The Dissertation Committee for Thiago Cardoso Carvalho Certifies that this is the approved version of the following dissertation:

Development of an Inhalational Formulation of Coenzyme Q_{10} to Treat Lung Malignancies

Committee:

Jason T. McConville, Supervisor

James W. McGinity

Krishnendu Roy

Hugh D. Smyth

Robert O. Williams, III

Development of an Inhalational Formulation of Coenzyme Q_{10} to Treat Lung Malignancies

by

Thiago Cardoso Carvalho, Farmacêutico

Dissertation

Presented to the Faculty of the Graduate School of

The University of Texas at Austin

in Partial Fulfillment

of the Requirements

for the Degree of

Doctor of Philosophy

The University of Texas at Austin

December, 2011

Dedication

Ye shall know the truth and the truth shall make you free.

(John, 8:32) – Message engraved in the South face of the UT tower.

I am the way and the truth and the life.

(John, 14:6)

To Jesus Christ be the glory.

To my loving wife Simone, for joining me in this adventure and for sticking with me through thick and thin.

To my devoted parents, who have always and unconditionally supported all my dreams.

Acknowledgements

More than a degree, the endeavor of my graduate studies has been an adventure into my soul and, ultimately, a vivid experience of self-awareness. While I first thought that the mere purpose of coming to the United States was to acquire a higher education, God's plans were different. I am deeply grateful for Him bringing me to the University of Texas at Austin so that I could find and get to know Him intimately. Besides giving me courage and strength, He put people in my life that has made and will continue to make a difference in years to come. These people have become essential players in this achievement and to whom I am profoundly indebted.

I am extremely grateful to my parents, Célia and Antônio Carvalho, and no words could describe their love and their restless efforts in always supporting my dreams unconditionally throughout my life. This accomplishment is significantly owed to their vision and value towards education that was instilled in me and my siblings. From our childhood in a small town in Brazil, we understood that our professional successes implied sacrifices that we, as a united family, were willing to make. For this reason, I also thank my brother, André Carvalho, and my sister, Celiane Carvalho, for all their advice in helping to keep me on-track with my dreams in moments of doubt and for assuring that our physical distance apart would never overcome our emotional bonds.

My lovely wife, Simone, is a very brave woman for accepting this challenge to move with me to another country so that I could follow my dreams. She has taught me that happiness is found in the small things of daily life and that serving is a joy for those who love. I am very thankful for her understanding, friendship, courage, patience and love. I extend my gratitude to her family in accepting the hardship that the physical distance has brought as a consequence of our choices.

I thank my supervisor, Dr. Jason T. McConville, to whom I have enormous gratitude for offering me this amazing opportunity. He has given me guidance, friendship, a willingness to find ways in lightening personal hardships, and help in seeing the positive facet that exists in every uncertainty. I am also thankful to Dr. James W. McGinity, Dr. Krishnendu Roy, Dr. Hugh D. Smyth and Dr. Robert O. Williams, III, for serving in my committee and offering advice and encouragement. I am especially thankful to Dr. Robert O. Williams, III, for opening the doors of the world to me, and to Dr. James W. McGinity, whose professional advice has enabled me to reach victories that go far beyond my initial dreams.

I am very gratified by the financial support from Berg Pharma to this work. I would like to thank Mr. Niven R. Narain, Dr. Rangaprasad Sarangarajan, Mr. Nikunj Tanna and Dr. Shen Luan for their technical support and advice. Most especially, my gratitude goes to Mr. John T. McCook for his patience, encouragement and understanding during my development in the graduate program.

Texas and its ability to change the world is made so by the invaluable knowledge acquired by students from an outstanding Faculty, supported by an amazing Staff who ensure a smooth running of procedures during daily activities. I extend my gratitude to Professors Dr. Robert Pearlman, Dr. Zhengrong Cui, Dr. Salomon A. Stavchansky and Dr. Carlton Erickson, all of whom have enriched my experience and shared of their friendship. I thank our great Graduate Coordinators, Ms. Stephanie Crouch and Ms. Mickie Sheppard. Special thanks go to Ms. Mickie Sheppard, with assistance from my great friend Dr. Milli Reddy, for going above and beyond their call of duty in helping me settle in a new country. Thanks to Ms. Yolanda Abasta and Ms. Claudia McClelland for their administrative assistance. To Ms. Joyce McClendon, Ms. Belinda G. Lehmkuhle, Mr. Jay Hamman, Mr. Oliver Gomez and all Information Technology squad members, I

am thankful for their help in ensuring that my work could be presented in the best way possible. I also thank Mr. James Baker and Mr. Joe D. Adcock for their continuous efforts in purchasing and delivering laboratory supplies at the earliest possible convenience. I am especially appreciative to Ms. Jamye O'Neal and Dr. Alan B. Watts for their understanding of my research needs while using equipment at the TherapeUTex facilities from the Drug Dynamics Institute. I would like to also thank my graduate student, *post doc* and intern fellows whom I have had the pleasure in interacting with, were always available for long scientific discussions and helped with daily research laboratory duties, including: Dr. Yoen-Ju Son, Dr. Sumalee Thitinan, Shih-Fan Jang, Javier Morales, Simone Carvalho, Ping Du, Ashkan Yazdi, Michelle Horng, Zachary Warnken, Ashley Jewett, Christine Joseph, Gero Joks, Simone Dietz, Dr. Alan Watts, Dr. Shawn Kucera, Dr. Sandra Schilling, Dr. Dorothea Sauer, Dr. Caroline Bruce, Dr. Dave Miller, Dr. Wei Yang, Dr. Shayna McGill, Dr. Martin Donovan, Dr. Ikumasa Ohno, Dr. Aileen Gibbons, Dr. Ashish Rastogi, Dr. Kevin O'Donnell, Dr. Nicole Beinborn, Dr. Steve Marek, Dr. Jasmine Rowe, Dr. Piyanuch Wonganan, Dr. James DiNunzio, Dr. Masao Nagao, Dr. Yasuhiro Tsutsumi, Dr. Eric Wang, Jin Huk Choi, Justin Hughey, Lonique Coots, Tarik Khan, Bo Lang, Hélène Dugas, Justin Keen, Ryan Bennett, Stephanie Bosselmann, Chris Brough, Ju Du, Matthew Herpin, Amit Kumar, Xinran Li, Letty Rodriguez, Meimei Zhang, John Yang, Michael Sandoval, and Yi-Bo Wang.

Throughout my life, I have had "unofficial mentors", people who have voluntarily spent a significant amount of their time to help me in shaping my career. For that, my gratitude goes to Dr. Jeffrey Hemenway and Mr. Sergio Brocca. I especially acknowledge my cousin, Mr. Rolando Dias, who showed me that the world can be of the size of our dreams, and my aunt, Ms. Maria do Carmo Cardoso, for her dedication

throughout my early school career in teaching me that preparedness is a key factor in success.

Finally, this achievement is enormously backed up by my “safety net”. These are people who have cheered me up, whom I have cried and laughed together with, who encouraged, and prayed for me. They include my extended family (aunties, uncles and cousins), my long-life friends from my hometown, Carmo do Rio Claro, my college friends from Belo Horizonte, my friends from Montes Claros and from Austin. It would be a mistake to list them, risking to leave names out. But each one of you knows how much you have done for me and how much I appreciate you! I cannot fully express how thankful I am for you always being there for me!

Development of an Inhalational Formulation of Coenzyme Q_{10} to Treat Lung Malignancies

Thiago Cardoso Carvalho, Ph.D.

The University of Texas at Austin, 2011

Supervisor: Jason T. McConville

Cancer is the second leading cause of death in the United States and its onset is highly incident in the lungs, with very low long-term survival rates. Chemotherapy plays a significant role for lung cancer treatment, and pulmonary delivery may be a potential route for anticancer drug delivery to treat lung tumors. Coenzyme Q_{10} (CoQ_{10}) is a poorly-water soluble compound that is being investigated for the treatment of carcinomas. In this work, we hypothesize that formulations of CoQ_{10} may be developed for pulmonary delivery with a satisfactory pharmacokinetic profile that will have the potential to improve a pharmacodynamic response when treating lung malignancies. The formulation design was to use a vibrating-mesh nebulizer to aerosolize aqueous dispersions of CoQ_{10} stabilized by phospholipids physiologically found in the lungs.

In the first study, a method was developed to measure the surface tension of liquids, a physicochemical property that has been shown to influence the aerosol output characteristics from vibrating-mesh nebulizers. Subsequently, this method was used, together with analysis of particle size distribution, zeta potential, and rheology, to further evaluate the factors influencing the capability of this nebulizer system to continuously and steadily aerosolize formulations of CoQ_{10} prepared with high pressure homogenization. The aerosolization profile (nebulization performance and *in vitro* drug

deposition of nebulized droplets) of formulations prepared with soybean lecithin, dimyristoylphosphatidylcholine (DMPC), dipalmitoylphosphatidylcholine (DPPC) and distearoylphosphatidylcholine (DSPC) were evaluated. The rheological behavior of these dispersions was found to be the factor that may be indicative of the aerosolization output profile. Finally, the pulmonary deposition and systemic distribution of CoQ_{10} prepared as DMPC, DPPC, and DSPC dispersions were investigated *in vivo* in mice. It was found that high drug amounts were deposited and retained in the mouse lungs for at least 48 hours *post* nebulization. Systemic distribution was not observed and deposition in the nasal cavity occurred at a lower scale than in the lungs. This body of work provides evidence that CoQ_{10} may be successfully formulated as dispersions to be aerosolized using vibrating-mesh nebulizers and achieve high drug deposition in the lungs during inhalation.

Table of Contents

List of Tables

List of Figures

Chapter 1: Introduction

1.1. Formulations for Pulmonary Administration of Anticancer Agents to Treat Lung Malignancies

Abstract

Chemotherapy plays a significant role both as primary and as supportive care for lung cancer treatment. The majority of currently available anticancer agents are administrated intravenously, causing side effects due to the systemic drug distribution. Alternatively, the bioavailability of orally administrated anticancer agents is usually compromised by the first-pass metabolism. Pulmonary administration may be a potential route for anticancer drug delivery to treat lung tumors, due to its site specific delivery, avoidance of first-pass metabolism, possibility of fewer side effects, and improved comfort for cancer patients using a needle-free delivery device. However, to attain an effective inhalational delivery, there is a requirement to design a formulation with appropriate aerodynamic properties with well-suited excipients. This review explores work to date related to the formulations developed for pulmonary delivery of small molecule antineoplastic agents to treat primary and metastatic lung carcinomas. Ultimately, it highlights the importance of formulation design to define the role of inhalational chemotherapy.

1.1.1. Introduction

Parts of this chapter were taken from *Carvalho TC, Carvalho SR, McConville JT. Formulations for Pulmonary Administration of Anticancer Agents to Treat Lung Malignancies. Journal of Aerosol Medicine and Pulmonary Drug Delivery.*

2011;24(2):1-20 and from *Carvalho TC, Peters JI, Williams III RO. Influence of particle size on regional lung deposition - What evidence is there? Int J Pharm. 2011;406(1-2):1-10*. The co-authors in these publications have contributed by providing comments to improve the quality of these review papers.

Second only to heart disease, cancer is the leading cause of death in the United States. Although a total of $228.1 billion USD was spent on cancer treatments in 2008[1] there was still an estimated 565,650 deaths in that year.[2] These cancer related deaths represented 25% of total mortality when compared to other diseases.[3] Among the many different possible sites for the onset of cancer, this disease has a high incidence in the lungs. It has been estimated that 219,440 new cases of lung cancer were diagnosed in 2009, which represents 15% of the total incidence of cancer. Moreover, lung tumors are the most lethal amongst all types of cancer. Alone, it accounts for 28% of all the cancer deaths estimated for 2009. This means it is expected to kill more than the next three most deadly cancers in men put together (i.e. prostate, colon, and pancreatic cancer). Tobacco is the most expressive risk factor for lung cancer development in both males and females[4] and is related to quantity and duration of exposure to tobacco smoke.[1]

Lung cancer is classified as two subtypes, according to the histological characteristics of the tumor: small cell lung cancer (SCLC) and non-small cell lung cancer (NSCLC). Their distinct biological profiles lead to different prognosis and, consequently, different clinical treatments. Without treatment, the median survival of a diagnosed SCLC patient is less than 4 months, due to its rapid growth and high propensity for dissemination throughout the body. Although this malignancy presents an aggressive nature, its response to chemotherapy and radiotherapy is greater than NSCLC.[5] The incidence of SCLC in the United States in 2002 was approximately 13% of all new cases, with a decreasing annual rate of 2.4% since 1973.[6] Inversely, at the

time of diagnosis, NSCLC represents the greatest majority among all new cases of lung cancer. Usually, several different types of cancer cells are presented at the NSCLC tumor aggregate, including squamous cell carcinoma, large cell carcinoma, and adenocarcinoma which is currently the most expressive type.[4, 7] Malignancy to the lungs may also be a result of metastases from tumors originated in other organism sites, such as melanoma, and breast cancer.[8, 9]

The Tumor-Node-Metastasis (TNM) staging system is the most commonly used classification in the clinical practice.[10] Given the nature of SCLC, to easily metastasize; a simpler concept of the staging system is also used: Limited Disease (LD) and Extensive Disease (ED).[11-13]

Surgery, radiotherapy, and chemotherapy are the treatment options for lung cancer patients. Due to the high mortality outcomes from this cancer subset, different treatment modalities are frequently combined in several ways, attempting to increase the life expectancy of the patients.

Surgery is considered effective when the early stage tumor is localized in a defined area. NSCLC patients normally benefit more with this modality, given the intrinsic characteristic of the tumor cells to spread less than SCLC.[14] Although surgery alone is not recommended, this medical procedure should always be considered as part of a multi-modality treatment, including neoadjuvant (or induction) and adjuvant therapy. For instance, both neoadjuvant chemoradiation after tumor resection and postoperative chemotherapy have provided favorable survival outcomes in NSCLC patients.[15, 16] Supposedly, these treatment modalities shrink the tumor prior to surgery and/or attempt to avoid disease relapses in the long-term.

Radiotherapy is recommended for patients with localized tumors, usually in the early stages of lung cancer. However, individuals that are medically inoperable or refuse

surgery may also benefit with radiation treatment. Radiotherapy can be used for both types of lung cancer.[17] For instance, given the radiosensitivity of SCLC cells, radiotherapy is a good treatment option for LD patients, requiring a lower radiation dose. Studies have shown a significant decrease in the recurrence of local failure and increase in the survival rate of LD-SCLC patients when chemotherapy is combined to radiotherapy.[18-22] Interestingly, LD-SCLC has different types of cells and, consequently, different morphological and biologic characteristics. Although, these kinds of LD-SCLC react with different intensity to small radiation, they are still more reactive than normal tissue. However, the incidence of metastases and local recurrence is still very common in those patients.[18]

Either alone or in combination with other modalities, chemotherapy plays a significant role in the treatment of cancer. In general, numerous drug delivery strategies for different routes of administration have been applied in the formulation development of anticancer drugs, regardless of tumor site. For instance, liposomes, solid lipid nanoparticles (SLNs) and polymeric micro/nanospheres, have been investigated as possible colloidal delivery systems.[23]

When it comes to lung cancer, in most cases, the currently available drugs are to be administered by the intravenous route (bolus or infusion). For instance, the paclitaxel formulation designed for intravenous (IV) infusion administration contains the water-insoluble Active Pharmaceutical Ingredient (API) solubilized in a mixture of Cremophor EL (polyoxyethylated castor oil) and dehydrated alcohol. However, as thoroughly reviewed by Marupudi *et al.*., hypersensitivity reactions, myalgias and hematologic, neuro and cardiac toxicities have been reported due to infusion administration of paclitaxel, which lead to a certain limitation in treating cancer patients.[24] While myelosuppression (mainly neutropenia) and peripheral neuropathy appear as fairly

common adverse effects, others are not only related to paclitaxel itself, but also to the presence of cremophor in the formulation (certain neurotoxic events and hypersensitivity reactions). Nevertheless, the review also highlights that paclitaxel having characteristics of lipophilicity, high protein affinity, and a volume of distribution much higher than total water volume in the body; make the current infusion treatment with paclitaxel demonstrate a low therapeutic index. This small concentration of anticancer agent administered that reaches the site of interest is also caused by the presence of cremophor in the formulation, altering the drug pharmacokinetic profile.[24]

To a lesser extent, some anticancer agents have also been administered orally.[25] For instance, etoposide treats lung malignancies and is commercially available as soft gelatin capsules containing 50 mg of API in a solution of purified water, citric acid, glycerin and polyethylene glycol 400. Although the need of hospitalization has been surpassed with the advent of this dosage form, etoposide bioavailability is still a concern, ranging from 40 to 75% and varying inter and intra-patient doses.[26] In addition, ethanol, bile salts, cimetidine, metaclopromide and propantheline administered along with etoposide have not shown to be successful in improving bioavailability and avoiding patient variability.[26, 27]

Generally speaking, either IV or oral administration routes are able to provide relatively high systemic drug concentrations. However, a rather low drug amount effectively reaches the desired site of the lungs.[28] As a result, this small lung-to-plasma ratio of drug concentration could lead to a low therapeutic efficacy and increased systemic side effects. Thus it has been the goal of several research groups to develop a locally acting anticancer delivery system for the lung using aerosol delivery.

1.1.1.1. Pulmonary Delivery

The lungs can potentially be a route of administration for both local action and systemic absorption. In either case, pulmonary delivery exposes the lung tissue to drug concentration levels significantly higher as compared to other routes of administration, such as intravenous or oral. For instance, pulmonary administration of itraconazole in mice has achieved lung tissue concentrations greater than 10-fold as compared to oral administration.[28] As for other respiratory diseases, such as asthma and Chronic Obstructive Pulmonary Disease (COPD), inhalation therapy for treatment of lung cancer might be considered reasonable for the same pharmacokinetic and pharmacodynamic reasons. With the lungs as the target organ, a focused drug exposure may avoid potential systemic side effects due to high plasma levels. Any reduction in systemic side effects could be highly beneficial to lung cancer patients given the current available chemotherapy options. From this standpoint, by local delivery of anticancer agents, lower doses compared to intravenous or oral routes would be expected to achieve higher drug levels at the site of lung malignancy. Consequently, more effective treatments may potentially be achieved, while systemic toxicity could possibly be reduced by decreasing plasma levels. The rationale and potential limitations for inhaled chemotherapy are discussed in detail in the literature.[29, 30]

To generate the aerosol particles, there are currently three major categories of devices for clinical use: nebulizers, pressurized-metered dose inhalers (pMDI), and dry powder inhalers (DPI). More detailed information on these delivery technologies are explained elsewhere in the literature.[31, 32] Nebulizer formulations can be administered by passive breathing; therefore lung cancer patients should not experience any difficulty in using this type of device whatsoever. On the other hand, pMDIs require patient synchronization to actuate the device and inhale the drug in an active maneuver. This can

be overcome when pMDIs are coupled with spacers that may act to assist the necessary effective inhalation maneuver. DPIs and pMDIs have been extensively investigated for the therapies to treat asthma and COPD. The fact that severe COPD patients are able to use these devices may allow us to assume that lung cancer patients could also potentially operate them in an effective manner. However, a consideration has to be made for the use of pMDIs to deliver the currently available anticancer drugs. Considering their relative low potencies, the dose necessary to treat a lung cancer patient via inhalation may well be in the order of milligrams. To deliver this level of dose, the number of actuations in a pMDI device may easily approach the order of the hundreds. Therefore this requisite would turn it into a low patient adherence therapy, nullifying one of the advantages of inhalation therapy. Therefore, despite the potential to deliver anticancer drugs using pMDI, the limitation of this device should be carefully evaluated.

Despite the potential of regional chemotherapy for primary and metastatic lung carcinomas, the development of inhalational formulations is in general very technically challenging. Aerosol particle size is of extreme importance for inhalational formulations, and is a determinant factor in the drug deposition region in the respiratory airways and, consequently the lung clearance mechanism. Given their different delivery methods, aerosol formulations are very device-specific. Hence, aerodynamic characterization of formulations for pulmonary delivery is essential to determine the likelihood of the drug to reach a specific lung region. Cascade impactors can be used for this purpose.[33] In general, particles with a mass median aerodynamic diameter (MMAD) of 1-5 μm are considered to deposit in the deep lung and settle by inertial impaction. In the alveolar region, they may be cleared mainly by dissolution followed by diffusion through the lung tissue, macrophage uptake and subsequent phagocytosis (unless they are smaller than about 260 nm), or metabolism.[34-36] On the other hand, aerosol particles smaller than

approximately 1 μm are predominantly exhaled at normal breathing patterns whereas those with an MMAD of about 5-10 μm are considered to deposit predominantly in the upper airways (oropharynx), being subsequently swallowed due to mucociliary clearance.[34, 36, 37] Along with MMAD, the geometric standard deviation (GSD) should be reported as it indicates the magnitude of dispersity from the MMAD value.[33] These particle aerodynamic profiles are influenced by particle size, shape and density. Recently, an *in vitro*/*in vivo* comparison has shown that particles of 1-3 μm are the ones that more effectively deposit in the lower airways.[38] Therefore, formulation aerodynamic properties may be a determining factor defining the fate of the drug in the pulmonary tissue. Alternatively, laser diffractometry equipments allow comparative evaluation for *in vitro* characterization during formulation development.[39]

1.1.1.2. Dose and Drug Deposition in the Lungs

Lung carcinomas can both be presented with diffuse nature (e.g. SCLC and bronchoalveolar carcinomas) or as solid tumors; and yet localized anywhere from the bronchi (central portion) to the alveoli (lung periphery). Thus, in many cases the pulmonary administration of anticancer agents should be expected to target very specific areas of the lungs. However, aerosol particles are more likely to deposit in well ventilated areas of the lungs, such as the central airways (trachea and bronchi). With that, solid tumors positioned in peripheral regions of the lungs may be limitedly exposed to inhaled drugs, thereby restricting treatment efficacy. Recently, an investigation has shown that co-administration of phospholipids induces particle migration towards lung periphery.[40] Although this finding brings some expectation for improvement of poorly-water soluble drug distribution throughout the lungs, it is still a major challenge to develop formulations that can effectively be deposited in the vicinity of the lung

carcinoma in order to potentially provide the desired pharmacodynamic response. Yet, even if the drug is available for absorption at the carcinoma site, the asymmetric diffusion throughout the solid tumor may cause a heterogeneous delivery.[41] Ruenraroengsak *et al.*.[42] discusses that not even the advances in nanotechnology for drug delivery systems may be able to enhance drug uptake into the tumor. This may be due to the low probability of the nanoparticles to find, bind and consequently been up taken by the tumor cells in a complex *in vivo* structure. From this standpoint, formulation scientists face a huge obstacle to turn antineoplastic agents into an effective chemotherapy inhalation option. For this reason, recently some believe that the role of antineoplastic inhalation may be restricted to adjuvant therapy.[41] With tumor removal by surgery, tumor penetration is no longer needed. Alternatively, aerosolized chemotherapy may also potentially be applied to treat more diffuse forms of lung cancer, such as bronchoalveolar carcinoma. In this case, the chemotherapy treatment via inhalation would possibly reduce the side effects to patients that could eligibly benefit from it. Nonetheless, the studies presented later in this review mainly focus on pulmonary delivery as primary treatment to eliminate the tumors.

No matter which treatment modality the anticancer inhalation therapy may fall within, determining the dose exposed to the lungs is also a challenging task for *in vivo* studies. Aerosol formulation performance is highly dependent on aerodynamics of formulation provided by a specific aerosol device.[43] The many different aerosol systems and animal dosing methods that can be used are able to produce different droplet/particle sizes. Consequently, different profiles of drug deposition can be achieved.[44] Therefore, dose determination of inhalation formulations is challenging, as opposed to other dosage forms, such as tablets, in which the API dose is very well defined. Planar gamma scintigraphy is the most widely used direct method to determine

the drug deposition in the lungs.[45, 46] By mixing the drug with radiolabeled substances (e.g. Technetium-99m, ^{99m}Tc), the deposited drug may be estimated using scintigraphic images. One major drawback of this method is that it requires the formulation itself to be altered in order to contain the radionuclide. This formulation modification may misrepresent the actual drug deposition. Nonetheless, the two-dimensional image results are not sensitive to drug deposition differences in distinct planes throughout the pulmonary tridimensional structure. Being able to identify the drug deposition three dimensions is an important feature when the aim is to target solid tumors in specific lung regions. This could be accomplished, with certain limitations, by single photon emission computed tomography (SPECT) or positron emission tomography (PET). Alternatively, calculation of estimated deposited drug has been used to determine inhaled dose from nebulizers.[47] This method is based on the minute-volume of respiration,[48] the estimated deposited index (both species-specific), the duration of treatment and the drug concentration in aerosol volume. Analysis of the later is more suitable for homogeneous systems (e.g. solutions) than for disperse dosage forms (e.g. emulsions and liposomes) due to their content uniformity during nebulization. By changing the respiratory patterns, the inhalation of 5% CO_2-enriched air increases drug deposition by approximately 3-fold.[49] Whenever this technique is applied, the CO_2 factor is also added to the calculation of the estimated dose. It is also worth mentioning that, although better dose control may be achieved by endotracheal instillation, since it bypasses nasal deposition, this technique does not allow assessment of the aerodynamic characteristics of the formulation. Therefore, conclusions from studies using this technique should be done using caution. Despite the estimation that the aforementioned methods provide, the accurate determination of drug deposition in the lungs remains yet a major issue to be considered in preclinical studies.

For clinical studies, concerns should be addressed in order to protect health care providers from fugitive aerosol. As we will see later in this review, this can appear as device adaptations, scavenging tents equipped with HEPA filters covering the patient, or special gowning.

1.1.1.3. Formulation Aspects

The physicochemical properties of a drug play a significant role in formulation design. For instance, the poor water solubility of taxanes (e.g. paclitaxel and docetaxel) and some recently discovered camptothecin derivatives, such as 9-Nitrocamptothecin (9NC), are a challenge for the development of aqueous formulations for nebulization delivery.[50] The partition coefficient (log P) and acid dissociation constant (pK_a) also provide important information about drug clearance from the lungs. Schanker and coworkers have previously demonstrated that, in general, hydrophilic drugs (log $P < 0$) present lung residence times in the magnitude of hours. Conversely, lipophilic drugs (log $P > 0$) are absorbed from the lungs in matter of minutes.[51, 52] Additionally, they have demonstrated that nonionized drugs are more rapidly absorbed as compared to the ionized form.[53] In order to achieve the desirable pharmacodynamic response, it is obvious that antineoplastic agents need to be available to tumor cells for a minimum period of time. Drugs readily absorbed by the lungs may then not effectively treat the disease. Table 1 shows the water solubility and log P values of selected drugs, including the use and dosage regimen to combat lung cancer.[54]

By suitably designing a formulation for lipophilic drugs, the delivery system can maintain sustained release of the anticancer agent to potentially prolong the drug exposure time to carcinomas. There are a number of excipients that can provide the sustained release feature for oral administration. However, for certain formulation

components, the relatively low clearance rate in the alveolar bronchial region may render an exceedingly long residence time. Consequently, the accumulation of poorly or non-biodegradable materials in the lungs may compromise pulmonary function.[34] When considering lung cancer patients in a later stage disease state, this accumulation may be of significant negative health impact. This fact restricts the use of a large number of excipients well tolerated by administration through other routes in the drug development of pulmonary delivery systems.

Still, a major issue for choosing appropriate excipients for aerosol medications has been the scarce information about their pulmonary delivery safety. In a recent study, Montharu and coworkers have investigated the safety of delivering water (control), ethanol (10%), propylene glycol (30%), and polysorbate 80 (10%) to the lungs.[55] Rats receiving 150 μL of solutions for four consecutive days via intratracheal instillation presented signs of local reaction only with polysorbate 80 (foamy macrophage and inflammation). In contrast, lower levels of polysorbate 80 can apparently be aerosolized to mice with no signs of inflammation or changes in pulmonary histology.[56] Excipients in previously approved products by the United States Food and Drug Administration (US FDA) can be found elsewhere.[57] Also, scale-up capabilities of the process used to prepare the formulation must highly be considered to turn preclinical results into clinical trials and successively into a market product.

Finally, it cannot be excluded the possibility that pulmonary delivery may impact lung function according to the formulation design. Possible pulmonary toxicity caused by excipients may then compromise the lung tolerance to the neoplastic agent. This in turn may lead to a reduction in the maximum tolerated dose (MTD) and consequently affect the chemotherapy efficacy.

1.1.2. Anticancer Agents

The next part of this review invites the reader to a commentary of the formulation aspects of delivery systems, which have been investigated specifically for the inhalation of anticancer small molecule drugs for the treatment of lung malignancies. This section of the review is subdivided into the different antineoplastic agents. The formulation of biopharmaceutical (macromolecules) and chemopreventive agents are not discussed as they are beyond the scope of this review. Summary tables from preclinical and clinical studies discussed in this review are presented in Tables 2, 3 and 4.

1.1.2.1. Methotrexate

Although not used alone for the primary treatment of lung cancer, methotrexate has been used as proof of concept for the inhalation delivery of chemotherapeutic agents using a pMDI delivery system.[58] Chlorofluorcarbon (CFC)-free formulations were prepared by cryomilling methotrexate, with or without Poloxamer 217 as a physical mixture. The low solubility of this drug in 10% ethanol/hydrofluoroalkane (HFA) 134a gave rise to a suspension dosage form. As investigated by X-ray diffraction, the grinding process did not alter the crystalline drug morphology. The first evident result from this study is that cryomilling only was not an effective method to reduce particle size for pulmonary delivery of methotrexate. The highest Respirable Fraction (RF) was achieved by taking the cryomilled particles and further processing by sieving (5 μm sieve). The values were as high as 35% RF for this formulation, while non-sieved preparations did not greatly vary from about 15% RF, regardless of grinding media and duration of process. Respirable fractions were defined as the percentage of particles deposited in stages of an Andersen cascade impactor with diameter less than 4.7 μm, to the total amount of drug emitted from the device (including all impactor stages, throat and

actuator). These results show that characterization of particle size distribution prior to formulation is highly beneficial to assess the potential to deliver the drug to the lungs. In general, the formulations presented MMADs of 2.2 to 3.2 μm and GSDs greater than 2. Undoubtedly, a greater reduction in particle size would be necessary to decrease GSD and consequently improve the respirable fraction results. Nevertheless, with this model anticancer drug, the investigators found *in vitro* cytotoxicity results of greater than 50% cell kill and comparable results between aerosolized and non-aerosolized doses were obtained. This outcome was sufficient to encourage further investigation of the pulmonary route for the delivery of other chemotherapeutic agents.

1.1.2.2. COX-2 inhibitors

The aerosol characteristics of different combinations of anticancer agents and selective COX-2 inhibitors against NSCLC cell lines have been examined for the *in vitro* cytotoxicity. For these studies, aerosolized nimesulide and aerosolized celecoxib have been formulated to evaluate cytotoxicity potentiation in conjunction with, respectively, doxorubicin and docetaxel.[59, 60] The COX-2 inhibitors nimesulide and celecoxib are practically insoluble in water and slightly soluble in ethanol.[61] After a solubility study in both HFAs 134a and 227 of the drug to be aerosolized, solution formulations for pMDI delivery were prepared. Water soluble drugs can be simply dissolved in an aqueous mixture prior to nebulization. Alternatively, solutions may be prepared for pMDI devices, by dissolving the drug in the propellant. In these cases, given the relatively recent change of propellant type from CFC to HFA,[62] it may be necessary to have a co-solvent (to dissolve the drug) that is miscible with HFA. Ethanol can often fulfill these two requirements. Stages 3 to 6 of the cascade impactor (particles with cutoff diameters of

less than 4.7 μm) were used to assess respirable fraction. The formulations, the devices and the particle size characterization are shown in Table 2.

The formulations of COX-2 inhibitors presented in Table 2 demonstrated feasible MMADs for drug delivery to the lungs, although with a relatively broad GSD for nimesulide formulation. From the studies with celecoxib, the formulations with higher drug loading have presented higher medication delivery. Also, it has been previously shown that as ethanol concentration decreases, either in HFA 134a or 227, the fine particle fraction increases.[63] This event has also been observed for aerosolized celecoxib formulations. Importantly, the aerosolization process has been reported not to alter the activity of the aerosolized drug. In addition, these two formulations presented satisfactory physical and chemical stability for 1 month at room temperature, and elevated temperature (40 ºC). The celecoxib formulation also presented a similar stability at room temperature only. The aerosolized selective COX-2 inhibitors have shown to satisfactorily decrease IC_{50} values of the aforementioned anticancer agents in lung cancer cell lines. But, are COX-2 inhibitors potent enough to be delivered via pMDI? In the case of COX-2 inhibitors, each actuation was able to deliver about 50 to 100 μg of drug. From this, only about 40 to 50% was potentially able to reach the deep lungs. That means that at least 20 actuations may be needed to achieve about 1 mg of COX-2 inhibitors to the lungs. Once more, we emphasize the dose restriction of pMDI delivery of anticancer drugs. Therefore, the capability of pMDI formulations of COX-2 inhibitors to effectively treat lung cancer in conjunction with other chemotherapeutic agents is yet to be answered.

Celecoxib has also been prepared as an emulsion for inhalation delivery via nebulizer.[64] Based on a previous study,[65] the antitumor activity was tested in a human orthotopic NSCLC xenograft model. Aerosolized celecoxib was compared with

oral delivery, both concurrently with an intravenous administration of docetaxel. Celecoxib (5 mg/mL) was dissolved in ethanol and polyethylene glycol (PEG) 400 before emulsification with molten D-α-tocopheryl polyethylene glycol 1000 succinate (vitamin E TPGS). Vitamin E TPGS has previously demonstrated to increase drug bioavailability via oral administration by inhibition of the multidrug resistant transporter P-glycoprotein.[66] The expression of P-glycoprotein in NSCLC patients is activated during chemotherapy.[67] Therefore, the use of vitamin E TPGS could potentially be more important than simply acting as an emulsifier agent. On the other hand, to our knowledge, there has been no report so far on the safety of pulmonary administration of this excipient. A Pari LC Star® jet nebulizer was used to generate particles with MMAD of 1.68 μm and GSD of 1.36 as measured by a Mercer Cascade Impactor (airflow rate not reported). Female Nu/Nu mice were exposed to aerosolized drug using a nose-only inhalation chamber for 30 minutes per day during 28 days. According to the authors, the estimated total deposited dose was 4.56 mg/kg/day, this calculation was based on concentration of drug in aerosol volume, volume of air inspired by the animal during 1 min, estimated deposition index for mice and duration of treatment. Compared to a control group, reduction in the tumor volume was 61 and 54%, following aerosolized and oral treatments in combination with IV docetaxel, respectively. The accuracy of the estimated deposited dose is questionable. To explain, this dispersion system may be considered to present similar thermodynamic characteristics to that of liposomes. Due to the stress applied, liposome structure is significantly disrupted by jet nebulizers.[68] In the study of aerosolized celecoxib emulsion, the system behavior under aerosolization via jet nebulizers was not evaluated. This could raise questions as whether the drug was homogeneously released from the device throughout the duration of exposure. Nevertheless, other factors are very relevant from the formulation aspect and therefore

should also have been evaluated, such as the particle size distribution of the emulsion and its stability over time.

1.1.2.3. Gemcitabine

In combination with other antineoplastic agents, gemcitabine has shown effectiveness against a number of types of cancer, including advanced stages of NSCLC.[69] A salt form is currently commercialized under the trade name Gemzar® (Gemcitabine HCl) by Eli Lilly. Gemzar® is supplied as a freeze-dried powder with mannitol and sodium acetate, hydrochloric acid, and sodium hydroxide as excipients. Reconstitution with saline gives the final solution of this marketed injection formulation, with pH ranging from 2.7 to 3.3. Clinical and toxicological studies have been performed by drug aerosolization using this solution for injection in mice, rats, dogs and baboons.[70-74] The most important features of these studies can be seen in Table 3.

The accuracy in the characterization of aerodynamic profile and drug deposition in some of these studies are questionable, particularly as one of the studies fails to mention the specified type of nebulizer used. Nonetheless, these gemcitabine preclinical studies give very significant therapeutical and toxicological data about inhaled solution for both primary and metastatic lung cancer. For instance, five weekly treatments of 8 mg/kg to mice bearing human orthotopic NSCLC tumors were able to significantly inhibit the primary cancer growth. Meanwhile, increasing the dose to 12 mg/kg caused acute and fatal pulmonary edema events.[71] Similarly, lung metastases incidence was significantly reduced by doses of 1.0 mg/kg biweekly for 6.5 weeks.[70] Also, gemcitabine has been shown to be safe in rats and dogs at a MTD of 9 weekly treatments of 4 mg/kg and 20 biweekly treatments of 2.38 mg/kg, respectively.[72, 74] Pharmacokinetic studies in baboons have shown that t_{max} is achieved at approximately 10

minutes after starting nebulization (in this case, still during inhalation process).[73] After 60 minutes, the drug was undetectable in the plasma; not a surprising result, given the low partition coefficient of gemcitabine (log P = -1.24).[75]

Despite the number of studies in different species, so far, only the commercialized injection formulation of this anticancer agent has been investigated for the possibility of aerosolization to the lungs. With an acidic pH, the desired water dissolution of gemcitabine for injection (pK_a = 3.58) is assured.[76] When inhaled, the prompt drug availability for lung absorption will highly contribute to a rapid pulmonary clearance by diffusion mechanism. On one hand, the hydrophilic characteristic of gemcitabine provides an advantageous lung residence time as compared to its lipophilic chemotherapeutic counterpart. On the other hand, more investigation exploring its water solubility properties are yet to be performed so as to ascertain the full potential of gemcitabine to treat lung malignancies.

1.1.2.4. Doxorubicin

Doxorubicin is a relatively lipophilic and water soluble drug that has long been used for the treatment of pulmonary malignancies. Based on its physicochemical characteristics, namely water solubility and partition coefficient (see Table 1), one would expect a prompt absorption of doxorubicin by the lungs.

A DPI formulation was studied to evaluate the *in vitro* cytotoxicity of doxorubicin nanoparticles.[77] The drug was incorporated into poly(butylcyanoacrylate) nanoparticles by emulsion polymerization and coated with polysorbate 80 (0.5 % v/v). Poly(butylcyanoacrylate) had previously been used for the intravenous administration of anticancer drugs for the treatment of brain tumors.[78] Inclusion of a surfactant coating has been shown to facilitate particles translocation across the capillary barrier.[79] The

doxorubicin-loaded nanoparticles were then mixed with lactose (carrier) in a spray freeze-drying procedure. This manufacturing process, which may be scaled up, was able to yield a loading capacity of 1.39 μg of doxorubicin per mg of powder. The results from this study showed that doxorubicin-loaded nanoparticles of 173 ± 43 nm mean particle sizes were effectively incorporated into a 10 ± 4 μm overall lactose geometric particle size. Using a passive DPI, the MMAD obtained was 3.41 ± 0.22 μm, as measured at 60 L/min by Mark II Anderson Cascade Impactor. This powder formulation has demonstrated an increased cytotoxicity against A549 and, more significantly, against H460 lung cancer cell lines as compared to free drug. However, the presence of polysorbate 80 in the formulation does not provide confirmation that endocytosis of doxorubicin-loaded nanoparticles has occurred more readily due to drug particle size alone or by some improvement in the translocation of these particles across the cancer cell barrier. Interestingly, the blank formulation (drug-free nanoparticles) showed certain levels of cytotoxicity as well. While similar low levels of polysorbate 80 has been safely aerosolized to mice,[56] to our knowledge, there has been no report to date verifying the safety of delivering poly(butylcyanoacrylate) to the lungs. Therefore, despite the encouraging cytotoxicity and aerodynamic results as well as the possibility of process scale up, this formulation may find restrictions for pulmonary delivery. Nevertheless, more studies are yet to be performed in order to define the feasibility of nanoparticle uptake by cancer cell lines.[42]

Dogs with naturally occurring primary or metastatic lung tumors were also treated with doxorubicin.[80] A solution was prepared by dissolving the drug in 20% ethanol at a concentration of 16 mg/mL. Under anesthesia, the dogs were exposed to the drug during a certain period of time by means of a Pari LC® jet nebulizer coupled to an endotracheal tube; this special assembly was designed to prevent fugitive aerosolization. The animals

received 6 treatments of 3 mg of doxorubicin once every 2 weeks. The dose calculation was based, not only on stabilized minute-volume of respiration under light anesthesia, but also assuming a body surface area of 1 m^2 (as a result small dogs were naturally exposed to a higher drug concentration in this study). Although 22% of the treated dogs (n = 18) achieved partial responses (a tumor volume reduction greater than 50%), no formulation characterization was reported. This lack of information does not allow us to evaluate whether the outcomes were maximized due to formulation and device performances. For instance, airflow rates, viscosity and surface tension may all influence the aerosol output from jet nebulizers.[81] Nevertheless, no systemic toxicity was evident, while pulmonary toxicity was observed (mainly as a cough).

The encouraging outcomes from the previous study have set the stage for a clinical trial. Doxorubicin was selected to be nebulized in patients with primary or metastatic tumors to the lungs for a phase I study.[82] The inhalation solution was provided at 16 and 24 mg/mL in ethanol:water 1:4 (pH 3). The aerosolization system consisted of a Pari LC Plus® jet nebulizer in a sealed, mouth-only inhalation apparatus (OncoMyst® model CDD-2a). As a precaution in this study, a demistifier tent with a HEPA filter was setup to protect the health care provider from potential fugitive aerosol. The dose was calculated on the bases of inhaled technetium-99m deposition and scintigraphy, and a limited pharmacokinetic evaluation was performed in this study. Due to the required number of breaths in the aerosolization system, administration of higher drug concentrations resulted in dosing times as long as 45-60 minutes. During this period, no drug plasma levels were analyzed. Maximal plasma concentration was observed at the first sampling point, 5 minutes after finishing treatment. Similarly to the study in dogs, no systemic toxicity was observed while cough was the most frequent adverse event observed in the patient population. Dose limiting pulmonary toxicity was observed at 7.5

mg/m^2 every 3 weeks. Therefore, dose escalation of this formulation by pulmonary administration has been suggested not to be adequate. Despite the nominal nebulizer capability to generate aerosol particles of 2-3 μm mentioned by the authors, again, the aerodynamic characteristics of the formulation were not confirmed by *in vitro* analytical tests. On one hand, the acidic solution (pH 3) present ionizes the doxorubicin (pK_a = 8.34) increasing the drug solubility.[83] On the other hand, the drug lipophilicity favors diffusion across membranes, considering the partition coefficient of doxorubicin (log P = 0.65). As a result, the fraction of unionized drug would be quickly absorbed and a relatively low lung residence time would be expected. Therefore, the long dosing time required to administer high drug concentrations may have biased these pharmacokinetic data. Another important aspect from this formulation is its pH. Previous studies have demonstrated that acidic aerosols stimulate coughing and increase lung resistance, with consequent bronchoconstriction.[84-86] In this study, pulmonary toxicity has been observed at high delivered doses, in so far as higher volume of liquid formulation was deposited. As the formulation pH increases the drug solubility, the acidic solution evokes airway irritation that may potentially be aggravated by increase in volume of liquid formulation deposited from the aerosol. Therefore, this formulation parameter appears as a confounding factor that may compromise the determination of the MTD of doxorubicin.

Doxorubicin is one of the few drugs to advance from preclinical studies to clinical trials for the pulmonary delivery to treat lung malignancies. Whether its intrinsic dose limiting toxicity may impose restrictions to its use as a single chemotherapy treatment modality is yet to be determined. In our opinion, formulations containing doxorubicin should be more appropriately designed and characterized prior to defining their intrinsic dose limiting toxicity, before an adequate assessment of the associated benefits of inhalational therapy. This will ultimately determine the role of this chemotherapeutic

option as single modality treatment. Furthermore, a neoadjuvant strategy is yet another option that still needs to be investigated prior to defining the role for pulmonary delivery of doxorubicin in lung cancer treatment.

1.1.2.5. Farnesol

Farnesol is a lipophilic (log P = 5.31) and very slightly water soluble drug that induces apoptosis in lung carcinoma cells.[87-89] An emulsion of this anticancer agent was prepared for nebulization by mixing farnesol (10.5 mg/mL) with polysorbate 80 (0.5 mg/mL) in a 20% v/v ethanol/normal saline mixture.[90] Emulsion stability was verified by storing a mixture of farnesol, ethanol and polysorbate 80 at 4 ºC for up to 14 days, with saline added just before use. The aerodynamic profile of this formulation was measured by a Phase Doppler Anemometer coupled to a breath simulator (average airflow rate of 18 L/min and tidal volume of 0.75 L).[91] According to this method, Pari LC Star® and LC Plus® nebulizers were able to generate aerosol particles with MMADs of 4.96 μm and 6.87 μm and GSDs of 1.48 and 1.67, for each nebulizer respectively. Also, the nebulization efficiency of this emulsion was estimated to be approximately 30% deposited drug out of the total volume submitted to aerosolization for either device. Finally, *in vitro* cytotoxic effects of nebulized farnesol were observed against A549 and H460 lung cancer cells. In our opinion, these data suggest that a low drug deposition *in vivo* as well as fast lung clearance may be expected. Firstly, only one-third of drug amount from the emulsion volume was effectively aerosolized by these jet nebulizers Considering solution dosage forms, both jet and ultrasonic nebulizers have similar performances to deliver the drug to the lungs. When it comes to suspensions though, drug aerosolization is more effective using jet nebulizers since the ultrasonic effect may aerosolize empty droplets (no drug present).[92] Now, fragile disperse systems like

emulsions may be vastly disrupted by the high energy imparted by jet nebulizers. Therefore, the amount of drug that ends up reaching the deep lungs may be compromised. Secondly, the aerodynamic results of this system are not very favorable for deposition in the lower airways. With MMAD values varying from 5 to 7 μm, most of the aerosol droplets would be deposited in the throat and upper airways, subsequently being swallowed. Finally, farnesol is a very lipophilic drug, with a log P value considerably higher than zero; an almost instantaneous absorption is more likely to occur.

In case of poorly-water soluble drugs, emulsification may be a preferred strategy for delivering the agent to the lungs. However, some important formulation characteristics should always be evaluated. The particle size distribution of the emulsion internal phase may be determined by the energy input during nebulization process. The emulsion particle size may greatly influence the final droplet size aerosolized. Also, it is important to determine whether the type of device chosen for aerosolization will be able to gently deliver the drug, without disrupting the emulsion formulation. In addition, the excipients and production method applied may influence the short and long-term emulsion formulation stability. In selecting the excipients, the scientist should strive to extend the drug release from the delivery system while being aware of possible toxic effects due to low clearance rates. Considering its physicochemical properties, the potential of farnesol as an anticancer agent to treat lung malignancies via inhalation may be improved with different formulation designs.

1.1.2.6. Paclitaxel

In the study of primary or metastatic lung tumors naturally occurring in dogs being treated with doxorubicin, a paclitaxel solution was also investigated.[80] The taxol (75 mg/mL) was dissolved in a mixture of polyethylene glycol 200 and ethyl alcohol.

Using the same drug deposition system and regimen, the doses ranging from 10 to 90 mg/m^2 were administered with no signs of systemic toxicity. As opposed to doxorubicin, local toxicity was not evidenced either. Out of 15 treated dogs, only one partial and one complete response were observed. The drug plasma levels after aerosolization for both doxorubicin and paclitaxel were less than one-tenth of plasma levels observed in normal dogs after intravenous injection of therapeutic range doses. However, the lack of information about the formulation characteristics makes it difficult task to speculate on the performance of this solution.

Drugs formulated within biodegradable polymers can present pharmacokinetic profiles with a delayed and/or extended release compared to the free drug. This sustained-release system can be controlled based on size and porosity of prepared spheres.[93] The feasibility of delivering anticancer agents within this type of dosage form has been investigated using paclitaxel.[94] Microspheres of the polymer poly-(L-glutamic acid) (PGA) were loaded with 20% (w/w) paclitaxel (PGA-PTX). For comparison purposes, 0.6% w/w paclitaxel was dissolved in cremophor, making a similar taxol solution to the commercially available product (Taxol®, Bristol-Myers Squibb). Aerosol output ratio tests demonstrated that PGA-PTX formulation was able to deliver 80-400 times faster than taxol solution. Although the drug was only deposited in mice lungs via intratracheal injection, the aerosol characteristics was evaluated when generated by a Salter Labs® 8900 jet nebulizer at 5 or 9 L/min. Using a 7-stage cascade impactor, the authors reported that approximately 50% (wt) of the aerosolized polymer formulation presented droplets with less than 5 μm. However, the amount of drug in each stage was measured by weighting the filters pre- and post-aerosolization instead of using an analytical method such as an UV spectrophotometer. Notably, this can render significant measurement errors. Firstly, the authors did not consider the differences in concentration from the taxol

solution (6 mg/mL) to the PGA-PTX formulation (not specifically mentioned, but ranging from 3 to 25 mg/mL). Secondly, the instrumental errors generated by the balance to measure formulation amounts in the milligrams were neglected. Therefore, the aerosol characteristics of this formulation are highly questionable. Nevertheless, the authors reported a concentration- and time-dependent *in vitro* cytotoxicity against H358 and H460 NSCLC cell lines. In addition, after single intratracheal administration, a MTD of 30 mg/kg (paclitaxel equivalents) was observed. Three weekly doses of taxol solution (2.5 mg/kg) or PGA-PTX (20 mg/kg paclitaxel equivalents) were both sufficient to significantly improve survival at about 135 days. Although the results may seem encouraging for further preclinical studies with pulmonary delivery of this formulation, the authors did not consider a potential accumulation of the polymers in the lungs. Due to a 10-fold greater dose of PGA-PTX needed to provide a similar survival as with the taxol solution, the dosage regimen outlines multiple administrations needed. Therefore, the PGA lung accumulation may be significantly high and could consequently compromise even more the pulmonary function of the lung cancer patients.

The pharmacokinetics and the therapeutic efficacy of a liposomal paclitaxel aerosol have also been investigated against pulmonary metastases in a murine renal carcinoma model. Since the excipients used are mainly surfactants naturally occurring in the lung fluid (e.g. phosphatidylcholine), liposomes present a relatively low local toxicity. Also, given their lipophilic nature, formulations of this type are able to encapsulate poorly-water soluble drugs.[95] Liposomes of paclitaxel (10 mg/mL) were composed of dilauroylphosphatidylcholine (DLPC) at drug-to-lipid ratio of 1:10 (w/w). Both components were prepared in t-butanol and subsequently lyophilized.[96] Prior to use, the formulation was reconstituted with sterile water and vortexed until homogeneously dispersed. With this method to produce liposomes, scaling up is feasible.

However, as there was no energy input to form the liposomes (e.g. high pressure homogenization), it is not surprising that particle size analysis revealed a wide size distribution (2.0 to 25.3 μm). An Aeromist® jet nebulizer generated aerosols with an MMAD and a GSD of 2.2 μm and 1.9, respectively, as measured using an Andersen Cascade Impactor at 10 L/min. Interestingly, the shear force applied by the jet nebulizer was able to disrupt the liposomes during the nebulization process. The particle size was reduced drastically to less than 0.4 μm. Despite that, the authors estimated the dose to be of 5 mg/kg by chamber aerosol exposure for pharmacokinetic studies. Compared to intravenous injection, the AUC in the aerosol treated group was 26-fold higher, with distribution half life of only 0.71 hours. Nevertheless, treatment 3 times a week over 2 weeks with paclitaxel-DLPC aerosolized liposomes, resulted in significant reduction in tumor number and an increased survival time compared to untreated and DLPC-only treated mice. These results were encouraging for further studies.

Paclitaxel-induced resistance is related to over expression of plasma membrane glycoprotein (P-gp), which acts as an efflux pump decreasing the intracellular drug concentration. Cyclosporin A (CsA) has the capacity of reversing this resistance, and, when co-administrated with paclitaxel, CsA also acts as an inhibitor of cytochrome P450-mediated metabolism (enzymes that are involved in the metabolism of this anticancer agent).[97] These findings and a dose-limiting toxicity not mentioned in the previous study prompted evaluation of the antitumor effect of co-administration of CsA and paclitaxel in the same animal model. Paclitaxel liposomes were prepared as mentioned above while CsA liposomes differed only by the drug to lipid ratio (1:7.5 w/w) and concentration (5 mg/mL). Similarly to the aerosol characteristics measurement in the study above, CsA-DLPC liposomes presented an MMAD of 1.6 μm and a GSD of 2.2. Chamber aerosol exposure provided an estimated dosage deposition of paclitaxel and

CsA liposomes to the lungs of 7.8 and 6.1 mg/kg, respectively. CsA/paclitaxel treated animals showed lung weights and tumor surface areas significantly lower than paclitaxel-only and untreated groups. Dose escalation of CsA has shown to be more effective to decrease area and number of tumors. However, the treatment (3 times per week for 2 weeks) had to be discontinued during toxicity studies due to expressive systemic toxicity (body weight loss).[98]

In terms of safety, the use of phospholipids as excipients to aid the drug delivery to the lungs is a viable option. In addition, they have shown to improve particle migration to the lung periphery owing to the reduction in surface tension provided by these surfactants.[40] In theory, this applies especially to poorly-water soluble drugs, such as the taxols. However, the encapsulation efficiency of any method to produce liposomes is an issue that should always be addressed. Previous studies have shown that, using the same process with similar phospholipids, somewhat low encapsulation efficiencies were achieved at a constant drug concentration (<45%).[99] When seeking for a controlled release, not only the encapsulation efficiency becomes important, but the selection of phospholipids may be crucial. Transition temperatures of phospholipids are highly dependent on the saturation and extension of the carbon chain.[100] For instance, DLPC (12 saturated carbons) presents a transition temperature of about -1 ºC. At the temperature of the human body, the fluid nature of this surfactant will promptly release the drug. On the other hand, dipalmitoylphosphatidylcholine (DPPC – 16 saturated carbons), with a transition temperature of approximately 41 ºC, may control the drug release for the encapsulated drug. In the study above, the lipophilic nature of paclitaxel together with the fluid-like characteristics of DLPC at body temperature justifies the low lung residence time.

After it has been shown *in vitro* that paclitaxel efficacy is more related to exposure time than to increased dose, a conjugation of paclitaxel with fullerene (C_{60}) was developed to sustain the release of the anticancer drug at the site of administration. Liposomes of paclitaxel-C_{60} conjugates have been formulated with DLPC similarly to the previous method. A mean diameter of 2.77 μm as measured by light scattering was determined for the fullerene-DLPC-paclitaxel liposomes. Cytotoxicity tests against A549 lung cancer cell lines have demonstrated IC_{50} values similar to those of DLPC-paclitaxel liposomes.[101] Impressively, aerosolization of this excipient to the lungs 3 hours per day for 10 consecutive days has presented minimal toxicity. Even so, lung half-lives for nano- and microparticles of C_{60} were 26 and 29 days, respectively.[102] These results hold promise of increasing exposure time of the anticancer agent at a tumor site, although safety studies are warranted. Pharmacokinetic and antitumor activity studies of C_{60}-paclitaxel are still being performed *in vivo* by the same group.

Conversely to previous studies of COX-2 inhibitors where docetaxel was studied along with aerosolized celecoxib, aerosolized docetaxel in conjunction with celecoxib has also been evaluated.[103] Considering the similarities in their physicochemical properties and formulation design, aerosolized docetaxel study will not be further discussed. The formulation and its characteristics are summarized in Table 2.

1.1.2.7. Camptothecins

Camptothecins are topoisomerase I inhibitor drugs that demonstrate significant toxicity, especially myelosuppression.[104] Camptothecin (CPT) and its likewise poorly-water soluble derivative, 9-nitrocamptothecin (9NC), also known as rubitecan, were some of the first anticancer drugs to be aerosolized to animal lungs. Similarly to liposomal paclitaxel, CPT (10 mg/mL) and 9NC (100 mg/mL) were prepared with DLPC and their

anticancer effect tested against human lung cancer xenografts in mice. Following lyophilization and reconstitution, an Aerotech II® nebulizer operating at 10 L/min aerosolized the formulation into a whole body exposure chamber. In this study, the formulations were characterized for liposome encapsulation efficiency by Percoll® gradient analysis. In summary, the studies demonstrated that an increase in drug concentration required a higher proportion of lipids for efficient drug incorporation. Rubitecan concentrations varying from 0.1 to 1.0 mg/mL, in the nebulizer reservoir, resulted in MMADs ranging from 0.8 to 1.6 μm. The encapsulation efficiency of 9NC and CPT liposomes at a drug to lipid ratio of 1:50 (w/w) and 0.5 mg/mL were approximately 80%. To achieve high encapsulation efficiency, the drug concentration was compromised and these formulations were chosen to evaluate their anticancer effect. The MMAD of the 9NC formulation was 1.2 μm. Significantly reduced tumor growth was shown in animals receiving an estimated 9NC dosage of 76.7 μg/kg/day, 5 days per week for 35 days. CPT treated animals also presented decrease in tumor volume, although 9NC was more effective. Similarly to the liposomal paclitaxel formulation, a shear effect promoted a higher than 6-fold decrease in mean size of liposome after nebulization process. Nevertheless, this study also demonstrated that aerosol exposure of 9NC liposomes were more effective to reduce tumor growth than by oral administration. This is a significant indication that the drug absorbed following oral administration, due to mice grooming has very little antitumor effect on lung carcinomas.[105] Finally, evaluation of the effect of delivery route using nose-only aerosol exposure or intramuscular administration indicated that the latter showed a significant decrease in tumor volume compared to untreated animals, however this was not as nearly effective as with nose-only aerosol exposure. Delivering the drug directly to the lungs has been shown therefore to be essential for the effective reduction in the tumor growth. No

myelosuppression signs were observed in this study, and 9NC liposomes have also been shown to be effective against murine melanoma and human osteosarcoma pulmonary metastases in mice.[106]

Following this study, the authors reported the pharmacokinetics of CPT in mice after liposomal aerosol inhalation. The formulation containing CPT (0.5 mg/mL) to DLPC ratio of 1:50 (w/w) presented an MMAD of 1.6 μm and a GSD of 2.1, as measured using an Andersen Cascade Impactor. The same device model used previously aerosolized an estimated dose of 80.9 μg/kg after 30 minutes of nebulization. CPT concentrations in the lungs after aerosolization using either nose-only or whole body exposure chambers were up to 16-fold greater than that found in the blood. Intramuscular solution injection (233 μg/kg) provided only trace amounts of CPT that could be detected in the lungs, even 2 hours after administration when 80% of the drug had been released from the site of injection. The authors compared this aerosolization study with previous reports of camptothecin concentration in the lungs after oral, intravenous and intramuscular administration. Aerosol treated mice in 50-fold lower concentrations presented 7 to 10-fold higher concentrations in the lungs after 30 minutes of exposure, compared to the other routes of administration.[47] As discussed earlier, the doses reported may be the best estimation possible rather than an accurate measurement. Despite this, subacute toxicity of the 9NC liposome aerosol in beagle dogs was not observed after an estimated aerosol dose of 24.7 μg/kg/day, 5 days per week, for 8 weeks.[107] DLPC-only liposomes were determined to be non-toxic as well. Following these results, a phase I study has shown that advanced pulmonary malignancy patients tolerated this treatment well in doses of 13.3 μg/kg/day, 5 days per week for an 8 week period.[108] However, the aerodynamic characteristics of the formulation were not reported in this case. Nevertheless, the doses were administered by a mouth breathing-

only face mask with a HEPA-filtered airborne scavenging tent covering the patient and nebulization system, to protect the health care professional. Finally, the authors recommended the aforementioned dosage regimen for phase II studies, which have not yet been reported.

Rubitecan liposomes of soybean lecithin and cholesterol were also formulated for different studies: *in vitro* release, biodistribution in mice and local toxicity in rats.[109] The thin-film hydration method was used, followed by filtration (0.45 μm) prior to lyophilization. The liposomes presented Z-averages of less than 200 nm as measured by dynamic light scattering. For the *in vivo* studies, a 9NC solution (0.25 mg/mL) was prepared in dimethyl sulfoxide (DMSO)/PEG400 mixture for comparison purposes. Although the authors failed to report the drug concentration and drug-to-lipid ratio of the liposomes, which limits the discussion herein, entrapment efficiencies greater than 90% were obtained before and after freeze-drying, as measured by centrifugation method. The sustained release properties of the formulation were also verified. Using the dialysis method, the drug release from the liposomes was 32.5% in 1 hour and approximately 90% after 24 hours. Following intratracheal administration of 0.8 mg/kg, the biodistribution study in mice showed that the mean lung residence time of 9NC liposomes and solution was 1.24 and 0.37 hours, respectively. In addition, the sustained release formulation presented an AUC in the lungs 3.4-fold higher than 9NC solution, and 4.73 times when compared to that of an intravenous administration. Finally, intratracheal instillation of rubitecan liposomes demonstrated lower toxicity than the solution dosage form, as investigated by histological studies in rats. These results illustrate that the use of soybean lecithin and cholesterol may be a feasible option to improve lung residence time of anticancer drugs. Yet, aerodynamic characterization of

the nebulizer-formulation system followed by further preclinical studies is still needed to evaluate the potential of delivering this formulation to human lungs.[109]

1.1.2.8. Cisplatin

Platinum derivatives, such as cisplatin and carboplatin, are the most traditional drugs used for the treatment of lung malignancies. Sustained Release Lipid Inhalation Targeting (SLIT) Cisplatin has been investigated in a phase I study of aerosol dosage form for the treatment of primary and metastatic lung cancers. Liposomes of cisplatin (1 mg/mL) were composed of DPPC and cholesterol at drug to lipid ratios of 1:16 and 1:7.5 (w/w), respectively. Sodium chloride was present as iso-osmotic agent and to enhance the stability of cisplatin. The PARI LC Star® nebulizer generated aerosols at 15 L/min with an MMAD of 3.7 μm and a GSD of 1.9, as measured using a Next Generation Impactor (NGI) at 5 ºC and 15 L/min. The impactor refrigeration increases the relative humidity in the inner environment of the NGI to close to 100%, diminishing droplet evaporation prior to impaction.[110] In this study, the dose limiting toxicity (DLT) could not be reached after dose escalation using different strategies: increasing dose level, reducing interval between cycles, increasing number of nebulization sessions per day, and increasing amount of drug inhaled (by flow rate increment of the compressor). Although the liposome size distribution was not reported, the authors evaluated the dispersion stability under nebulization. Approximately 40-50% of total cisplatin is released from the liposomes during the aerosolization process. In this case, the cisplatin liposome structure is being partially disrupted due to the shear force generated by the jet nebulizer, as discussed earlier. Considering the physicochemical properties of cisplatin (water soluble and negative log P), one would expect a relatively slow systemic absorption of the free drug over time. With that, the supposed liposome capacity of slowly releasing the drug

may be confounded with the intrinsic characteristics of the antineoplastic agent. In addition, considering that the liposomes are not cleared by macrophages, it is uncertain whether any therapeutic effect may be elicited by the drug that remains encapsulated after deposited in the lungs. On the other hand, the liposomes may possibly be engulfed by the pulmonary macrophages, resulting in no systemic exposure of the anticancer agent, but no therapeutic efficacy either. Nonetheless, stabilization of the disease in 12 out of 17 patients was the best overall response with this treatment.[111] As with doxorubicin treatment, long administration times were required for inhalational cisplatin therapy, which could reduce patient compliance. This may then impose an alternative criterion, as opposed to local and/or systemic toxicity endpoints. On the other hand, defining a tolerable administration time will certainly restrict high dose requirements for some antineoplastic drugs. Finally, the authors reported their intention to pursue further studies to define DLT with a higher cisplatin concentration in the liposomes (3 mg/mL) as an alternative strategy. Lately, a phase Ib/IIa study was published with relapsed/progressive osteosarcoma metastatic patients. No systemic, but only minor local toxicity was observed. The drug was well tolerated by heavily pre-treated patients with one year cumulative doses of up to 1020 mg. After the same time period, 2 out of 14 patients remained pulmonary disease free.[112] The DLT of this formulation is yet to be accurately determined. Furthermore and despite these encouraging results, the effectiveness of this formulation is still to be proven throughout the upcoming phases of the pharmaceutical product development process.

1.1.2.9. 5-Fluoruracil

The neoplastic agent 5-Fluorouracil (5-FU) has long been used for cancer treatment, although not the first line drug to treat lung malignancies. Liposomes,

microspheres and Lipid Coated Nanoparticles (LNP) of 5-FU have been prepared to investigate their sustained-release properties, as measured by microdialysis.[113] Lipid coated nanoparticles consist of a drug-loaded core coated by a lipid shell; the dosage form is dispersed in water in the presence of a surfactant. The submicronized hydrophilic core can contain either the drug alone or in combination with other excipients.

Firstly, DPPC and hydrogenated soy phosphatidylcholine (HSPC) liposomes were prepared by the thin film hydration method, and cholesterol was included to further sustain the drug release. Also evaluated was whether the presence of negatively charged lipids in some formulations, such as dipalmitoyl phosphatidic acid (DPPA) and dipalmitoyl phosphatidylglycerol (DPPG), would promote physical stability by inhibiting liposome aggregation and fusion. Extruded liposomes with vesicle diameter of approximately 0.5 μm presented a higher release constant from a first-order release model than nonextruded liposomes. The presence of DPPA was effective in decreasing the release rate of extruded liposomes, whilst it was not able to provide the same effect in nonextruded preparations. Among the various liposome formulations studied, drug loading was not higher than 7% w/w (measured by centrifugation method) and the drug release was extended to about 8 hours. Based on these results and considering the drug lipophilicity, the authors estimate drug administration three or four times daily by inhalation, deeming this formulation ineligible for sustained-release purposes.

In this same study, polymeric microspheres were formulated by spray drying different proportions of the following copolymers: poly-(lactide-co-glycolide) (PLGA), poly-(lactide-co-caprolactone) (PLCL) and poly-(lactide) (PLA). In this study the drug loading was approximately 8% w/w and the particle size, characterized by light scattering of the drug in suspension, was 1.2 to 1.5 μm. Based on microdialysis measurements of 5-FU, a release constant was calculated from a first order release model. The drug released

in 24 hours was about 70 to 90% of the loaded dose. The results also demonstrated that an increase in the lactide moiety of the polymer progressively decreased the 5-FU release from the microspheres. Microspheres of 5-FU within PLA presented the longest duration of release (>32 hours). Importantly, the low 5-FU loading capacity (8% w/w) of this dosage form would require a high amount of polymer to be deposited into the lungs of cancer patients, especially following repeated administrations. The complete degradation time of PLA and PLGA polymers have been reported to be relatively high for this application.[114] Therefore, unknown toxicity and respiratory function-related consequences, due to cumulative deposition of these polymers in the lungs, has thus far prevented further development for the delivery of 5-FU microspheres to the lung.

Finally, LNPs of 5-FU were prepared by spray drying the drug with poly-(glutamic acid), poly-lysine, or lactose to form the dosage form core. These cores were further spray dried with various combinations of lipids (tripalmitin, tristearin, cetyl alcohol, and stearyl alcohol) to form an outer shell. The drug, released over 24 hours, was about 70 to 90% of the loaded dose for the different formulations studied, with core and total LNP diameters of 500 and 1000 nm, respectively. Based on the release constants, the most appropriate combination of core and shell materials for sustained-release aerosolization formulation was poly-(glutamic acid):5-FU (4:1), and tripalmitin:cetyl alcohol (2:1). The predominance of naturally occurring surfactants (e.g. triglycerides) in this dosage form alleviates the concern about low lung clearance rates of polymers. Thus, although it presented as low drug loading as microspheres (5% w/w), the LNPs of 5-FU were chosen to be further studied by the authors. The myelosuppression and bone marrow toxicity caused by 5-FU is expected to be overcome by inhalation delivery of this anticancer agent loaded with LNPs (5-FU LNP). Also, a low release rate of this dosage form would provide a sustained-release delivery system for aerosolized drugs.[113]

Following this, investigation of influence of core diameter and lipid shell thickness suggested the latter to be the rate limiting step for the release of 5-FU. Based on this, the authors have developed a release model from polydispersed cores and shells consisting of a sequential zero-order/first-order kinetics. Accordingly, a delivery system consisting of 600 nm diameter poly-(glutamic acid):5-FU (4:1) cores and 200 nm thick tripalmitin:cetyl alcohol (2:1) shells was chosen for *in vivo* studies in hamsters. The particle size of this formulation measured by dynamic light scattering was 1.02 ± 0.26 μm. From a diluted dispersion, an ultrasonic nebulizer (model not specified) generated aerosol droplets that were subsequently dried to the drug particle unit (reflux drying process). The formulation aerodynamic properties were then measured using an Andersen cascade impactor (airflow not reported). The MMAD was 1.15 μm with a GSD of 2.15 and neither the reflux drying process nor the ultrasonic nebulization demonstrated an influence on the release rate. Hamsters in whole body aerosol exposure units presented estimated drug deposition in the lungs as high as 3.4 ± 0.3%, based on nebulizer output rate and respiratory minute volume.[115]

Next, fluorescein isothiocyanate dextran (FITC-dextran) was added to the formulation and hamsters were exposed to a nose only aerosol chamber for an eight-component pharmacokinetic modeling study. Separate HPLC analysis of FITC-dextran and 5-FU ensured distinction of entrapped and released 5-FU. LNPs demonstrated a 5-FU peak concentration of 0.13 μg/g at 1.02 hours. In addition, the half-life of LNPs in the lungs was 4.95 ± 0.38 hours with an almost complete clearance in 24 hours. Using pharmacokinetic modeling, the authors estimated that the effective dose (0.065 to 0.13 μg/g, for DNA synthesis inhibition) would be maintained for up to 5.4 hours. The pharmacokinetic model used also predicted that, using this route of administration, lung levels would be 5.5 times higher than the systemic circulation.[116] In their conclusion,

the authors discuss that, when considering greater than 20% drug deposition (which can easily be achieved by modern medical aerosol devices) doses of about 100 mg can be translated to humans.

This thorough 5-fluorouracil formulation study is a great illustration of how the dosage form may potentially improve the drug delivery to the lungs. Selection of excipients combined to careful assessment of drug characteristics and, consequently, well elaborated formulations are crucial to achieve performances that will indeed explore the full antineoplastic potential of each drug. However, further studies are warranted to confirm these predicted pharmacokinetic modeling data.

1.1.3. Conclusions

Lately, there has been a shortage in new drug discovery to aid more effective treatment for pulmonary malignancies, which has translated into a poor prognosis for lung cancer patients. Inhalation chemotherapy can noticeably target the disease site to treat lung malignancies. By delivering appropriate chemotherapeutic agents to the specific disease site, at the proper dose, at a convenient and appropriate interval may lead to better patient outcomes.

Clinical studies have shown improved drug tolerability via pulmonary administration, consequently enabling higher MTDs to be achieved. Despite that, oncologists may decide to insist on continuing systemic chemotherapy due to the high dissemination profile of lung cancer. For this reason, improvements in the early diagnosis of the disease are highly desirable for the potential success of aerosol delivery of anticancer agents. To date, the results from the early clinical development with inhaled chemotherapeutics have not yet justified the choice of this type of therapy over systemic administration. Notably, this is in part due to the nature of patient selection in these early

phase clinical trials, where extensive disease patients that in general had previously failed treatments with similar compounds were enrolled. In addition, significant issues remain to be understood in order to facilitate properly designed aerosol formulations of anticancer agents:

A. The traditional MTD methods clinically used may not be adequate to establish the required lung dose of inhaled chemotherapeutics. For instance, pulmonary toxicity may be confounded by disease progression. In addition, lung doses that require unreasonably long administration times may be considered "no-go" during early phases of pharmaceutical development;
B. An appropriate parameter to correlate a pharmacokinetic profile and a pharmacodynamic response is yet to be determined (e.g. peak levels in the lungs, AUC or alternatively a minimum lung concentration akin to an IC_{50});
C. Obstacles to drug penetration in solid tumors following pulmonary administration may impose significant barriers to treatment efficacy. For instance, the delivery of drug nanoparticles to the tumor vicinity may not be as effective as the beneficial EPR effect achieved when nanoparticles are systemically administered. Also, other characteristics of the particles, such as charge and shape, may also affect tumor penetration. If tumor penetration cannot be surpassed, neoadjuvant therapy may still benefit from inhalation chemotherapy, as well as the treatment of more diffuse forms of cancer, such as bronchoalveolar carcinoma;
D. Targeting the aerosol delivery site within the respiratory system may impose increased complexity. As the aerodynamic particle size predominantly determines drug deposition, tumors located anywhere from the trachea/main bronchus to peripheral lung regions will require different challenges. The capacity to deliver the formulation to peripheral lung regions occupied by the disease is a different

challenge than that of avoiding the mucociliary clearance of particles when targeting tumors close to the trachea;

E. An antineoplastic agent suitable for pulmonary delivery may need to be selected based on proper physicochemical properties (e.g. solubility, log P), and pharmacodynamic characteristics (e.g. required lung dose, sensitivity of cancer cells to drug, etc.). A balance of these factors may be added to the right choice of device and excipients used in the formulation to provide the proper pharmacokinetic profile (e.g. lung levels, pulmonary drug clearance, etc.) and therefore to achieve the desirable therapeutic efficacy.

Even with these challenges, the formulation development of inhaled anticancer agents appears to be an exciting and emergent field that must be further and more extensively explored. As shown in this review paper, many dosage forms have been studied for the delivery of anticancer agents using pulmonary administration. Despite these attempts, in our opinion, the results are unsatisfying from a formulation standpoint. Before considering preclinical and clinical trials, a formulation scientist, as part of a multi-disciplinary team must consider the different formulation designs applied to the different routes of administration; each one with its own idiosyncrasies. In the same way that an oral formulation is not likely to be intravenously administered, a pulmonary dosage form should not be based on formulations for other routes of administration. An ideal dosage form depends highly on the physicochemical properties of the drug and the method of aerosolization that will be used. In addition, safety, tolerability and clearance of the excipients chosen must be considered. Therefore, the formulation for each antineoplastic agent should be carefully designed according to these aspects. Consequently, inappropriate or incomplete characterization of aerosolization performance

can mislead the results from inhalation chemotherapy studies. As a result, the formulation must be thoroughly characterized in order to ensure the expected dose is delivered to the lungs. Without considering the full aspects of formulation design and characterization, any conclusions made about the future of inhalation therapy are deprived of the potential that this type of therapy may render to treat lung malignancies.

1.2. INFLUENCE OF PARTICLE SIZE ON REGIONAL LUNG DEPOSITION – WHAT EVIDENCE IS THERE?

Abstract

The understanding of deposition of particles in the respiratory tract is of great value to risk assessment of inhalation toxicology and to improve efficiency in drug delivery of inhalation therapies. There are three main basic mechanisms of particle deposition based primarily on particle size: inertial impaction, sedimentation and diffusion. The regional deposition in the lungs can be evaluated in regards to the aerodynamic particle size, in which particle density plays a significant role. In this part of the review, we first introduce the available imaging techniques to confirm regional deposition of particles in the human respiratory tract, such as planar scintigraphy, single photon emission computed tomography (SPECT) and positron emission tomography (PET). These technologies have widely advanced and consequently benefited the understanding of deposition pattern, although there is a lack of lung dosimetry techniques to evaluate the deposition of nanoparticles. Subsequently, we present a comprehensive review summarizing the evidence available in the literature that confirms the deposition of smaller particles in the smaller airways as opposed to the larger airways.

1.2.1. Introduction

Particles are deposited in the respiratory tract when they are removed in a definitive fashion from the flow streamline generated by the breathing maneuver. Understanding this process and the factors influencing particles settlement in the surface of specific regions of the airway tree has implications to the development of

pharmaceutical inhalation products for aerosol therapy and to risk assessment of air pollutants that concerns toxicology.

Besides pulmonary physiology of patients (e.g. breathing pattern and lung geometry), particle deposition is also known to be influenced by aerosol characteristics.[117, 118] Namely, the physicochemical properties of inhaled aerosols that can determine deposition are: size, size distribution, shape, charge, density and hygroscopicity.[119] In the field of aerosol medicine, particle size is a formulation design variable that can be engineered accordingly, aiming the development of pulmonary drug delivery systems.[35, 120] As we can examine from the mechanisms of deposition, particle diameter is the primary factor determining pulmonary deposition of aerosols in the various regions of the respiratory tract. Ultimately, inspiratory flow rate also plays an important role in the particle deposition following pulmonary administration.[121]

In this section, the evidence available in the literature to confirm that smaller particles delivered to the lungs are deposited in the smaller airways as opposed to the larger airways is summarized (Figure 1.1). So, the mechanisms of particle deposition and the relevance of particle aerodynamic diameter for regional lung deposition are firstly presented. Following the description of particle deposition, experimental techniques that can be used to confirm regional deposition of particles in the respiratory tract are highlighted. Our focus herein is on evidence of deposition patterns applied to inhalation therapies in humans, based on available data about particle aerodynamic size.

1.2.2. Mechanisms of Particle Deposition

There are five different mechanisms by which particle deposition can occur in the lungs: inertial impaction, sedimentation, diffusion, interception, and electrostatic precipitation. The two latter mechanisms are related, respectively, to particle shape (e.g.

elongated particles) and electrostatic charges; and have been reviewed in detail elsewhere.[117, 118] The mechanisms of deposition directly (or inversely) related to particle size are presented in Figure 1.2.

1.2.2.1. Inertial Impaction

Inertial impaction occurs when airborne particles possess enough momentum to keep its trajectory despite changes in direction of the air stream, consequently colliding with the walls of the respiratory tract. The chances of deposition by impact are increased when the particles are more likely to travel longer distances, *S*, which is based on the particle mobility (velocity per unit force), *B*, mass, *m*, and velocity, *v*, according to Equation 1.1:[117]

$$S = B \cdot m \cdot v \qquad \text{(Equation 1.1)}$$

The dimensionless Stokes' number, *Stk*, more specifically describes the probability of particle deposition in the airways via impaction. The higher the Stokes' number, the more readily particles will be deposited by inertial impaction, according to Equation 1.2:

$$Stk = \frac{\rho_p \cdot d^2 \cdot V}{18 \cdot \eta \cdot R} \qquad \text{(Equation 1.2)}$$

Where ρ_p is the particle density, d is the particle diameter, V is the air velocity, η is the air viscosity and R is the airway radius. Therefore, considering the bifurcated architecture of the lungs, large particles travelling through the airways at high airflow

velocity are more likely to impact in the proximal portion of the respiratory tract (upper airways).[118]

1.2.2.2. Sedimentation

Sedimentation is a time-dependent process in which particles settle due to the influence of gravity. Hence, breathing maneuvers in which more time is allowed for the particles to sediment (e.g. breath-holding) may increase lung deposition.[118] The Stokes' Law assumes that the relative velocity between the surface of the particle and the airstream is null. Considering unit density spheres of 1 to 40 μm, Stokes' law can be used to predict the terminal settling velocity, V_{ts}, according to Equation 1.3:

$$V_{ts} = \frac{(\rho_p - \rho_a) \cdot d^2 \cdot g}{18 \cdot \eta} \qquad \text{(Equation 1.3)}$$

Where ρ_a is the density of air ($\rho_p > \rho_a$) and g is the gravitational acceleration.[117] However, for particles smaller than 10 μm, a slip correction factor (C_c) derived by Cunningham should be applied to Stokes' law, as described in Equation 1.4:[122]

$$C_c = 1 + K_n \cdot \left(A_1 + A_2^{-A_3/K_n}\right) \qquad \text{(Equation 1.4)}$$

Where K_n is the Knudsen Number, and A_1, A_2 and A_3 are constants. The size-dependence of this equation is related to the balance between the downward force exerted by the particle and the resistant force for which Stokes' law is valid. With increased air flow, the stream becomes turbulent and the deposition by impaction increases.[118] Therefore, this equation assumes laminar flow within the airways, as defined by the Reynolds number, Re (Equation 1.5).

$$R_e = \frac{\rho_a \cdot V \cdot d}{\eta} \qquad \text{(Equation 1.5)}$$

Interestingly, the effect of gravity on particle sedimentation has recently been evaluated by the National Aeronautics and Space Administration (NASA). Inhalation of lunar dust is a concern for potential toxicological effects to future explorers of the moon.[123] Six healthy subjects were administered aerosols with particle diameters of 0.5 and 1.0 μm on the ground (1 g) and during short periods of lunar gravity (1/6 *g*). In this study, the researchers found that, although the deposition of fine particles is greater on earth, peripheral deposition was improved at low gravity for those particles that are actually deposited in the lunar environment.

1.2.2.3. Diffusion

Diffusion occurs when particles are sufficiently small to undergo a random motion due to molecular bombardment. This process, also known as Brownian motion, is correlated to particle size, according to Stokes-Einstein equation (Equation 1.6):[117]

$$Dif = \frac{k \cdot T}{3\pi \cdot \eta \cdot d} \qquad \text{(Equation 1.6)}$$

Where *Dif* is the diffusion coefficient, *k* is the Boltzmann's constant and *T* is the absolute temperature. Different from impaction and sedimentation mechanisms, diffusional deposition is therefore inversely related to particle size.

1.2.3. Particle Aerodynamic Diameter

Aerosols for inhalation vary not only on geometric particle size and size distribution, but in a number of other factors that influence particle deposition: physical state (liquid or solid), density, shape and velocity. In addition, a dynamic system of forces is interacting with the airborne particles throughout the airways, namely: gravity, resistant force of the inspiratory air and inertial force. The balance between these forces and the aerosol properties ultimately determines the mechanism of particle deposition in the lungs.[39]

The aerodynamic diameter, d_{ae}, is, by definition, the diameter of a sphere with unit density ($\rho = 1$), having the same terminal settling velocity in still air as the particle in consideration.[39] Considering the particle characteristics, this independent variable can therefore correlate the effect of geometric diameter and particle density, as described in Equation 1.7:

$$d_{ae} = d \cdot \sqrt{\frac{\rho}{\rho_0}} \qquad \text{(Equation 1.7)}$$

Where d is the actual diameter of the sphere, ρ is the spherical particle density and ρ_0 is unit density. For non-spherical particles, which are more prone to deposition via interception, the particle shape also influences the aerodynamic diameter and therefore correction for shape factors is applied.[117, 118]

The relationship between the geometric diameter and the particle density for aerodynamic diameter is illustrated by a study of large porous particles for pulmonary delivery.[124] In this investigation, Edwards *et al.*. have effectively delivered very light weight large particles (ρ = 0.1 g/cm^3; d = 8.5 μm) to the deep lung. Therefore, aerodynamic diameter, as opposed to geometric diameter, must be used as independent

variable to relate to particle deposition governed primarily by inertial impaction.[33] *In vitro* determination of the aerodynamic size of inhalation products can be performed using cascade impactors, including: the Andersen Cascade Impactor, Multi-Stage Liquid Impinger, and the Next Generation Cascade Impactor.[39] This characterization is essential to evaluate the particle deposition in the lungs. Usually, the mass median aerodynamic diameter (MMAD) and the geometric standard deviation (GSD) are reported. MMAD is the cut off particle size in which 50% of the mass of the aerosol is smaller and the other 50% is larger than the referred parameter.[125] MMAD is a measure of central tendency while GSD indicates the magnitude of dispersity from the MMAD value.[126]

During the inhalation process of pharmaceutical products, a specific device is positioned in the mouth of the patients and the drug particles are aerosolized. These particles travel throughout the airways with a number of factors determining its deposition in the respiratory tract, which can be anywhere from the oral cavity to the alveoli. There are a number of mathematical models and computational tools available in the literature that aids in predicting the deposition patterns of particles in the whole lung and in its specific regions, even considering different disease states. These topics have recently been reviewed and beyond the scope of this review.[127-130]

1.2.4. Assessment of Regional Lung Deposition

An overview of the commonly used techniques is presented in Figure 1.3. There are two basic methods to identify drug deposition in the lungs following inhalation: pharmacokinetic methods and gamma-scintigraphy techniques.[44] The former one can only provide information about total lung dose, based on plasma concentrations and/or urinary recovery.[45, 131] On the other hand, besides quantifying total lung deposition,

radionuclide imaging (or gamma-scintigraphy) is the primary technology used to differentiate between depositions into different zones of human lungs.[132] This *in vivo* imaging technology is greatly valued due to its ability to provide visual confirmation (and therefore convincing evidence) that the dosage form is functioning in the way it is designed to, by demonstrating that the drug particles are being deposited into the lungs following inhalation. Initially, two-dimensional gamma-scintigraphy was used as imaging technique for delivery of inhaled drugs. Lately, tridimensional imaging technologies have been applied for more accurate particle deposition in the human respiratory tract, including Single Photon Emission Computed Tomography (SPECT) and Positron Emission Tomography (PET). More recently, a new experimental technique based on Magnetic Resonance Imaging (MRI) has been published and is herein discussed briefly.

1.2.4.1. Two-Dimensional Gamma Scintigraphy

This planar imaging technique has been extensively used to assess the delivery efficiency of inhaled drugs,[133, 134] in which deposition patterns can be determined for different formulations and devices used for pulmonary administration. Usually, the radiolabelling process involves adsorbing the imaging agent to the surface of the drug particle[135] or adding the radionuclide to the nebulizer solution.[136, 137] The radionuclide Technetium-99m (^{99m}Tc, half life of 6 hours) has been widely utilized as radiolabelling agent for imaging of structure and function of different organs.[138] Other radionuclides include Indium-111 (^{111}In), Iodine-123 (^{123}I), and Gallium-67 (^{67}Ga).[139] Mucociliary clearance, coughing and rapid permeability of the tracer through the airways limit the process to a short period of time when evaluating particle deposition patterns.[45] Despite this, accurate quantification of particle deposition in the lungs can be obtained, as long as drug and radionuclide distributions for comparative particle size

ranges are equivalent and the radiolabelling process does not affect the particle size distribution of the drug.[140]

Gamma scintigraphy operates with either a single-headed or dual-headed gamma camera positioned to take static images. When fitted into a two-dimensional perspective these images can provide information about the distribution of the radiolabelling agent in the organ of interest.[141] To determine the specific region at which particles are deposited onto the lung using gamma scintigraphic methods, it is common practice to spatially divide the lungs into sections of interest (e.g. central, intermediate and peripheral) using computer tools. Based on the regions of interest, the Peripheral to Central (P/C) ratio (or, inversely, the Central to Peripheral C/P ratio) of particle deposition is widely used as planar index.[45, 139] In this image division, the peripheral zone refers mainly to the small airways (≤ 2 mm) while the central portion of the lung represents the larger airways. Hence, the P/C ratio correlates to the proportion of drug particles deposited in the respiratory bronchiole/alveolar region as compared to tracheobronchial regions of the lung.

One of the main drawbacks of the planar scintigraphy though is the projection of the (three-dimensional) lung structure into a two-dimensional image. Relative particle deposition at different plane levels of the lungs may obscure the real deposition pattern when using this technique. Consequently, the lack of three-dimensional resolution can cause overestimation of deposition due to overlapping airways. Based on a coronal position image, this effect is considerably higher in the hilar region and gradually decreases towards the small airways in the periphery. Hence, it has been highly recommended to correct for attenuation of the radioactivity in the chest wall.[121, 142] To overcome this issue, SPECT and PET provide information about three-dimensional intrapulmonary deposition pattern that can reduce this source of error.

1.2.4.2. Single Photon Emission Computed Tomography (SPECT)

With the gamma camera rotating through 360º, SPECT provides three-dimensional image of the lungs.[45] Similar to gamma scintigraphy, the single-headed cameras rotate around the chest of the patient laid in supine position. However, with single detector cameras the scanning time can be unacceptably long (e.g. greater than 15 min), since relative quantification can be erroneous due to significant absorption, mucociliary clearance (1 mm/min), or cough.[143, 144] For this reason, twin-headed or even triple-headed cameras have been used to boost analysis efficiency.

Using the same radiolabelling method as in gamma scintigraphy, the obtained scans can be used to reconstruct the three-dimensional distribution of the particles in the lungs using an algorithm.[139] SPECT can then be used to determine regional lung deposition by differentiating between small and large airways.[145] As opposed to planar sections (based on pixels), the lung structure can be divided into volumes of interest, also known as voxels. For instance, in one of these techniques, the airway tree is arbitrarily divided into lung layers in the shape of concentric "shells" with the main bronchial bifurcation as the reference point.[146, 147] Based on gamma camera counts, these shells are further converted into spatial distributions that can consequently be used in the definition of Penetration Index (PI = P/C or C/P ratio). Given the arbitrary definition of this index established according to the research group, they should be analyzed on a case-by-case basis.

More recently, the development of 3D *in silico* models that can be superimposed on laboratory images of SPECT and PET may improve the interpretation of regional particle deposition in the lungs from clinical data.[148, 149] In this manner, the individual anatomy is preserved and, based on the airway dimensions of a lung model;

the airway generation contribution to each shell can be detailed. Unquestionably, such 3D *in silico* model is a powerful tool to better elucidate regional particle deposition patterns in the airways.

1.2.4.3. Positron Emission Tomography (PET)

While in SPECT the formulation is radiolabelled with surrogate markers like ^{99m}Tc, PET incorporates positron emitters such as Carbon-11 (^{11}C) and Fludeoxyglucose (^{18}F) into the drug molecule.[45, 139, 150] Although the radiolabelling method in PET is considerably more elaborated, some drugs have been used for PET studies as aerosols, including: ^{11}C-triamcinolone,[151] ^{11}C-formoterol,[152] ^{18}F-insulin,[153] ^{124}I-insulin, and ^{125}I-insulin.[154] Alternatively, the lung physiology can be studied by using aerosols of ^{18}F-Fluorodeoxyglucose (FDG).[155] The need to formulate the radiolabelled drug into an inhaled dosage form (e.g. dry powder) and further load it into the respective delivery device (e.g. dry powder inhaler) requires consideration of the isotope decay from the time the radiolabelling process is finished. This procedure can be very challenging when considering the short half lives of these radionuclides: 20 min for ^{11}C and 110 min for ^{18}F.[156]

In studying pulmonary deposition based on particle size, changes in the physicochemical properties of the particles due to the addition or incorporation of the radionuclide into the drug molecule or formulation may occur. Therefore, a verification that the particle size distribution after introduction of the tracer into the formulation has not changed significantly is required.[147] For instance, an investigation of budesonide delivered with pressurized Metered Dose Inhaler (pMDI), pMDI with Nebuhaler®, a large volume spacer, and Turbuhaler®, a dry powder inhaler (DPI) in eight asthmatic patients using gamma scintigraphy showed a P/C ratio of 1.24, 1.22 and 0.64, respectively.[157]

Despite the increased peripheral deposition of the pMDI device, however, the incorporation of ^{99m}Tc tracer to the formulation did not present similar sizes before and after the radiolabelling process. In this case, underestimation of particle deposition may have occurred.

1.2.4.4. Magnetic Resonance Imaging (MRI)

More recently, a MRI method of measuring regional lung deposition has been published based on superparamagnetic iron oxide nanoparticles.[158] The feasibility of this method was demonstrated in a study where mice were administered colloidal suspensions of the nanoparticles via a nose-only inhalation chamber. The MMAD of the aerosol droplets formed using a Pari LC Star® jet nebulizer was 5.6 ± 0.8 μm, with a geometric standard deviation (GSD) of 1.30 ± 0.03 (n=6), as measured by time-of-flight technique.[159] The longitudinal relaxation time of 12 axial slices of the lungs was analyzed using MRI and subsequently converted to iron concentration. The methodology showed potential for analysis of regional lung deposition, resulting in greater concentration of iron in central regions of the mice lungs. This is an expected result, based on MMAD value, as it is discussed in more details in the next section. As such, this technique has a potential as an alternative for scintigraphic methods for determining deposition patterns in the various regions of the lungs. Additionally, this experimental technique also shows considerable promise for evaluation of magnetic-based formulations for pulmonary drug delivery, in which particles are already loaded with iron oxide.[160]

1.2.5. Particle Deposition in the Lungs

Stahlhofen and coworkers have previously studied the effect of particle size on lung deposition in a systematic experimental design with subjects inhaling monodisperse aerosols during tidal breathing.[161] With a tube inserted into the mouth, the oropharyngeal (mouth and throat) deposition for particles greater than 10 μm was more than 90% and 50% at 60 and 18 L/min, respectively. In their study, the smaller airways were differentiated by the larger airways according to the time of particle clearance from the lungs based on scintigraphic methods. A "fast-cleared" fraction was correlated to lung deposition at the tracheobronchial region (or larger airways), attributed to the known mechanism of mucociliary clearance in this area. Alternatively, a "slow-cleared" fraction was correlated to the absence of cilia in the terminal portion of the airway, indicating deposition in the lower airways and an expected particle clearance at approximately one day. By subtracting the slow-cleared fraction observed after a period of about 24 hours from the initial total lung dose, the regional deposition of particles is determined.[162] According to this experimental design and with particle aerodynamic diameter measured at an airflow rate of 30 L/min, it was found by Stahlhofen *et al.,* that particles of approximately 6 and 3 μm are deposited predominantly in the larger and smaller airways, respectively. Notably a high intersubject variability was observed.[161] These results are in agreement with the particular mechanisms of deposition: inertial impaction and sedimentation. Interestingly, it was also found in this study that as particle sizes decrease to submicron dimensions the total lung deposition also decreased. With further decrease in particle size into the nanometric scale, the total lung deposition increased back to levels equivalent or greater than micronized particles[163] This minimum of total lung deposition may be attributed to a crossover between predominance of diffusion versus impaction/sedimentation mechanisms based on their particle sizes.[162]

Similar studies in terms of experimental design are reported in the literature.[164] However, there is evidence supporting that some particles depositing in the tracheobronchial region are actually cleared slowly and independent on their geometric diameters.[165] Therefore, the accuracy in determining regional pulmonary deposition from different particle sizes based on particle clearance should be evaluated with caution.

Early on, evidence about the deposition of smaller particles in the smaller airways also emerged from related therapeutic response. According to the pathophysiology of asthma, inflammation may occur throughout the entire airway. Given the easy accessibility of the large airways, early studies related to this chronic inflammation had been done in the proximal central region, neglecting the occurrence in the distal airways.[166] In a series of studies, Zanen and coworkers demonstrated a significant improvement in lung function of stable asthma patients may be influenced by disease severity as well as particle characteristics. In the first study, monodisperse solutions of ipratropium bromide were aerosolized to mild asthma patients, with MMADs of 1.5, 2.8 and 5.0 μm and GSDs smaller than 1.2.[167] Improvement in forced expired volume was observed for patients inhaling equivalent doses of aerosols with MMADs of 1.5 and 2.8 μm only. Following this study, monodisperse salbutamol or ipratropium bromide solutions were administered in equal doses to asthma patients with severe obstruction.[168] For aerosols with the same aerodynamic characteristics as in the previous study, only particles with MMADs of approximately 3 μm presented improvement in the respiratory tract in this subset of patients. Not able to visualize the deposition patterns with imaging techniques, the authors were unable to explain why the aerosol with small particles (MMAD of 1.5 μm) presented similar lung function improvement as the solution aerosolized presenting larger particles (MMAD of 5.0 μm). These data suggest that aerodynamic diameter, geometric standard deviation and the

degree of underlying airway disease may all impact the delivery as well as the therapeutic response to inhaled medications. Finally, Zanen *et al.*. compared the monodisperse ipratropium bromide aerosol (MMAD 2.8 μm; GSD 1.1) with a polydispersed pMDI formulation of the same drug (MMAD 1.8; GSD 2.0).[169] The wide distribution of particle sizes of the pMDI formulation was found to be not as efficacious as the monodisperse delivery of the aerosol, based on lung function improvement. Subsequent studies have found that inflammation at distal portions of the lungs play a significant role in development and persistence of asthma symptoms.[170]

More evidence for the deposition of smaller particles in the lower airways occurred after chlorofluorocarbons (CFC) were mandated to be removed from pMDIs, according to the 1987 Montreal Protocol on Substances that Deplete the Ozone Layer.[171] Gradually, the propellant CFC was being phased out and substituted by hydrofluoroalkanes (HFA), given its safety profile.[62] The need for reformulation provided the opportunity to produce solutions of inhaled corticosteroids (e.g. flunisolide and beclomethasone) with the propellant HFA, as opposed to the then available CFC-based suspensions.[172, 173] The HFA-based formulation of beclomethasone dipropionate (QVAR®) was able to produce aerosols with MMADs of 1.1-1.2 μm, much smaller aerodynamic particle sizes than the CFC-based formulations with MMADs varying from 3.5 to 4.0 μm. Several studies comparing QVAR® and CFC-based formulations were performed for inhaled corticosteroids like beclomethasone and flunisolide.[172, 174, 175] The deposition patterns were based on percentage of ^{99m}Tc radiolabelled particles deposited in the oropharyngeal cavity (upper airways) versus the deposition in the deep lung (lower airways). The smaller aerodynamic particles of the HFA-based solution formulation were consistently deposited in the deep lungs in a considerably higher proportion than with the CFC-based suspension formulations. Such

findings have not been consistent with all HFA formulations though. Scintigraphic studies for beclomethasone and flunisolide HFA show dramatically increased lung deposition (50-70 %) when compared to CFC formulations (5-20 %).[170] The increased solubility in HFA for some drugs is likely the reason for smaller particle size. The importance of solubility on the particle size is illustrated by the scintigraphic studies of mometasone furoate HFA. Unlike the HFA-soluble drugs beclomethasone and flunisolide, mometasone furoate is currently delivered in an aerosol suspension. Studies by Pickering *et al.*. demonstrated lung deposition of mometasone furoate HFA of approximately 14% for a formulation presenting only approximately 20% of particles smaller than 5.8 μm.[176] Thus, in evaluating the reduction in particle size with HFA-based formulations, one must take into account drug solubility. Therefore, the relatively low lung deposition of mometasone furoate HFA has been shown to be similar to the CFC-based suspension formulations. Importantly, both present larger particle sizes than the HFA-based solution formulations.

pMDIs represent a high ballistic effect when actuated and therefore the particles are more prone to deposit via inertial impaction.[177] On the other hand, aerosols generated by nebulizers may be more dependent on the breathing pattern of patients.[178] Sangwan and coworkers have investigated the regional deposition patterns from aerosols generated by Misty-Neb® (MMAD = 3.1 μm) and AeroEclipse® (MMAD = 2.2 μm).[179] The total lung deposition measured by two-dimensional scintigraphy was two-fold smaller for the aerosols with larger particle size, and therefore presented a proportional increase in oropharyngeal deposition. The peripheral deposition though was higher for the aerosols generated from Misty-Neb®, with a C/P ratio of 1.5 as compared to 1.9 for AeroEclipse®. This controversial finding was attributed to the relatively extended time required for nebulization with the breath-actuated nebulizer AeroEclipse®

(20 minutes). As discussed earlier, the use of single-headed SPECT presents the disadvantage of long scanning times, allowing for particle clearance to occur. In the same manner, the effect of extended time due to aerosol generation may have hindered the evidence of small particles depositing in the alveoli. Nevertheless, the evidence that the larger particles were deposited in the upper airways was confirmed.

Also using planar gamma-scintigraphy, an evaluation of the regional deposition of monodisperse particles was performed in twelve asthma patients in a more recent study.[180] Albuterol was radiolabelled with ^{99m}Tc and aerosolized using a spinning-disk aerosol generator able to provide a GSD smaller than 1.22. For regional deposition analysis, the lung images were divided in three different zones: central, intermediate and peripheral. The penetration index (P/C ratio) results for particles with MMADs of 1.5, 3.0 and 6.0 μm were 0.79, 0.60 and 0.36, respectively. When considering central and intermediate zones together, the percentage of deposition in the peripheral lung zone compared to the total lung dose was still high for smaller particles: 44, 34 and 25%, respectively. The increase in penetration index values with decreasing particle sizes observed in this study clearly confirms the deposition of smaller particles in the smaller airways (peripheral lung region). On the other hand, larger particles are more likely to deposit in the upper airways that present a larger caliber. The deposition pattern of monodispersed particles with aerodynamic diameters of 1, 2.75 and 4.75 μm were reported likewise in another study.[181] In this investigation, 90% of the larger particles (MMAD 4.75 μm) were deposited in the upper airways. Also, increase in airflow rate demonstrated the effect of inertial impaction in larger particles, by increasing deposition in the upper respiratory tract.

With the advances in SPECT instrumentation, multi-headed cameras have been used to decrease the image acquisition time and provide more reliable regional deposition

patterns in the lungs. Eberl and coworkers have introduced a dynamic SPECT technique in which acceptable image quality was obtained with 2-min frame using a triple-detector gamma camera.[181-183] In this study, the investigators compared the sensitivity of planar scintigraphy data with fast acquisition of three-dimensional images from SPECT. For the comparison, saline solutions containing ^{99m}Tc-DTPA tracer with different tonicity (hypertonic and normal saline) and droplet sizes (MMADs of 3.2 and 6.5 μm and span indices of 1.8 and 1.7, respectively) were aerosolized to six human subjects during tidal breathing. Using laser diffractometry, the span index was defined as the difference between the 90 and 10% cumulative volumes, divided by volume mean diameter: span = $(Dv_{(90)} - Dv_{(10)})/Dv_{(50)}$. The hypertonic saline aerosols were expected to undergo hygroscopic growth as the droplets travel through the humid airways. Though, due to insufficient time for growth coupled with effect of mass transfer, the increase in aerodynamic diameter by small hypertonic saline droplets was expected by the authors to reach an intermediate size between 3.2 and 6.5 μm. Consequently, it would be expected to demonstrate a pulmonary deposition pattern intermediate to the smaller and bigger airways. Based on the work by Fleming *et al.*.,[146] the lung images from SPECT were likewise subdivided into concentric shells as previously explained and the regional deposition of the particles in the lungs was determined according to the penetration index (P/C ratio). However, only deposition in the right lung was considered, since the image of the left lung may include confounding factors from the stomach and cardiac shadow.

In fact, the three-dimensional imaging technique proved to demonstrate a higher sensitivity than the planar scintigraphy. Not surprisingly, both techniques were able to detect the significant differences in penetration index that could be observed between the small normal saline and the large (both hypertonic and normal saline) droplets. However, the dynamic SPECT imaging was able to additionally identify significant differences in

intermediate particle sizes being deposited in intermediate regions of the airways that could not be achieved by the two-dimensional scintigraphic method. More importantly, the study was able to demonstrate that smaller particles are deposited more peripherally in the lungs. The mean (± SEM) penetration indexes as measured by SPECT for small normal saline, small hypertonic saline, large normal saline and large hypertonic saline droplets were, respectively, 0.501 ± 0.043, 0.432 ± 0.022, 0.358 ± 0.024, and 0.338 ± 0.017. Interestingly, no significant difference in regional pulmonary deposition was found between the different tonicities of large droplets. This finding may be related to the already central deposition of these larger aerodynamic particles, with little further hygroscopic effect to the large hypertonic saline aerosol.

A similar study has recently been published to confirm the deposition of small particles in the peripheral region of the lungs, following pulmonary administration using an Aeroliser® DPI device.[184] Eight healthy volunteers were dosed with powder aerosols of mannitol radiolabelled with ^{99m}Tc complexed to Diethylene Triamine Pentaacetic Acid (DTPA) prepared by co-spray drying. The incorporation of radionuclide to mannitol did not present difference in particle sizes. This indicates the validity of using this radiolabelling method to determine the mannitol deposition in the lungs by measuring the radioactivity. The three different formulations evaluated presented particles with MMADs of 2.7, 3.6 and 5.4 μm and GSDs of 2.6, 2.4 and 2.7. The lungs of the human subjects were analyzed using SPECT and the images were divided into 10 concentric shells: central (5 innermost shells), peripheral (2 outermost shells) and intermediate (remaining 3 shells). An interesting finding from this study was that decreasing the particle aerodynamic diameter from 5.4 to 3.6 μm significantly increased the peripheral deposition. However, decreasing MMAD further from 3.6 to 2.7 μm did not improve significantly particle deposition in the lung periphery. With a greater

deposition of the smaller particles more diffusively throughout the lungs consequently provided a greater lung dose. Alternatively, the deposition in the upper airways was significantly higher for bigger particles (> 70%).

In addition, Glover and coworkers investigated an intersubject variation in total lung dose based on individual subject flow patterns and inspiratory airflow rate. With peak inhalation flow greater than 90 L/min for all patients, no correlation could be drawn since no difference in *in vitro* deposition was found between airflow rates of 60 and 100 L/min. Results of airflow rate and deposition patterns have been previously correlated, however using different DPI devices (Inhalator^{TM})[185] or the same device with different airflow rate ranges.[186] Although a consistent polydispersity characteristic was observed for the three different formulations of mannitol powder, the results obtained in this investigation using a more reliable imaging tool (SPECT) for regional lung deposition helps to support the evidence that aerodynamically smaller particles deposit in the smaller airways.

While regional lung deposition of micronized aerosols is more frequently reported, the investigation of nanometer aerosols deposition in specific regions of the lungs is not available in the literature. Considering the late advances in nanotechnology, the regional dosimetry of nanoaerosols has been identified as a specific gap by the National Institute for Occupational Safety and Health.[187] More recently, Ruzer and Apte discussed the difficulties related to available experimental techniques for assessment of local deposition of nanoparticles (i.e. particles ranging from 1 to 100 nm) in humans.[188] The authors then go on to propose a potential method to be used for this purpose based on the unattached fraction of radon progeny. This marker forms naturally by decay of the inert radioactive gas radon and presents the smallest radioactive size, 1 nm. Through diffusion mechanism, this marker can deposit onto the surface of particles

ranging from nanometer to micrometer dimensions and therefore has a potential for application in the regional dosimetry of nanoparticle aerosols. This approach has been previously used for determining extrathoracic deposition patterns in the human respiratory tract following nose- and mouth-breathing.[189]

Nonetheless, a formulation of salbutamol with primary particles in the geometric nanosize range has been investigated for the local lung deposition.[190] The Quasi-Elastic Light Scattering (QELS) results from this study showed that more than 70% of the particles prepared by spray-drying had a diameter smaller than 100 nm. The particle size results were confirmed by Scanning Electron Microscopy (SEM), which also demonstrated a well-defined round shaped morphology. The nanoparticles obtained were then compared to micronized particles of salbutamol in terms of aerodynamic diameter and regional deposition following inhalation with a Rotahaler® DPI device. The nano-salbutamol formulation presented an MMAD of 1.6 μm, with the discrepancy to the geometric diameter attributed to a potential aggregation due to interparticle adhesion in the dry state. Despite of that, the distribution of particle deposition in the Andersen Cascade Impactor showed that approximately 20% of the formulation presented aerodynamic diameter smaller than 150 nm. The MMAD of the micronized drug was approximately 3.1 μm. The healthy volunteers were trained to retain the breath for 10s following deep inhalation and exhale into a collecting bag. Considering the diffusion mechanism related to ultrafine particles, an improvement in deposition of particles is expected with this breath-holding maneuver.[191] The planar scintigraphy imaging results, using the tracer ^{99m}Tc, showed a peripheral deposition of the nanoparticles greater than 2-fold higher than the micronized salbutamol and a minimal exhaled fraction (< 1% of the emitted dose).

Similarly to the results obtained with humans, the studies in animals have presented the same evidence for the deposition of small particles in the lower (smaller) airways, despite the differences in the structure of their respiratory tract and breathing characteristics (nose versus mouth breathing).[192] Intraspecies variability has been reported to be similar to that of humans in animal species that include: rodents, dogs, minipigs, and monkeys.[193-195] Besides the scintigraphic techniques generally used for studies in humans, more recently a fluorescent imaging method has been introduced to study deposition patterns in lungs of animals.[196]

Age is a determinant factor in the airway caliber of humans, with both increasing gradually from the newborn to the adult phase. Considering this fact, formulations developed for inhalation therapy based on adults may not be appropriate or applicable for infants and young children. The relatively smaller airways of this subset of patients are a critical factor for the drug to reach the lower airways.[197, 198]

Due to the focus on pulmonary delivery to adult populations, some studies have investigated specifically the importance of aerosol formulations with smaller aerodynamic particle sizes to be delivered to children. In certain studies, the distinction in particle deposition is based solely on the difference in radioactivity observed in intra- and extrathoracic regions. Although they lack distinctive information on more specific pulmonary regions (e.g. terminal airway region), these investigations provide valuable data from a different viewpoint, in which they are based on differences in particle deposition between oropharyngeal (larger airways) and deep lung (lower airways). Comparing deposition in the lower versus the upper respiratory tract, budesonide droplets radiolabelled with ^{99m}Tc presented MMADs of 2.5 μm (GSD of 1.25) and 4.2 μm (GSD of 2.0) after nebulization with eFlow® and Pari LC Plus® nebulizers, respectively.[199] Using planar gamma scintigraphy to analyze six asymptomatic three-year old children,

Schuepp and coworkers found that lung deposition was 36-38% and 5-8%, for children inhaling particles with MMADs of 2.5 and 4.2 μm respectively. In a similar study, jet nebulizers were used to produce aerosols with MMADs of 3.6 and 7.7 μm.[200] With twenty asymptomatic cystic fibrosis patients, ages 3- to 24-months old, lung deposition of nebulized small particles was also greater than large particles. The ideal size of particles and best method of delivery; however, have not been clearly established in infants and young children.

1.2.6. Establishing Clear Relationships

The respiratory tract is a complex anatomical structure in which the upper airways gradually decrease in diameter down to the small dimensions of the terminal airways and alveoli. The *in vitro* determination of aerodynamic diameters has long been explored as a parameter to correlate regional lung deposition with *in vivo* studies. For the development of inhalation products, the use of cascade impactors greatly benefits the fast screening of formulations. Hence, since the studies from Stahlhofen *et al.*., in the late 1980's, the optimal particle sizes for inhalation products have been highly speculated. Consequently, rules-of-thumb have arisen. The most common one found in publications related to development of formulations for pulmonary delivery is that particles in the range of 1 to 5 μm are deposited in the deep lungs; while those larger than 10 μm are generally deposited in the oropharyngeal region and the particles smaller than 1 μm are exhaled.[120, 201-203] In an attempt to determine a more consistent in vitro/in vivo relationship, Newman and Chan have evaluated the results available in the literature for DPIs and pMDIs.[38] Comparing the whole-lung deposition as a function of fine particle fraction, they found that the scattered data straddled the line of identity when particles were smaller than 3 μm. This may suggest an upper limit for particle size related to

deposition in the deep lungs. So far, this finding in conjunction with the published data summarized in this review paper may be the best guide to predict deposition in the small airways, although it does not present a high level of accuracy, since other factors influence deposition (e.g. particle shape and degree of airway inflammation).

Just as it is important to define an upper limit of particle size distributed in various regions of the lung, it is also important to define the lower limit for each region. Considering the gradual, but not stepwise, decrease in the dimensions from the upper to the lower airways and the often polydispersed characteristic of orally inhaled products, it is reasonable to expect difficulties though in determining a specific cut off particle size range that translate into regional deposition in the lungs. One reason for that is the fact that the current available methods provide information on deposition via inertial impaction only, regardless of the other two significant mechanisms that can occur: sedimentation and diffusion.[33] Elutriation is the process by which particles are separated when moving upwards suspended in a fluid at a determined velocity. Elutriators have been developed to operate based on the principle of sedimentation; however they have not yet been widely applied to characterization of pharmaceutical formulations for inhalation therapy.[204] Specifically for the diffusion mechanism, not only methods for characterization of aerosols are not available, but also dosimetry techniques are yet to be developed, as discussed earlier. The lack of information on the determination of aerodynamic particle sizes based on the three possible mechanisms of deposition may be the gap to determine more specific ranges of MMAD that correlates to regional deposition in the lungs. The late advances in *in vivo* experimental techniques, mainly related to three-dimensional imaging, have certainly developed towards meeting this need. Even though the optimal particle size range is yet to be defined, the reports

available in the literature are evident about the deposition of smaller particles in the deep lungs, as opposed to deposition in the larger airways.

1.2.7. Conclusions

Despite the limitations in early imaging techniques used to determine particle deposition in specific zones of the lungs, the technological advances in imaging techniques are gradually improving the capability of differentiating the deposition patterns of particles with increasingly smaller differences in aerodynamic dimensions. With the advances in SPECT and PET, more confirmatory studies are being reported of the evidence of deposition of small particles in the smaller airways, as opposed to deposition in the larger airways. Nonetheless, the imaging techniques can also be used for less specific studies in the respiratory tract by comparing extrathoracic (upper airways: oropharyngeal cavity) versus intrathoracic (lower airways: lower trachea, bronchi, bronchioles and alveoli) particle deposition. This has been more frequently reported in studies with children.

The desire to establish clear relationships between *in vitro* aerodynamic determination and *in vivo* particle deposition has led to comparisons between fine particle fraction and total lung deposition of particles. Results based on impaction studies indicate that particles smaller than 3 μm are more likely to deposit in the deep lungs. However, there is a lack of information about the regional lung deposition of particles affected by non-impaction mechanisms (e.g. sedimentation and diffusion), largely due to lack of applicable *in vitro* and *in vivo* experimental techniques; however, there is sufficient evidence reported in the literature showing that smaller aerodynamic particles deposit in the lower portion of the respiratory tract where the airways are gradually smaller. As imaging techniques advance, investigation of how particle size, shape, charge, and

composition affect deposition and movement through both the airway and the lung's mucous gel layer. An overall understanding related to the fate of inhaled particles for a given formulation type will be required in order to optimize drug delivery using the pulmonary route of administration.

1.3. THE FUNCTION AND PERFORMANCE OF AQUEOUS AEROSOL DEVICES

1.3.1. Introduction

Commercially available technologies to transform a liquid dosage form into an aerosol for medical inhalation purposes have evolved significantly over the last century. Fundamentally, aerosol generation in the form of droplets has evolved from using human-powered techniques (manually compressed hand bulbs), followed by the advent of gas-powered devices (the air-jet stream principle), and through to electronic powered systems (using the ultrasound effect, including recent adaptations to create vibrating-mesh micropumps). More recently, mechanical and electromechanical systems have been applied to develop novel aerosol production technologies (i.e. soft mist inhalers). The emerging technologies still include new nebulizing concepts involving mechanisms like electrohydrodynamic atomization and surface acoustic wave microfluidic atomization as well as capillary aerosol generators. Nebulizers are usually selected over other medical inhalers (e.g. pressurized metered dose inhaler (pMDI), or dry powder inhaler (DPI)) either due to the high drug deposition potential, or the negation of required patient training of complex inhalation maneuvers. Additionally, nebulizers have an innate capacity to aerosolize special formulations (e.g. recombinant human deoxyribonuclease (rhDNAse), or antibiotics not available as other inhalation dosage forms).[205]

In addition to the progress of the basic principles of nebulization, the innovation has advanced further to encompass the so-called “smart” technologies with the objective to increase drug deposition to the lungs. Breath-enhanced nebulizer systems such as the Pari LC Star® and AeroEclipse® devices have an inspiratory flow rate to match that of the patient, increasing delivery of droplets, while going back to baseline during exhalation.[206] In addition, breath-actuated devices like the AeroEclipse® and Halolite® deliver aerosols after pre-profiling a patient’s breathing pattern. The I-neb Adaptive

Aerosol Delivery by Respironics® delivers aerosol only during the initial phase of inhalation.[207-209] And the Aer$_X$™ insulin Diabetes Management System (iDMS®) is a breath-activated inhalation system developed by Aradigm and Novo Nordisk that also allows for patient monitoring to ensure compliance to an adequate inhalation technique at optimal breathing conditions.[210, 211] Other technologies are available to monitor adherence of patients to MDI's, like the SmartMist®, the Doser CT®, and the MDILog®.[212]

Nebulization is the use of a particular device for the conversion of a liquid dosage form into fine droplets. Therefore, specific properties of bulk formulations in conjunction with the functional mechanism of a specific inhaler can dramatically influence the droplet characteristics and overall aerosol production. These droplet characteristics, together with patient dependent factors in turn determine the quality and extent of drug deposition to the lungs (Figure 1.4).

Deposition throughout the respiratory airways of particles with different sizes is governed by different forces. Larger particles are highly affected by velocity, due to their relatively high mass, and therefore deposit by inertial impaction. Alternatively, sedimentation generally occurs to particles when gravitational forces are significant. Overall, larger particles are more likely to deposit in the upper airways while smaller sized particles tend to reach the deep lungs via sedimentation. At the smallest end of the scale, particles moving by Brownian motion are prone to be exhaled. More often than not, the droplets formed in most nebulizer systems present somewhat a heterogeneous size distribution. Thus, the dispersity of the size distribution is also an important parameter to be considered in deposition. Overall, it is generally accepted that particles with aerodynamic sizes between 1 and 5 μm may be deposited in the deep lungs.[213]

Essentially, two methods have become prominent in analyzing droplet sizes generated by nebulizers; these are cascade impactor (CI) and laser diffraction (LD). The first one relates to the drug concentration and is correlated to the hydrodynamic airflow and inertial impaction of droplets with specific sizes; the distribution of droplets is evaluated gravimetrically to determine a Mass Median Aerodynamic Diameter (MMAD). This parameter is the equivalent droplet size in which half (50%) of the droplets are smaller and 50% are larger than the specified cutoff diameter. The MMAD is calculated by following the evaluation of drug amount deposited in different stages of an inertial impactor. Commonly, the Geometric Standard Deviation (GSD) is reported to indicate the dispersity droplet size distribution around the MMAD. Laser diffraction is only applied to solution systems since it is derived from a volume-based measurement and is supported by the principle of homogeneous drug concentration of these dosage forms. For this technique, the MMAD is usually interchangeably referred to as Volume Mean Diameter (VMD) and the dispersity is sometimes given as span (10% percentile subtracted from 90% percentile and divided by VMD).

A reduced nebulization time is always desired in order to boost patient compliance to treatment, and nebulizer systems capable of delivering relatively high amounts of drug are generally preferred. Therefore, measurement of aerosol output (amount and rate) is essential to establish nebulization performance. This analysis has been traditionally performed either by determining the difference in drug amount or by gravimetrical analysis (by simply weighing a nebulizer reservoir before and after nebulization). However, care should be practiced when relying on the gravimetric method. For instance, weight loss analysis can overestimate drug output due to evaporative effects of jet nebulizers[214, 215], or due to a heterogeneous nebulization of drug containing droplets (i.e. the generation of droplets that contain varying amounts of

drug) during aerosolization. These effects could potentially be exacerbated during the nebulization of dispersed systems like suspensions or liposomes.[216]

In this section, the different mechanisms of aerosol generation are presented: the transformation of bulk liquids into droplets. Although some nebulizer systems are generally sub classified as “soft mist inhalers” (SMI) due to the slow velocity of their emitted aerosol, they were included herein from the standpoint of their functioning mechanism. The nebulization performance of different methods of aerosol generation were explored for solution and dispersed systems based on the bulk characteristics of liquids, with emphasis on the influence of changes in surface tension and viscosity on aerosol production. Additionally, the importance of density is recognized, but because the vast majority of the nebulizing formulations are based on aqueous systems overall changes might be small and its influence may be limited. Importantly, the nebulizer system comprises all components attached to the aerosol generation system, due to the fact that the nebulizer performance varies with respect to factors in addition to droplet formation, for example flow characteristics and airway connection tubing properties.[178]

1.3.2. Jet nebulizers

The basic functioning principle of jet nebulization is that a compressed gas (e.g. air) is forced through a tubing system which is in turn connected to a nozzle. As the air velocity increases with the decrease in the tubing cross-sectional area, a zone of low pressure is created around the nozzle (Venturi effect). As the high velocity jet passes tangentially or co-axially through the Venturi nozzle, the pressure drop created causes the liquid formulation to rise up on a feed tube from the liquid reservoir (Bernoulli effect). A primary droplet is then formed as an aerosol; a large droplet may subsequently impact on

baffles or onto the nebulizer walls, recycling into the reservoir. Droplets small enough circumvent these barriers (secondary droplets) and form the respirable aerosol generated from jet nebulizers.[217] Therefore, nebulizer design and dimensions greatly influence the characteristics of the secondary aerosol formation. This reason reinforces that nebulizers should be evaluated as a multicomponent system for the respirable aerosol generation, as opposed to characterization of the inhalation formulations based on isolating the single mechanism of aerosol production itself (primary aerosol generation). Although the influence of surface tension and viscosity on the size of primary droplets is well described, the secondary aerosol characteristic is a complex function of jet nebulizer systems.[217, 218]

The performance of these nebulizer systems (compressor/nebulizer combinations) to produce water droplets has been compared extensively, with MMAD values measured using laser diffraction varying from 2.6 to 10.2 μm.[219] Treatment time reduction with these systems can be achieved by increasing airflow rate and by using a small initial fill volume, although these measures can slightly change the aerosol characteristics.[217, 219] Overall, decrease in droplet size (with increased aerosol polydispersity) and increase in aerosol output can be expected for higher airflow rates and higher initial fill volumes.[220, 221] Irrespective of initial fill volume, this study with water clearly showed that output rate was not constant over time for the twenty three jet nebulizer systems investigated, varying anywhere from 0.05 to 0.29 mL/min at different time points within the same aerosolization event. This was an important study comparing the capacity of different nebulizer/compressor combinations to aerosolize a reference liquid (water). However, the fact that these systems promoted a device-specific variable decrease in temperature (4 to 8 °C)[222] does not allow us to evaluate the effect of the

important temperature-dependent properties (i.e. surface tension and viscosity) and their effect on nebulization performance.

Nebulizer systems are capable of delivering high amounts of drug, and nebulizer formulations are primarily comprised of aqueous systems that can avoid damage to lung physiology. However, the presence of different excipients will almost certainly alter the physicochemical properties of liquids, even given the limited options for inhalation delivery due to potential toxicological effects of certain inactive ingredients.[119] For this reason, the characterization of the liquid formulation in conjunction with nebulization performance has been investigated in a number of recent studies. Very small droplet sizes (MMAD between 0.5 and 1 μm as measured by a 6-stage cascade impactor) were generated from jet nebulization of a simple hydroalcoholic solution (4% v/v ethanol in water) of Prostaglandin E_1, aiming to treat neonatal hypoxemic respiratory failure.[223] The small ethanolic content was of a sufficient amount to decrease surface tension and viscosity values to approximately 61 mN/m and 0.982 cP, respectively. Cyclodextrin complexation of poorly-water soluble formoterol has provided solutions with surface tension and viscosity values of 54-56 mN/m and 1.16-1.18 cP, respectively.[215] Jet nebulization of these solutions has shown VMD values varying between 3 to 5 μm, with drug output rates of approximately 30-60 μg/min for four different nebulizer systems. Interestingly, the authors report that rate of formulation output is greater than rate of the formoterol emitted, indicative of the formation of aerosol droplets with varying drug concentration.

The effect of surface tension on jet nebulization output of solutions was clearly illustrated when Ventolin® (albuterol sulfate) was added to a tobramycin intravenous solution supplied by Eli Lilly Canada.[221] The presence of benzalkonium chloride as preservative in the Ventolin® formulation caused the surface tension of the final mixture

to change from 66 mN/m (tobramycin IV solution diluted with saline) to 31 mN/m.[224] As a result, an increased drug output (10-50%) was observed for the lower surface tension solution. Similar results have been reported in another investigation that used three different jet nebulizer systems.[222] Importantly, authors from both studies highlighted the magnitude of increased drug output further related to differences in jet nebulizer systems and parameters (e.g. airflow rate) studied. Conversely, studies on solutions with increasing concentrations of heparin have shown a concomitant increase in kinematic viscosity, but no change in surface tension.[220] This increase in viscosity is in general translated into increased output rate and decreased droplet sizes when solutions of calcium, sodium, and low molecular weight heparin are jet nebulized. Interestingly, analysis of droplet size over time within a 15-minute nebulization run using a highly concentrated sodium heparin solution (19,900 IU/mL) displayed a decrease in MMAD from 2.5 to 1.9 μm, with no change in GSD.

A drop in temperature caused by the latent heat of evaporation of the nebulizer solution is only one formulation attribute changing over time during jet nebulization.[225] According to Steckel and Eskandar, while studying the changes occurring within a 10-minute nebulization period, an increased drug concentration can also be expected as the water evaporates. This can be attenuated by the presence of buffer in saline solution, which causes a drop in the saturated vapor pressure. Moreover, the investigators found that while viscosity increases due to temperature drop of the nebulizer solution, surface tension decreases due to the increased nebulizer solution concentration. Most importantly, the authors explain that, within a 10-minute nebulization period, as jet nebulization occurs and water starts to evaporate, the temperature drop promotes an increase in viscosity and a reduction in saturated vapor pressure. Consequently, an initial increase in droplet size is observed. As the process continues and the nebulizer solution

concentrates, the reduction in surface tension provides droplets with smaller VMD values.

As indicated, it is very valuable to have knowledge during formulation development with respect to an understanding of the influence of physicochemical properties of liquids (i.e. surface tension and viscosity) on aerosol droplet size and output for these inhaler devices.[81] The addition of surface active agents to water changes the secondary aerosol properties in a device-specific manner, with an overall inverse relationship relative to aerosol output.[226] However, a more intricate relationship between surface tension and droplet size can be expected. In some cases this relationship between surface tension and droplet size may be inversely related, and in other cases it may reach a peak value. Irrespective of the observed relationship, the size of the emitted droplets appears to be independent of the critical micelle concentration, and respirable output results overall agree with total output trends.[226] Viscosity effects are clearer, with jet nebulization being more efficient in terms of respirable output with liquids of low viscosity (1 to 6 cP). Thereafter and up to ceasing nebulization, increased viscosity increases MMAD as well as aerosol output, also in a device-specific manner.[81, 227]

Jet nebulizers have been shown to be capable of aerosolizing protein solutions. Recombinant human deoxyribonuclease I (RhDNase I, also known as dornase alfa) has been tested and successfully delivered to the cystic fibrosis patient airways using jet nebulizer systems, to alleviate excessive mucus accumulation.[228, 229] In fact, there are only three different jet nebulizer systems approved for delivery of dornase alfa to treat cystic fibrosis patients and these are (nebulizer/compressor system): the Marquest Acorn II/DeVilbiss Pulmo-Aide; the Hudson T Up-draft/DeVilbiss Pulmo-Aide; and the Pari LC Jet Plus/Pari Inhalier Boy.[230, 231] However, studies to evaluate jet nebulization on protein degradation must always be considered. It is apparent that through different

mechanisms, the micellar properties of tween 80 and the hydrodynamic size as well as the influence of polyethylene glycol (PEG) on the conformational structure of protein in the air-water interface have shown to aid in protein stabilization during air jet nebulization.[232] Chitosan provides an additional protective effect, possibly via ionic interactions between its positive charge and the negatively charged enzyme[233]. Moreover, protein solutions are commonly freeze-dried to provide greater physicochemical stability.[234] When sodium polyphosphate, calcium chloride, or magnesium sulfate are used as cryoprotectants in a protein formulation (aviscumine), decreased surface tension and increased viscosity are seen.[235] The droplet size of jet nebulized formulations was observed to be slightly decreased when containing these excipients as compared to normal saline. Meanwhile, these components also provide protection to aviscumine destabilization caused by the air-jet process. For the treatment of emphysema, and potentially cystic fibrosis, the addition of antifoams such as span 65, or a mixture of cetyl alcohol and tyloxapol to protein solutions of α_1 protease inhibitor also decreased surface tension without altering viscosity.[236] An overall increased amount of jet nebulized protein was observed while the cetyl alcohol/tyloxapol antifoam mixture provided an improved respirable fraction.

Dispersed dosage forms can also be delivered to the lungs using jet nebulizers.[237] The aerosolization efficiency is highly device-dependent.[238, 239] For instance, thirty different jet nebulizer systems show respirable fractions of Pulmicort Respules® (budesonide suspensions) ranging from 15 to 50% but with very different output rates.[240] Reportedly, these suspensions present drug particle sizes of 2-3 μm.[241] Nanoemulsions of budesonide (10.9 nm) prepared using ultrasonication presented improved aerosol characteristics for pulmonary delivery following jet nebulization. MMAD values were around 5.0-5.5 μm for the nanoemulsion compared to

7.0-8.0 μm for the standard suspension, additionally the nanoemulsion had better aerosol output, thus allowing for a much improved respirable fraction.[242] Jet nebulization of nanoparticle dispersions of deoxyribonuclease I (DNase I) show similar results, while greater than 50% activity of the protein is maintained.[243] Importantly, the nebulization performance of suspensions using jet nebulizers is also dependent on formulation properties, with different excipients and methods of preparation providing rather variable drug deposition patterns.[244] In addition, drug nanoparticle aggregation may also occur during jet nebulization.[245]

Many liposomal formulations have been aerosolized with this method. Liposome components included soy (SPC) or egg phosphatidylcholine (EPC), cholesterol, and a variety of synthetic phospholipids, such as 1,2-dimyristoyl-sn-glycero-3-phosphocholine (DMPC), 1,2-dipalmitoyl-sn-glycero-3-phosphocholine (DPPC) and 1,2-distearoyl-sn-glycero-3-phosphocholine (DSPC).[95] With increased phospholipid concentration (1,2-dilauroyl-sn-glycero-3-phosphocholine – DLPC), an increase in the Non-Newtonian apparent viscosity of budesonide and cyclosporine A liposomes has been observed, promoting reduction in drug mass output rate following jet nebulization.[246] Nevertheless, the differences in nebulizer design as well as lipid concentration (and therefore viscosity) are factors influencing secondary droplet sizes.[247] Ultimately, the type of phospholipid influences the jet nebulization performance differently for particular compounds.[248]

Powders of phospholipid-coated particles (proliposomes) are ready for hydration to form liposomes and can be directly dispersed within the jet nebulizer reservoir for efficient aerosolization.[216] However, the shear effect of air-jet aerosolization can be expected to affect the physical stability of multi lamellar vesicles (MLV).[249] A slightly higher physical stability of liposomes to jet nebulization can be achieved when MLVs are

extruded through 1 μm polycarbonate filters.[68] Further reduction in particle size of MLVs by extrusion through 0.4 μm filters did not improve physical stability, in terms of retained entrapped drug following jet nebulization, but did provide an improved drug-to-aerosol mass output. *In vitro* studies suggest that liposomal drug encapsulation with DPPC is beneficial for deposition to the deep lungs with air jet nebulization when compared to free drug, mainly for poorly-water soluble compounds.[250] Supposedly, the decrease in surface tension caused by this phospholipid can bring advantages to the adsorption kinetics of the liposomes to lung surfactants.[251]

1.3.3. Ultrasonic nebulizers

During the function of an ultrasonic nebulizer, acoustic waves are generated by a piezoelectric transducer that converts electrical signal into oscillatory mechanical movement. With frequencies of approximately 20 KHz, this mechanism creates oscillatory pressure disturbances that travel through a bulk liquid which is to be aerosolized. Cavitation occurs when pressure disturbances propagating through the liquid cause zones of low pressure, this creates vapor bubbles. At the collapse of these bubbles, shock waves conveniently close to the air-liquid interfacial region lead to surface destabilization creating the droplets. Alternatively, liquid excitation by ultrasonication causes capillary waves going outwards from the surface region up to a collapsing point in which droplets are generated. These two widely discussed possible mechanisms, for wave destabilization at the liquid surface are responsible for producing droplets, namely cavitation and capillary.[252]

Conversely to air-jet systems, ultrasonic nebulizers promote an increase in solution temperatures to as much as 10°C above the starting temperature after a 5 to 7 minute aerosolization period.[222] This phenomenon of increasing temperature is caused

by the high energy input of the piezoelectric crystal. Additionally a higher magnitude of increase in drug concentration within a 10-minute nebulization period is observed than that of jet nebulizers.[225] On the other hand, the addition of buffer salts or saline solution has also a relatively greater effect in decreasing drug concentration differences as well. Nonetheless, ultrasonic nebulizers are capable of maintaining a more constant VMD over time during the same nebulization event, while causing viscosity as well as saturated vapor pressure at the air-water interface to drop during aerosolization.[225] Increased concentration of buffer solution promotes increase in VMD caused by increase in viscosity, decrease in saturated vapor pressure and/or a surface tension drop.

Considering the functioning mechanisms of aerosol generation, it is extremely important to independently evaluate formulations by comparison of different devices. For instance, for formulations of heparin with increased concentration (and therefore increased kinematic viscosity, but no variation in surface tension), aerosol characteristics were unsatisfactory for ultrasonic nebulizers, presenting variable MMADs from 5.5 to 7 μm. This variation was not observed for air-jet nebulizers, as previously discussed.[220] The ultrasonic aerosolization of solutions containing macromolecules is another concern. For instance, activity of the protein aviscumine is highly affected by ultrasonic nebulizers compared to air-jet systems.[235] Notably, a device in which water was used as medium to propagate the ultrasonic waves presented less accentuated protein degradation in this study than when the protein solution was used as transducer medium. Nevertheless, this investigation also showed that salts used as cryoprotectants decreased surface tension and increased viscosity, but did not alter droplet size significantly. In addition, the salts were not as capable of providing protection to the protein solution during ultrasonic aerosolization as they were for jet nebulization, and could not be ruled out as a possible contributor to extensive protein instability. On the other hand, aerosolization of a protein

solution of α1 protease inhibitor (viscosity of 1.25 mPa and surface tension of 53 mN/m) using a variable frequency ultrasonic nebulizer (up to 2.4 MHz) provides adequate VMDs of approximately 1.6 μm at different vibration levels of the piezoelectric crystal.[253] More importantly, the protein molecular weight and antielastase activity are maintained despite the stress caused by the ultrasonic nebulization. As the protein is a thermo-labile compound, this stabilization is related to the heat absorption of a coupling liquid that is designed with the ultrasonic nebulizer to act as a buffer; avoiding excessive temperature increases in the formulation to be aerosolized. Therefore, it appears that the thermal and mechanical stresses caused by ultrasonic nebulization are potential reasons for the unsuitability of these devices to aerosolize large molecules. However, when studying nebulization of lactate dehydrogenase solutions, no simplistic evaluation could be inferred for the capability of different types of nebulizers (jet and ultrasonic) to effectively aerosolize this protein solution, as enzyme activity was maintained across the board.[254] This reinforces the need to specifically determine the effectiveness of a device to aerosolize protein solutions.

Overall, ultrasonic nebulizers are incapable of generating aerosols from high viscosity liquids (i.e. greater than 6 cP).[81, 227] For less viscous liquids, an inverse relationship to the respirable output occurs. And comparing liquids with decreasing surface tension, peak values for VMDs outbalance the trough values of total output resulting in an optimal respirable output from ultrasonic nebulizers concurring with droplet size patterns generated.[81, 226] In general, ultrasonic nebulizers present a less heterodisperse aerosol than jet nebulizer systems.[81]

Ultrasonic devices are well known for not being appropriate to deliver microparticulate dispersed dosage forms, such as budesonide suspensions, and MLV liposomes.[92, 95, 216] Radiolabelled solid lipid nanoparticles however have been

effectively delivered to the lungs using this aerosol generation mechanism to study lymphatic uptake.[255] Furthermore, recent studies show that ultrasonication does not rupture nor does it cause aggregation or agglomeration of drug particle size encapsulated in lipid nanocarriers.[256] Further investigations are warranted to determine nebulization performance of these formulations as well as whether this resistance of solid lipid nanoparticles to nebulization is related to particle composition or structure and size.

1.3.4. Vibrating-mesh nebulizers

Vibrating-mesh nebulizers can be classified as micropump systems because aerosol generation from this technology is a result of ultrasonic energy forcing liquid to flow through small apertures of a plate or membrane. There are two types of micropump nebulizers: passive or active vibrating-mesh systems. The passive vibrating-mesh nebulizer (e.g. Omron MicroAir®) is composed of a piezoelectric crystal which generates vibration from electrical force to a transducer horn that is in contact with the liquid formulation. The ultrasonic vibration then creates waves in the nebulizer reservoir that travel towards a perforated plate positioned in front of the transducer horn. Consequently, aerosol droplets are created once the fluid flowing through the membrane is enough to cause drop detachment. Alternatively, active vibrating-mesh nebulizers (e.g. Aerogen Aeroneb®, and Pari eFlow®) have a dome-shaped membrane directly connected to a vibrating piezo electric element. Following application of electric current, the liquid formulation is rapidly extruded through the mesh as a consequence of the downward and upward movements of said membrane, this action generates the droplets.[31, 257]

These devices present the lowest change in temperature of the nebulizer solution among the inhalers discussed so far, with a small increase of about 3 °C over a 5-minute nebulization period.[222] This particular technological advance in functioning

mechanism offers the benefit of promoting its selection for clinical trials use of inhalation therapies.[258, 259] Both active and passive vibrating-mesh nebulizers are highly dependent on formulation characteristics. The influence of bulk liquid characteristics on aerosol generation of solutions has been systematically evaluated.[260, 261] Both systems have been demonstrated their ineffectiveness to produce aerosols from solutions that have viscosities of higher than 2 cP, with their total aerosol output being independent of physicochemical properties of liquids. The passive mesh technology yields slightly larger droplets than the active mesh system, but compensates to provide a similar respirable output by having a higher total aerosol output. An increased viscosity provides a decrease in droplet size, and a consequently higher respirable output from both mesh systems, but the overall output rate is compromised for passive mesh nebulizers. The influence of surface tension on aerosol properties are less clear, but it is known that fluids with low viscosity and low surface tension seem more desirable for greater nebulization performance.[260] A low ion concentration is crucial for providing less variable aerosol generation.[260-262] It should be noted that not all available apertures produce droplets all of the time though, this is highly dependent on the interactions between the bulk liquid formulation and the vibrating membrane.[261]

Importantly, the orifices of a mesh can get clogged over time, despite emphasizing cleaning instructions to patients that aerosolize solutions.[263] As a result of clogging, dramatic variations in output rate and subsequent delivered dose can be problematic. In extreme clogging situations the device may even be caused to switch-off automatically. For these reasons, thorough cleaning of the vibrating-mesh must be conducted and the membrane should be periodically evaluated for clogging. In a clinical setting, timely replacement of the membrane as well as dedication of device to specific formulations should be considered to avoid cross contamination.

Active vibrating-mesh nebulizers more efficiently deliver solutions than jet nebulizers, while passive devices present comparable performance.[264-266] On the other hand, passive vibrating-mesh nebulizers more efficiently deliver protein solutions than the air-jet systems.[208, 229, 267] Vibrating-mesh nebulizers can successfully deliver poorly-water soluble drugs to the lungs from dispersed systems, such as nanosuspensions.[28, 268, 269] Active devices have been shown to be capable of delivering liposomal formulations of water-soluble drugs as well,[270] demonstrating a superior performance when compared to air-jet and ultrasonic systems (greater physical stability and output rate).[216, 249] Manufacturer customization of the active vibrating-mesh with larger aperture sizes (8 μm as opposed to the commonly available 4 μm) have been shown to provide a lower extent of MLV liposome disruption than that of air-jet nebulization, but no significant difference when compared to the normal aperture size vibrating-mesh.[68, 249] Extrusion of MLV liposomes through 1 μm membrane filters improved drug output from large mesh aperture nebulizers, but further decrease in lamellarity (using a 0.4 μm filter) was not deemed beneficial.[68] Despite being able to better aerosolize drug suspensions than jet nebulizers, the delivery of nanoemulsions of budesonide demonstrates an even more pronounced improvement, with better drug output and fine particle fraction.[242] The drug particle size of nanosuspensions can be maintained for this particular aerosolization, including nanoparticles prepared using freeze-drying with different lyoprotectants.[271, 272]

Reconstitution of liposomal formulations with various hydration media provides differences in aerosolization performance of active vibrating-mesh nebulizers, based on the physicochemical properties of the medium.[273] Interestingly, the drug particle size increases have been observed in the nebulizer reservoir. This increase could indicate that aggregation and/or accumulation can occur due to a cutoff size of liposomes that may be

extruded through the mesh during aerosolization. Thus, formulation properties highly influence the nebulization performance of these devices. Therefore, it is imperative to evaluate many of the properties of the dispersion (e.g. drug particle size distribution, zeta potential, rheology, etc.) when considering aerosolization of this dosage form.

1.3.5. Colliding jets (Respimat®)

A compressed coiled spring positioned in the bottom of a liquid reservoir serves to store the energy necessary to operate this system. When the spring is released, the formulation is pushed through two precisely engineered nozzles (uniblock) positioned in a specific pre-set angle that allows liquid jets to converge and thus collide against each other. The uniblock is comprised of finely engineered microchannels that filter the solution prior to jet formation in the outlet nozzle. As a result, aerosols are generated at a slow speed. Hence, the name soft mist inhaler (SMI), which, based on the definition of conversion from liquid to aerosol droplet, can be considered a subcategory of nebulizers. It has been recently found that a high deposition of small particles in the mouthpiece occurs with the current Respimat® design, due to a zone of recirculation created around the nozzle outlet.[274, 275]

The rationale for developing this system was to overcome the disadvantages of other inhalers. The aerosol cloud lasts longer and travels slower (10 m/s for aqueous drug solutions) than aerosols generated by pressurized metered dose inhalers (pMDI) (50 m/s).[276] Other comparisons show that the mist generated from Respimat® can be up to ten times slower than pMDIs and last 1.2 to 1.6 seconds in the air.[277] The characteristic slow velocity mist avoids high drug deposition in the oropharynx and negates the need for patient synchronization as seen with all pMDI devices.[278] Mixing the concepts of the functional mechanism of nebulizers with the advantage of having a portable inhaler,

Respimat® is currently available for clinical use in Europe, but not approved for the United States yet.[279] It provides a multidose of 120 actuations that are precisely delivered[280] using this mechanical-powered platform. In addition to being independent on inspiratory effort (as observed in some dry powder inhaler systems), it is portable and user-friendly to patients.[32, 281]

Respimat® is designed to deliver drug solutions, but not dispersed systems.[282] Successful clinical trials in asthma patients with an aqueous solution containing ipratropium bromide and fenoterol hydrobromide led to the approval of Berodual®.[283, 284] Follow up studies demonstrated its efficacy and safety, despite the presence of benzalkonium chloride and EDTA in the formulation.[285, 286] In fact, Berodual® was shown to provide better efficiency in drug delivery to the lungs, and the nominal dose of the active ingredients could be decreased by 2- to 4-fold when using this device, compared to conventional DPI or pMDIs (with or without the use of spacers).[275, 287, 288] Similar results were found when treating Chronic Obstructive Pulmonary Disease (COPD) patients.[289-292] Inhalation solutions of tiotropium have been shown to be safe in asthma patients,[293] but an increased risk of mortality has been reported for COPD patients using Respimat®.[294] The high efficiency of this device also allows for the delivery of acidic solutions with pH values as low as 2.7, as well as ethanolic solutions, to be safely delivered to asthma patients without causing adverse events.[295, 296] The flexibility of this platform has allowed the use of a novel β_2 agonist solution (olodaterol) to be evaluated for pulmonary delivery using this technology in a hydroalcoholic mixture.[297]

Although, to our knowledge, there is no report on a systematic investigation, surface tension and viscosity of liquids may also play a role in the performance of this device. Analysis of an ethanolic solution of the steroid flunisolide showed a higher fine

particle fraction and slower aerosol cloud speed (7.5 m/s) than that of an aqueous solution of β_2 agonist fenoterol containing also benzalkonium chloride and Ethylenediaminetetraacetic acid (EDTA).[276] The physicochemical properties that result from the components utilized in each of the aforementioned formulations are likely to have been responsible for the apparent differences in nebulization performance. Finally, device handling is considered safe, with unintentional misuse being likely to show no harmful or unwanted side effects due to facial and/or ocular deposition.[298]

1.3.6. Extruded jets (Aer$_X^{TM}$ and Medspray®)

A three-layer laminate strip is assembled to form the unit dose package of this technology for the pulmonary delivery of aqueous formulations. The first layer contains a microvolume liquid reservoir blister that is heat sealed to the second (lid) layer. A nozzle array completes the third layer where micrometer holes are laser drilled. Index holes align the multilayer system, which is then connected to a handle to form a final assembled package (strip) fit to the device accordingly. During operation, a piston forces the first layer of the strip towards the nozzle array, a minimum pressure, dependent on the surface tension, is needed to impart the necessary velocity to the liquid jet stream. As the liquid ruptures the lid layer and rapidly extrudes through the microholes, liquid break up occurs. This break up is dependent on the liquid viscosity that generating the aerosol droplets.[299] This functioning mechanism produces a slow velocity mist and is commercialized as Aer$_X^{TM}$.

This technology is capable of aerosolizing solution dosage forms, including testosterone[300] and opioids[301, 302] (e.g. morphine[303-306] and fentanyl[307]) . An ethanolic formulation containing a poorly-water soluble prodrug candidate for pulmonary delivery was also successfully delivered using this device.[308] The prodrug had an

MMAD of 3 μm and a GSD of 1.3, with a pharmacokinetic study showing systemic absorption following pulmonary delivery comparable to that of intravenous administration. Patient posture, and breathing maneuver were not shown to influence the diffuse pattern in lung distribution of aerosols generated using this technology.[144] Despite its usual small volume reservoir (e.g. 45 μL), Aer$_X^{TM}$ is capable of delivering high doses of therapeutic agents in solution. Two inhalations from this system were twice as effective in delivering an inhaled drug candidate to the lungs as up to 15 minutes of aerosolization using conventional air-jet nebulizers. The superior performance can be attributed to the improved aerosol output (higher respirable dose) that the soft mist inhaler provides.[309]

Furthermore, protein solutions can also be aerosolized using the extruded jets mechanism. When an interleukin-4 receptor drug was aerosolized to the lungs, together with a radiolabelling compound in a saline solution, a higher peripheral deposition was found when compared to air-jet nebulization.[310] The higher peripheral deposition could be explained by differences in aerosol properties that showed MMAD values of 2.0 and 3.5 μm, and GSDs of 1.35 and 2.5, for the Aer$_X^{TM}$ and air-jet nebulizer respectively. Importantly, Aer$_X^{TM}$ delivered five times faster, three to four times more drug (relatively to their initial protein charge) than the air-jet system. Similar results were found when compared to a pMDI device for the deposition profile of a radiolabelling solution.[311] Importantly, bolus inhalation of dornase alfa using this extruded jets mechanism to treat cystic fibrosis patients may in the future be a possible alternative to the currently approved jet nebulizer systems.[312]

However, the possibility of macromolecule degradation must always be considered on a case-by-case basis. DNA-based drug products can be prone to degradation following extruded jet nebulization.[313] Plasmid DNA protected by

encapsulation in cationic lipids (lipoplexes) can avoid such degradation when this nonviral gene therapy formulation is aerosolized to the lungs using Aer$_X^{TM}$. Ion concentration plays an important role in production of aerosols via this mechanism due to suppression of electrostatic charges.[314] And the addition of sodium chloride to lipoplex formulations has shown an improved emitted dose.[313]

The possibility of delivering insulin to diabetes patients via the lungs is a subject that has been widely investigated.[315] Insulin solutions have also been delivered with this technology.[302, 316] In particular, this has been the only system used for inhaled insulin in liquid dosage form when most of the other attempts are with formulations in dry powder form.[210, 317] Recently, a long term study comparing prandial inhaled insulin compared to subcutaneous administration showed encouraging results.[318] In this insulin study using the iDMS technology, the authors concluded that, after one year, both routes of administration of insulin were comparably safe and efficacious, although further optimization was needed to avoid risk of nocturnal hypoglycemia with the inhaled dosage form.

When drug particles are in the nanoscale size range, this technology can also produce aerosol from dispersed systems. Solid lipid nanosuspensions of ketoprofen and indomethacin were prepared via supercritical fluid extraction of emulsions. Aerosolization using Aer$_X^{TM}$ and Aer$_X^{TM}$ Essence (electronically and mechanically controlled) produced fine particle fractions of 60-80% and emitted doses of 50-60%, which resulted in fine particle doses of approximately 40%.[319, 320] Importantly, suspensions of a few hundred nanometers were not as effectively delivered using micron-sized nozzle extruders as those suspensions with drug particle sizes below 100 nm.[319, 321] Sub-micron sized nozzle extruders are also being considered for development, in which viscosity and drug particle size of dispersions are expected to have a greater

impact on the aerosolization profile.[320] In addition, a miniaturized version of Aer$_X^{TM}$ has been developed and is due to be used in large animals (e.g. dogs).[322] This system might bring great value to future proof-of-concept studies for safety and tolerability of drug candidates for inhalation therapy.

Medspray® is a recently developed technology that applies the extruded jets principle from the Rayleigh break-up theory to produce aerosols.[323, 324] It is a hand-held, liquid metered dose inhaler in which lithography (wafer stepper and etching techniques) is used to engineer different micron sized spray nozzles. Following actuation by the patient, a loaded spring mechanically controls the release of the drug solution contained in a metering valve. As the liquid formulation is extruded through the spray nozzle, the patient's inspiratory flow pulls the formed droplets from a Venturi-like mouthpiece channel into the lungs. The device therefore requires some synchronization, with the patient pushing the drug release button a few seconds after initializing the inspiratory maneuver. On the other hand, since the aerosol production rate is controlled by the device (spring), it avoids dose emission variability that could be caused by differences in pressure and speed of actuation by a patient. A slow mist (4 m/s) is created at an inspiratory flow of 30 L/min by a patient. Weber further considered the influence of liquid viscosity on Rayleigh's basic analysis of jet instability to describe a relationship between water aerosol droplets and nozzle diameters.[323, 325] During the development phase of the Medspray® inhaler, nozzles of 1.5, 2.0, and 2.5 μm in diameter generated droplets with aerodynamic diameters of 4.0, 5.0, and 6.0 μm, respectively. Further studies showed that the larger droplets (6.0 μm) are more effective for improving the pulmonary function in asthmatic patients.[326]

1.3.7. Electrohydrodynamic mechanism (Mystic™)

A liquid is slowly fed to a positive potential, electronically-controlled capillary nozzle surrounded by a gas flow sheath. An electric field is then created between the nozzle and a counter-electrode; also positively charged, independently from the capillary nozzle. A Taylor cone-jet is formed between the capillary nozzle and the counter-electrode once the electrical stress outbalances the surface tension, generating charged droplets. Subsequently, a corona discharge controls the droplet charge generating a monodisperse aerosol.[327] This functioning mechanism is called electrohydrodynamic atomization (EHDA) or electrospray and has been recently adapted for pulmonary delivery of drugs.[328] Under the trade name Mystic™, it is currently being developed by the Battelle Memorial Institute.[329] This technique is also widely used in pharmaceutical applications for ionization in mass spectroscopy,[330] thin film formation[331, 332] and particle engineering.[333-336] Particularly, this technique can consistently produce highly monodisperse aerosols (with GSD values between 1.2 and 1.4).[337]

Control of certain variables during EHDA can greatly benefit the aerosol generation for inhalation purposes. Flow rate is directly related to droplet size while surface tension presents an inverse relationship.[327, 337] The surrounding gas sheath influences the electric breakdown threshold, preventing corona discharge at the tip of the nozzle. Utilization of a small concentration of carbon dioxide (0.5%) in the gas sheath helps stabilize the electrospray in cases when fluids of high surface tension (e.g. pure water) require a voltage greater than the electric breakdown threshold. Ion concentration can also help stabilize the electrospray and produce smaller droplet sizes. When adding low concentrations of sodium chloride (0.005% w/w) to pure water, increased water conductivity can be achieved while not affecting surface tension. Thus, electrical current

can flow more effectively, producing smaller particle sizes.[337] However, higher concentrations of NaCl can increase polydispersity, which can be a problem for pulmonary delivery of certain pharmaceutical preparations (e.g. isotonic solutions).[327] Viscosity also appears to influence aerosol generation with this mechanism, although systematic investigation is warranted.[337] Droplet charge control through the corona discharge system can avoid deposition in the oropharynx despite droplet size.[327] An increase in drug concentration can increase droplet size and polydispersity, but does not change MMAD and GSD values significantly over time for the same aerosolized system.[337]

Clinical trials using EHDA aerosol generation have shown the feasibility of delivering ethanolic solutions of beclomethasone dipropionate.[338] Interestingly, evaluation of monodisperse aerosols (GSD < 1.2) shows bioavailability of larger droplets (MMADs of 2.5 and 4.5 μm) to be greater than that of small droplet aerosols (MMAD of 1.5 μm). Additionally, this technology can produce aerosols from dispersed dosage forms.[339] Electrospraying of negatively charged nanoliposomes of DPPC, 1,2-Dipalmitoyl-sn-Glycerol-3-[Phospho-rac-(1-glycerol)] sodium salt (DPPGNa) and cholesterol presented a bimodal size distribution (35 and 100 nm) caused by different agglomeration patterns inside the capillary nozzle during aerosolization.[340] Head-to-tail and side-by-side juxtaposition were identified during aerosolization of suspensions with high lipid mass concentration. Notably, the characteristics of the dispersed system (i.e. drug particle size of nanosuspension) can influence the jet break-up characteristics.[341] Nevertheless, EHDA is a gentle technique that can be successfully used in the ionization of macromolecules for analysis with mass spectroscopy.[342, 343] Not surprisingly, large biomolecules are aerosolized with this mechanism without suffering thermal degradation, even at high concentrations of protein solutions.[344]

Very importantly, this technology has shown to be more effective for aerosol delivery of gene therapy than jet, ultrasonic, and vibrating-mesh nebulizers.[345]

1.3.8. Surface Acoustic Wave Microfluidic Atomization

Much like the traditional ultrasonic nebulizers, this novel technology uses propagating waves to generate aerosols. However, it is designed in a way that, instead of millimeter order wavelengths propagating through the bulk liquid, the nanometer amplitude Raleigh waves travel on the surface of a piezoelectric substrate at a much higher frequency (10-20 MHz).[346-348] The Surface Acoustic Wave (SAW) is therefore a highly efficient method to drive fluid motion. With a microsyringe pump continuously delivering a solution on top of the lithium niobate ($LiNbO_3$) substrate, the x-propagating acoustic waves generate aerosol from the formed capillary waves.[346] With a significantly more efficient energy transfer, a considerably lower energy input is required (1-3 W). A lower energy input results in the feasibility of a portable hand-held device.[349]

The droplet diameter during SAW atomization is directly proportional to surface tension and inversely proportional to the viscosity of liquids.[350] Due to the higher surface tension and lower viscosity, water produces larger droplets when compared to fluids like ethanol and octanol.[349] Ethanol and octanol have similar surface tensions (22-27 mN/m) but the latter presents a greater viscosity of 7.3 cP, compared to 1.1 cP. Aerosolization of octanol using SAW results in smaller droplets than with ethanol. Further development of this system could therefore be an alternative to jet nebulizers for aerosolization of highly viscous fluids due to the limitations described above for other nebulizer types (e.g. ultrasonic and vibrating-mesh). Of equal importance, the aerosol output is directly related to the power input, but its increase compromises droplet size and

dispersity.[351] In general, an optimal power input to produce aerosols for delivery to the deep lung at a reasonable rate has been shown to be around 1.5 watts.[349]

The delivery of large molecules is expected to be feasible since proteins have been shown to maintain their activity.[352, 353] Insulin solutions have been successfully aerosolized.[351] The SAW microfluidic process may be unsuitable for atomization of dispersed systems (i.e. suspensions) due to concentration of particles via nucleation templating.[354, 355] But this *a priori* disadvantage has further found an application in the production of pharmaceutical nanoparticles.[352, 356, 357]

1.3.9. Capillary Aerosol Generator (CAG)

In this aerosolization process, a liquid solution is pumped into one end of a heated micro-capillary. Once inside the tube, the formulation vaporizes before it exits from the other end where it mixes with the cooler surrounding air. This cooling causes the vapor to supersaturate and therefore initiate nucleation. A subsequent increase in droplet size occurs due to condensation of the surrounding vapor onto the formed nuclei, generating the desired aerosol for pulmonary delivery.[358, 359] The appropriate particle size can be achieved by controlling droplet coagulation using reservoir chambers.[360]

The surface tension and the viscosity of liquids appear to greatly influence the production of aerosols from CAG. Using a variety of vehicles, the values found for MMAD varied greatly, up to ten times.[361] Furthermore, both concentration and the physicochemical characteristics of solutes influence the aerosol generation.[362] Importantly, by dissolving benzil in propylene glycol, it has been shown that both evaporate and condensate simultaneously.[360] The aerosol droplet is also dependent on energy input, with trough in MMAD at about 40 Joules.[363] It is not feasible to aerosolize thermolabile substances using CAG, since the vapor jet temperature reaches

between 150 to 200 °C.[363] Studies with the antiemetic perphenazine dissolved in propylene glycol required a higher energy input (84-95 J), but still showed acceptable stability of this substance with the CAG aerosolization process.[364]

1.3.10. Characterization of Nebulizer Formulations

In spite of the great significance of nebulization therapy in clinical practice, very little has been done to standardize the characterization of nebulizer formulations. Assessment of the nebulizer device itself is available under a European Standard[365] and the European Respiratory Society presents guidelines on nebulization therapy.[205] Nebulizers were not covered, in the United States Pharmacopoeia (USP) General Chapter *<601> Aerosols, Nasal Sprays, Metered-Dose Inhalers, and Dry Powder Inhalers*. Only very recently, the first supplement of USP 34 – NF 29 brings the standardization of characterization tests for nebulizer products.

The General Chapter *<1601> Products for Nebulization – Characterization Test* of the USP now establishes, based on the dose delivered to a patient intrinsic to the formulation characteristics in conjunction with the device chosen (nebulizer system), two analyses for assessment of nebulization performance:

- Drug Substance Delivery Rate and Total Drug Substance Delivered (TDD); and
- Aerodynamic Assessment of Nebulized Aerosols.

The first test determines the rate and total amount of drug delivered. A breathing simulator is recommended to be used at specific airflow rates, established depending on the targeted patient population (neonates, infants, children or adults).[179] Instead of

continuous delivery, breathing patterns more appropriately measure drug mass output from nebulizers. In this analysis, a volume of formulation specified for therapy is filled to the nebulizer reservoir. The device, positioned as intended to use, is connected to a filter enclosed in a holder, which is then connected to the breathing simulator. The nebulization is started and, at regular intervals, the filter is substituted for a new one. The drug mass deposited in each filter is then suitably analyzed and used to calculate the results as follows:

$$R_i = \frac{m_i}{t_i} \qquad \text{(Equation 1.8)}$$

$$TDD = \sum_{i=1}^{n} m_i \qquad \text{(Equation 1.9)}$$

Where R_i, m_i, and t_i are the rate, the drug mass and the time interval used for collection at the i^{th} interval, respectively, and n is the total number of filters collected.

Among various cascade impactors, the Next Generation Impactor (NGI) is the apparatus recommended by the USP for assessment of aerodynamic droplet sizes from nebulizer systems, because it is a direct measurement of drug mass deposited based on aerodynamic droplet sizes.[33, 366-370] Alternatively, laser diffractometry is accepted for droplet size measurement specifically for homogeneous solutions, but not for dispersed systems or when significant droplet evaporation occurs.[39, 371] The test should be performed at airflow of 15 L/min and with a cooled impactor to avoid droplet evaporation.[110, 372, 373] The seven stages of the NGI therefore present the following cutoff diameters: 0.98, 1.36, 2.08, 3.30, 5.39, 8.61, and 14.1 μm. Besides the micro-orifice collector (MOC) plate, an external filter is also recommended to collect very small droplets. Plate coating to avoid droplet bounce and re-entrainment, and the use of a pre-

separator are unnecessary. Impactor stage overloading should be avoided by adequately establishing a feasible time interval for drug deposition during the test, a balancing capability with that of sensitivity of the analytical method employed to determine drug mass.

If a normal distribution of the deposited drug is observed, the MMAD and GSD can be determined from the log cutoff size versus probability scale (probit) of cumulative mass, starting at the MOC/external filter. Intercept of this curve identifies MMAD, since probit of 50% is equal to zero. GSD can be determined from the slope of the linear portion of the curve or as follows:

$$GSD = \sqrt{\frac{Size\ relative\ to\ 84.13\%\ deposition}{Size\ relative\ to\ 15.87\%\ deposition}} \qquad \text{(Equation 1.10)}$$

The mass fraction of drug deposited in each plate should also be presented, including the deposition in the induction port.

Nevertheless, the characterization of the physicochemical properties of the formulations is very important to help determine the factors influencing droplet formation from nebulization systems with different functioning mechanisms. There are innumerous methods available to measure surface tension, including the Capillary Rise and the Du Noüy ring methods.[374, 375] As described earlier in this chapter, our group has developed a simple and quick method using a texture analyzer.[376] Likewise, viscosity can be measured using various techniques such as: capillary (or Ostwald-Cannon-Fenske) viscometer, falling-sphere viscometer, and rotational (cup-and-bob, and cone-and-plate) viscometers.[377, 378]

When dispersed systems (e.g. suspensions, liposomes, etc.) are to be nebulized, it is very important to characterize the drug particles in bulk liquid in order to better

understand the nebulization performance based on the different mechanisms of aerosol generation from the appropriate devices.[379] Among the different methods, measurement of drug particle size and charge should be considered. Particle size and particle size distribution can be analyzed via laser diffraction or dynamic light scattering.[159] Measurement of zeta potential based on the principle of dynamic electrophoretic mobility can inform the magnitude of attraction or repulsion between particles.[380, 381] Very importantly, it should be considered that the rheology of dispersions (i.e. suspensions and emulsions) is much more complex than the simple measurement of viscosity for Newtonian fluids.[382, 383] Non-Newtonian behavior of fluids may be a factor influencing the nebulization performance of these systems depending on the type of nebulizer used. In addition, the aerosol output from these systems, based on gravimetrical analysis, may be misleading with respect to the real drug mass that is being aerosolized.

1.3.11. Conclusions

The technology to produce aerosols from liquid formulations for inhalation therapy has greatly evolved in a continuous manner from the traditional jet and ultrasonic nebulizers to emerging technologies based on techniques like surface acoustic waves, electrohydrodynamic atomization, and capillary aerosol generation. And smart technologies have further improved success through monitoring of patient adherence to therapy. The recent establishment of compendial characterization tests for nebulization products will greatly favor *in vitro* comparison of devices, which should ultimately translate into better *in vivo* efficiency. The physicochemical properties of the formulations in conjunction with the nebulizer design and mechanism of function greatly determines the aerosolization performance. Overwhelmingly it is surface tension and

viscosity that can highly influence these results and a greater understanding of their role in nebulization performance is a large part of the puzzle towards improved nebulization therapies.

1.4. TABLES

Drug	Use and Dosage Regimen[54]	Log P	Water Solubility[54]
Cisplatin	SCLC and NSCLC. Combination therapy: 75-100 mg/m^2; IV infusion once every 3-4 weeks.	-2.19 [384]	Soluble
Doxorubicin (HCl)	ED-SCLC. Monotherapy: 60-75 mg/m^2 single dose at 21 days interval; or 20 mg/m^2 once weekly; or 30 mg/m^2 daily on 3 successive days every 4 weeks. Combination therapy: 40-60 mg/m^2 single IV dose and repeated at 21- to 28-days intervals.	0.65 [385]	
Gemcitabine (HCl)	Advanced NSCLC and metastatic disease. Optimum dosage regimen not established. Commonly, for monotherapy: 1 or 1.25 g/m^2 30-min IV infusion once weekly for 3 weeks followed by 1 week of rest. Combination therapy: 1 g/m^2 once weekly for 3 weeks on 4-week cycle; or 1.25 g/m^2 once weekly for 2 weeks on 3-week cycle.	-1.24 [75]	
Etoposide	Not preferred chemotherapy for NSCLC. For SCLC, combination therapy: IV infusion ranging from 35 mg/m^2 daily for 4 consecutive days to 50 mg/m^2 daily for 5 consecutive days every 3-4 weeks. Alternatively, oral administration: twice the IV dosage rounded to the nearest 50 mg.	0.60 [384]	Sparingly soluble
5-Fluorouracil	Not a conventional treatment	-0.89 [384]	

Drug	Use and Dosage Regimen[54]	Log P	Water Solubility[54]
Farnesol	Not a conventional treatment	5.31 [88]	Very Slightly Soluble
Methotrexate	Recurrent SCLC and squamous cell type NSCLC. Not preferred chemotherapy option.	0.54 [385]	
Docetaxel	Advanced NSCLC: 75 mg/m^2 1-hour IV infusion once every 3 weeks	4.10 [386]	
Paclitaxel	For NSCLC, combination therapy: 135 mg/m^2 24-hour IV infusion or 175 mg/m^2 3-hour IV infusion with cycles repeated every 3 weeks. For SCLC, no survival benefits of adding paclitaxel to standard combination regimens (platinums and etoposide). Phase II studies presented only partial responses with monotherapy of 250 mg/m^2 24-hour IV infusion every 3 weeks or combination therapy of 175 mg/m^2 3-hour IV infusion every 3 weeks.	3.50 [387]	Practically insoluble
Celecoxib	Not a conventional treatment	3.68 [61]	
Nimesulide	Not a conventional treatment	2.60 [384]	

ED: extended disease; IV: intravenous; SCLC: small cell lung cancer; NSCLC: non-small cell lung cancer.

Table 1.1 - Use, dosage regimen and physicochemical properties of selected drugs to treat lung malignancies.

Drug	Dosage Form	Formulation	Device	MMAD test specification	MMAD (μm) / GSD	Cell Line	Medication Delivery (μg/shot)	Respirable Fraction (%)
Methotrexate [58]	Suspension	0.66% w/w in 10% w/w ethanol/HFA 134a. Drug co-milled with Poloxamer 217 (3:1).	pMDI	Six-stage viable Andersen Cascade Impactor at 28.3 L/min	2.2 to 3.2 / 2.7 to 3.7	HL-60 (leukemia)	29 to 52	14 to 17
Nimesulide [59]	Solution	0.1% w/w in 15% w/w ethanol/HFA 134a	Proventil HFA	Eight-stage Mark II Andersen Cascade Impactor at 28.3 L/min	1.1 ± 0.3 / 2.8 ± 0.6	A549 (lung cancer)	51.1 ± 3.3	42.4 ± 4.2
Celecoxib [60]	Solution	0.25-0.45% w/w in 10-15% w/w ethanol/HFA 134a or 227	Qvar80	Eight-stage Mark II Andersen Cascade Impactor at 28.3 L/min	1.3 to 1.4 / 1.9	A549 and H460 (lung cancer)	72 to 117	35 to 53
Doxorubicin [77]	Dry Powder	Drug loaded poly(butylcyanoacrylate) nanoparticles: 1.39 μg per mg powder. Carrier: lactose	Passive DPI	Mark II Andersen Cascade Impactor at 60 L/min	3.41 ± 0.22 / N/A	A549 and H460 (lung cancer)	N/A	N/A
Farnesol [90]	Emulsion	10.5 mg/mL of drug and polysorbate 80 (0.5 mg/mL) in 20% v/v ethanol/water	Pari LC Star® and Pari LC Plus® jet	Phase Doppler Anemometer coupled to breath simulator (airflow:	4.96 / 1.48 6.87 / 1.67	A549 and H460 (lung cancer)	N/A	N/A

Drug	Dosage Form	Formulation	Device	MMAD test specification	MMAD (μm) / GSD	Cell Line	Medication Delivery (μg/shot)	Respirable Fraction (%)
			nebulizers	18 L/min; tidal volume: 0.75 L)				
Paclitaxel [101]	Liposomes	Drug-fullerene (C_{60}) conjugation in DLPC	N/A	N/A	N/A	A549 (lung cancer)	N/A	N/A
Docetaxel [103]	Solution	0.25% w/w in 15% w/w ethanol/HFA 134a	Proventil HFA	Eight-stage Mark II Andersen Cascade Impactor at 28.3 L/min	1.58 ± 0.4 / 3.2 ± 0.5	A549 (lung cancer)	80.0 ± 2.3	42.2 ± 3.2
5-Fluorouracil [113]	Liposomes	Combinations of DPPC, HSPC, cholesterol, DPPA and DPPG.	N/A	N/A	N/A	N/A	N/A	N/A
	Polymer Microspheres	Combinations of PLGA, PLCL and PLA	N/A	N/A	N/A	N/A	N/A	N/A
	Lipid Coated Nanoparticles	Combinations of: Core: poly-(glutamic acid), poly-lysine, or lactose; Shell: tripalmitin, tristearin, cetyl alcohol, and stearyl alcohol.	N/A	N/A	N/A	N/A	N/A	N/A

MMAD: mass median aerodynamic diameter; GSD: geometric size distribution; HFA: hydrofluoroalkane; pMDI: pressurized metered dose inhaler; DPI: dry powder inhaler; DLPC: dilauroylphosphatidylcholine; DPPC: dipalmitoylphosphatidylcholine HSPC: hydrogenated soy phosphatidylcholine; DPPA: dipalmitoyl phosphatidic acid; DPPG: dipalmitoyl phosphatidylglycerol; PLGA: poly-(lactide-co-glycolide); PLCL: poly-(lactide-co-caprolactone); PLA: poly-(lactide); N/A: not available or not applicable.

Table 1.2 - Summary of *in vitro* studies of anticancer agents for pulmonary delivery.

Drug	Dosage Form	Formulation	Device	MMAD test specification	MMAD (μm) / GSD	Specie	Tumor Model	Dosing Method	Drug Deposition Estimative Method
Celecoxib [64]	Emulsion	5 mg/mL dissolved in ethanol and PEG 400. Emulsification with molten vitamin E TPGS	Jet nebulizer (Pari LC® Star)	Mercer Cascade Impactor (airflow rate not reported)	1.68 / 1.36	Mice	Human orthotopic NSCLC xenograft	Nose only inhalation chamber	Estimated dose
Gemcitabine [70-74]	Solution	Gemzar® (Eli Lilly)	Microsprayer + high pressure syringe	N/A	18 / 3	Mice	Human orthotopic NSCLC xenograft	Endotracheal spray	Scintigraphic images
			Jet nebulizer (AeroTech II®)	Andersen Cascade Impactor (airflow rate not reported)	0.8 / 2.1	Mice	Osteosarcoma lung metastases	Unrestrained chamber	Estimated dose
			Not specified	Andersen Cascade Impactor at 10 L/min	0.8 / 2.1	Dogs	Osteosarcoma lung metastases	Unrestrained outdoors	Not specified
			Microsprayer + high pressure syringe	N/A	18 / 3	Rats	N/A	Endotracheal spray	Scintigraphic images

Drug	Dosage Form	Formulation	Device	MMAD test specification	MMAD (μm) / GSD	Specie	Tumor Model	Dosing Method	Drug Deposition Estimative Method
			Jet nebulizer (Atomisor NL9M®) with Atomisor Abox+ compressor	Ten-stage cascade impactor (IMPAQ GS-1) operated at 1 L/min	3.7 / 0.8	Baboons	N/A	Inhalation cabin	Scintigraphic images
Doxorubicin [80]	Solution	16 mg/mL in 20% ethanol	Jet nebulizer (Pari LC®)	N/A	N/A	Dogs	Spontaneously occurring primary or metastatic lung tumors	Endotracheal tube (anesthesia)	Estimated dose (time, body surface area and minute-volume of respiration)
Paclitaxel	Solution [80]	75 mg/mL in PEG 200 and ethanol	Jet nebulizer (Pari LC®)	N/A	N/A	Dogs	Spontaneously occurring primary or metastatic lung tumors	Endotracheal tube (anesthesia)	Estimated dose (time, body surface area and minute-volume of respiration)
	Polymer Microspheres [94]	poly-(L-glutamic acid) (PGA) were loaded with 20% (w/w) paclitaxel	Jet nebulizer (8900, Salter Labs, USA)	Seven-stage cascade impactor (In-Tox Products) at 5 or 9 L/min	Not calculated	Mice	Human orthotopic NSCLC xenograft	Intratracheal injection	N/A

Drug	Dosage Form	Formulation	Device	MMAD test specification	MMAD (μm) / GSD	Specie	Tumor Model	Dosing Method	Drug Deposition Estimative Method
		(PGA-PTX)							
	Liposomes [96]	10 mg/mL with DLPC (1:10 w/w)	Jet nebulizer (Aeromist®)	Andersen Cascade Impactor at 10 L/min	2.2 / 1.9	Mice	Renal carcinoma lung metastases	Whole body inhalation chamber	Not reported
Camptothecin and Rubitecan (9NC) [47, 105, 106]	Liposomes	10 and 100 mg/mL with DLPC (1:50 w/w), respectively	Jet nebulizer (AeroTech II®)	Six-stage Andersen cascade impactor at 10 L/min	0.8 to 1.6 / 1.8 to 2.6	Mice	Human orthotopic NSCLC xenograft	Whole body and nose only inhalation chambers	Estimated dose
Rubitecan (9NC)	Liposomes [107]	DLPC (1:50 w/w)	Jet nebulizer (AeroTech II®)	Six-stage Andersen cascade impactor at 10 L/min	1.41 ± 0.29 / 2.37 ± 0.15 (average ± SD measured weekly over 53 days)	Beagle dogs	N/A	N/A	Estimated dose
	Liposomes [109]	soybean lecithin and cholesterol	N/A	N/A	N/A	Mice Rats	N/A	Intratracheal injection	N/A

Drug	Dosage Form	Formulation	Device	MMAD test specification	MMAD (μm) / GSD	Specie	Tumor Model	Dosing Method	Drug Deposition Estimative Method
5-Fluorouracil [115, 116]	Lipid Coated Nanoparticles	Core: 600 nm diameter poly-(glutamic acid):5-FU-FITC dextran (3:1:1 wt); Shell: 200 nm thick tripalmitin:cetyl alcohol (2:1 wt).	Ultrasonic nebulizer (model not specified)	Eight-stage Mark II Andersen cascade impactor (airflow rate not reported). Formulation droplets pre-evaporated.	1.15 / 2.15 0.95 / 1.57	Hamster	N/A	Intratracheal injection; and whole body and nose only inhalation chambers	Estimated dose

MMAD: mass median aerodynamic diameter; GSD: geometric standard deviation; SD: standard deviation; PEG: polyethylene glycol; PGA: poly-(L-glutamic acid); DLPC: dilauroylphosphatidylcholine; 5-FU: 5-fluorouracil; FITC: fluorescein isothiocyanate; N/A: not available or not applicable.

Table 1.3 - Preclinical (*in vivo*) studies of anticancer agents for pulmonary delivery.

Drug	Dosage Form	Study Phase	Formulation	Device	Population	Dose Calculation	Dose and Regimen	Outcomes
Doxorubicin [82]	Solution	I	16 and 24 mg/mL in ethanol:water 1:4 (pH 3).	Jet nebulizer (Pari LC Plus®) with OncoMyst™ model CDD-2a	Metastatic Tumors (n = 53)	Technetium 99m deposition test and scintigraphy	0.4 to 9.4 mg/m^2 every 3 weeks	No systemic toxicity; Dose limiting pulmonary toxicity: 7.5 mg/m^2 every 3 weeks; 1 partial response (spindle cell sarcoma) after 6^{th} cycle of 1.9 mg/m^2; 8 stable disease patients (2 bronchoalveolar carcinoma, 2 soft tissue sarcoma, 1 endometrial carcinoma and 3 thyroid cancer) after 5-15 cycles.
Rubitecan (9NC) [108]	Liposomes	I	0.2 mg/mL in DLPC (1:50 w/w)	Jet nebulizer (Aeromist®) with mouth breathing-only face mask and HEPA-filtered airborne scavenging tent	Primary or metastatic tumors (n = 25)	N/A	6.7 to 26.6 µg/kg/day, 5 days per week for 8 weeks	Dose limiting toxicity: 13.3 µg/kg/day, 5 days per week during 8 weeks; 2 partial remissions (uterine cancer); stable disease in 3 patients (primary lung cancer).
Cisplatin	Liposomes	I [111]	SLIT CPT (1 mg/mL), DPPC (1:16 w/w) and cholesterol (1:7.5 w/w) in 0.9%	Jet nebulizer (Pari LC Star®) with Pari filter® in Demistifier Canopy model 2000® tent	NSCLC (n = 16) and SCLC (n = 1)	Body Surface Area	Escalation from 1.5 mg/m^2 until DLT for 1-4 consecutive days every 1-3	Dose Limiting Toxicity not reached: increasing dose level (inhalation time: up to 8h), reducing interval between cycles, increasing number of nebulization

Drug	Dosage Form	Study Phase	Formulation	Device	Population	Dose Calculation	Dose and Regimen	Outcomes
			NaCl.				weeks	sessions per day, and increasing amount of drug inhaled; stable disease in 12 patients.
		Ib/IIa [112]	SLIT CPT (concentration not disclosed)	Nebulizer (not specified)	Relapse osteosarcoma metastasis (n = 14)	Body Surface Area	24 and 36 mg/m^2 every 2 weeks	Cumulative doses of 840 to 1020 mg per year in heavily pre-treated patients. Two patients with pulmonary disease free after 1 year.

DLPC: dilauroylphosphatidylcholine; DPPC: dipalmitoylphosphatidylcholine; SLIT: sustained-release lipid inhalation targeting; CPT: camptothecin; 9NC: 9-nitrocamptothecin or rubitecan; SCLC: small cell lung cancer; NSCLC: non-small cell lung cancer; HEPA: high efficiency particulate arresting; DLT: dose limiting toxicity; N/A: not available or not applicable.

Table 1.4 - Clinical studies of anticancer agents via inhalation.

1.5. FIGURES

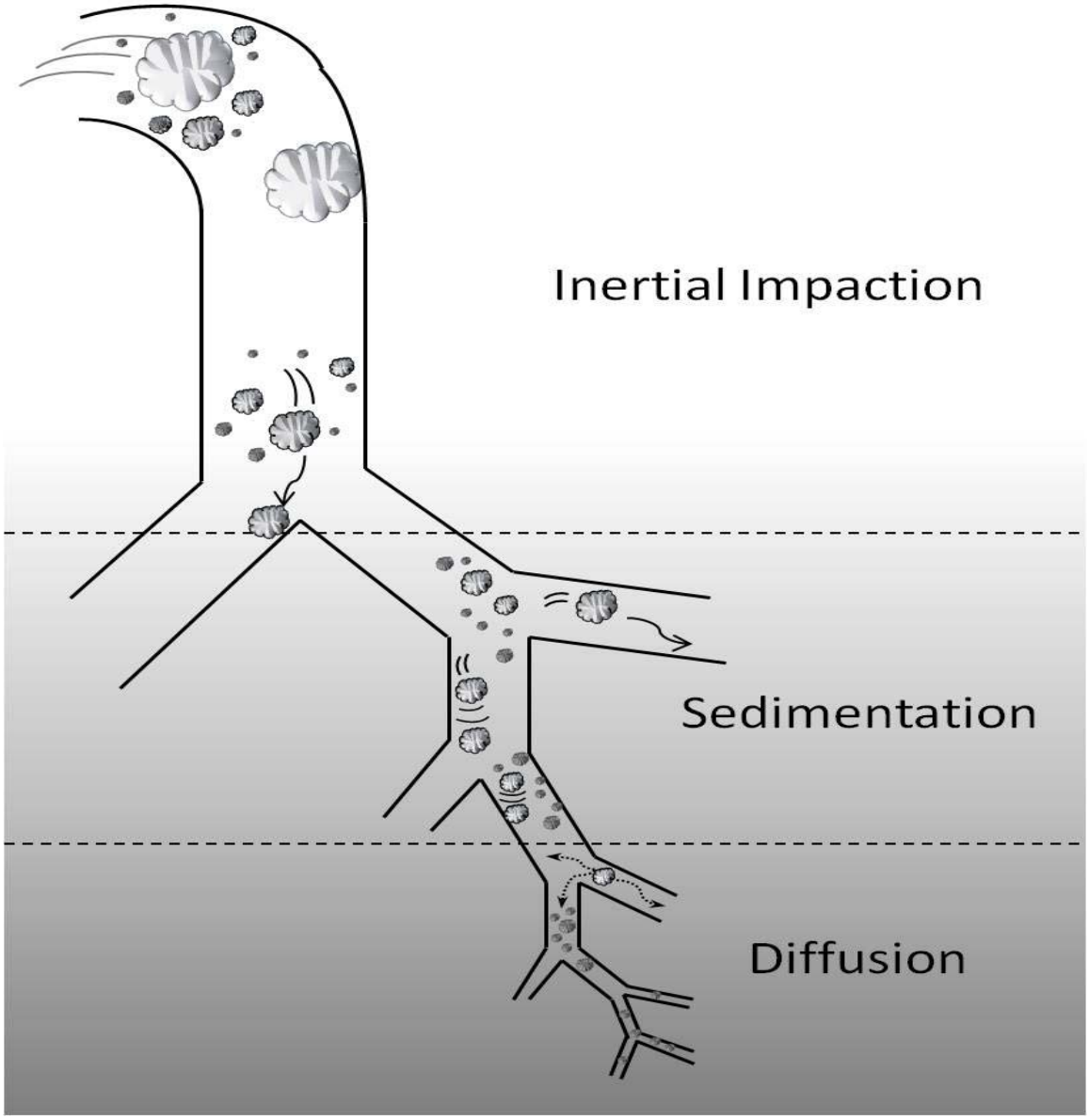

Figure 1.1 – Schematic diagram representing particle deposition in the lungs according to different mechanisms related to particle size: inertial impaction, sedimentation and diffusion. The diagram presents the smaller particles depositing in the lower airways as opposed to the larger airways. The GI tract is omitted in this diagram.

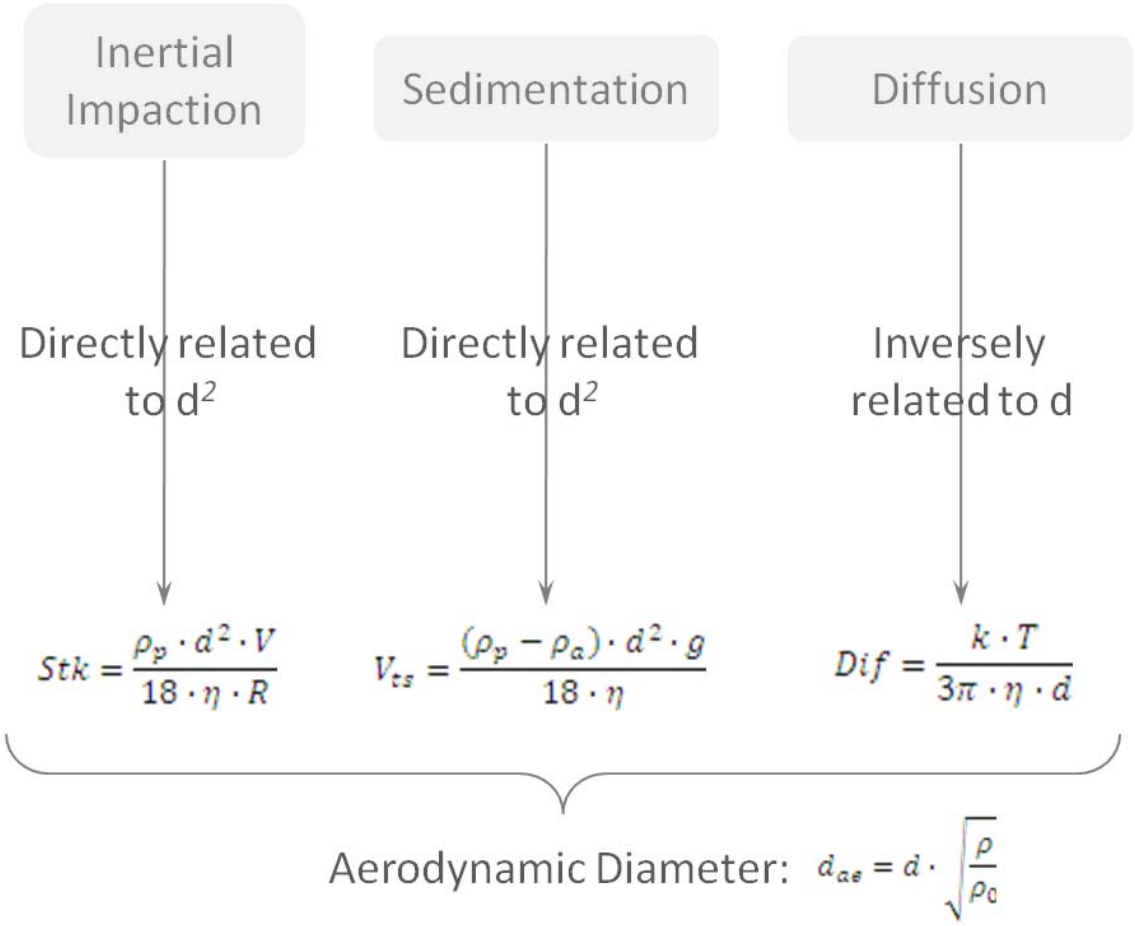

Figure 1.2 – The influence of particle size on deposition. *d*: particle diameter; *Stk*: Stokes number; ρ_p: particle density; *V*: air velocity; η: air viscosity; *R*: airway radius; V_{ts}: terminal settling velocity; ρ_a: air density; *g*: gravitational accelaration; *Dif*: diffusion coefficient; *k*: Boltzmann's constant; *T*: absolute temperature; d_{ae}: aerodynamic diameter; ρ_0: unity density.

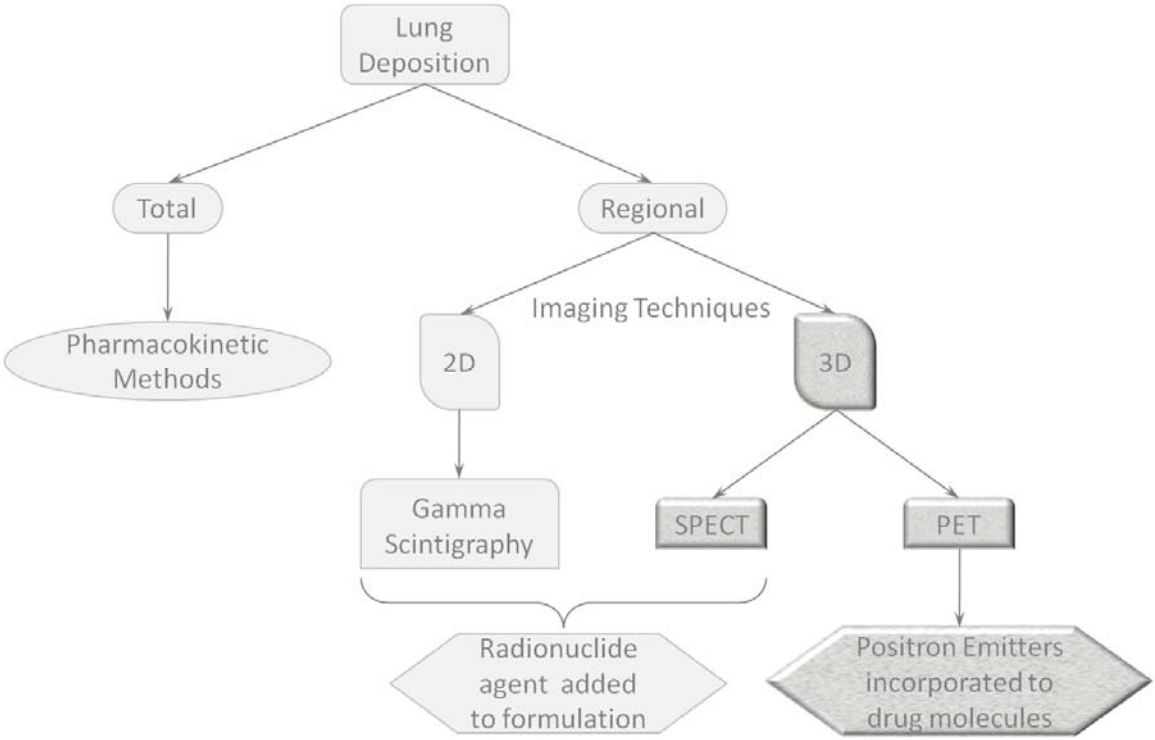

Figure 1.3 – Commonly used methods for assessment of regional lung deposition. 2D: two-dimensional; 3D: three-dimensional; SPECT: Single Photon Emission Computed Tomography; PET: Positron Emission Tomography.

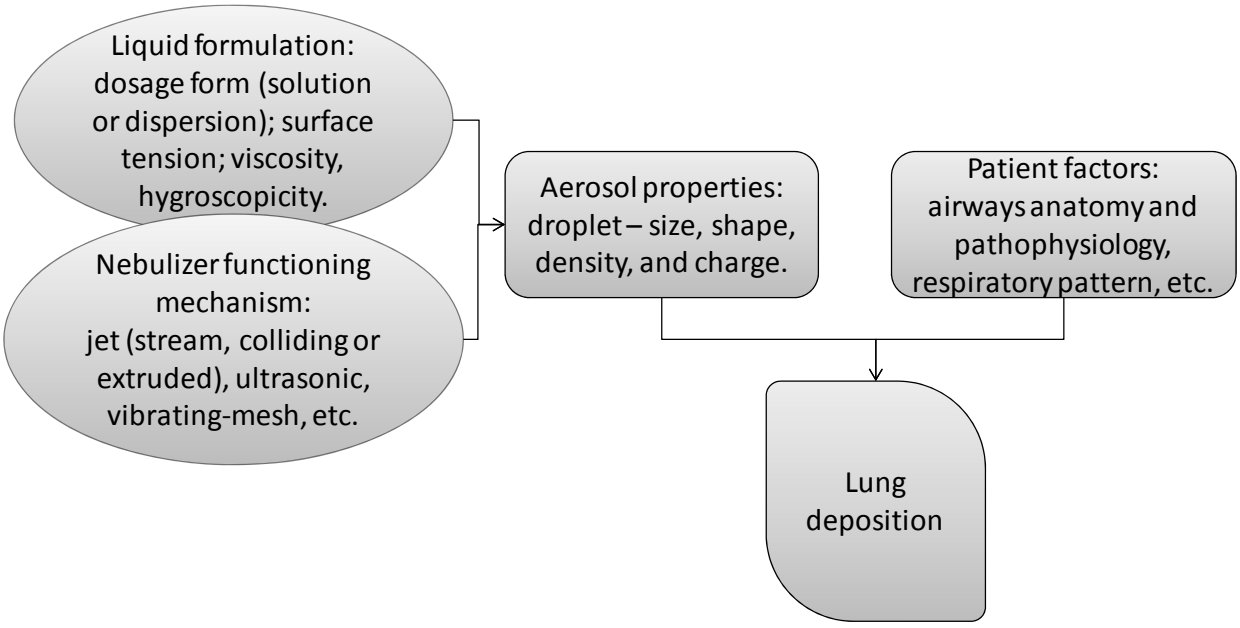

Figure 1.4 – Factors influencing lung deposition from nebulizer formulations.

1.6. REFERENCES

[1] Cancer Facts & Figures 2009: American Cancer Society; 2009.

[2] Cancer Facts & Figures 2008: American Cancer Society; 2008.

[3] Cancer Facts & Figures 2007: American Cancer Society; 2007.

[4] Alberg AJ, Samet JM. Epidemiology of lung cancer. Chest. 2003 Jan;123(1):21S-49S.

[5] Physicians Data Query (PDQ): Small Cell Lung Cancer Treatment (health professional version). 07/01/2009 [cited 02/22/2010]; Available from: http://www.cancer.gov/cancertopics/pdq/treatment/small-cell-lung/healthprofessional

[6] Govindan R, Page N, Morgensztern D, Read W, Tierney R, Vlahiotis A, et al.. Changing Epidemiology of Small-Cell Lung Cancer in the United States Over the Last 30 Years: Analysis of the Surveillance, Epidemiologic, and End Results Database. J Clin Oncol. 2006 October 1, 2006;24(28):4539-44.

[7] Physician Data Query (PDQ): Non-Small Cell Lung Cancer Treatment (health professional version). 02/05/2010 [cited 02/22/2010]; Available from: http://www.cancer.gov/cancertopics/pdq/treatment/non-small-cell-lung/healthprofessional

[8] Ballo MT, Ross MI, Cormier JN, Myers JN, Lee JE, Gershenwald JE, et al.. Combined-modality therapy for patients with regional nodal metastases from melanoma. Int J Radiat Oncol Biol Phys. 2006;64(1):106-13.

[9] Chen F, Fujinaga T, Sato K, Sonobe M, Shoji T, Sakai H, et al.. Clinical features of surgical resection for pulmonary metastasis from breast cancer. Ejso. 2009;35(4):393-7.

[10] Mountain CF. Revisions in the International System for Staging Lung Cancer. Chest. 1997 Jun;111(6):1710-7.

[11] Simon GR, Wagner H. Small cell lung cancer. Chest. 2003 Jan;123(1):259S-71S.

[12] Riedel RF, Crawford J. Small-cell lung cancer: a review of clinical trials. Semin Thorac Cardiovasc Surg. 2003;15(4):448-56.

[13] Davies AM, Lara PN, Lau DH, Gandara DR. Treatment of extensive small cell lung cancer. Hematol Oncol Clin N Am. 2004 Apr;18(2):373-85.

[14] Posther KE, Harpole DH. The surgical management of lung cancer. Cancer Invest. 2006;24(1):56-67.

[15] Fischer S, Darling G, Pierre AF, Sun A, Leight N, Waddell TK, et al.. Induction chemoradiation therapy followed by surgical resection for non-small cell lung cancer (NSCLC) invading the thoracic inlet. Eur J Cardiothorac Surg. 2008;33(6):1129-33.

[16] Hotta K, Matsuo K, Kiura K, Ueoka H, Tanimoto M. Advances in our understanding of postoperative adjuvant chemotherapy in resectable non-small-cell lung cancer. Curr Opin Oncol. 2006 Mar;18(2):144-50.

[17] Al Hebshi A, Al Hadab A. An overview of radiation therapy in the treatment of non-small-cell lung cancer. Annals of Thoracic Medicine. 2008;3(6):S89-S96.

[18] Erridge SC, Murray N. Thoracic radiotherapy for limited-stage small cell lung cancer: Issues of timing, volumes, dose, and fractionation. Semin Oncol. 2003 Feb;30(1):26-37.

[19] Faivre-Finn C, Lee LW, Lorigan P, West C, Thatcher N. Thoracic Radiotherapy for Limited-stage Small-cell Lung Cancer: Controversies and Future developments. Clin Oncol. 2005;17(8):591-8.

[20] De Ruysscher D, Vansteenkiste J. Chest radiotherapy in limited-stage small cell lung cancer: facts, questions, prospects. Radiother Oncol. 2000;55(1):1-9.

[21] Warde P, Payne D. DOES THORACIC IRRADIATION IMPROVE SURVIVAL AND LOCAL-CONTROL IN LIMITED-STAGE SMALL-CELL CARCINOMA OF THE LUNG - A METAANALYSIS. J Clin Oncol. 1992 Jun;10(6):890-5.

[22] Pignon JP, Arriagada R, Ihde DC, Johnson DH, Perry MC, Souhami RL, et al.. A METAANALYSIS OF THORACIC RADIOTHERAPY FOR SMALL-CELL LUNG-CANCER. N Engl J Med. 1992 Dec;327(23):1618-24.

[23] Kim CK, Lim SJ. Recent progress in drug delivery systems for anticancer agents. Arch Pharm Res. 2002 Jun;25(3):229-39.

[24] Marupudi NI, Han JE, Li KW, Renard VM, Tyler BM, Brem H. Paclitaxel: a review of adverse toxicities and novel delivery strategies. Expert Opin Drug Saf. 2007 Sep;6(5):609-21.

[25] Partridge AH, Avorn J, Wang PS, Winer EP. Adherence to therapy with oral antineoplastic agents. J Natl Cancer Inst. 2002;94(9):652-61.

[26] Hande KR. Etoposide: Four decades of development of a topoisomerase II inhibitor. Eur J Cancer. 1998;34(10):1514-21.

[27] Joel SP, Clark PI, Heap L, Webster L, Robbins S, Craft H, et al.. PHARMACOLOGICAL ATTEMPTS TO IMPROVE THE BIOAVAILABILITY OF ORAL ETOPOSIDE. Cancer Chemother Pharmacol. 1995 Nov-Dec;37(1-2):125-33.

[28] Vaughn JM, McConville JT, Burgess D, Peters JI, Johnston KP, Talbert RL, et al.. Single dose and multiple dose studies of itraconazole nanoparticles. Eur J Pharm Biopharm. 2006;63(2):95-102.

[29] Gagnadoux F, Hureaux J, Vecellio L, Urban T, Le Pape A, Valo I, et al.. Aerosolized chemotherapy. J Aerosol Med Pulm Drug Deliv. 2008 2008;21(1):61-70.

[30] Sharma S, White D, Imondi AR, Placke ME, Vail DM, Kris MG. Development of inhalational agents for oncologic use. J Clin Oncol. 2001 Mar;19(6):1839-47.

[31] Watts AB, McConville JT, Williams RO. Current therapies and technological advances in aqueous aerosol drug delivery. Drug Dev Ind Pharm. 2008;34(9):913-22.

[32] Son YJ, McConville JT. Advancements in dry powder delivery to the lung. Drug Dev Ind Pharm. 2008;34(9):948-59.

[33] Mitchell JP, Nagel MW. Cascade impactors for the size characterization of aerosols from medical inhalers: Their uses and limitations. J Aerosol Med-Depos Clear Eff Lung. 2003;16(4):341-+.

[34] Rytting E, Nguyen J, Wang XY, Kissel T. Biodegradable polymeric nanocarriers for pulmonary drug delivery. Expert Opin Drug Deliv. 2008;5(6):629-39.

[35] Shoyele SA, Cawthome S. Particle engineering techniques for inhaled biopharmaceuticals. Adv Drug Delivery Rev. 2006;58(9-10):1009-29.

[36] Phalen RF. The Respiractory Tract. In: Phalen RF, ed. *Inhalation Studies: Foundations and Techniques*. New York, NY, USA: Informa Health Care 2008:33-68.

[37] Labiris NR, Dolovich MB. Pulmonary drug delivery. Part I: Physiological factors affecting therapeutic effectiveness of aerosolized medications. Br J Clin Pharmacol. 2003;56(6):588-99.

[38] Newman SP, Chan HK. In vitro/in vivo comparisons in pulmonary drug delivery. Journal of Aerosol Medicine and Pulmonary Drug Delivery. 2008 Mar;21(1):77-84.

[39] de Boer AH, Gjaltema D, Hagedoorn P, Frijlink HW. Characterization of inhalation aerosols: a critical evaluation of cascade impactor analysis and laser diffraction technique. Int J Pharm. 2002;249(1-2):219-31.

[40] Ganguly S, Moolchandani V, Roche JA, Shapiro PS, Somaraju S, Eddington ND, et al.. Phospholipid-Induced In Vivo Particle Migration to Enhance Pulmonary Deposition. Journal of Aerosol Medicine and Pulmonary Drug Delivery. 2008;21(4):343-50.

[41] Yi D, Wiedmann TS. Inhalation Adjuvant Therapy for Lung Cancer. Journal of Aerosol Medicine and Pulmonary Drug Delivery. 2010:ahead of print.

[42] Ruenraroengsak P, Cook JM, Florence AT. Nanosystem drug targeting: Facing up to complex realities. J Controlled Release. 2009;141(3):265-76.

[43] Atkins PJ, Barker NP, Mathisen D. Drugs and the Pharmaceutical Sciences. In: Hickey AJ, ed. *Pharmaceutical Inhalation Aerosol Technology*. New York, New York, USA.: Marcel Dekker, Inc. 1992:155-85.

[44] Cryan S-A, Sivadas N, Garcia-Contreras L. In vivo animal models for drug delivery across the lung mucosal barrier. Adv Drug Delivery Rev. 2007;59(11):1133-51.

[45] Chrystyn H. Methods to identify drug deposition in the lungs following inhalation. Br J Clin Pharmacol. 2001;51(4):289-99.

[46] Dolovich MB. Drugs and the Pharmaceutical Sciences. In: Hickey AJ, ed. *Pharmaceutical Inhalation Aerosol Technology*. New York, New York, USA.: Marcel Dekker, Inc. 1992:171-213.

[47] Koshkina NV, Gilbert BE, Waldrep JC, Seryshev A, Knight V. Distribution of camptothecin after delivery as a liposome aerosol or following intramuscular injection in mice. Cancer Chemother Pharmacol. 1999 Sep;44(3):187-92.

[48] Phalen RF. In: Phalen RF, ed. *Inhalation Studies: Foundations and Techniques*. New York, NY, USA: Informa Health Care 2008:187-214.

[49] Koshkina NV, Knight V, Gilbert BE, Golunski E, Roberts L, Waldrep JC. Improved respiratory delivery of the anticancer drugs, camptothecin and paclitaxel, with 5% CO2-enriched air: pharmacokinetic studies. Cancer Chemother Pharmacol. 2001 May;47(5):451-6.

[50] Koshkina NV, Waldrep JC, Knight V. Camptothecins and lung cancer: Improved delivery systems by aerosol. Curr Cancer Drug Targets. 2003 August;3(4):251-64.

[51] Brown RA, Schanker LS. ABSORPTION OF AEROSOLIZED DRUGS FROM THE RAT LUNG. Drug Metab Dispos. 1983;11(4):355-60.

[52] Patton JS, Fishburn CS, Weers JG. The lungs as a portal of entry for systemic drug delivery. Proc Am Thorac Soc. 2004;1(4):338-44.

[53] Schanker LS, Less MJ. LUNG PH AND PULMONARY ABSORPTION OF NONVOLATILE DRUGS IN RAT. Drug Metab Dispos. 1977;5(2):174-8.

[54] In: McEvoy GK, ed. *American Hospital Formulary Service (AHFS) Drug Information® 2010*. Bethesda, MD: American Society of Health-System Pharmacists, Inc. 2010:902-1260.

[55] Montharu J, Le Guellec S, Kittel B, Rabemampianina Y, Guillemain J, Gauthier F, et al.. Evaluation of Lung Tolerance of Ethanol, Propylene Glycol, and Sorbitan Monooleate as Solvents in Medical Aerosols. Journal of Aerosol Medicine and Pulmonary Drug Delivery. 2010;23(1):41-6.

[56] Vaughn JM, Wiederhold NP, McConville JT, Coalson JJ, Talbert RL, Burgess DS, et al.. Murine airway histology and intracellular uptake of inhaled amorphous itraconazole. Int J Pharm. 2007 Jun;338(1-2):219-24.

[57] Mogalian E, Myrdal PB. In: Augustijns P, Brewster M, eds. *Solvent systems and their selection in pharmaceutics and biopharmaceutics*: Springer; AAPS PRESS 2007:427-41.

[58] Shaik MS, Haynes A, McSween J, Ikediobi O, Kanikkannan N, Singh M. Inhalation delivery of HFA-based metered dose anticancer agents via inhaler using methotrexate as a model drug. J Aerosol Med-Depos Clear Eff Lung. 2002 Fal;15(3):261-70.

[59] Haynes A, Shaik MS, Chatterjee A, Singh M. Evaluation of an aerosolized selective COX-2 inhibitor as a potentiator of doxorubicin in a non-small-cell lung cancer cell line. Pharm Res. 2003 Sep;20(9):1485-95.

[60] Haynes A, Shaik MS, Chatterjee A, Singh M. Formulation and evaluation of aerosolized celecoxib for the treatment of lung cancer. Pharm Res. 2005 Mar;22(3):427-39.

[61] Seedher N, Bhatia S. Solubility enhancement of Cox-2 inhibitors using various solvent systems. AAPS PharmSciTech. 2003;4(3):E33.

[62] Emmen HH, Hoogendijk EMG, Klopping-Ketelaars WAA, Muijser H, Duistermaat E, Ravensberg JC, et al.. Human safety and pharmacokinetics of the CFC alternative propellants HFC 134a (1,1,1,2-tetrafluoroethane) and HFC 227 (1,1,1,2,3,3,3-

heptafluoropropane) following whole-body exposure. Regul Toxicol Pharmacol. 2000;32(1):22-35.

[63] Myrdal PB, Karlage KL, Stein SW, Brown BA, Haynes A. Optimized dose delivery of the peptide cyclosporine using hydrofluoroalkane-based metered dose inhalers. J Pharm Sci. 2004 Apr;93(4):1054-61.

[64] Fulzele SV, Chatterjee A, Shaik MS, Jackson T, Singh M. Inhalation delivery and anti-tumor activity of celecoxib in human orthotopic non-small cell lung cancer xenograft model. Pharm Res. 2006 Sep;23(9):2094-106.

[65] Shaik MS, Chatterjee A, Jackson T, Singh M. Enhancement of antitumor activity of docetaxel by celecoxib in lung tumors. Int J Cancer. 2006 Jan;118(2):396-404.

[66] Dintaman JM, Silverman JA. Inhibition of P-glycoprotein by D-alpha-tocopheryl polyethylene glycol 1000 succinate (TPGS). Pharm Res. 1999;16(10):1550-6.

[67] Berger W, Setinek U, Hollaus P, Zidek T, Steiner E, Elbling L, et al.. Multidrug resistance markers P-glycoprotein, multidrug resistance protein 1, and lung resistance protein in non-small cell lung cancer: prognostic implications. J Cancer Res Clin Oncol. 2005;131(6):355-63.

[68] Elhissi AMA, Faizi M, Naji WF, Gill HS, Taylor KMG. Physical stability and aerosol properties of liposomes delivered using an air-jet nebulizer and a novel micropump device with large mesh apertures. Int J Pharm. 2007;334(1-2):62-70.

[69] Esteban E, Casillas M, Cassinello A. Pemetrexed in first-line treatment of non-small cell lung cancer. Cancer Treat Rev. 2009;35(4):364-73.

[70] Koshkina NV, Kleinerman ES. Aerosol gemcitabine inhibits the growth of primary osteosarcoma and osteosarcoma lung metastases. Int J Cancer. 2005 Sep;116(3):458-63.

[71] Gagnadoux F, Pape AL, Lemarie E, Lerondel S, Valo I, Leblond V, et al.. Aerosol delivery of chemotherapy in an orthotopic model of lung cancer. Eur Respir J. 2005 October 1, 2005;26(4):657-61.

[72] Gagnadoux F, Le Pape A, Urban T, Montharu J, Vecellio L, Dubus JC, et al.. Safety of pulmonary administration of gemcitabine in rats. J Aerosol Med-Depos Clear Eff Lung. 2005 Sum;18(2):198-206.

[73] Gagnadoux F, Leblond V, Vecellio L, Hureaux J, Le Pape A, Boisdron-Celle M, et al.. Gemcitabine aerosol: in vitro antitumor activity and deposition imaging for preclinical safety assessment in baboons. Cancer Chemother Pharmacol. 2006 Aug;58(2):237-44.

[74] Rodriguez CO, Crabbs TA, Wilson DW, Cannan VA, Skorupski KA, Gordon N, et al.. Aerosol Gemcitabine: Preclinical Safety and In Vivo Antitumor Activity in Osteosarcoma-Bearing Dogs. Journal of Aerosol Medicine and Pulmonary Drug Delivery. 2009.

[75] Stella B, Arpicco S, Rocco F, Marsaud V, Renoir JM, Cattel L, et al.. Encapsulation of gemcitabine lipophilic derivatives into polycyanoacrylate nanospheres and nanocapsules. Int J Pharm. 2007;344(1-2):71-7.

[76] Pili B, Bourgaux C, Meneau F, Couvreur P, Ollivon M. Interaction of an anticancer drug, gemcitabine, with phospholipid bilayers. J Therm Anal Calorim. 2009;98(1):19-28.

[77] Azarmi S, Tao X, Chen H, Wang Z, Finlay WH, Lobenberg R, et al.. Formulation and cytotoxicity of doxorubicin nanoparticles carried by dry powder aerosol particles. Int J Pharm. 2006;319(1-2):155-61.

[78] Rautio J, Chikhale PJ. Drug delivery systems for brain tumor therapy. Curr Pharm Des. 2004;10(12):1341-53.

[79] Kato T, Yashiro T, Murata Y, Herbert DC, Oshikawa K, Bando M, et al.. Evidence that exogenous substances can be phagocytized by alveolar epithelial cells and transported into blood capillaries. Cell Tissue Res. 2003 Jan;311(1):47-51.

[80] Hershey AE, Kurzman ID, Forrest LJ, Bohling CA, Stonerook M, Placke ME, et al.. Inhalation Chemotherapy for Macroscopic Primary or Metastatic Lung Tumors: Proof of Principle Using Dogs with Spontaneously Occurring Tumors as a Model. Clin Cancer Res. 1999 September 1, 1999;5(9):2653-9.

[81] McCallion ONM, Taylor KMG, Thomas M, Taylor AJ. Nebulization of Fluids of Different Physicochemical Properties with Air-Jet and Ultrasonic Nebulizers. Pharm Res. 1995 Nov;12(11):1682-8.

[82] Otterson GA, Villalona-Calero MA, Sharma S, Kris MG, Imondi A, Gerber M, et al.. Phase I study of inhaled doxorubicin for patients with metastatic tumors to the lungs. Clin Cancer Res. 2007 Feb;13(4):1246-52.

[83] Kleeberger L, Rottinger EM. EFFECT OF PH AND MODERATE HYPERTHERMIA ON DOXORUBICIN, EPIRUBICIN AND ACLACINOMYCIN-A CYTOTOXICITY FOR CHINESE-HAMSTER OVARY CELLS. Cancer Chemother Pharmacol. 1993;33(2):144-8.

[84] Lou YP, Lundberg JM. INHIBITION OF LOW PH EVOKED ACTIVATION OF AIRWAY SENSORY NERVES BY CAPSAZEPINE, A NOVEL CAPSAICIN-RECEPTOR ANTAGONIST. Biochem Biophys Res Commun. 1992;189(1):537-44.

[85] Simonsson BG, Jacobs FM, Nadel JA. ROLE OF AUTONOMIC NERVOUS SYSTEM AND COUGH REFLEX IN INCREASED RESPONSIVENESS OF AIRWAYS IN PATIENTS WITH OBSTRUCTIVE AIRWAY DISEASE. J Clin Invest. 1967;46(11):1812-&.

[86] Lalloo UG, Fox AJ, Belvisi MG, Chung KF, Barnes PJ. CAPSAZEPINE INHIBITS COUGH INDUCED BY CAPSAICIN AND CITRIC-ACID BUT NOT BY HYPERTONIC SALINE IN GUINEA-PIGS. J Appl Physiol. 1995;79(4):1082-7.

[87] Joo JH, Liao G, Collins JB, Grissom SF, Jetten AM. Farnesol-induced apoptosis in human lung carcinoma cells is coupled to the endoplasmic reticulum stress response. Cancer Res. 2007;67(16):7929-36.

[88] Cantrell CL, Franzblau SG, Fischer NH. Antimycobacterial plant terpenoids. Planta Med. 2001;67(8):685-94.

[89] Hornby JM, Jensen EC, Lisec AD, Tasto JJ, Jahnke B, Shoemaker R, et al.. Quorum sensing in the dimorphic fungus Candida albicans is mediated by farnesol. Appl Environ Microbiol. 2001;67(7):2982-92.

[90] Wang Z, Chen HT, Roa W, Finlay WH. Farnesol for aerosol inhalation: Nebulization and activity against human lung cancer cells. J Pharm Pharm Sci. 2003 Jan-Apr;6(1):95-100.

[91] Prokop RM, Finlay WH, Stapleton KW. AN IN-VITRO TECHNIQUE FOR CALCULATING THE REGIONAL DOSAGES OF DRUGS DELIVERED BY AN ULTRASONIC NEBULIZER. J Aerosol Sci. 1995;26(5):847-60.

[92] Nikander K, Turpeinen M, Wollmer P. The conventional ultrasonic nebulizer proved inefficient in nebulizing a suspension. J Aerosol Med-Depos Clear Eff Lung. 1999 Sum;12(2):47-53.

[93] Freiberg S, Zhu X. Polymer microspheres for controlled drug release. Int J Pharm. 2004;282(1-2):1-18.

[94] Zou Y, Fu H, Ghosh S, Farquhar D, Klostergaard J. Antitumor Activity of Hydrophilic Paclitaxel Copolymer Prodrug Using Locoregional Delivery in Human Orthotopic Non-Small Cell Lung Cancer Xenograft Models. Clin Cancer Res. 2004 November 1, 2004;10(21):7382-91.

[95] Gaspar MM, Bakowsky U, Ehrhardt C. Inhaled Liposomes-Current Strategies and Future Challenges. J Biomed Nanotechnol. 2008;4(3):245-57.

[96] Koshkina NV, Waldrep JC, Roberts LE, Golunski E, Melton S, Knight V. Paclitaxel Liposome Aerosol Treatment Induces Inhibition of Pulmonary Metastases in Murine Renal Carcinoma Model. Clin Cancer Res. 2001 October 1, 2001;7(10):3258-62.

[97] Sonnichsen DS, Liu Q, Schuetz EG, Schuetz JD, Pappo A, Relling MV. VARIABILITY IN HUMAN CYTOCHROME-P450 PACLITAXEL METABOLISM. J Pharmacol Exp Ther. 1995 Nov;275(2):566-75.

[98] Knight V, Koshkina NV, Golunski E, Roberts LE, Gilbert BE. Cyclosporin a aerosol improves the anticancer effect of Paclitaxel aerosol in mice. Trans Am Clin Climatol Assoc. 2004 2004;115:395-404.

[99] Zaru M, Mourtas S, Klepetsanis P, Fadda AM, Antimisiaris SG. Liposomes for drug delivery to the lungs by nebulization. Eur J Pharm Biopharm. 2007;67:655-66.

[100] Mabrey S, Sturtevant JM. INVESTIGATION OF PHASE-TRANSITIONS OF LIPIDS AND LIPID MIXTURES BY HIGH SENSITIVITY DIFFERENTIAL SCANNING CALORIMETRY. Proc Natl Acad Sci U S A. 1976;73(11):3862-6.

[101] Zakharian TY, Seryshev A, Sitharaman B, Gilbert BE, Knight V, Wilson LJ. A fullerene-paclitaxel chemotherapeutic: Synthesis, characterization, and study of biological activity in tissue culture. J Am Chem Soc. 2005 Sep;127(36):12508-9.

[102] Baker GL, Gupta A, Clark ML, Valenzuela BR, Staska LM, Harbo SJ, et al.. Inhalation toxicity and lung toxicokinetics of C-60 fullerene nanoparticles and microparticles. Toxicol Sci. 2008;101(1):122-31.

[103] Fulzele SV, Shaik MS, Chatterjee A, Singh M. Anti-cancer effect of celecoxib and aerosolized docetaxel against human non-small cell lung cancer cell line, A549. J Pharm Pharmacol. 2006;58:327-36.

[104] Hatefi A, Amsden B. Camptothecin delivery methods. Pharm Res. 2002 Oct;19(10):1389-99.

[105] Knight V, Koshkina NV, Waldrep JC, Giovanella BC, Gilbert BE. Anticancer exffect of 9-nitrocamptothecin liposome aerosol on human cancer xenografts in nude mice. Cancer Chemother Pharmacol. 1999 Sep;44(3):177-86.

[106] Knight V, Kleinerman ES, Waldrep JC, Giovanella BC, Gilbert BE, Koshkina NV. 9-Nitrocamptothecin Liposome Aerosol Treatment of Human Cancer Subcutaneous Xenografts and Pulmonary Cancer Metastases in Mice. Ann N Y Acad Sci. 2000;922(1):151-63.

[107] Gilbert BE, Seryshev A, Knight V, Brayton C. 9-nitrocamptothecin liposome aerosol: Lack of subacute toxicity in dogs. Inhal Toxicol. 2002 Feb;14(2):185-97.

[108] Verschraegen CF, Gilbert BE, Loyer E, Huaringa A, Walsh G, Newman RA, et al.. Clinical Evaluation of the Delivery and Safety of Aerosolized Liposomal 9-Nitro-20(S)-Camptothecin in Patients with Advanced Pulmonary Malignancies. Clin Cancer Res. 2004 April 1, 2004;10(7):2319-26.

[109] Zhang L-J, Xing B, Wu J, Xu B, Fang X-L. Biodistribution in mice and severity of damage in rat lungs following pulmonary delivery of 9-nitrocamptothecin liposomes. Pulm Pharmacol Ther. 2008 2008 (Epub 2007 May;21(1):239-46.

[110] Berg E, Svensson JO, Asking L. Determination of nebulizer droplet size distribution: A method based on impactor refrigeration. J Aerosol Med-Depos Clear Eff Lung. 2007;20(2):97-104.

[111] Wittgen BPH, Kunst PWA, van der Born K, van Wijk AW, Perkins W, Pilkiewicz FG, et al.. Phase I study of aerosolized SLIT cisplatin in the treatment of patients with carcinoma of the lung. Clin Cancer Res. 2007 Apr;13(8):2414-21.

[112] Chou AJ, Bell MD, Mackinson C, Gupta R, Meyers PA, Gorlick R. Phase Ib/IIa study of sustained release lipid inhalation targeting cisplatin by inhalation in the treatment of patients with relapsed/progressive osteosarcoma metastatic to the lung. J Clin Oncol (Meeting Abstracts). 2007;25(18_suppl):9525.

[113] Hitzman CJ, Elmquist WF, Wattenberg LW, Wiedmann TS. Development of a respirable, sustained release microcarrier for 5-fluorouracil I: In vitro assessment of liposomes, microspheres, and lipid coated nanoparticles. J Pharm Sci. 2006 May;95(5):1114-26.

[114] Fu YJ, Shyu SS, Su FH, Yu PC. Development of biodegradable co-poly(D,L-lactic/glycolic acid) microspheres for the controlled release of 5-FU by the spray drying method. Colloids and Surfaces B-Biointerfaces. 2002 Aug;25(4):269-79.

[115] Cory J. Hitzman WFETSW. Development of a respirable, sustained release microcarrier for 5-fluorouracil II: *In vitro* and *in vivo* optimization of lipid coated nanoparticles. J Pharm Sci. 2006;95(5):1127-43.

[116] Hitzman CJ, Wattenberg LW, Wiedmann TS. Pharmacokinetics of 5-fluorouracil in the hamster following inhalation delivery of lipid-coated nanoparticles. J Pharm Sci. 2006 Jun;95(6):1196-211.

[117] Gonda I. Targeting by Deposition. In: Hickey AJ, ed. *Pharmaceutical Inhalation Aerosol Technology*. New York, New York, USA.: Marcel Dekker, Inc. 2004:65-88.

[118] Zeng XM, Martin GP, Marriott C. Medicinal Aerosols. In: Zeng XM, Martin GP, Marriott C, eds. *Particulate interactions in dry powder formulations for inhalation*. New York, NY: Taylor & Francis 2001:65-102.

[119] Pilcer G, Amighi K. Formulation strategy and use of excipients in pulmonary drug delivery. Int J Pharm. 2010;392(1-2):1-19.

[120] Chow AHL, Tong HHY, Chattopadhyay P, Shekunov BY. Particle engineering for pulmonary drug delivery. Pharm Res. 2007;24(3):411-37.

[121] Dolovich MA. Influence of inspiratory flow rate, particle size, and airway caliber on aerosolized drug delivery to the lung. Respir Care. 2000;45(6):597-608.

[122] Crowder TM, Rosati JA, Schroeter JD, Hickey AJ, Martonen TB. Fundamental effects of particle morphology on lung delivery: Predictions of Stokes' law and the particular relevance to dry powder inhaler formulation and development. Pharm Res. 2002;19(3):239-45.

[123] Darquenne C, Prisk GK. Deposition of inhaled particles in the human lung is more peripheral in lunar than in normal gravity. Eur J Appl Physiol. 2008;103(6):687-95.

[124] Edwards DA, Hanes J, Caponetti G, Hrkach J, BenJebria A, Eskew ML, et al.. Large porous particles for pulmonary drug delivery. Science. 1997;276(5320):1868-71.

[125] Jaafar-Maalej C, Andrieu V, Elaissari A, Fessi H. Assessment methods of inhaled aerosols: technical aspects and applications. Expert Opin Drug Deliv. 2009;6(9):941-59.

[126] Pilcer G, Vanderbist F, Amighi K. Correlations between cascade impactor analysis and laser diffraction techniques for the determination of the particle size of aerosolised powder formulations. Int J Pharm. 2008;358(1-2):75-81.

[127] Martonen T, Fleming J, Schroeter J, Conway J, Hwang D. In silico modeling of asthma. Adv Drug Delivery Rev. 2003;55(7):829-49.

[128] Kleinstreuer C, Zhang Z, Donohue JF. Targeted drug-aerosol delivery in the human respiratory system. Annu Rev Biomed Eng. 2008;10:195-220.

[129] Rostami AA. Computational Modeling of Aerosol Deposition in Respiratory Tract: A Review. Inhal Toxicol. 2009;21(4):262-90.

[130] Balashazy I, Alfoldy B, Molnar AJ, Hofmann W, Szoke I, Kis E. Aerosol drug delivery optimization by computational methods for the characterization of total and regional deposition of therapeutic aerosols in the respiratory system. Curr Comput-Aided Drug Des. 2007 Mar;3(1):13-32.

[131] Koehler E, Sollich V, Schuster-Wonka R, Huehnerbein J. Lung Deposition in Cystic Fibrosis Patients Using an Ultrasonic or a Jet Nebulizer. J Aerosol Med. 2003;16(1):37-46.

[132] Moller W, Meyer G, Scheuch G, Kreyling WG, Bennett WD. Left-to-Right Asymmetry of Aerosol Deposition after Shallow Bolus Inhalation Depends on Lung Ventilation. Journal of Aerosol Medicine and Pulmonary Drug Delivery. 2009;22(4):333-9.

[133] Davis SS, Hardy JG, Newman SP, Wilding IR. GAMMA-SCINTIGRAPHY IN THE EVALUATION OF PHARMACEUTICAL DOSAGE FORMS. Eur J Nucl Med. 1992;19(11):971-86.

[134] Newman SP. Scintigraphic assessment of therapeutic aerosols. Crit Rev Ther Drug Carrier Syst. 1993;10(1):65-109.

[135] Newman S, Malik S, Hirst P, Pitcairn G, Heide A, Pabst J, et al.. Lung deposition of salbutamol in healthy human subjects from the MAGhaler dry powder inhaler. Respir Med. 2002 Dec;96(12):1026-32.

[136] Schmekel B, Hedenstrom H, Hedenstierna G. Deposition of terbutaline in the large or small airways: A single-center pilot study of ventilation-perfusion distributions and airway tone. Current Therapeutic Research-Clinical and Experimental. 2002;63(9):536-48.

[137] Coates AL, Green M, Leung K, Chan J, Ribeiro N, Louca E, et al.. Rapid pulmonary delivery of inhaled tobramycin for pseudomonas infection in cystic fibrosis: A pilot project. Pediatr Pulmonol. 2008 Aug;43(8):753-9.

[138] Clark A, Kuo MC, Newman S, Hirst P, Pitcairn G, Pickford M. A comparison of the pulmonary bioavailability of powder and liquid aerosol formulations of salmon calcitonin. Pharm Res. 2008;25(7):1583-90.

[139] Newman SP, Pitcairn GR, Hirst PH, Rankin L. Radionuclide imaging technologies and their use in evaluating asthma drug deposition in the lungs. Adv Drug Delivery Rev. 2003 Jul;55(7):851-67.

[140] Farr SJ. The physico-chemical basis of radiolabelling metered dose inhalers with Tc-99m. J Aerosol Med-Depos Clear Eff Lung. 1996;9:S27-S36.

[141] Newman SP, Wilding IR. Imaging techniques for assessing drug delivery in man. Pharm Sci Technol Today. 1999 May;2(5):181-9.

[142] Moller W, Felten K, Meyer G, Meyer P, Seitz J, Kreyling WG. Corrections in Dose Assessment of Tc-99m Radiolabeled Aerosol Particles Targeted to Central Human

Airways Using Planar Gamma Camera Imaging. Journal of Aerosol Medicine and Pulmonary Drug Delivery. 2009 Mar;22(1):45-54.

[143] Berridge MS, Lee ZH, Heald DL. Regional distribution and kinetics of inhaled pharmaceuticals. Curr Pharm Des. 2000 Nov;6(16):1631-51.

[144] Chan HK, Daviskas E, Eberl S, Robinson M, Bautovich G, Young I. Deposition of aqueous aerosol of technetium-99m diethylene triamine penta-acetic acid generated and delivered by a novel system (AER(x)) in healthy subjects. Eur J Nucl Med. 1999;26(4):320-7.

[145] Eberl S, Chan HK, Daviskas E. SPECT imaging for radioaerosol deposition and clearance studies. J Aerosol Med-Depos Clear Eff Lung. 2006;19(1):8-20.

[146] Fleming JS, Hashish AH, Conway JH, HartleyDavies R, Nassim MA, Guy MJ, et al.. A technique for simulating radionuclide images from the aerosol deposition pattern in the airway tree. J Aerosol Med-Depos Clear Eff Lung. 1997;10(3):199-212.

[147] Berridge MS, Heald DL, Lee Z. Imaging studies of biodistribution and kinetics in drug development. Drug Dev Res. 2003 Jun;59(2):208-26.

[148] Martonen T, Isaacs K, Hwang DM. Three-dimensional simulations of airways within human lungs. Cell Biochem Biophys. 2005;42(3):223-49.

[149] Martonen TB, Schroeter JD, Fleming JS. 3D in silico modeling of the human respiratory system for inhaled drug delivery and imaging analysis. J Pharm Sci. 2007 Mar;96(3):603-17.

[150] van Waarde A, Maas B, Doze P, Slart RH, Frijlink HW, Vaalburg W, et al.. Positron emission tomography studies of human airways using an inhaled beta-adrenoceptor antagonist, S-C-11-CGP 12388. Chest. 2005 Oct;128(4):3020-7.

[151] Berridge MS, Lee Z, Heald DL. Pulmonary distribution and kinetics of inhaled [C-11]triamcinolone acetonide. J Nucl Med. 2000 Oct;41(10):1603-11.

[152] Visser TJ, van Waarde A, Doze P, Elsinga PH, van der Mark TW, Kraan J, et al.. Characterisation of beta(2)-adrenoceptors, using the agonist [C-11]formoterol and positron emission tomography. Eur J Pharmacol. 1998;361(1):35-41.

[153] Guenther KJ, Yoganathan S, Garofalo R, Kawabata T, Strack T, Labiris R, et al.. Synthesis and in vitro evaluation of F-18- and F-19-labeled insulin: A new radiotracer for PET-based molecular imaging studies. J Med Chem. 2006;49(4):1466-74.

[154] Iozzo P, Osman S, Glaser M, Knickmeier M, Ferrannini E, Pike VW, et al.. In vivo imaging of insulin receptors by PET: preclinical evaluation of iodine-125 and iodine-124 labelled human insulin. Nucl Med Biol. 2002;29(1):73-82.

[155] Dolovich MB. 18F-fluorodeoxyglucose positron emission tomographic imaging of pulmonary functions, pathology, and drug delivery. Proc Am Thorac Soc. 2009;6(5):477-85.

[156] Dolovich M, Labiris R. Imaging drug delivery and drug responses in the lung. Proc Am Thorac Soc. 2004;1(4):329-37.

[157] Thorsson L, Kenyon C, Newman SP, Borgstrom L. Lung deposition of budesonide in asthmatics: a comparison of different formulations. Int J Pharm. 1998;168(1):119-27.

[158] Martin AR, Thompson RB, Finlay WH. MRI Measurement of Regional Lung Deposition in Mice Exposed Nose-Only to Nebulized Superparamagnetic Iron Oxide Nanoparticles. Journal of Aerosol Medicine and Pulmonary Drug Delivery. 2008;21(4):335-41.

[159] Shekunov BY, Chattopadhyay P, Tong HHY, Chow AHL. Particle size analysis in pharmaceutics: Principles, methods and applications. Pharm Res. 2007;24(2):203-27.

[160] Xie YY, Zeng PY, Siegel RA, Wiedmann TS, Hammer BE, Longest PW. Magnetic Deposition of Aerosols Composed of Aggregated Superparamagnetic Nanoparticles. Pharm Res. 2010;27(5):855-65.

[161] Stahlhofen W, Rudolf G, James AC. Intercomparison of Experimental Regional Aerosol Deposition Data. J Aerosol Med. 1989;2(3):285-308.

[162] Finlay WH. Particle Deposition in the Respiratory Tract. In: Finlay WH, ed. *The mechanics of inhaled pharmaceutical aerosols: an introduction*. San Diego, CA: Academic Press 2001:119-74.

[163] Hinds WC. Respiratory Deposition. In: Hinds WC, ed. *Aerosol technology: properties, behavior, and measurement of airborne particles*. second ed. New York: Wiley 1999:233-59.

[164] Meyer T, Muellinger B, Sommerer K, Scheuch G, Brand P, Beckmann H, et al.. Pulmonary deposition of monodisperse aerosols in patients with chronic obstructive pulmonary disease. Exp Lung Res. 2003;29(7):475-84.

[165] Smith JRH, Bailey MR, Etherington G, Shutt AL, Youngman MJ. Effect of particle size on slow particle clearance from the bronchial tree. Exp Lung Res. 2008 2008;34(6):287-312.

[166] Carroll N, Elliot J, Morton A, James A. THE STRUCTURE OF LARGE AND SMALL AIRWAYS IN NONFATAL AND FATAL ASTHMA. Am Rev Respir Dis. 1993 Feb;147(2):405-10.

[167] Zanen P, Go LT, Lammers JWJ. THE OPTIMAL PARTICLE-SIZE FOR PARASYMPATHICOLYTIC AEROSOLS IN MILD ASTHMATICS. Int J Pharm. 1995;114(1):111-5.

[168] Zanen P, Go LT, Lammers JWJ. Optimal particle size for beta(2) agonist and anticholinergic aerosols in patients with severe airflow obstruction. Thorax. 1996;51(10):977-80.

[169] Zanen P, Go LT, Lammers JWJ. The efficacy of a low-dose, monodisperse parasympathicolytic aerosol compared with a standard aerosol from a metered-dose inhaler. Eur J Clin Pharmacol. 1998;54(1):27-30.

[170] Martin RJ. Therapeutic significance of distal airway inflammation in asthma. J Allergy Clin Immunol. 2002 Feb;109(2):S447-S60.

[171] UNEP. The Montreal Protocol on substances that deplete the ozone layer. United Nations Environment Programme, Nairobi. 1987:54.

[172] Corren J, Tashkin DR. Evaluation of efficacy and safety of flunisolide hydrofluoroalkane for the treatment of asthma. Clin Ther. 2003 Mar;25(3):776-98.

[173] Vanden Burgt JA, Busse WW, Martin RJ, Szefler SJ, Donnell D. Efficacy and safety overview of a new inhaled corticosteroid, QVAR (hydrofluoroalkane-beclomethasone extrafine inhalation aerosol), in asthma. J Allergy Clin Immunol. 2000;106(6):1209-26.

[174] Leach CL, Davidson PJ, Hasselquist BE, Boudreau RJ. Influence of particle size and patient dosing technique on lung deposition of HFA-beclomethasone from a metered dose inhaler. J Aerosol Med-Depos Clear Eff Lung. 2005;18(4):379-85.

[175] Leach CL, Davidson PJ, Boudreau RJ. Improved airway targeting with the CFC-free HFA-beclomethasone metered-dose inhaler compared with CFC-beclomethasone. Eur Respir J. 1998;12(6):1346-53.

[176] Pickering H, Pitcairn GR, Hirst PH, Bacon RE, Newman SP, Affrime MB, et al.. Regional lung deposition of a technetium 99m-labeled formulation of mometasone furoate administered by hydrofluoroalkane 227 metered-dose inhaler. Clin Ther. 2000 Dec;22(12):1483-93.

[177] Labiris NR, Dolovich MB. Pulmonary drug delivery. Part II: The role of inhalant delivery devices and drug formulations in therapeutic effectiveness of aerosolized medications. Br J Clin Pharmacol. 2003;56(6):600-12.

[178] Gurses BK, Smaldone GC. Effect of tubing deposition, breathing pattern, and temperature on aerosol mass distribution measured by cascade impactor. J Aerosol Med-Depos Clear Eff Lung. 2003;16(4):387-94.

[179] Sangwan S, Condos R, Smaldone GC. Lung deposition and respirable mass during wet nebulization. J Aerosol Med-Depos Clear Eff Lung. 2003;16(4):379-86.

[180] Usmani OS, Biddiscombe MF, Barnes PJ. Regional lung deposition and bronchodilator response as a function of beta(2)-agonist particle size. Am J Respir Crit Care Med. 2005;172(12):1497-504.

[181] Brand P, Haussinger K, Meyer T, Scheuch G, Schulz H, Selzer T, et al.. Intrapulmonary distribution of deposited particles. J Aerosol Med-Depos Clear Eff Lung. 1999 Win;12(4):275-84.

[182] Eberl S, Chan HK, Daviskas E, Constable C, Young I. Aerosol deposition and clearance measurement: a novel technique using dynamic SPET. Eur J Nucl Med. 2001;28(9):1365-72.

[183] Chan HK, Eberl S, Daviskas E, Constable C, Young I. Changes in lung deposition of aerosols due to hygroscopic growth: A fast SPECT study. J Aerosol Med-Depos Clear Eff Lung. 2002;15(3):307-11.

[184] Glover W, Chan H-K, Eberl S, Daviskas E, Verschuer J. Effect of particle size of dry powder mannitol on the lung deposition in healthy volunteers. Int J Pharm. 2008 2008 Feb 12 (Epub 2007 Aug;349(1-2):314-22.

[185] Glover W, Chan HK, Eberl S, Daviskas E, Anderson S. Lung deposition of mannitol powder aerosol in healthy subjects. J Aerosol Med-Depos Clear Eff Lung. 2006;19(4):522-32.

[186] Meyer T, Brand P, Ehlich H, Kobrich R, Meyer G, Riedinger F, et al.. Deposition of Foradil P in human lungs: Comparison of in vitro and in vivo data. J Aerosol Med-Depos Clear Eff Lung. 2004;17(1):43-9.

[187] NIOSH. Strategic Plan for NIOSH Nanotechnology Research and Guidance - Filling the Knowledge Gap. Nanotechnology Research Program, Centers for Disease Control and Prevention, National Institute for Occupational Safety and Health 2005:103.

[188] Ruzer LS, Apte MG. Unattached radon progeny as an experimental tool for dosimetry of nanoaerosols: Proposed method and research strategy. Inhal Toxicol. 2010;22(9):760-6.

[189] Butterweck G, Vezzu G, Schuler C, Muller R, Marsh JW, Thrift S, et al.. In vivo measurement of unattached radon progeny deposited in the human respiratory tract. Radiat Prot Dosimetry. 2001;94(3):247-50.

[190] Bhavna, Ahmad FJ, Mittal G, Jain GK, Malhotra G, Khar RK, et al.. Nano-salbutamol dry powder inhalation: A new approach for treating broncho-constrictive conditions. Eur J Pharm Biopharm. 2009 Feb;71(2):282-91.

[191] Kim CS, Jaques PA. Total lung deposition of ultrafine particles in elderly subjects during controlled breathing. Inhal Toxicol. 2005;17(7-8):387-99.

[192] Miller FJ, Mercer RR, Crapo JD. LOWER RESPIRATORY-TRACT STRUCTURE OF LABORATORY-ANIMALS AND HUMANS - DOSIMETRY IMPLICATIONS. Aerosol Sci Technol. 1993;18(3):257-71.

[193] Schlesinger RB. COMPARATIVE DEPOSITION OF INHALED AEROSOLS IN EXPERIMENTAL-ANIMALS AND HUMANS - A REVIEW. J Toxicol Environ Health. 1985;15(2):197-214.

[194] Cheng YS, Irshad H, Kuehl P, Holmes TD, Sherwood R, Hobbs CH. Lung Deposition of Droplet Aerosols in Monkeys. Inhal Toxicol. 2008;20(11):1029-36.

[195] Windt H, Kock H, Runge F, Hubel U, Koch W. Particle deposition in the lung of the Gottingen minipig. Inhal Toxicol. 2010;22(10):828-34.

[196] Yi D, Price A, Panoskaltsis-Mortari A, Naqwi A, Wiedmann TS. Measurement of the distribution of aerosols among mouse lobes by fluorescent imaging. Anal Biochem. 2010;403(1-2):88-93.

[197] Schuepp KG, Straub D, Moller A, Wildhaber JH. Deposition of aerosols in infants and children. J Aerosol Med-Depos Clear Eff Lung. 2004;17(2):153-6.

[198] Amirav I, Newhouse MT, Minocchieri S, Castro-Rodriguez JA, Schuepp KG. Factors that affect the efficacy of inhaled corticosteroids for infants and young children. J Allergy Clin Immunol. 2010 Jun;125(6):1206-11.

[199] Schuepp KG, Devadason S, Roller C, Wildbaber JH. A complementary combination of delivery device and drug formulation for inhalation therapy in preschool children. Swiss Med Wkly. 2004;134(13-14):198-200.

[200] Mallol J, Rattray S, Walker G, Cook D, Robertson CF. Aerosol deposition in infants with cystic fibrosis. Pediatr Pulmonol. 1996;21(5):276-81.

[201] Haughney J, Price D, Barnes NC, Virchow JC, Roche N, Chrystyn H. Choosing inhaler devices for people with asthma: current knowledge and outstanding research needs. Respir Med. 2010;104(9):1237-45.

[202] Malcolmson RJ, Embleton JK. Dry powder formulations for pulmonary delivery. Pharm Sci Technol Today. 1998;1(9):394-8.

[203] Usmani OS. Delivery of drugs to the airways. In: Usmani OS, ed. *Lung Biol Health Dis* 2009:143-61.

[204] Tillery M, Buchan R. Determination of large aerosol particle size by elutriation. Appl Occup Environ Hyg. 2002 2002;17(10):717-22.

[205] Boe J, Dennis JH, O'Driscoll BR. European Respiratory Society Guidelines on the use of nebulizers. Eur Respir J. 2001;18(1):228-42.

[206] Leung K, Louca D, Coates AL. Comparison of breath-enhanced to breath-actuated nebulizers for rate, consistency, and efficiency. Chest. 2004 Nov;126(5):1619-27.

[207] Denyer J, Dyche T. The Adaptive Aerosol Delivery (AAD) Technology: Past, Present, and Future. Journal of Aerosol Medicine and Pulmonary Drug Delivery. 2010 Apr;23:S1-S10.

[208] Hardaker LEA, Hatley RHM. In Vitro Characterization of the I-neb Adaptive Aerosol Delivery (AAD) System. Journal of Aerosol Medicine and Pulmonary Drug Delivery. 2010 Apr;23:S11-S20.

[209] Geller DE. The science of aerosol delivery in cystic fibrosis. Pediatr Pulmonol. 2008 Sep;43(9):S5-S17.

[210] Mudaliar S. Inhaled insulin using AERx (R) insulin diabetes management system (AERx (R) iDMS). Expert Opin Investig Drugs. 2007 Oct;16(10):1673-81.

[211] Owens DR, Zinman B, Bolli G. Alternative routes of insulin delivery. Diabet Med. 2003 Nov;20(11):886-98.

[212] Julius SM, Sherman JM, Hendeles L. Accuracy of three electronic monitors for metered-dose inhalers. Chest. 2002 Mar;121(3):871-6.

[213] Carvalho TC, Peters JI, Williams III RO. Influence of particle size on regional lung deposition - What evidence is there? Int J Pharm. 2011;406(1-2):1-10.

[214] Ocallaghan C, Clarke AR, Milner AD. Inaccurate Calculation of Drug Output from Nebulizers. Eur J Pediatr. 1989 Feb;148(5):473-4.

[215] Thi THH, Azaroual N, Flament MP. Characterization and in vitro evaluation of the formoterol/cyclodextrin complex for pulmonary administration by nebulization. Eur J Pharm Biopharm. 2009 May;72(1):214-8.

[216] Elhissi AMA, Taylor KMG. Delivery of liposomes generated from proliposomes using air-jet, ultrasonic, and vibrating-mesh nebulisers. Journal of Drug Delivery Science and Technology. 2005;15(4):261-5.

[217] McCallion ONM, Taylor KMG, Bridges PA, Thomas M, Taylor AJ. Jet nebulisers for pulmonary drug delivery. Int J Pharm. 1996 Mar;130(1):1-11.

[218] Mercer TT. Production of Therapeutic Aerosols - Principles and Techniques. Chest. 1981;80(6):813-8.

[219] Smith EC, Denyer J, Kendrick AH. Comparison of 23 Nebulizer Compressor Combinations for Domiciliary Use. Eur Respir J. 1995;8(7):1214-21.

[220] Bendstrup KE, Newhouse MT, Pedersen OF, Jensen JI. Characterization of heparin aerosols generated in jet and ultrasonic nebulizers. J Aerosol Med-Depos Clear Eff Lung. 1999 Spr;12(1):17-25.

[221] Coates AL, MacNeish CF, Meisner D, Kelemen S, Thibert R, MacDonald J, et al.. The choice of jet nebulizer, nebulizing flow, and addition of albuterol affects the output of tobramycin aerosols. Chest. 1997 May;111(5):1206-12.

[222] Arzhavitina A, Steckel H. Surface active drugs significantly alter the drug output rate from medical nebulizers. Int J Pharm. 2010;384(1-2):128-36.

[223] Sood BG, Peterson J, Malian M, Galli R, Geisor-Walter M, McKinnon J, et al.. Jet nebulization of prostaglandin E-1 during neonatal mechanical ventilation: Stability, emitted dose and aerosol particle size. Pharmacol Res. 2007 Dec;56(6):531-41.

[224] MacNeish CF, Meisner D, Thibert R, Kelemen S, Vadas EB, Coates AL. A comparison of pulmonary availability between ventolin (albuterol) nebules and ventolin (albuterol) respirator solution. Chest. 1997 Jan;111(1):204-8.

[225] Steckel H, Eskandar F. Factors affecting aerosol performance during nebulization with jet and ultrasonic nebulizers. Eur J Pharm Sci. 2003 Aug;19(5):443-55.

[226] McCallion ONM, Taylor KMG, Thomas M, Taylor AJ. The influence of surface tension on aerosols produced by medical nebulisers. Int J Pharm. 1996;129(1-2):123-36.

[227] McCallion ONM, Patel MJ. Viscosity effects on nebulisation of aqueous solutions. Int J Pharm. 1996;130(2):245-9.

[228] Diot P, Palmer LB, Smaldone A, deCelieGermana J, Grimson R, Smaldone GC. RhDNase I aerosol deposition and related factors in cystic fibrosis. Am J Respir Crit Care Med. 1997 Nov;156(5):1662-8.

[229] Johnson JC, Waldrep JC, Guo J, Dhand R. Aerosol Delivery of Recombinant Human DNase I: In Vitro Comparison of a Vibrating-Mesh Nebulizer With a Jet Nebulizer. Respir Care. 2008 Dec;53(12):1703-8.

[230] Fiel SB, Fuchs HJ, Johnson C, Gonda I, Clark AR, Cipolla CC, et al.. Comparison of Three Jet Nebulizer Aerosol Delivery Systems used to Administer Recombinant Human DNase-I to Patients with Cystic Fibrosis. Chest. 1995 Jul;108(1):153-6.

[231] Geller DE, Eigen H, Fiel SB, Clark A, Lamarre AP, Johnson CA, et al.. Effect of smaller droplet size of dornase alfa on lung function in mild cystic fibrosis. Pediatr Pulmonol. 1998 Feb;25(2):83-7.

[232] Niven RW, Prestrelski SJ, Treuheit MJ, Ip AY, Arakawa T. Protein nebulization .2. Stabilization of G-CSF to air-jet nebulization and the role of protectants. Int J Pharm. 1996 Feb;127(2):191-201.

[233] Albasarah YY, Somavarapu S, Taylor KMG. Stabilizing protein formulations during air-jet nebulization. Int J Pharm. 2010 Dec 15;402(1-2):140-5.

[234] Chang LQ, Pikal MJ. Mechanisms of Protein Stabilization in the Solid State. J Pharm Sci. 2009 Sep;98(9):2886-908.

[235] Steckel H, Eskandar F, Witthohn K. Effect of cryoprotectants on the stability and aerosol performance of nebulized aviscumine, a 57-kDa protein. Eur J Pharm Biopharm. 2003 Jul;56(1):11-21.

[236] Flament MP, Leterme P, Burnouf T, Gayot A. Influence of formulation on jet nebulisation quality of alpha(1) protease inhibitor. Int J Pharm. 1999 Feb;178(1):101-9.

[237] Terzano C, Ricci A, Burinschi V, Nekam K, Lahovsky J. Comparison of the efficacy of beclometasone dipropionate and fluticasone propionate suspensions for nebulization in adult patients with persistent asthma. Respir Med. 2003 Feb;97:S35-S40.

[238] Barry PW, O'Callaghan C. An in vitro analysis of the output of budesonide from different nebulizers. J Allergy Clin Immunol. 1999 Dec;104(6):1168-73.

[239] Dahlstrom K, Thorsson L, Larsson P, Nikander K. Systemic availability and lung deposition of budesonide via three different nebulizers in adults. Annals of Allergy,

Asthma & Immunology: Official Publication of the American College of Allergy, Asthma, & Immunology. 2003;90(2):226-32.

[240] Berg EB, Picard RJ. In Vitro Delivery of Budesonide From 30 Jet Nebulizer/Compressor Combinations Using Infant and Child Breathing Patterns. Respir Care. 2009 Dec;54(12):1671-8.

[241] Vaghi A, Berg E, Liljedahl S, Svensson JO. In vitro comparison of nebulised budesonide (Pulmicort Respuless (R)) and beclomethasone dipropionate (Clenil (R) per Aerosol). Pulm Pharmacol Ther. 2005;18(2):151-3.

[242] Amani A, York P, Chrystyn H, Clark BJ. Evaluation of a Nanoemulsion-Based Formulation for Respiratory Delivery of Budesonide by Nebulizers. AAPS PharmSciTech. 2010 Sep;11(3):1147-51.

[243] Osman R, Kan PL, Awad G, Mortada N, El-Shamy A, Alpar O. Enhanced properties of discrete pulmonary deoxyribonuclease I (DNaseI) loaded PLGA nanoparticles during encapsulation and activity determination. Int J Pharm. 2011 Apr;408(1-2):257-65.

[244] Tadros MI. The influence of sodium hyaluronate, L-leucine and sodium taurocholate on the nebulization of aqueous betamethasone-17-valerate suspensions. AAPS PharmSciTech. 2008 Mar;9(1):243-9.

[245] Dailey LA, Schmehl T, Gessler T, Wittmar M, Grimminger F, Seeger W, et al.. Nebulization of biodegradable nanoparticles: impact of nebulizer technology and nanoparticle characteristics on aerosol features. J Controlled Release. 2003;86(1):131-44.

[246] Waldrep JC, Arppe J, Jansa KA, Knight V. High dose cyclosporin A and budesonide-liposome aerosols. Int J Pharm. 1997 Jun;152(1):27-36.

[247] Bridges PA, Taylor KMG. An investigation of some of the factors influencing the jet nebulisation of liposomes. Int J Pharm. 2000 Aug;204(1-2):69-79.

[248] Desai TR, Hancock REW, Finlay WH. A facile method of delivery of liposomes by nebulization. J Controlled Release. 2002 Nov;84(1-2):69-78.

[249] Elhissi AMA, Karnam KK, Danesh-Azari MR, Gill HS, Taylor KMG. Formulations generated from ethanol-based proliposomes for delivery via medical nebulizers. J Pharm Pharmacol. 2006;58(7):887-94.

[250] Chimote G, Banerjee R. In Vitro Evaluation of Inhalable Isoniazid-Loaded Surfactant Liposomes as an Adjunct Therapy in Pulmonary Tuberculosis. Journal of Biomedical Materials Research Part B-Applied Biomaterials. 2010 Jul;94B(1):1-10.

[251] Chimote G, Banerjee R. Evaluation of antitubercular drug-loaded surfactants as inhalable drug-delivery systems for pulmonary tuberculosis. J Biomed Mater Res Part A. 2009 May;89A(2):281-92.

[252] Yeo LY, Friend JR, McIntosh MP, Meeusen ENT, Morton DAV. Ultrasonic nebulization platforms for pulmonary drug delivery. Expert Opin Drug Deliv. 2010 Jun;7(6):663-79.

[253] Flament MP, Leterme P, Gayot A. Influence of the technological parameters of ultrasonic nebulisation on the nebulisation quality of alpha 1 protease inhibitor (alpha 1I). Int J Pharm. 1999 Nov;189(2):197-204.

[254] Khatri L, Taylor KMG, Craig DQM, Palin K. An assessment of jet and ultrasonic nebulisers for the delivery of lactate dehydrogenase solutions. Int J Pharm. 2001 Oct 4;227(1-2):121-31.

[255] Videira MA, Botelho MF, Santos AC, Gouveia LF, de Lima JJP, Almeida AJ. Lymphatic uptake of pulmonary delivered radiolabelled solid lipid nanoparticles. J Drug Target. 2002 2002;10(8):607-13.

[256] Pardeike J, Weber S, Haber T, Wagner J, Zarfl HP, Plank H, et al.. Development of an Itraconazole-loaded nanostructured lipid carrier (NLC) formulation for pulmonary application. Int J Pharm. 2011.

[257] Lass JS, Sant A, Knoch M. New advances in aerosolised drug delivery: vibrating membrane nebuliser technology. Expert Opin Drug Deliv. 2006;3(5):693-702.

[258] Coates AL, Denk O, Leung K, Ribeiro N, Chan J, Green M, et al.. Higher Tobramycin Concentration and Vibrating Mesh Technology Can Shorten Antibiotic Treatment Time in Cystic Fibrosis. Pediatr Pulmonol. 2011 Apr;46(4):401-8.

[259] Coates AL, Leung K, Vecellio L, Schuh S. Testing of Nebulizers for Delivering Magnesium Sulfate to Pediatric Asthma Patients in the Emergency Department. Respir Care. 2011 Mar;56(3):314-8.

[260] Ghazanfari T, Elhissi AMA, Ding Z, Taylor KMG. The influence of fluid physicochemical properties on vibrating-mesh nebulization. Int J Pharm. 2007;339(1-2):103-11.

[261] Zhang G, David A, Wiedmann TS. Performance of the vibrating membrane aerosol generation device: Aeroneb micropump nebulizer (TM). J Aerosol Med-Depos Clear Eff Lung. 2007 Win;20(4):408-16.

[262] Chan JGY, Kwok PCL, Young PM, Chan HK, Traini D. Mannitol Delivery by Vibrating Mesh Nebulisation for Enhancing Mucociliary Clearance. J Pharm Sci. 2011 Jul;100(7):2693-702.

[263] Rottier BL, van Erp CJP, Sluyter TS, Heijerman HGM, Frijlink HW, de Boer AH. Changes in Performance of the Pari eFlow (R) Rapid and Pari LC Plus (TM) during 6 Months Use by CF Patients. Journal of Aerosol Medicine and Pulmonary Drug Delivery. 2009;22(3):263-9.

[264] Pitance L, Vecellio, L., Leal, T., Reychler, G., Reychler, H., Liistro, G. Delivery Efficacy of a Vibrating Mesh Nebulizer and a Jet Nebulizer under Different Configurations. Journal of Aerosol Medicine and Pulmonary Drug Delivery. 2010;23(6):389-96.

[265] Ari A, Atalay OT, Harwood R, Sheard MM, Aljamhan EA, Fink JB. Influence of Nebulizer Type, Position, and Bias Flow on Aerosol Drug Delivery in Simulated Pediatric and Adult Lung Models During Mechanical Ventilation. Respir Care. 2010 Jul;55(7):845-51.

[266] Skaria S, Smaldone GC. Omron NE U22: Comparison Between Vibrating Mesh and Jet Nebulizer. Journal of Aerosol Medicine and Pulmonary Drug Delivery. 2010 Jun;23(3):173-80.

[267] Harris K, Morra L, Shah A, Smaldone G. *In vitro* effects of vibrating mesh nebulization and radiopharmaceuticals on interferon gamma. European Respiratory Society; 2007; 2007.

[268] McConville JT, Overhoff KA, Sinswat P, Vaughn JM, Frei BL, Burgess DS, et al.. Targeted high lung concentrations of itraconazole using nebulized dispersions in a murine model. Pharm Res. 2006 May;23(5):901-11.

[269] Tam JM, McConville JT, Williams RO, Johnston KP. Amorphous Cyclosporin Nanodispersions for Enhanced Pulmonary Deposition and Dissolution. J Pharm Sci. 2008 Nov;97(11):4915-33.

[270] Li ZL, Zhang YL, Wurtz W, Lee JK, Malinin VS, Durwas-Krishnan S, et al.. Characterization of nebulized liposomal amikacin (Arikace (TM)) as a function of droplet size. Journal of Aerosol Medicine and Pulmonary Drug Delivery. 2008;21(3):245-53.

[271] Beck-Broichsitter M, Gauss J, Packhaeuser CB, Lahnstein K, Schmehl T, Seeger W, et al.. Pulmonary drug delivery with aerosolizable nanoparticles in an ex vivo lung model. Int J Pharm. 2009 Feb;367(1-2):169-78.

[272] Packhaeuser CB, Lahnstein K, Sitterberg J, Schmehl T, Gessler T, Bakowsky U, et al.. Stabilization of Aerosolizable Nano-carriers by Freeze-Drying. Pharm Res. 2009 Jan;26(1):129-38.

[273] Elhissi A, Gill H, Ahmed W, Taylor K. Vibrating-mesh nebulization of liposomes generated using an ethanol-based proliposome technology. J Liposome Res. 2011 Jun;21(2):173-80.

[274] Longest PW, Hindle M. Evaluation of the Respimat Soft Mist Inhaler using a Concurrent CFD and In Vitro Approach. Journal of Aerosol Medicine and Pulmonary Drug Delivery. 2009 Jun;22(2):99-112.

[275] Pitcairn G, Reader S, Pavia D, Newman S. Deposition of corticosteroid aerosol in the human lung by Respimat (R) Soft Mist (TM) Inhaler compared to deposition by metered dose inhaler or by Turbuhaler (R) dry powder inhaler. J Aerosol Med-Depos Clear Eff Lung. 2005 Fal;18(3):264-72.

[276] Zierenberg B. Optimizing the in vitro performance of Respimat. J Aerosol Med-Depos Clear Eff Lung. 1999;12:S19-S24.

[277] Hochrainer D, Holz H, Kreher C, Scaffidi L, Spallek M, Wachtel H. Comparison of the aerosol velocity and spray duration of Respimat (R) Soft Mist (TM) Inhaler and pressurized metered dose inhalers. J Aerosol Med-Depos Clear Eff Lung. 2005 Fal;18(3):273-82.

[278] Dalby R, Spallek M, Voshaar T. A review of the development of Respimat((R)) Soft Mist (TM) Inhaler. Int J Pharm. 2004 Sep;283(1-2):1-9.

[279] Dolovich MB, Dhand R. Aerosol drug delivery: developments in device design and clinical use. Lancet. 2011 Mar;377(9770):1032-45.

[280] Spallek MW, Hochrainer, D., Wachtel, H. Optimizing Nozzles for Soft Mist Inhalers. In: Dalby RN, Byron, P. R., Peart, J., Farr, S. J., editor. Respiratory Drug Delivery VIII; 2002; Tucson, AZ, USA: Virginia Commonwealth University, Richmond, VA, USA; 2002. p. 375-8.

[281] Islam N, Gladki E. Dry powder inhalers (DPIs) - A review of device reliability and innovation. Int J Pharm. 2008 Aug;360(1-2):1-11.

[282] Kesser KC, Geller DE. New Aerosol Delivery Devices for Cystic Fibrosis. Respir Care. 2009 Jun;54(6):754-67.

[283] Kunkel G, Magnussen H, Bergmann KC, Juergens UR, de Mey C, Freund E, et al.. Respimat (R) (a new soft mist inhaler) delivering fenoterol plus ipratropium bromide provides equivalent bronchodilation at half the cumulative dose compared with a

conventional metered dose inhaler in asthmatic patients. Respiration. 2000 May-Jun;67(3):306-14.

[284] Goldberg J, Freund E, Beckers B, Hinzmann R. Improved delivery of fenoterol plus ipratropium bromide using Respimat (R) compared with a conventional metered dose inhaler. Eur Respir J. 2001 Feb;17(2):225-32.

[285] Hodder R, Pavia D, Dewberry H, Alexander K, Iacono P, Ponitz H, et al.. Low incidence of paradoxical bronchoconstriction in asthma and COPD patients during chronic use of Respimat (R) soft mist (TM) inhaler. Respir Med. 2005 Sep;99(9):1087-95.

[286] Koehler D, Pavia D, Dewberry H, Hodder R. Low incidence of paradoxical bronchoconstriction with bronchodilator drugs administered by Respimat (R) Soft Mist (TM) Inhaler: Results of phase II single-dose crossover studies. Respiration. 2004;71(5):469-76.

[287] von Berg A, Jeena PM, Soemantri PA, Vertruyen A, Schmidt P, Gerken F, et al.. Efficacy and safety of Ipratropium bromide plus fenoterol inhaled via Respimat (R) Soft Mist (TM) inhaler vs. a conventional metered dose inhaler plus Spacer in children with asthma. Pediatr Pulmonol. 2004 Mar;37(3):264-72.

[288] Vincken W, Bantje T, Middle MV, Gerken F, Moonen D. Long-term efficacy and safety of ipratropium bromide plus fenoterol via Respimat (R) Soft Mist (TM) inhaler (SMI) versus a pressurised metered-dose inhaler in asthma. Clin Drug Investig. 2004 2004;24(1):17-28.

[289] Iacono P, Velicitat P, Guemas E, Leclerc V, Thebault JJ. Improved delivery of ipratropium bromide using Respimat (R) (a new soft mist inhaler) compared with a conventional metered dose inhaler: cumulative dose response study in patients with COPD. Respir Med. 2000 May;94(5):490-5.

[290] Kilfeather SA, Ponitz HH, Beck E, Schmidt P, Lee A, Bowen I, et al.. Improved delivery of ipratropium bromide/fenoterol from Respimat (R) Soft Mist (TM) Inhaler in patients with COPD. Respir Med. 2004 May;98(5):387-97.

[291] Anderson P. Use of Respimat Soft Mist inhaler in COPD patients. Int J Chron Obstruct Pulmon Dis. 2006 2006;1(3):251-9.

[292] ZuWallack R, De Salvo MC, Kaelin T, Bateman ED, Park CS, Abrahams R, et al.. Efficacy and safety of ipratropium bromide/albuterol delivered via Respimat (R) inhaler versus MDI. Respir Med. 2010 Aug;104(8):1179-88.

[293] Kerstjens HAM, Disse B, Schroder-Babo W, Bantje TA, Gahlemann M, Sigmund R, et al.. Tiotropium improves lung function in patients with severe uncontrolled asthma: A randomized controlled trial. J Allergy Clin Immunol. 2011 Aug;128(2):308-14.

[294] Singh S, Loke YK, Enright PL, Furberg CD. Mortality associated with tiotropium mist inhaler in patients with chronic obstructive pulmonary disease: systematic review and meta-analysis of randomised controlled trials. Br Med J. 2011 Jun;342.

[295] Leclerc V, Lafferre M, Pavia D. Acute local tolerability of acidic aqueous vehicles delivered via Respimat (R) soft Mist(TM) inhaler in hyperreactive asthma patients. Respiration. 2007;74(6):691-6.

[296] Patel KR, Pavia D, Lowe L, Spiteri M. Inhaled ethanolic and aqueous solutions via respimat soft mist inhaler are well-tolerated in asthma patients. Respiration. 2006;73(4):434-40.

[297] Bouyssou T, Casarosa P, Naline E, Pestel S, Konetzki I, Devillier P, et al.. Pharmacological Characterization of Olodaterol, a Novel Inhaled beta(2)-Adrenoceptor Agonist Exerting a 24-Hour-Long Duration of Action in Preclinical Models. J Pharmacol Exp Ther. 2010 Jul;334(1):53-62.

[298] Newman SP, Steed KP, Reader SJ, Pavia D, Sohal AK. An in vitro study to assess facial and ocular deposition from Respimat (R) Soft Mist (TM) inhaler. J Aerosol Med-Depos Clear Eff Lung. 2007 Spr;20(1):7-12.

[299] Schuster J, Rubsamen R, Lloyd P, Lloyd J. The AER(X)(TM) aerosol delivery system. Pharm Res. 1997 Mar;14(3):354-7.

[300] Davison S, Thipphawong J, Blanchard J, Liu K, Morishige R, Gonda I, et al.. Pharmacokinetics and acute safety of inhaled testosterone in postmenopausal women. J Clin Pharmacol. 2005 Feb;45(2):177-84.

[301] Farr SJ, Otulana BA. Pulmonary delivery of opioids as pain therapeutics. Adv Drug Delivery Rev. 2006 Oct;58(9-10):1076-88.

[302] Gonda I, Schuster JA, Rabsamen RM, Lloyd P, Cipolla D, Farr SJ. Inhalation delivery systems with compliance and disease management capabilities. J Controlled Release. 1998 Apr;53(1-3):269-74.

[303] Otulana B, Okikawa J, Linn L, Morishige R, Thipphawong J. Safety and pharmacokinetics of inhaled morphine delivered using the AERx System in patients with moderate-to-severe asthma. Int J Clin Pharmacol Ther. 2004 Aug;42(8):456-62.

[304] Thipphawong JB, Babul N, Morishige RJ, Findlay HK, Reber KR, Millward GJ, et al.. Analgesic efficacy of inhaled morphine in patients after bunionectomy surgery. Anesthesiology. 2003 Sep;99(3):693-700.

[305] Dershwitz M, Walsh JL, Morishige RJ, Conners PM, Rubsamen RM, Shafer SL, et al.. Pharmacokinetics and pharmacodynamics of inhaled versus intravenous morphine in healthy volunteers. Anesthesiology. 2000 Sep;93(3):619-28.

[306] Ward ME, Woodhouse A, Mather LE, Farr SJ, Okikawa JK, Lloyd P, et al.. Morphine pharmacokinetics after pulmonary administration from a novel aerosol delivery system. Clin Pharmacol Ther. 1997 Dec;62(6):596-609.

[307] Mather LE, Kam, P.C., Morishige, R.J., Otulana, B.A., Dayton, F., Rubsamen, R.M. Pharmacokinetics of Orally Inhaled Fentanyl in Healthy Subjects. The Journal of Clinical Pharmacology. 2000;40(9):1060.

[308] Okumu FW, Lee RY, Blanchard JD, Queirolo A, Woods CM, Lloyd PM, et al.. Evaluation of the AERx pulmonary delivery system for systemic delivery of a poorly soluble selective D-1 agonist, ABT-431. Pharm Res. 2002 Jul;19(7):1009-12.

[309] Cipolla DC, Boyd, B., Evans, R.M., Warren, S., Taylor, G., Farr, S.J. Bolus Administration of INS365: Studying the Feasibility of Delivering High Doses of Drugs Using the AERx Pulmonary Delivery System. In: Dalby RN, Byron, P.R., Farr, S.J., Peart, J. , editor. Respiratory Dru Delivery VII; 2000 May 14 to 18, 2000; Tarpon Springs, FL, USA: Serentec Press, Raleigh, NC, USA; 2000. p. 231-40.

[310] Sangwan S, Agosti JM, Bauer LA, Otulana BA, Morishige RJ, Cipolla DC, et al.. Aerosolized protein delivery in asthma: Gamma camera analysis of regional deposition and perfusion. J Aerosol Med-Depos Clear Eff Lung. 2001 Sum;14(2):185-95.

[311] Farr SJ, Warren SJ, Lloyd P, Okikawa JK, Schuster JA, Rowe AM, et al.. Comparison of in vitro and in vivo efficiencies of a novel unit-dose liquid aerosol generator and a pressurized metered dose inhaler. Int J Pharm. 2000 Mar;198(1):63-70.

[312] Geller D, Thipphawong J, Otulana B, Caplan D, Ericson D, Milgram L, et al.. Bolus inhalation of rhDNase with the AERx system in subjects with cystic fibrosis. J Aerosol Med-Depos Clear Eff Lung. 2003 Sum;16(2):175-82.

[313] Deshpande D, Blanchard J, Srinivasan S, Fairbanks D, Fujimoto J, Sawa T, et al.. Aerosolization of lipoplexes using AERx (R) Pulmonary Delivery System. AAPS PharmSci. 2002;4(3).

[314] Rosell J. SJ, Liu K., Gonda, I., Srinivassan, S., Deshpande, D. Suppression of electrostatic changing of AERx aerosols. J Aerosol Med. 2001;14(3):405-.

[315] Heinemann L. New ways of insulin delivery. Int J Clin Pract. 2011 Feb;65:31-46.

[316] Boyd B, Noymer P, Liu K, Okikawa J, Hasegawa D, Warren S, et al.. Effect of gender and device mouthpiece shape on bolus insulin aerosol delivery using the AER(x) pulmonary delivery system. Pharm Res. 2004 Oct;21(10):1776-82.

[317] Mastrandrea LD, Quattrin T. Clinical evaluation of inhaled insulin. Adv Drug Delivery Rev. 2006 Oct 31;58(9-10):1061-75.

[318] Moses RG, Bartley P, Lunt H, O'Brien RC, Donnelly T, Gall MA, et al.. Safety and efficacy of inhaled insulin (AERx((R)) iDMS(1)) compared with subcutaneous insulin therapy in patients with Type 1 diabetes: 1-year data from a randomized, parallel group trial. Diabet Med. 2009 Mar;26(3):260-7.

[319] Wilbanks TM, Schuster JA. Aerosol drug delivery to the lung periphery using nano-scale technologies. *2005 International Conference on MEMS, NANO and Smart Systems, Proceedings* 2005:127-8.

[320] Chattopadhyay P, Shekunov BY, Yim D, Cipolla D, Boyd B, Farr S. Production of solid lipid nanoparticle suspensions using supercritical fluid extraction of emulsions (SFEE) for pulmonary delivery using the AERx system. Adv Drug Delivery Rev. 2007;59:444-53.

[321] Yim D. CD, Boyd B. Feasibility of Pulmonary Delivery of Nano-suspension Formulations using the AERx® System. J Aerosol Med. 2001;18(1):101-2.

[322] Deshpande DS, Blanchard JD, Schuster J, Fairbanks D, Hobbs C, Beihn R, et al.. Gamma scintigraphic evaluation of a miniaturized AERx (R) pulmonary delivery system for aerosol delivery to anesthetized animals using a positive pressure ventilation system. J Aerosol Med-Depos Clear Eff Lung. 2005 Spr;18(1):34-44.

[323] de Boer AH, Wissink J, Hagedoorn P, Heskamp I, de Kruijf W, Bunder R, et al.. In vitro performance testing of the novel medspray (R) wet aerosol inhaler based on the principle of Rayleigh break-up. Pharm Res. 2008 May;25(5):1186-92.

[324] Rayleigh L. On the Instability of Jets. Proceedings of the London Mathematical society. 1878;10:4-13.

[325] Weber C. Zum Zerfall eines Flussigkeitsstrahles. Journal of Applied Mathematics and Mechanics / Zeitschrift fur Angewandte Mathematik und Mechanik. 1931;11(2):136-54.

[326] Munnik P, de Boer AH, Wissink J, Hagedoorn P, Heskamp I, de Kruijf W, et al.. In Vivo Performance Testing of the Novel Medspray (R) Wet Aerosol Inhaler. Journal of Aerosol Medicine and Pulmonary Drug Delivery. 2009 Dec;22(4):317-21.

[327] Tang K, Gomez A. Generation by Electrospray of Monodisperse Water Droplets for Targeted Drug-Delivery by Inhalation. J Aerosol Sci. 1994 Sep;25(6):1237-49.

[328] Zimlich WC, Ding, J.Y., Busick, D.R., Moutvic, R.R., Placke, M.E., Hirst, P.H., Pitcairn, G.R., Malik, S., Newman, S.P., Macintyre, F., Miller, P.R., Shepherd, M., Lukas, T.M. The Development of a Novel Electrohydrodynamic Pulmonary Drug Delivery Device. In: Dalby RN, Byron, P.R., Farr, S.J., Peart, J. , editor. Respiratory Dru Delivery VII; 2000 May 14 to 18, 2000; Tarpon Springs, FL, USA: Serentec Press, Raleigh, NC, USA; 2000. p. 241-6.

[329] Clear N, Ticehurst, M., Clarke, J., Miller, P., Shepherd, M. Electrohydrodynamic Aerosol Drug Delivery: Experience in Early Clinical Development. J Aerosol Med. 2004;17(1):95-.

[330] Smyth WF, Rodriguez V. Recent studies of the electrospray ionisation behaviour of selected drugs and their application in capillary electrophoresis-mass spectrometry and liquid chromatography-mass spectrometry. J Chromatogr A. 2007 Aug;1159(1-2):159-74.

[331] Yurteri CU, Hartman RPA, Marijnissen JCM. Producing Pharmaceutical Particles via Electrospraying with an Emphasis on Nano and Nano Structured Particles - A Review. Kona Powder and Particle Journal. 2010 2010(28):91-115.

[332] Kumbar SG, Bhattacharyya S, Sethuraman S, Laurencin CT. A preliminary report on a novel electrospray technique for nanoparticle based biomedical implants coating: Precision electrospraying. Journal of Biomedical Materials Research Part B-Applied Biomaterials. 2007 Apr;81B(1):91-103.

[333] Xie J, Lim LK, Phua Y, Hua J, Wang C-H. Electrohydrodynamic atomization for biodegradable polymeric particle production. J Colloid Interface Sci. 2006;302(1):103-12.

[334] Ding L, Lee T, Wang C-H. Fabrication of monodispersed Taxol-loaded particles using electrohydrodynamic atomization. J Controlled Release. 2005;102(2):395-413.

[335] Jung JH. Electrohydrodynamic nano-spraying of ethanolic natural plant extracts. J Aerosol Sci. 2011;42(10):725-36.

[336] Jaworek A. Electrostatic micro- and nanoencapsulation and electroemulsification: A brief review. J Microencapsul. 2008;25(7):443-68.

[337] Ijsebaert JC, Geerse KB, Marijnissen JCM, Lammers JWJ, Zanen P. Electro-hydrodynamic atomization of drug solutions for inhalation purposes. J Appl Physiol. 2001 Dec;91(6):2735-41.

[338] Esposito-Festen JE, Zanen P, Tiddens HAWM, Lammers JWJ. Pharmacokinetics of inhaled monodisperse beclomethasone as a function of particle size. Br J Clin Pharmacol. 2007 Sep;64(3):328-34.

[339] Davies DN, Pollard M, Coffee RA, inventors; Battelle Memorial Institute, Columbus, OH (US), assignee. Liquid formations for electrohydrodymanic spraying containing polymer and suspended particles. USA patent USPTO 7,891,578 B2. 2011 Feb. 22, 2011.

[340] Chattopadhyay S, Modesto-Lopez LB, Venkataraman C, Biswas P. Size Distribution and Morphology of Liposome Aerosols Generated By Two Methodologies. Aerosol Sci Technol. 2010;44(11):972-82.

[341] Jayasinghe SN, Edirisinghe MJ. Jet break-up in nano-suspensions during electrohydrodynamic atomization in the stable cone-jet mode. J Nanosci Nanotechnol. 2005 Jun;5(6):923-6.

[342] Charvat A, Bogehold A, Abel B. Time-resolved micro liquid desorption mass spectrometry: Mechanism, features, and kinetic applications. Aust J Chem. 2006;59(2):81-103.

[343] Murariu M, Dragan ES, Drochioiu G. Model Peptide-Based System Used for the Investigation of Metal Ions Binding to Histidine-Containing Polypeptides. Biopolymers. 2010 Jun;93(6):497-508.

[344] Pareta R, Brindley A, Edirisinghe MJ, Jayasinghe SN, Luklinska ZB. Electrohydrodynamic atomization of protein (bovine serum albumin). Journal of Materials Science-Materials in Medicine. 2005 Oct;16(10):919-25.

[345] Lentz YK, Anchordoquy TJ, Lengsfeld CS. Rationale for the selection of an aerosol delivery system for gene delivery. J Aerosol Med-Depos Clear Eff Lung. 2006 Fal;19(3):372-84.

[346] Yeo LY, Friend JR. Ultrafast microfluidics using surface acoustic waves. Biomicrofluidics. 2009 Jan-Mar;3(1).

[347] Alvarez M, Friend JR, Yeo LY. Surface vibration induced spatial ordering of periodic polymer patterns on a substrate. Langmuir. 2008 Oct 7;24(19):10629-32.

[348] Friend J, Yeo LY. Microscale acoustofluidics: Microfluidics driven via acoustics and ultrasonics. Reviews of Modern Physics. 2011 Jun 20;83(2):647-704.

[349] Qi AS, Friend JR, Yeo LY, Morton DAV, McIntosh MP, Spiccia L. Miniature inhalation therapy platform using surface acoustic wave microfluidic atomization. Lab Chip. 2009;9(15):2184-93.

[350] Qi A, Yeo LY, Friend JR. Interfacial destabilization and atomization driven by surface acoustic waves. Phys Fluids. 2008 Jul;20(7).

[351] Alvarez M, Friend J, Yeo LY. Rapid generation of protein aerosols and nanoparticles via surface acoustic wave atomization. Nanotechnology. 2008 Nov 12;19(45).

[352] Alvarez M, Yeo LY, Friend JR, Jamriska M. Rapid production of protein-loaded biodegradable microparticles using surface acoustic waves. Biomicrofluidics. 2009 Jan-Mar;3(1).

[353] Qi A, Yeo L, Friend J, Ho J. The extraction of liquid, protein molecules and yeast cells from paper through surface acoustic wave atomization. Lab Chip. 2009 2010;10(4):470-6.

[354] Li H, Friend JR, Yeo LY. Surface acoustic wave concentration of particle and bioparticle suspensions. Biomedical Microdevices. 2007 Oct;9(5):647-56.

[355] Tan MK, Friend JR, Yeo LY. Microparticle collection and concentration via a miniature surface acoustic wave device. Lab Chip. 2007 2007;7(5):618-25.

[356] Friend JR, Yeo LY, Arifin DR, Mechler A. Evaporative self-assembly assisted synthesis of polymeric nanoparticles by surface acoustic wave atomization. Nanotechnology. 2008 Apr 9;19(14).

[357] Forde GM, Friend J, Williamson T. Straightforward biodegradable nanoparticle generation through megahertz-order ultrasonic atomization. Appl Phys Lett. 2006 Aug 7;89(6).

[358] Hindle M, Byron, P.R., Jashnani, R.N., Howell, T.M., Cox, K.A. High Efficiency Fine Particle Generation using Novel Condensation Technology. In: Dalby RN, Byron, P. R., Farr, S. J., editor. Respiratory Drug Delivery VI; 1998; Hilton Head, SC, USA: Interpharm Press, Buffalo Grove, IL, USA; 1998. p. 97-102.

[359] Howell TM, Sweeney WR, inventors; Philip Morris Incorporated. New York, N.Y., assignee. Aerosol and a Method and Apparatus for Generating Aerosol. USA patent USPTO 5,743,251 B2. 1998 Apr. 28, 1998.

[360] Hong JN, Hindle M, Byron PR. Control of particle size by coagulation of novel condensation aerosols in reservoir chambers. J Aerosol Med-Depos Clear Eff Lung. 2002 Win;15(4):359-68.

[361] Gupta R, Hindle M, Byron PR, Cox KA, McRae DD. Vehicle Effects On The Performance Of A Novel Pharmaceutical Condensation Aerosol Generator. AAPS PharmSci; 2001; 2001.

[362] Gupta R, Hindle M, Byron PR, Cox KA, McRae DD. Solute and Concentration Effects in a Novel Pharmaceutical Condensation Aerosol Generator. AAPS PharmSci; 2001; 2001.

[363] Shen X, Hindle A, Byron PR. Effect of energy on propylene glycol aerosols using the capillary aerosol generator. Int J Pharm. 2004 May;275(1-2):249-58.

[364] Li XH, Blondino FE, Hindle M, Soine WH, Byron PR. Stability and characterization of perphenazine aerosols generated using the capillary aerosol generator. Int J Pharm. 2005 Oct;303(1-2):113-24.

[365] CEN. Respiratory therapy equipment - Part 1: Nebulizing systems and their components. In: Standardization ECf, ed.: BSI 2007.

[366] Marple VA, Roberts DL, Romay FJ, Miller NC, Truman KG, Holroyd MJ, et al.. Next generation pharmaceutical impactor (A new impactor for pharmaceutical inhaler testing). Part I: Design. J Aerosol Med-Depos Clear Eff Lung. 2003 Fal;16(3):283-99.

[367] Mitchell J, Newman S, Chan HK. In Vitro and In Vivo Aspects of Cascade Impactor Tests and Inhaler Performance: A Review. AAPS PharmSciTech. 2007 Oct;8(4).

[368] Waldrep JC, Berlinski A, Dhand R. Comparative analysis of methods to measure aerosols generated by a vibrating mesh nebulizer. J Aerosol Med-Depos Clear Eff Lung. 2007 Fal;20(3):310-9.

[369] Mitchell J, Bauer R, Lyapustina S, Tougas T, Glaab V. Non-impactor-Based Methods for Sizing of Aerosols Emitted from Orally Inhaled and Nasal Drug Products (OINDPs). AAPS PharmSciTech. 2011;12(3):965-88.

[370] Mitchell JP, M.W. Nagel. Particle size analysis of aerosols from medicinal inhalers. KONA Powder and Particle. 2004;22:32-65.

[371] Mitchell JP, Nagel MW, Nichols S, Nerbrink O. Laser diffractometry as a technique for the rapid assessment of aerosol particle size from inhalers. J Aerosol Med-Depos Clear Eff Lung. 2006;19(4):409-33.

[372] Marple VA, Olson BA, Santhanakrishnan K, Roberts DL, Mitchell JP, Hudson-Curtis BL. Next generation pharmaceutical impactor: A new impactor for pharmaceutical inhaler testing. Part III. Extension of archival calibration to 15 L/min. J Aerosol Med-Depos Clear Eff Lung. 2004 Win;17(4):335-43.

[373] Berlinski A, Hayden JB. Optimization of a Procedure Used to Measure Aerosol Characteristics of Nebulized Solutions Using a Cooled Next Generation Impactor. Journal of Aerosol Medicine and Pulmonary Drug Delivery. 2010 Dec;23(6):397-404.

[374] Bummer PM. Interfacial Phenomena. In: Hendrickson R, ed. *Remington: The Science and Practice of Pharmacy*. 21st ed. Baltimore, MD: Lippincott Williams & Wilkins 2005:280-92.

[375] Minko T. Interfacial Phenomena. In: Sinko PJ, ed. *Martin's physical pharmacy and pharmaceutical sciences*. 5th ed. Baltimore, MD: Lippincott Williams & Wilkins 2006:437-67.

[376] Carvalho TC, Horng M, McConville JT. Measurement of Surface Tension of Liquids using a Texture Analyzer. AAPS PharmSci; 2010; 2010.

[377] Longer M. Rheology. In: Sinko PJ, ed. *Martin's physical pharmacy and pharmaceutical sciences*. 5th ed. Baltimore, MD: Lippincott Williams & Wilkins 2006:561-83.

[378] Schnaare RL, Block LH, Rohan LC. Rheology. In: Hendrickson R, ed. *Remington: The Science and Practice of Pharmacy*. 21st ed. Baltimore, MD: Lippincott Williams & Wilkins 2005:338-57.

[379] Nagvekar AA, Trickler WJ, Dash AK. Current Analytical Methods Used in the In Vitro Evaluation of Nano-Drug Delivery Systems. Curr Pharm Anal. 2009;5(4):358-66.

[380] Lyklema J. Molecular interpretation of electrokinetic potentials. Curr Opin Colloid Interface Sci. 2010 Jun;15(3):125-30.

[381] Kallay N, Preocanin T, Kovacevic D, Lutzenkirchen J, Chibowski E. Electrostatic Potentials at Solid/Liquid Interfaces. Croat Chem Acta. 2010 Oct;83(3):357-70.

[382] Barnes HA, Hutton JF, Walters K. Rheology of Suspensions. In: Walters K, ed. *An introduction to rheology*. Amsterdam, The Netherlands: Elsevier 1989:115-37.

[383] Derkach SR. Rheology of emulsions. Adv Colloid Interface Sci. 2009;151(1-2):1-23.

[384] Hansch C, Leo A, Hoekman D. Exploring QSAR: Volume 2: Hydrophobic, Electronic, and Steric Constants. Washington, DC: An American Chemical Society Publication 1995.

[385] Avdeef A. Absorption and drug development: solubility, permeability and charge state. Hoboken, NJ: John Wiley & Sons, Inc. 2003.

[386] Carstens MG, de Jong P, van Nostrum CF, Kemmink J, Verrijk R, De Leede LGJ, et al.. The effect of core composition in biodegradable oligomeric micelles as taxane formulations. Eur J Pharm Biopharm. 2008;68(3):596-606.

[387] Dhanikula AB, Panchagnula R. Localized paclitaxel delivery. Int J Pharm. 1999;183(2):85-100.

Chapter 2: Research Outline

2.1 OVERALL OBJECTIVES

The primary goal of this work, presented in this dissertation, was to develop formulations of Coenzyme Q_{10} (CoQ_{10}) with the potential to be delivered at high doses via inhalation, for the purpose of treating lung carcinomas in future work. Development of a pulmonary drug delivery system capable of carrying high drug amounts may provide flexibility in dosing strategies during treatment of lung cancer patients for either primary or supportive care. Nebulization was selected as the delivery mode of inhaler device to attain the desired high doses. Being a poorly-water soluble compound, it naturally presented formulation technology challenges for the delivery of aqueous dispersions of CoQ_{10} using the nebulization strategy. Consequently, it was most pertinent to investigate the physicochemical properties influencing the aerosolization profile of these dispersions. The research presented encompassed the definition of an appropriate manufacturing process, *in vitro* characterization and *in vivo* investigation. These studies were performed to identify the potential to deliver high doses of CoQ_{10} through the pulmonary route.

2.2 SUPPORTING OBJECTIVES

2.2.1. Measurement of Surface Tension of Liquids from the Maximum Pull on a Disk Theory using a Texture Analyzer

The surface tension of liquids has been shown to influence the aerosolization profile from nebulizers. There are several methods available to measure this

physicochemical property in bulk liquid matter. The DuNoüy ring is the most common method utilized to determine this interfacial phenomenon and employs analytical microbalances for the measurement of the detachment force of a platinum-iridium ring from the surface of the bulk liquid. Using a disk geometry probe, an increase in the detachment force leads to the substitution of the microgravimetric system by a texture analyzer. By extrapolating the previously published work from the maximum pull on a rod, the objective of the study presented in Chapter 3 was to develop a precise, accurate and reproducible analytical method based on the maximum pull on a disk using a texture analyzer to determine the surface tension of the liquids.

2.2.2 Development and Characterization of Phospholipid-Stabilized Submicron Aqueous Dispersions of Coenzyme Q_{10} Presenting Continuous Vibrating-Mesh Nebulization Performance

CoQ_{10} is a poorly-water soluble compound that is being investigated for the treatment of lung malignancies. In this study, the aim was to develop a suitable formulation of CoQ_{10} for pulmonary delivery. The rationale for the selection of excipients and vibrating-mesh nebulizer device are presented in Chapter 4, in conjunction with preformulation characterization of the drug limited to the intended purpose. High pressure homogenization was chosen as an appropriate manufacturing process based on the production of submicron drug particles in aqueous dispersions and potential scale up capabilities. Soybean lecithin was used as a model excipient to stabilize CoQ_{10} dispersions and analysis of the adequate number of passes in the microfluidization process was performed. It is known that the pores of vibrating-mesh nebulizers can clog, causing variations in the aerosol generation (i.e. intermittent mist). Therefore, in

conjunction with analysis of physicochemical properties, the nebulization performances of the CoQ_{10} formulations were also investigated.

2.3.2 Prediction of *In Vitro* Aerosolization Profiles Based on Rheological Behaviors of Aqueous Dispersions of Coenzyme Q_{10}

Phospholipids comprise the majority of the components in the human alveolar surfactants. Dimyristoylphosphatidylcholine (DMPC), dipalmitoylphosphatidylcholine (DPPC) and distearoylphosphatidylcholine (DSPC) are among these phospholipids and can be synthetically produced. Soybean lecithin is a mixture of phospholipids. The objective of the study presented in Chapter 5 was to determine the nebulization performances and *in vitro* particle deposition profiles of formulations of CoQ_{10} stabilized with synthetic phospholipids and compare them with that of lecithin dispersions presented in Chapter 4. The nebulization steadiness, aerosol output, and deposition profiles were evaluated. In addition, the physicochemical properties of these formulations were further investigated and compared to identify those that may have the greatest influence on the aerosolization profile. Particle size distribution, zeta potential, surface tension, and rheological behavior were all studied.

2.4.2 Pulmonary Deposition and Systemic Distribution in Mice of Inhalable Formulations of Coenzyme Q_{10}

Based on the *in vitro* characterization data, unprecedentedly high doses were observed with potential to reach the lungs based on their aerodynamic properties. Following-up, *in vivo* studies were performed to confirm the *in vitro* data. The goal of this investigation, presented in Chapter 6, was to determine the lung and nasal depositions as well as the systemic distribution of CoQ_{10} following nebulization of

formulations stabilized with DMPC, DPPC or DSPC. An estimated dose at which mice were to be exposed to was calculated for each formulation to be delivered. Mice were exposed to the drug aerosol for 15 minutes into a nose-only inhalation chamber, and the dosed and control groups were compared with respect to the estimated doses.

Chapter 3: Measurement of Surface Tension of Liquids from the Maximum Pull on a Disk Theory using a Texture Analyzer

Abstract

The intrinsic property of liquids serves as a vital indicator of formulation performance and stability. Therefore, investigation of the interfacial phenomenon of surface tension is a routine procedure in the development of products in a wide variety of areas including foods, pharmaceuticals, cosmetics, and painting technologies. In this work, it is hypothesized that studies related to the maximum pull on a rod can be extrapolated to disk geometry for application to measure surface tension using a texture analyzer. A glass disk probe was attached to the arm of a texture analyzer and pulled from the liquid surface. The maximum force of detachment was used to calculate surface tension extrapolated from the theory of maximum pull on a rod. The surface tension of water, ethanol and a hydroalcoholic solution were measured and compared to literature values to validate this hypothesis. The calculated values of surface tension for the liquids studied were within 5% of reported values. Probe diameter appears to have an important role on surface tension accuracy as compared to literature values. Slight discrepancies can be attributed to temperature control and leveling of the liquid surface, although still in accordance with reported values of surface tension measured using different methods. This study presents a simple, precise, and quick method to determine the surface tension of liquids from the maximum pull on a disk. Further studies are necessary to determine the optimum glass disk probe diameter for better accuracy.

3.1 INTRODUCTION

Interfacial phenomena are important aspects in the formulation development process of liquids in the pharmaceutical, cosmetics, consumer product, painting, and food industries. Particularly, this physicochemical property is critical in pharmaceutical formulation development of microemulsions, suppositories, topical and transdermal delivery systems, eye drops and nasal aerosols, as the presence of surface active agents in formulations aid in the stability of suspensions, emulsions, and foams.[1, 2] Surface tension properties can be affected by the addition of ingredients to a liquid. Of particular importance to the development of inhalable pharmaceutical product, the surface tension of liquids has been shown to influence the aerosolization performance of nebulizers.[3-5] Numerous methods exist for the determination of liquid surface tensions, and can be either dependent or independent of contact angle.[6, 7] Considering their widely established use and acceptance, the DuNoüy ring and the capillary rise methods are the most noteworthy techniques applied to the evaluation of surface tension.

Several types of probe geometries, including rings, cones and rods, have been used for the pull technique to measure surface tension from the menisci at a free liquid surface.[8-10] To date, there have been limited publications on the pull on a disk method after this technique was deemed not to offer applicable solutions for the measurement of surface tension.[7] According to Nietz and Lambert, disk geometry “presents complex problems” due to the exponential increase in force as a function of probe diameter. Ultimately, it was determined that the linear relationship found for rings, reasoned probe ring geometry to be the most suitable method for measurement of surface tension. However as an alternative approach, Padday and coworkers had previously determined the physical aspects governing the maximum pull on a rod.[11] They found that the maximum force to suspend the liquid underneath the rod, expressed as volume, is a

characteristic property of the system that can be numerically correlated to the probe radius for determination of surface tension.

In order to rapidly determine the suspension force of a liquid, the inclusion of a force measurement apparatus is essential in the evaluation of surface tension. Traditionally, analytical balances are the predominant apparatus used to measure force exerted, by raising the liquid above a general level.[12] The DuNoüy method requires a microbalance to measure the detachment force of the liquid surface from platinum – iridium ring. The texture analyzer is a force measurement instrument with a high force sensitivity and measurement range, although not capable of measuring the very small detachment force for a ring probe. The texture analyzer has in recent years become a standard for force measurement applications and has been widely used as a research tool in the pharmaceutical as well as the food industries.[13-16] With measurement time, arm speed and displacement distance as parameters that can be finely controlled, this versatile equipment offers the tools needed to investigate a variety of formulation aspects including material hardness, adhesiveness, stickiness, swelling, and penetration, properties.[17-19]

The larger relative diameter of disks, as compared to rods and rings, is capable of suspending a greater volume of liquid underneath the probe, therefore requiring a greater maximum force to be measured. This increase in the measured detachment force is sufficient to fall within the measurement range of the texture analyzer. Previous work has not focused on disk geometry due to the reasons described above. In this study, it is hypothesized that the work performed by Padday *et al.* on the theory of maximum pull on a rod, can be extrapolated to the application of disks as the probe geometry due to their similarities in shape. However, the large differences in dimensions may alter the dynamics of static interfacial phenomenon measurement by modifying the magnitude of

maximum detachment force. The objective of this study was to explore the feasibility of using a glass disk probe in conjunction with a texture analyzer instrument to develop an accurate, precise and reproducible analytical method for the determination of the surface tension of liquids. The novelty of this work is in exploring the disk geometry capability of suspending significant volume of liquid underneath its leveled surface, making the force measurement to fall within the range of measurement of the texture analyzer. Therefore, eliminating the need of an extremely sensitive instrument to measure force, like the analytical microbalances commonly used to measure surface tension. Given its versatile and widespread application in a variety of laboratory settings, expanding the capabilities of this instrument would greatly benefit the fast screening of formulations for diversified industries.

3.2 EXPERIMENTAL

3.2.1. Materials

A texture analyzer from Texture Technologies, model TA.XTPlus (Scarsdale, NY, USA) was used for all experiments in this study. A PYREX® 150 x 75 mm crystallizing dish (Product #3140-150) (Lowell, MA USA) was used as the liquid reservoir, and Alconox® Powdered Precision Cleaner (White Plains, NY, USA) was used as the cleaning agent. The ethanol used was procured from Fisher Science Education (Hanover Park, IL, USA) and the deionized water was obtained from a central reverse osmosis/demineralizer system commonly found in research laboratories. Duco® Cement from ITW Performance Polymers, Devcon (Danvers, MA, USA) was used to assemble the probes.

Two commissioned machine-made aluminum probes were constructed at the University of Texas at Austin department of Chemistry and Biochemistry machine shop. For each probe, an aluminum rod of radius 3.2 mm with thread on both ends was screwed perpendicularly into the probe housing of the texture analyzer on one end, and to a circular aluminum plate of radius 3.12 cm on the other. Two hand-made borosilicate glass disks were made by the University of Texas at Austin Chemistry Glass Shop, and the glass disks were adhered to the bottom of the aluminum plates with Duco® Cement (Figure 3.1). The small and large probes consisted of a radius of $X_S = 2.53860 \pm 0.00402$ cm and $X_L = 2.97375 \pm 0.00403$ cm; and a width of $W_S = 6.571 \pm 0.0547$ mm and $W_L = 6.684 \pm 0.060$ mm, respectively, using a caliper and average of 8 points about the circumference.

3.2.2. Methods

3.2.2.1. Preparation

Prior to testing, all probes and liquid containers were cleaned with concentrated detergent (Alconox®), rinsed with deionized water, sprayed with ethanol, allowed to air dry, and followed by a thorough drying with compressed air. Additionally, an internal height calibration was performed on the texture analyzer as reference prior to each series of tests, as well as weight calibration check.

3.2.2.2. Procedure

Surface tension was measured by attaching the probe to the texture analyzer arm and lowering the probe until the bottom surface of the glass probe contacted the surface of a test liquid contained in a reservoir (Figure 3.1). At the start of test, the probe was

raised from the surface of the liquid at a constant speed to a specific height, while the texture analyzer registered force as a function of time or distance. The maximum force represents the force of detachment of the probe from the surface of the liquid, which was used to calculate the surface tension as explained later. The settings on the texture analyzer were as shown in Table 3.1.

In this protocol, the probe was set to descend at a set speed until a trigger force was reached; this subsequently initiated the pre-programmed ascending movement to the return distance. The small trigger force of 0.20 mN was intentionally set to prevent the creation of disturbances on the liquid surface, from any descending movement. Therefore, contact time with liquid was maintained for a set period of time before the probe started its ascent.

3.2.2.3. Calculation of Surface Tension

Padday and coworkers have thoroughly investigated the surface tension measurement of liquids from the maximum pull on a rod.[11] Our study for calculation of surface tension from the maximum pull on a disk is derived from their work. The rationale for using specific equations developed by Padday and coworkers is described below.

By raising a probe from the free surface of a liquid, the maximum force, F_{max}, observed before meniscus breakaway is the result of hydrostatic pressure and surface tension contributions:

$$F_{max} = \pi X^2 Z \rho g + 2\pi X \gamma sin\theta \qquad \text{(Equation 3.1)}$$

Where X is the probe radius, Z is the distance above the free surface of a liquid, ρ and γ are respectively the density and surface tension differences between the liquid and the surrounding fluid, g is the gravitational acceleration and θ is the angle between the vertical longitudinal axis and the meniscus angle at the junction of the disk. Therefore, the determination of surface tension is based on the following relationship:

$$\gamma = \frac{F_{max} - F_V}{L \cdot cos\theta} \left(in \ \frac{mN}{m} \ or \frac{dyn}{cm} \right) \qquad \text{(Equation 3.2)}$$

Where F_V is the force related to the hydrostatic pressure created by the volume of liquid lifted by the probe, L is the probe perimeter and θ is the contact angle. The commonly used DuNoüy ring is made of platinum, a material that presents a zero contact angle with water, similar to glass.[20, 21]

In their work, Padday *et al.* express the maximum force as volume, V, according to the following equation:

$$V = \frac{F_{max}}{\rho \cdot g} \qquad \text{(Equation 3.3)}$$

By introducing a meniscus coefficient, k:

$$k = \sqrt[2]{\left(\frac{\gamma}{\rho \cdot g} \right)} \qquad \text{(Equation 3.4)}$$

The relationship between volume, probe radius and meniscus coefficient is established as:

$$\frac{X}{k} = a_0 + a_1 \cdot \left(\frac{X^3}{V}\right) + a_2 \cdot \left(\frac{X^3}{V}\right)^2 + a_3 \cdot \left(\frac{X^3}{V}\right)^3 \qquad \text{(Equation 3.5)}$$

According to the mathematical analysis made by Padday *et al.*, at different domains of X^3/V, different coefficients, a_n, of Equation 3.5 are defined. In general, the greater the probe radius, the fewer the degrees of the polynomial equation above, are necessary to determine surface tension. In their work, Padday and coworkers present an extensive table of coefficients focusing on the lower range of X^3/V to fit values from the maximum pull on a rod. A rod of small radius and capable of suspending a low volume of liquid from the surface justifies the focus of this work on the low range of X^3/V. Since the ratio X^3/V is largely determined by probe radius, and because our probe is significantly larger than a rod, the surface tension of liquids in this study was calculated using the coefficients related to the upper range of X^3/V as determined by the envelope construction technique used by Padday and coworkers. The studied equations are presented in Table 3.2.

More recently, Christian and coworkers have synthesized all 18 polynomial expressions developed by Padday *et al.* into one cumbersome formula (Equation H, presented below), regardless of the range of X^3/V:

$$\frac{X}{k} = 2.48573 \cdot \left(\frac{X^3}{V}\right)^{0.5} + 0.70985 \cdot \left(\frac{X^3}{V}\right) + 4.21654 \cdot \left(\frac{X^3}{V}\right)^{1.5} - 1.94468 \cdot \left(\frac{X^3}{V}\right)^2 + 2.30285 \cdot \left(\frac{X^3}{V}\right)^3 - 2.77894 \cdot \left(\frac{X^3}{V}\right)^4 + 1.65453 \cdot \left(\frac{X^3}{V}\right)^5 - 0.420300 \cdot \left(\frac{X^3}{V}\right)^6 + 0.0129372 \cdot \left(\frac{X^3}{V}\right)^8 \qquad \text{(Equation H)}$$

In this work, Equation H was also analyzed for accuracy in measuring surface tension from the maximum pull on a disk.

3.2.2.4. Validation Design

To validate this test, surface tensions of 300 mL of distilled water, ethanol (EtOH), or 10% w/w ethanol in distilled water (10% EtOH/H_2O), were analyzed for each of the two probes (n=5). These three liquids were chosen to cover a broad range of surface tensions according to their literature values (approximately, 22 to 72 mN/m). The liquid temperature was registered prior to each test. To compare with literature values, accuracy was measured according to Equation 3.6:

$$Accuracy(\%) = \left[\left(\frac{\gamma_{calc}}{\gamma_{lit}}\right) - 1\right] \times 100 \qquad \text{(Equation 3.6)}$$

Where γ_{calc} and γ_{lit} are the calculated and literature values of surface tension of liquids, respectively.

3.2.2.5. Statistical Analysis

The data is presented as average ± standard deviation. Samples were analyzed in quintuplicate and evaluated for statistical differences with *t-test* for significance when $p < 0.05$ using NCSS/PASS software Dawson edition.[22]

3.3 RESULTS AND DISCUSSION

Force increases as a function of time when considering the distance moved by the texture analyzer arm at a constant speed. A typical graph of the measurement of surface tension of liquids using this method is shown in Figure 3.2.

The peak (F_{max}) represents the force of probe detachment from the surface of the liquid. The F_{max} values measured for water, 10% w/w ethanol in water and ethanol and their respective calculated X^3/V are shown in Table 3.3. Considering the radius of the probes and the maximum force, the majority of the X^3/V values for liquids evaluated in this study do not fall within the ranges provided in the work from Padday and coworkers, namely: 0.01 – 1.85. Interestingly, both probe sizes presented very precise results, with coefficients of variation smaller than 1%, indicating the high reproducibility of this method. Nevertheless, F_{max} (and consequently X^3/V) was more precise for the large probe diameter. Based on the study from maximum pull on a rod, the equations related to the upper range of X^3/V (Table 3.2) were empirically used to calculate the surface tension values of the referred liquids for comparison with the literature values.[23] The results of X^3/V to Equation H as previously described were also fitted. The accuracy results are presented in Figure 3.3 for small and large diameter probes.

The surface tension of water, ethanol and the hydroalcoholic solution calculated using Equations A to H) presented overall underestimated values compared to literature data. Regardless of probe size, similar patterns were observed for the equation groups B/D and C/E/F/G. Besides more precise results, the large diameter probe presented more accurate values than the small probe. This may indicate that accuracy and precision may be dependent on an optimum probe diameter. Figure 3.4 helps to elucidate this trend. Considering the differences in accuracy of surface tension according to the probes investigated (radius of approximately 2.5 and 3.0 cm), it is believed that increasing the

probe radius to about 3.5 to 4.0 cm may provide even more accurate results. Further studies are warranted for verification of this relationship, but it is noteworthy to highlight that with increased radius, a wider container is necessary to maintain the infinite interface configuration later discussed, consequently requiring a greater sample volume. Nevertheless, using the large probe and Equation E, for instance, provided results with accuracy that was less than 5% from literature values for water (69.55 ± 0.34 mN/m), 10% w/w ethanol in water (45.20 ± 0.13 mN/m) and ethanol (21.40 ± 0.05 mN/m). Interestingly, Equations C, E, F and G, which provided similarly better accuracy results with the large probe, are either first or second order polynomial forms of X^3/V. This indicates that an exponential function does not necessarily model an increase in force as a function of disk diameter, as previously described by Nietz and Lambert.[7] Finally, Equation H appears to be unfeasible for use in the calculation of surface tension from maximum pull on a disk, since it is equally accurate compared to Equations C, E, F and G when X^3/V is below 2.0 but largely deviates from the literature values when this parameter increases.

Any slight discrepancy between the calculated values of surface tension measured by the large probe (e.g. using Equation E) and the literature values may be explained by a number of factors that could be considered limitations of this method. Most importantly, the probe and liquid surfaces must be in full and close contact throughout the measurement. To ensure this, probe and container surfaces were thoroughly cleaned prior to experiments with an abrasive detergent, adequately dried to remove any dust, and followed by careful handling to avoid particle settling. Additionally, our in-house constructed glass probe is prone to present a non-ideal edge roughness, as well as micro-chips and micro-cracks despite careful handling and storage. A glass probe produced and stored under strict specifications in terms of edge roughness, radius measurement, and

storage container, may potentially provide even more accurate results. Moreover, considering the large surface area of the probes, any tilt in probe position in relation to the surface of the liquid, must be avoided. In this study, leveling was performed by placing a level instrument on the texture analyzer platform and adjusting the legs of the equipment. Lastly, the operator must certify that any bubble underneath the probe is removed prior to starting the test. This has been performed in this study purely based on visual observation. When a high volume of sample is being analyzed (e.g. 300 mL as initially tested), the operator can easily identify the presence of bubbles by looking upwards at the liquid-probe contact point from a low eye position. In the case of opaque liquids (e.g. suspensions, emulsions) and low volume samples, the configuration in Figure 3.5 with a mirror positioned underneath the sample container is very useful. Frequently, a series of upward and downward movements with the texture analyzer arm is necessary to ensure that no bubbles are impeding the direct contact between glass probe and liquid surface. A container equipped with ultrasonication capability is an alternative option to help remove bubbles, both dissolved in the liquid and generated by the contact of the probe with the surface of the liquid.

Furthermore, temperature is highly influential in the determination of liquid surface tension and should be strictly controlled. In our proof-of-concept experiments, the liquid temperature was registered using an ordinary alcohol lab thermometer. Alternatively, a thermal cabinet adequately adapted to enclose the container (and possibly the texture analyzer arm) could provide improved temperature control. Furthermore, there must be sufficient distance between the probe and container walls to eliminate cross-interference in the measurement of surface tension of liquids (infinite interface).[24, 25] For this reason, and considering probe diameter, a wide circular container was used in our study, necessitating a sample volume of a few hundred milliliters. Further studies to

determine the minimum sample volume for this setup have also been performed. Using 50 mL, the surface tension of water analyzed at 24 °C was calculated using Equation E of this method and found to be 69.79 ± 0.24 mN/m. This is not statistically different from the measurement made with 300 mL of water. With smaller sample volumes, stricter temperature control is even more important because heat transfer to the liquid mass turns the sample more prone to temperature variation. Lastly, any difficulty in measuring the surface tension of surfactant solutions due to rise of liquid against the glass probe wall, may be circumvented via careful control of the ascending arm speed of the texture analyzer. This would allow adequate time for the liquid to drain down as the peak force is approached.

Remarkably, uncertainty in absolute values of surface tension of liquids using different methods has been widely described. For instance, the surface tension of water at 25°C has been reported between 71.82 and 73.0 mN/m.[26, 27] Therefore, our method presents an acceptable accuracy. Particularly, the method presents excellent precision, with coefficients of variation below 0.5% for the large probe (1.4% for the small probe). During our studies though, it was observed that more precise measurements were obtained at the end of a series of analysis. Studies on the dehydration of glass surfaces indicate an increase in contact angle as a function of water drying time.[28] These findings may indicate that the glass probe needs to be in contact with aqueous solutions for a certain period of time prior to analysis of surface tension.

3.4 CONCLUSION

A glass probe disk with radius of approximately 3 cm attached to the arm of a texture analyzer can be used to measure the detachment force from a liquid surface. This

maximum force can be extrapolated to equations previously developed to calculate surface tension from the maximum pull on a rod. Using this method, calculated absolute values of surface tension of selected liquids are within 5% from literature values. With this setup, sample volumes as low as 50 mL can be analyzed. Using a texture analyzer to determine surface tension provides an additional feature for this versatile equipment already used in a multitude of testing procedures and therefore widely available in such research laboratories. This experiment provides a precise, simple and quick method to determine the surface tension of liquids from the maximum pull on a disk. Further studies are necessary to ensure the optimal probe diameter necessary to improve accuracy in the values of surface tension compared to the literature.

3.5 TABLES

Parameter	Value
Texture analyzer protocol:	Adhesive test
Speed of descent:	0.5 mm/s
Trigger force:	0.20 mN
Contact time:	5 s
Return distance:	10 mm
Return speed:	0.05 mm/s
Data acquisition:	5 points per second

Table 3.1 – Settings on texture analyzer for measurement of surface tension of liquids from the maximum pull on a disk.

Equation	Range of X^3/V	Formula
A	0.50 – 0.60	$\frac{X}{k} = 0.378 + 5.8 \cdot \left(\frac{X^3}{V}\right)$
B	0.60 – 0.80	$\frac{X}{k} = 0.57211 + 5.15631 \cdot \left(\frac{X^3}{V}\right) + 0.533894 \cdot \left(\frac{X^3}{V}\right)^2$
C	0.80 – 1.00	$\frac{X}{k} = 0.299048 + 5.8626 \cdot \left(\frac{X^3}{V}\right) + 0.0783455 \cdot \left(\frac{X^3}{V}\right)^2$
D	1.00 – 1.20	$\frac{X}{k} = 0.676415 + 5.16281 \cdot \left(\frac{X^3}{V}\right) + 0.401204 \cdot \left(\frac{X^3}{V}\right)^2$
E	1.20 – 1.40	$\frac{X}{k} = 0.0408687 + 6.20312 \cdot \left(\frac{X^3}{V}\right) - 0.0240752 \cdot \left(\frac{X^3}{V}\right)^2$
F	1.40 – 1.60	$\frac{X}{k} = 0.253174 + 5.90351 \cdot \left(\frac{X^3}{V}\right) - 0.0814259 \cdot \left(\frac{X^3}{V}\right)^2$
G	1.60 – 1.85	$\frac{X}{k} = -0.013 + 6.2 \cdot \left(\frac{X^3}{V}\right)$

Table 3.2 – Relation of X/k as a function of X^3/V for the calculation of surface tension of liquids from the maximum pull on rods with different diameters.[11]

Liquid	F_{max} (mN)		X^3/V	
	X_S	X_L	X_S	X_L
Water	101.44 ± 0.65[a] (0.64%)	142.57 ± 0.36 (0.25%)	1.577 ± 0.010[a] (0.64%)	1.804 ± 0.005 (0.25%)
10% w/w ethanol in water	81.79 ± 0.16 (0.20%)	113.71 ± 0.16 (0.14%)	1.923 ± 0.004 (0.20%)	2.223 ± 0.003 (0.14%)
Ethanol	50.25 ± 0.17 (0.33%)	69.78 ± 0.08 (0.11%)	2.506 ± 0.008 (0.33%)	2.901 ± 0.003 (0.11%)

[a] The liquid temperature during measurement was 24 °C. F_{max}: maximum detachment force; X: probe radius; V: volume; S: small; L: large.

Table 3.3 – Values of measured F_{max} for three different liquids and their respective calculated X^3/V at 25°C, unless specified. Results are expressed as mean ± standard deviation (coefficient of variation) for 5 replicates.

3.6 FIGURES

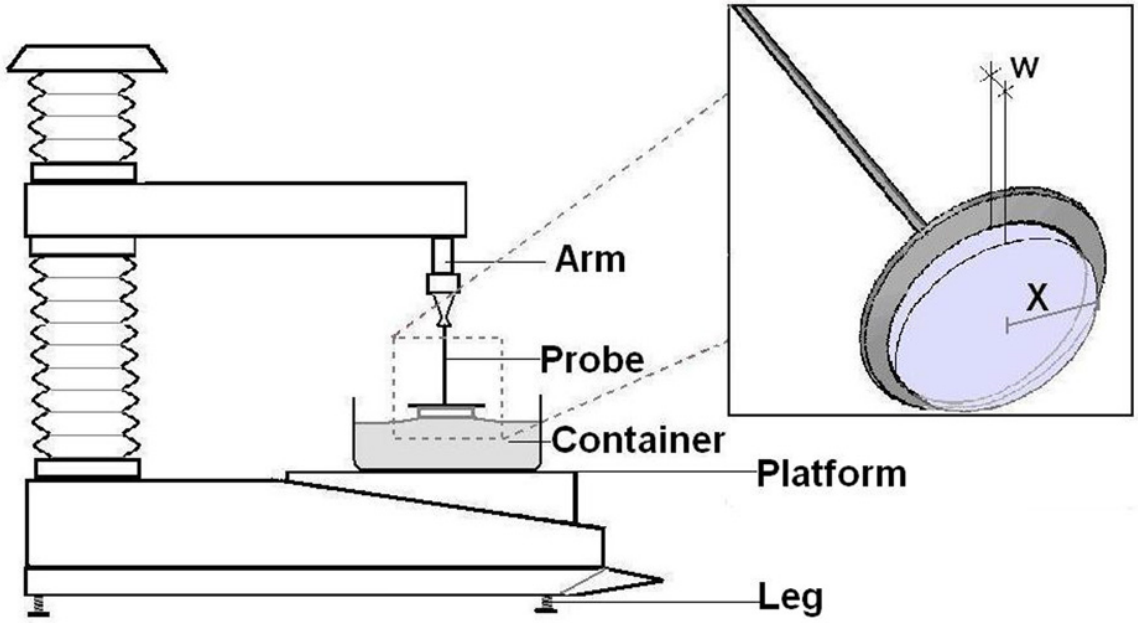

Figure 3.1 – Schematic diagram of texture analyzer used to measure the surface tension of liquid. Details of the probe appear in the zoomed-in area. *X* and *W* represent radius and width of the glass disk probe, respectively.

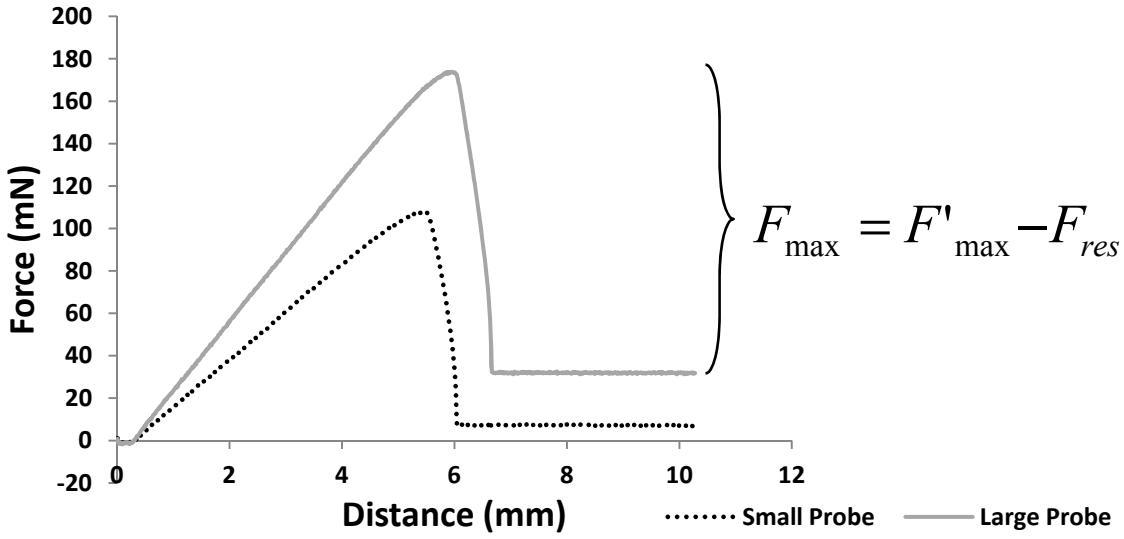

Figure 3.2 – A typical graph from the maximum pull on a disk using the present method for small and large probes.

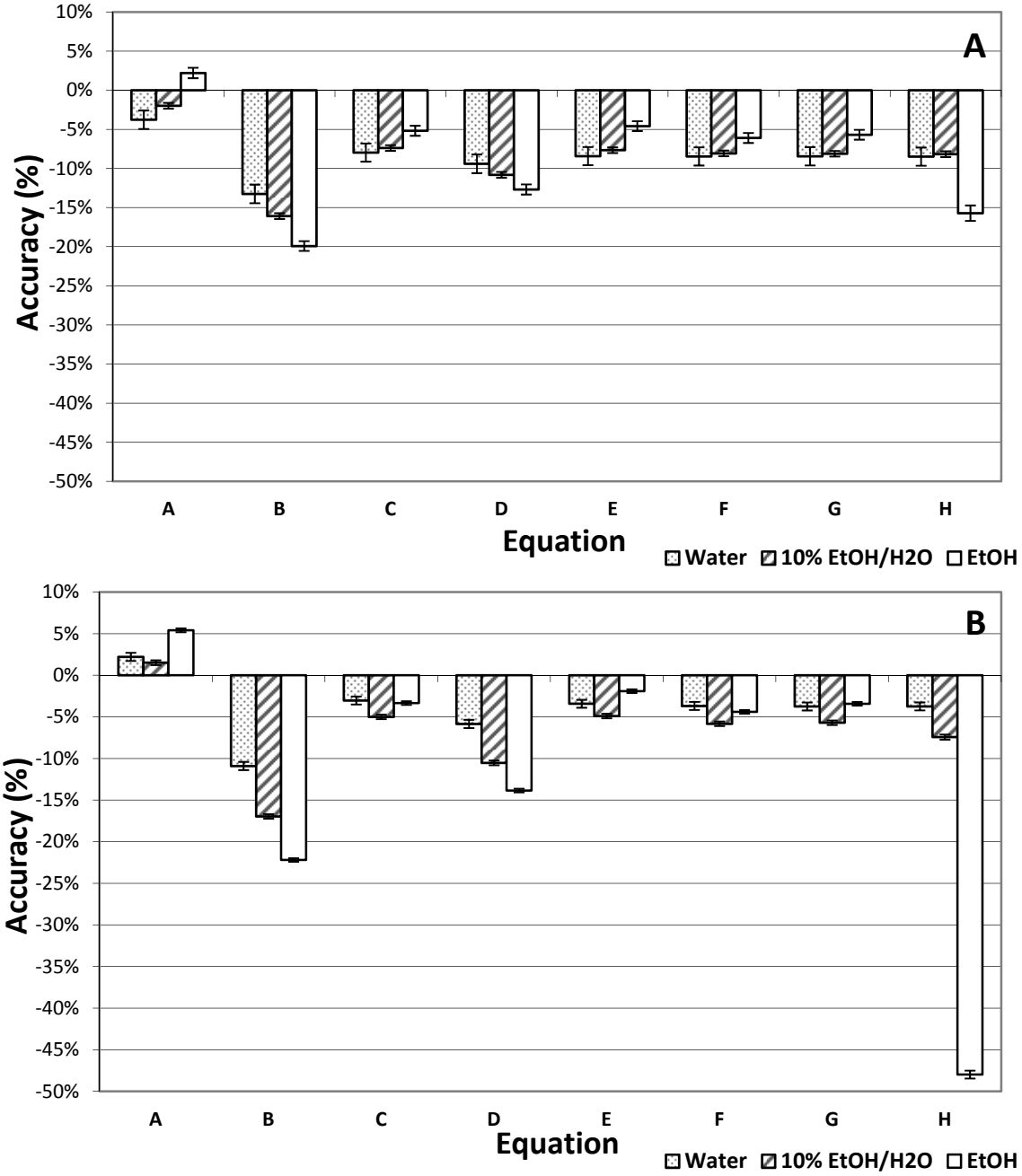

Figure 3.3 – Accuracy in measurement of surface tension of three different liquids based on extrapolation on the theory of maximum pull on a rod to the application of disks as probe geometries. Results are expressed as mean ± standard deviation (n = 5). Equations A to G are shown in Table 3.2 and Equation H is presented in section 3.2.2.3. A: small probe (X_S); B: large probe (X_L).

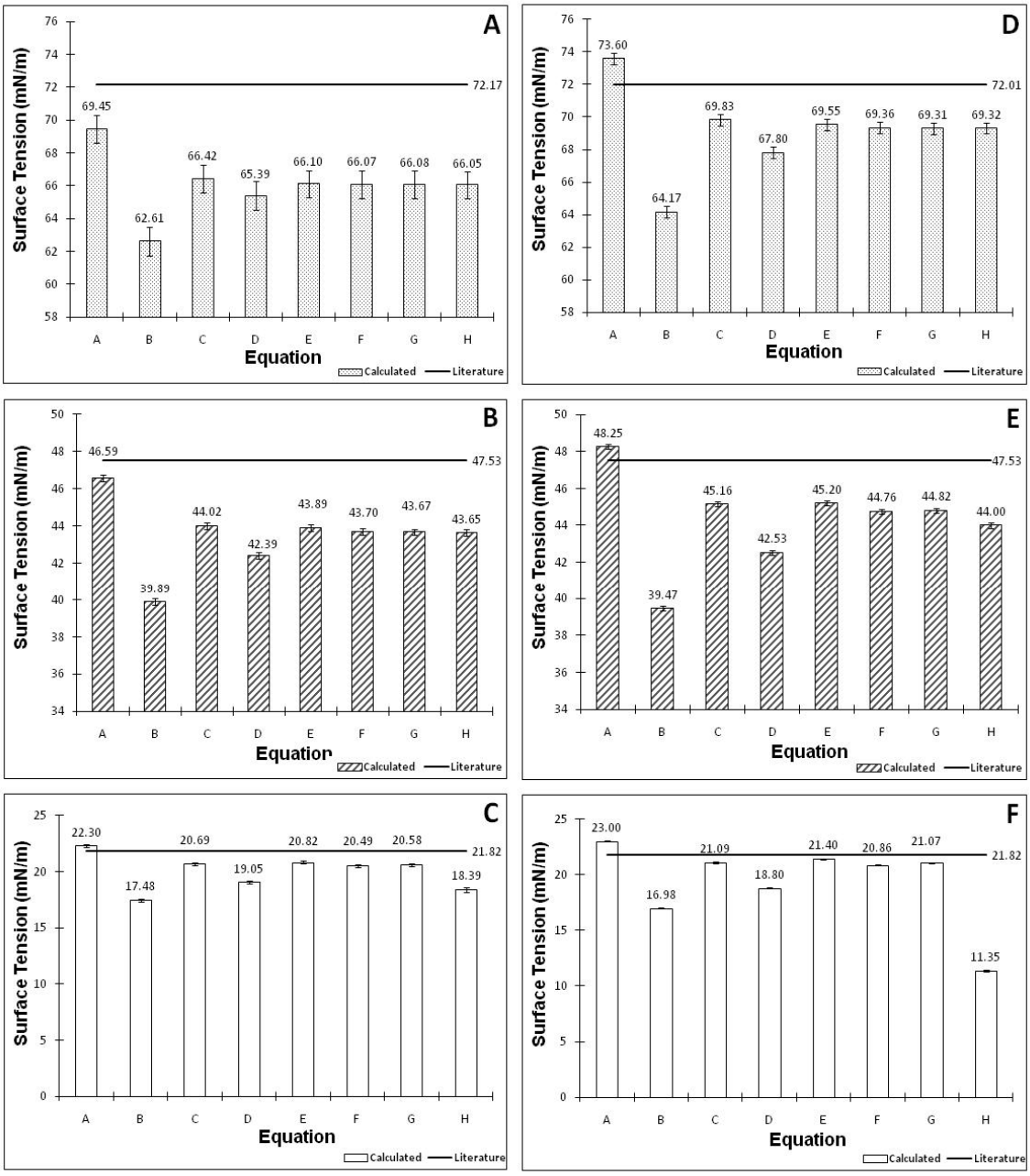

Figure 3.4 – Comparison with literature values of surface tension of water (dotted), 10% ethanol in water (diagonal) and ethanol (empty columns); based on extrapolation on the theory of maximum pull on a rod to the application of disks as probe geometries. Results are expressed as mean ± standard deviation (n = 5). Equations A to G are shown in Table 3.2 and Equation H is presented in the section 3.2.2.3. A-C: small probe (X_S); D-F: large probe (X_L). Measurements were performed at 25°C (except graph A: 24°C).

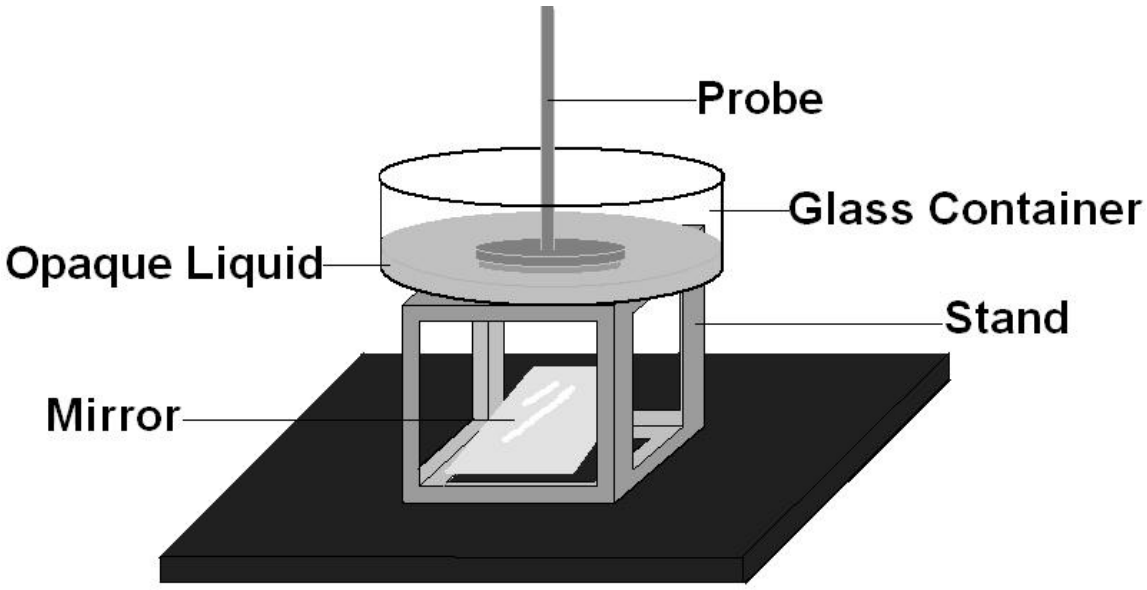

Figure 3.5 – Setup for measurement of surface tension of opaque liquids, such as suspensions and emulsions, and/or low volume samples for better visualization of the presence of bubbles between the liquid surface and the glass disk probe. The stand is a cube shaped structure with open walls in all faces. Therefore, the movement of the texture analyzer arm should be controlled to avoid breaking the glass container.

3.7 REFERENCES

[1] Fathi-Azarbayjani A, Jouyban A, Chan SY. Impact of Surface Tension in Pharmaceutical Sciences. J Pharm Pharm Sci. 2009;12(2):218-28.

[2] Bummer PM. Interfacial Phenomena. In: Hendrickson R, ed. *Remington: The Science and Practice of Pharmacy*. 21st ed. Baltimore, MD: Lippincott Williams & Wilkins 2005:280-92.

[3] Ghazanfari T, Elhissi AMA, Ding Z, Taylor KMG. The influence of fluid physicochemical properties on vibrating-mesh nebulization. Int J Pharm. 2007;339(1-2):103-11.

[4] McCallion ONM, Taylor KMG, Thomas M, Taylor AJ. The influence of surface tension on aerosols produced by medical nebulisers. Int J Pharm. 1996;129(1-2):123-36.

[5] McCallion ONM, Taylor KMG, Thomas M, Taylor AJ. Nebulization of Fluids of Different Physicochemical Properties with Air-Jet and Ultrasonic Nebulizers. Pharm Res. 1995 Nov;12(11):1682-8.

[6] Minko T. Interfacial Phenomena. In: Sinko PJ, ed. *Martin's physical pharmacy and pharmaceutical sciences*. 5th ed. Baltimore, MD: Lippincott Williams & Wilkins 2006:437-67.

[7] Nietz AH, Lambert RH. Effect of Some Factors on the Ring Method for determining Surface Tension. The Journal of Physical Chemistry. 1929;33(10):1460-7.

[8] Ugarcic Z, Vohra DK, Atteya E, Hartland S. Measurement of Surface Tension using a Vertical Cone. Journal of the Chemical Society-Faraday Transactions I. 1981;77:49-61.

[9] Freud BB, Freud HZ. A Theory of the Ring Method for the Determination of Surface Tension. J Am Chem Soc. 1930;52(5):1772-82.

[10] Harkins WD, Jordan HF. A Method for the Determination of Surface and Interfacial Tension from the Maximum Pull on a Ring. J Am Chem Soc. 1930;52(5):1751-72.

[11] Padday JF, Pitt AR, Pashley RM. Menisci at a Free Liquid Surface - Surface Tension from Maximum Pull on a Rod. Journal of the Chemical Society-Faraday Transactions I. 1975;71:1919-31.

[12] Christian SD, Slagle AR, Tucker EE, Scamehorn JF. Inverted vertical pull surface tension method. Langmuir. 1998;14(11):3126-8.

[13] Schulz M, Fussnegger B, Bodmeier R. Drug release and adhesive properties of crospovidone-containing matrix patches based on polyisobutene and acrylic adhesives. Eur J Pharm Sci. 2010 Dec;41(5):675-84.

[14] Majzoobi M, Ostovan R, Farahnaky A. Effects of Hydroxypropyl Cellulose on the Quality of Wheat Flour Spaghetti. J Texture Stud. 2011 Feb;42(1):20-30.

[15] Bansal K, Rawat MK, Jain A, Rajput A, Chaturvedi TP, Singh S. Development of Satranidazole Mucoadhesive Gel for the Treatment of Periodontitis. AAPS PharmSciTech. 2009 Sep;10(3):716-23.

[16] Mei XH, Etzler FM, Wang Z. Use of texture analysis to study hydrophilic solvent effects on the mechanical properties of hard gelatin capsules. Int J Pharm. 2006;324(2):128-35.

[17] Lu S, Chen JJ, Chen YK, Li CY, Lai P, Chen HH. Water mobility, rheological and textural properties of rice starch gel. J Cereal Sci. 2011 Jan;53(1):31-6.

[18] Tukaram BN, Rajagopalan IV, Shartchandra PSI. The Effects of Lactose, Microcrystalline Cellulose and Dicalcium Phosphate on Swelling and Erosion of Compressed HPMC Matrix Tablets: Texture Analyzer. Iranian Journal of Pharmaceutical Research. 2010 Fal;9(4):349-58.

[19] Li CB, Shi PL, Xu C, Xu XL, Zhou GH. Tracing processes of rigor mortis and subsequent resolution of chicken breast muscle using a texture analyzer. J Food Eng. 2010 Oct;100(3):388-91.

[20] Bernardin JD, Mudawar I, Walsh CB, Franses EI. Contact angle temperature dependence for water droplets on practical aluminum surfaces. Int J Heat Mass Transfer. 1997;40(5):1017-33.

[21] Richards TW, Carver EK. A Critical Study of the Capillary Rise Method of Determining Surface Tension, with Data for Water, Benzene, Toluene, Chloroform, Carbon Tetrachloride, Ether and Dimethyl Aniline[Second Paper]. J Am Chem Soc. 1921;43(4):827-47.

[22] Hintze J. NCSS and PASS. released January 29th, 2004 ed. Kaysville, UT, USA: Number Cruncher Statistical Systems 2001.

[23] Surface Tension of Aqueous Mixtures. In: Lide DR, ed. *CRC handbook of chemistry and physics, 90th edition (Internet Version 2010)*. Boca Raton, FL: CRC Press/Taylor and Francis 2010:6-131.

[24] Furlong DN, Hartland S. Wall Effects in Measurement of Surface Tension using a Vertical Cylinder.1. Theory. Journal of the Chemical Society-Faraday Transactions I. 1980;76:457-66.

[25] Furlong DN, Hartland S. Wall Effects in Measurement of Surface Tension using a Vertical Cylinder. 2. Experimental. Journal of the Chemical Society-Faraday Transactions I. 1980;76:467-72.

[26] Pallas NR, Pethica BA. The Surface Tension of Water. Colloids Surf. 1983;6(3):221-7.

[27] Gaonkar AG, Neuman RD. The Uncertainty in Absolute Values of Surface Tension of Water. Colloids Surf. 1987;27(1-3):1-14.

[28] Englander T, Wiegel D, Naji L, Arnold K. Dehydration of glass surfaces studied by contact angle measurements. J Colloid Interface Sci. 1996 May;179(2):635-6.

Chapter 4: Development and Characterization of Phospholipid-Stabilized Submicron Aqueous Dispersions of Coenzyme Q_{10} Presenting Continuous Vibrating-Mesh Nebulization Performance

Abstract

Coenzyme Q_{10} (CoQ_{10}) is a poorly-water soluble compound that is being investigated for the treatment of carcinomas. The aim of this research was to develop a suitable formulation for pulmonary delivery of this anticancer agent. An appropriate selection of excipients (phospholipids) and a suitable device (Aeroneb Pro® vibrating-mesh nebulizer) were selected initially after reviewing the literature. Initial characterization of the bulk drug using X-ray diffraction (XRD), Differential Scanning Calorimetry (DSC), Laser Diffractometry (LD) and Scanning Electron Microscopy (SEM) was performed. High shear mixing, high pressure homogenization or ultrasonication was then evaluated as feasible manufacturing processes to obtain small particle size dispersions of CoQ_{10}. Following selection of an appropriate process, the parameters affecting drug particle size were studied. Using LD and gravimetrical analysis, nebulization was evaluated to assess the performance of the inhalation system triad: drug-excipients-device. CoQ_{10} powder studied was crystalline with a melting point approximately at 51 °C with a particle size of 30 μm. Therefore, particle downsizing was deemed necessary for pulmonary delivery. Microfluidization was found to be a suitable method to prepare submicron drug particles in aqueous dispersions. The number of passes and type of phospholipids (lecithin or Dipalmitoyl Phosphatidylcholine – DPPC) used strongly affected final drug particle size of the dispersions. Nebulization performance of lecithin-stabilized CoQ_{10} dispersions varied according to number of passes in the microfluidizer. Most importantly, the rheology of these dispersions appeared to play a significant role in the aerosol generation from the active vibrating-

mesh nebulizer used. In conclusion, aqueous dispersions of CoQ_{10} were adequately produced using a microfluidizer with characteristics that were suitable for pulmonary delivery with an Aeroneb Pro® nebulizer.

4.1. INTRODUCTION

Coenzyme Q_{10}, also known as CoQ_{10}, ubiquinone or ubidecarenone, is a vitamin-like compound in that it is similar in structure to vitamin K. CoQ_{10} is absorbed in a similar fashion to vitamin E; this becomes enhanced in the presence of lipids.[1] Naturally found in the body, therefore not considered a vitamin, this compound primarily participates in electron transport and proton transfer in mitochondrial respiration.[2] It follows that altering the levels of this antioxidant may have an impact on aging, neurodegenerative and cardiovascular diseases, diabetes and cancer.[3] Endogenous CoQ_{10} has shown to be a prognostic factor for melanoma progression by observing that patients with higher levels presented a lower risk of metastasis.[4] Therapy using exogenous CoQ_{10} has long been reported in cases where a number of cancer patients were effectively treated against a variety of different types of carcinomas.[5, 6] Reports include survival ranging from 5 to 15 years for pancreas, rectum, breast, prostate, larynges, or lung cancer patients. Recent findings indicate that chemotherapeutic drugs (e.g. camptothecin, etoposide, doxorubicin, methotrexate) can increase levels of CoQ_{10} following treatment of cancer cell lines.[7] Further studies have shown that this endogenous compound may act against melanoma and other malignancies through modulation of the BCL-2 protein family.[8-10] Although improved survival rates for end stage cancer patients treated with CoQ_{10} have lately been confirmed in a pilot study, no rigorous trials have been carried out to substantiate these findings.[11] This anticancer

agent is a poorly-water soluble compound presented as a yellow or orange crystalline powder.[12]

The pulmonary delivery of such compounds has been attempted in dosage forms of nanosuspensions and liposomes where vibrating-mesh nebulizers have been used.[13-19] These devices generate aerosol by vibrating a mesh following application of electrical current to a piezoelectric membrane.[20] Studies have shown that surface tension, viscosity, and ion concentration play a significant role in the aerosol output from these devices.[21] Since droplet sizes of 1 to 5 μm generated from nebulizers are expected to reach the deep lungs following inhalation,[22] it is crucial to select appropriate excipients and a suitable delivery device.

The highest plasma concentration of CoQ_{10} reported in the literature is 10.7 μmol/L (approximately 9 μg/mL) from a solubilized formulation among several oral formulations available on the market as dietary supplements (nutraceutical).[23] Nevertheless, the maximum tolerated dose (MTD) has yet to be determined. We hypothesize that formulations of CoQ_{10} can be developed for pulmonary delivery with a satisfactory pharmacokinetic profile that will improve the pharmacodynamic response to treat lung malignancies. By delivering a high amount of drug to the disease site, a lower dose may be necessary compared to intravenous or oral administration. Additionally, systemic distribution from the lungs may favor treatment of carcinoma in different body organs. However, the systemic absorption from the lungs is unknown.

The main objective of this study was to develop an inhalable formulation of CoQ_{10}. We start by introducing the rationale for selection of the main elements of this formulation: device and excipients for pulmonary delivery. We then present preformulation characterization of bulk CoQ_{10} limited to our intended purpose. Next, we selected an appropriate manufacturing process with scale up potential. Finally, we

determined the nebulization capacity of this dispersion and investigated the possible physicochemical properties of the formulation that may be indicative of nebulization performance. We discovered out that rheology may play a significant role in the hydrodynamics of aerosol production using a vibrating-mesh nebulizer with CoQ_{10}.

4.2. RATIONALE FOR FORMULATION DESIGN

The intended purpose of this formulation is to deliver CoQ_{10} to treat lung malignancies via inhalation therapy. The formulation design of this poorly-water soluble compound is extremely important to ensure the safe delivery to patients. For this reason, consideration of the bulk physicochemical properties of this drug and an adequate selection of excipients and device ensures an appropriate formulation design. In turn, a feasible manufacturing process guarantees the development of the final dosage form for pulmonary delivery.

In general, a nebulizer is selected for inhalation therapy over pressurized Metered Dose Inhalers (pMDIs) and Dry Powder Inhalers (DPIs) by virtue of their capability of delivering high amounts of drugs via passive breathing.[24] Therefore, patients with impaired pulmonary function (e.g. lung cancer patients) are not expected to experience difficulty in using this type of device. Based on previous studies confirming the capability of this device in delivering poorly-water soluble drugs as a dispersed dosage form, we have designed the delivery of CoQ_{10} to the lungs using the Aeroneb Pro® micropump nebulizer (Aerogen Ltd, Galway, Ireland).[13-15] This autoclavable device, designed for mechanically ventilated patients in hospital settings, is an active vibrating-mesh nebulizer.[25] This functioning mechanism generates aerosol from aqueous-based formulations, including liposomes.[17-19] The device has a mesh placed on the bottom of

the nebulizer reservoir (medication cup capacity: 10 mL) that actively vibrates (frequency of nebulizer unit: 128 KHz) generating an aerosol from the liquid that is available in the reservoir (low residual volume in medication cup minimizes drug waste)[26]. Importantly, the performance of this nebulizer can be affected by mesh clogging, resulting in changes in the performance and ultimately automatic switch off of the device.[27] Therefore, thorough cleaning of the membrane must be ensured prior to performing each test run.

A very limited number of excipients are available for safe delivery of drugs via nebulization, which complicates the selection process.[28] Phospholipids are the main constituents of the human alveolar surfactant (90%), and there is a predominant occurrence of phosphatidylcholine (PC – 73% of phospholipids). Among the different saturated and unsaturated lipidic chains of PC, dipalmitoyl phosphatidylcholine (DPPC) is the main component (81% of PC), while dimyristoyl phosphatidylcholine (DMPC) and distearoyl phosphatidylcholine (DSPC) each comprise 3% of PC.[29] We have chosen to stabilize our formulations with phospholipids given their physiological occurrence in the lungs.

Lung surfactants are used for the treatment of Respiratory Distress Syndrome (RDS) in premature infants.[30] Survanta is an intratracheal suspension (25 mg/mL of phospholipids) of pulmonary surfactant extracted from natural bovine lungs. Other pulmonary surfactants include: Curosurf, from porcine extract (80 mg/mL of phospholipids); Exosurf, a synthetic phospholipid mixture of DPPC (13.5 mg/mL) with cetyl alcohol (1.5 mg/mL) and tyloxapol (1 mg/mL); and Infasurf, from calf lung lavage (35 mg/mL of phospholipids).[31] We have chosen 2.5% w/w to be the maximum phospholipid concentration in our formulations, which is the same as in the approved drug product Survanta®. DPPC is one of the components of the mixtures of phospholipids

that comprise soybean lecithin, with concentrations varying widely depending on the source and extraction method.[32, 33] Given that it is already in approved drug products for inhalation and available at a low cost, lecithin has been selected as a model phospholipid. DPPC was also selected and analyzed as a purified PC choice.

Figure 4.1 presents our vision of the pulmonary delivery of CoQ_{10} based on our formulation design. The bulk drug is formulated into a phospholipid-stabilized aqueous dispersion with small (drug) particle size that is aerosolized using the vibrating-mesh nebulizer into droplets containing small drug particles. For definition purposes, "particle" is referring the internal phase of the aqueous dispersion and "droplet" is referring the result of becoming aerosol generated. Ideally, each droplet contains a certain number of drug particles. The physicochemical characterization of bulk CoQ_{10} for our intended purposes and the selection of a manufacturing process are presented next.

4.3. MATERIALS AND METHODS

4.3.1. Materials

Coenzyme Q_{10} was supplied by Asahi Kasei Corp. (Tokyo, Japan). Lecithin (granular, NF) was purchased from Spectrum Chemical Mfg. Corp. (Gardena, CA, USA). Genzyme Pharmaceuticals (Liestal, Switzerland) provided 1,2-dipalmitoyl-sn-glycero-3-phosphocholine (DPPC). Sodium chloride (crystalline, certified ACS) was acquired from Fisher Chemical (Fisher Scientific, Fair lawn, NJ, USA) and the deionized water was obtained from a central reverse osmosis/demineralizer system commonly found in research laboratories. The dispersant 1,3-propanediol (98%) was purchased from Sigma-Aldrich (St. Louis, MO, USA). Ethanol 200 proof USP was purchased from Decon Laboratories (King of Prussia, PA, USA).

4.3.2. Bulk Characterization of CoQ_{10}

4.3.2.1. X-ray diffraction (XRD)

Testing was performed using a Philips Model 1710 X-ray diffractometer (Philips Electronic Instruments Inc., Mahwah, NJ, USA) with primary monochromated radiation (CuKα1, λ = 1.54056 Å) emitting at an accelerating voltage of 40 kV and 30 mA. The CoQ_{10} powder was placed into a stage and the sample was scanned for diffraction patterns from 5º to 50º at 0.05º intervals of 2θ angles, with dwell time of 3 seconds.

4.3.2.2. Differential Scanning Calorimetry (DSC)

DSC testing was performed using a 2920 Modulated DSC (TA Instruments, New Castle, DE, USA) and analyzed using TA Universal Analysis 2000 Software. Powder of CoQ_{10} was weighed (10.5 mg) into aluminum pan (kit 02190041, Perkin-Elmer Instruments, Norwalk, CT, USA) and crimped. At a heating rate of 10 °C/min, the thermal behavior of the sample was analyzed from 10 to 120 °C.

4.3.2.3. Laser Diffraction (LD)

Bulk CoQ_{10} powder was dispersed in 20% (v/v) 1,3-propanediol in deionized water for analysis of particle size distribution. This dispersed sample was then added to a small cell apparatus in a Malvern Mastersizer S® instrument (Malvern Instruments, Worcestershire, UK) equipped with a 300 mm lens until 5-10% obscuration was attained. The internal phase and dispersant refractive indexes were 1.45 and 1.33, respectively.

4.3.2.4. Scanning Electron Microscopy (SEM)

Analysis of physical appearance and estimation of particle size of bulk CoQ_{10} were performed using SEM. An aluminum stage with adhesive carbon tape held the powder sample. Coating was carried out in a rotary-planetary-tilt stage with platinum-iridium using a Cressington Sputter Coater 208 HR (Cressington Scientific Instruments, Watford, England) under argon atmosphere. The SEM pictures were captured using SmartSEM® graphical user interface software in a Carl Zeiss Supra® 40VP Scanning Electron Microscope (Carl Zeiss AG, Oberkochen, Germany) operated at a working distance of 19 mm and at 5 kV of Electron High Tension (EHT).

4.3.3. Determination of Manufacturing Process

We have tested three different manufacturing processes with the objective of obtaining an aqueous dispersion with a small drug particle size. A phospholipid dispersion containing 6% w/w of lecithin in water was added to the molten CoQ_{10} (1% w/w) at 55 °C. The lecithin concentration is above the critical micellar concentration (depending on soybean seed type and processing method, CMC varies from 1.3 to 5.5 mg/mL[33]). The formulation was then processed as follows.

4.3.3.1. High Shear Mixing

One hundred milliliters of formulation was stirred at 300 rpm and high shear mixed at 10,000-12,000 rpm for 45 minutes using an Ultra-Turrax® TP 18/10 Homogenizer with 8 mm rotor blade (IKA-Werke, Staufen, Germany).

4.3.3.2. High Pressure Homogenization

The microfluidization process works by having two jet streams in opposite directions. Each pass represents one chance that the drug particles have to collide against each other, breaking apart and becoming smaller. The formulation was predispersed using probe sonication for 2 minutes, followed by 30 passes at approximately 13,000 psi using an M-110Y High Pressure Pneumatic Microfluidizer® (Microfluidics, Newton, MA USA).

4.3.3.3. Ultrasonication

The formulation was ultrasonicated at 125W for 60 minutes using an Omni Sonic Ruptor-250® Ultrasonic Homogenizer with 5/32" (3.9mm) with a micro-tip probe (Omni International, Kennesaw, GA, USA).

4.3.4. Formulation Development

After selection of the manufacturing process, formulations were prepared with high pressure homogenization to determine the effect of the selected parameters and type of phospholipid on the particle size distribution of the drug dispersion. During preliminary studies, it has been observed that the high solute concentration of formulations containing 6% w/w of lecithin was not able to produce aerosol from the Aeroneb Pro® vibrating-mesh micropump nebulizer. Further preliminary studies have also shown that formulations containing a reduced concentration of lecithin (1% w/w, at 1:1 drug-to-lipid ratio) have presented sufficient stability for evaluation of nebulization performance following preparation. Therefore, reduction of phospholipid concentration

was necessary while simultaneously keeping the concentration of CoQ_{10} constant at an adequate drug-to-lipid ratio.

Following hydration, a phospholipid dispersion containing 1% w/w of phospholipid (lecithin or DPPC) in water was added to the molten CoQ_{10} (1% w/w) at 55 °C. The formulation was then predispersed using high shear mixing (Ultra-Turrax® TP 18/10 Homogenizer with 8 mm rotor blade, IKA-Werke, Staufen, Germany) for up to 5 minutes at 20,000 rpm. Subsequently, the formulation was passed through an M-110P Bench-top Microfluidizer® (Microfluidics, Newton, MA USA) up to 100 times at approximately 30,000 psi while maintaining the temperature between 50 and 60 °C.

In testing the effects that the type of phospholipid and number of passes have on particle size distribution of the formulations, phospholipid dispersions were hydrated for approximately 1 hour without stirring (Table 4.1, Formulations A and B). Formulations were then passed through a microfluidizer 10, 20, 30, 40 and 50 times when comparing different phospholipids; 20, 50, 70 and 100 times when evaluating the effect from number of passes. For nebulization performance tests, the phospholipid dispersions were hydrated overnight with stirring and 0.9% w/v of sodium chloride was added to the final formulation (Table 4.1, Formulation C).

The particle size distributions of the formulations were then analyzed using Laser Diffraction (LD) and/or Dynamic Light Scattering (DLS). The surface tension, zeta potential and rheology were also evaluated. For nebulization performance, aerosol output was performed using LD and gravimetrical analysis. Unless otherwise stated, samples were characterized following preparation.

4.3.5. Formulation Characterization

4.3.5.1. Particle Size Distribution

Particle size distribution testing of the dispersed formulations was performed with LD using a wet sample dispersion unit stirring at 1,000 rpm coupled to a Malvern Spraytec® (Malvern Instruments, Worcestershire, UK) equipped with a 300 mm lens. The dispersed formulations were added to distilled water (dispersant) until approximately 5% laser obscuration was attained. The internal phase and dispersant refractive indexes were set as 1.45 and 1.33, respectively, based on reports related to lecithin in the literature.[34] A timed measurement was performed for 45 seconds with 1 second sampling periods (a total of 45 measurements). Results are presented as $Dv_{(X)}$ and span, where X is the cumulative percentile of particles under the referred size (e.g. $Dv_{(50)}$ corresponds to the median volume of the particles). Span is a measurement of particle size distribution calculated as $[Dv_{(90)} - Dv_{(10)}]/Dv_{(50)}]$. Therefore the higher the span, the more polydisperse the particle size distribution was.

In addition, the nanoparticle hydrodynamic diameter of the dispersed formulations was characterized with DLS using a Malvern Zetasizer Nano S® (Malvern Instruments, Worcestershire, UK) at 25°C and pre-equilibrated for 2 minutes. The intercept of the correlation function was between 0.5 and 1.0. Dilution of the dispersion was done with distilled water.

4.3.5.2. Surface Tension

Surface tension testing was performed using a TA.XT.plus Texture Analyzer (Texture Technologies, Scarsdale, NY, USA) from the maximum pull on a disk as described in the previous chapter. Briefly, the container and glass disk probe were

thoroughly degreased, cleaned with ethanol and allowed to dry. The probe was attached to the texture analyzer arm, and lowered until the bottom surface of the probe contacted the surface of the liquid formulation contained in the reservoir. The temperature of the liquid was measured and recorded. At the start of testing, the probe was raised from the surface of the liquid at a constant speed (0.05 mm/s) for 10 mm, while the texture analyzer registered at 5 points per second the force exerted as a function of either time or distance. Using the maximum (detachment) force the surface tension was calculated using the equation below:

$$\frac{X}{k} = 0.0408687 + 6.20312 \cdot \left(\frac{X^3}{V}\right) - 0.0240752 \cdot \left(\frac{X^3}{V}\right)^2 \qquad \text{(Equation 4.1)}$$

Where X is probe radius, V is volume and k is the meniscus coefficient. For more details, see Chapter 3. The density values used to calculate surface tension were assumed to be the same as the density of water at the measurement temperature.

4.3.5.3. Zeta Potential

Electrophoretic light scattering was used to perform zeta potential testing with a ZetaPlus Zeta Potential Analyzer (Brookhaven Instruments Corp., Holtsville, NY, USA). The samples were analyzed at a constant temperature of 25°C and constant (neutral) pH. Samples were diluted with distilled water to conductance values of 300 to 550 μS. Each sample was subjected to 10 runs each, with a 5 second interval between measurements.

4.3.5.4. Rheology

Rheological behavior of the dispersed formulations were tested using a AR-G2 rheometer (TA Instruments, New Castle, DE, USA) equipped with a cone-and-plate geometry (cone diameter: 40 mm; truncation: 54 μm). Zero-gap and rotational mapping, respectively, were performed prior to testing. All measurements were executed with fresh sample dispersion at a constant temperature of 25°C with no pre-shear. Excess sample around the edge of the probe was trimmed and water added to the solvent trap compartment. The samples were measured at steady state flow step over a range of shear rates (300 to 10 s^{-1}) decreasing logarithmically (10 points per decade). The upper limit of shear rate was determined by hydrodynamic limitations (high probe speed will cause the liquid sample to spill away from the measurement zone). The sample period was 10 seconds and considered in equilibrium after 2 consecutive analyses within 5% tolerance, not exceeding a maximum point time of 2 minutes. The results were evaluated using Rheology Advantage Data Analysis software (TA Instruments, New Castle, DE, USA).

4.3.5.5. Nebulization Performance

Based on previous experience, the performance of vibrating-mesh nebulizers can be affected by mesh clogging, resulting in variable aerosol emission (i.e. intermittent mist), since this formulation is a dispersed system.[27] To analyze the nebulization performance of these formulations, we evaluate the changes in transmission over time from LD technique measurements. The nebulization performance of the dispersions was evaluated using the "open bench" method with a Malvern Spraytec® instrument (Malvern Instruments, Worcestershire, UK) equipped with 300 mm lens.[35] The nebulizer reservoir was positioned with the membrane at 25 mm above the upper edge of the laser beam and a distance of 25 mm between the lens and the center of the aerosol cloud. Air

suction was positioned 10 cm beneath the laser beam. The device and air suction apparatus positions were maintained still throughout the whole measurement period. The internal phase and dispersant refractive indexes were 1.33 (water) and 1.00 (air), respectively. Formulation (10 mL) was added to the nebulizer reservoir. At the start of nebulization, aerosol characteristics were continuously measured every second for 15 minutes. The slope of the transmission-time curves (transmittograms) were considered when comparing the different phospholipid formulations.

In addition, the Total Aerosol Output (TAO) was gravimetrically measured for each of the formulations studied. Before aerosolization, the nebulizer was weighed after each formulation was dispensed into the reservoir. The remaining formulation in the nebulizer reservoir was re-weighed after undergoing 15 minutes of nebulization. The difference in weight before and after nebulization results in the calculated TAO. The weight of the nebulizer mouthpiece was not considered during the measurements.

Importantly, neither transmittogram nor TAO provide information regarding drug output from the nebulizer. Information is limited solely to total mass output (droplets emitted over time). In the aerosolization of these dispersions, droplets not containing drug particles (empty droplets) are potentially generated. However, our purpose with this test is to investigate the capability of the Aeroneb Pro® nebulizer to continuously and steadily aerosolize the aqueous dispersions of Coenzyme Q_{10} over time. Intermittent mist can be identified in the transmittograms while TAO elucidates the magnitude of total mass being aerosolized. Saline solution (12 mL of 0.9% w/v NaCl in water) was used as the control.

4.3.6. Statistical Analysis

The data is expressed as mean ± standard deviation with the exception of surface tension and zeta potential results, which were expressed as mean ± standard error. For rheology studies, standard errors were provided by the software used to analyze the best fit of the results to the rheological models. Samples were analyzed at least in triplicate and evaluated for statistical differences with One-Way ANOVA for significance when $p < 0.05$ using NCSS/PASS software Dawson edition.[36] *Post hoc* comparisons were performed to identify statistically significant differences among groups using Tukey-Kramer method. A paired *t-test* was performed to analyze statistical differences ($p < 0.05$) within the same formulation for stability of drug particle size over time and to analyze the effect of different phospholipids processed at the same microfluidization conditions.

4.4. RESULTS AND DISCUSSION

In this study, the feasibility in the development of a suitable formulation of CoQ_{10} for pulmonary delivery has been explored. Following selection of excipients and nebulizer, the step starting the process was to perform a characterization analysis of the bulk powder for our intended purpose. The need to identify a suitable manufacturing process to prepare a colloidal dispersion of the drug was soon evident upon analyzing the powder characteristics. The selection for the manufacturing process consisted of formulating drug particles with small diameters in dispersion. This was suitably achieved with the microfluidizer, notably at different magnitudes of particle size according to type of phospholipid used and the number of passes. The ultimate purpose was to identify how the different physicochemical properties of the CoQ_{10} dispersions were influencing the nebulization performance of the Aeroneb Pro® vibrating-mesh nebulizer. Considering the

functioning mechanism of this type of nebulizer, surface tension and viscosity of formulations were expected to influence aerosol output. Most importantly, transmission data from LD and gravimetrical analysis of nebulizer output rendered a feasible method to evaluate steady aerosolization over time.

The XRD pattern of bulk CoQ_{10} shows two high intensity peaks (2θ) at approximately 18.65 and 22.80, indicating the crystalline structure of this drug (Figure 4.2). An endothermic peak at approximately 51°C in the DSC thermogram indicates the low melting point of this physiologically occurring compound (Figure 4.3). Most importantly, the drug particles are unsuitable for pulmonary delivery as presented in the bulk material, with $Dv_{(50)}$ of 29.87 μm and span value of 2.051. The magnitude of the particle dimensions were also confirmed by SEM pictures (Figure 4.4). The first approach to reduce particle size was performed with ball milling for 18 hours; however, the fluff appearance of the drug turned into a cluster of drug mass. This visual observation was confirmed by an increased particle size ($Dv_{(50)}$ = 29.87 μm, span = 2.282). Due to the low melting point of CoQ_{10}, heat generated during the process and mechanical impact may have both contributed to this outcome. Similar results were found when bulk powder was cryomilled.

A more elaborate approach to engineer the particles for pulmonary delivery then turned out to be mandatory. Therefore, high shear mixing, high pressure homogenization and ultrasonication were subsequently tested. The results shown in Figure 4.5 indicate that formulations prepared using shear force presented drug particles in dispersion with nearly a bimodal distribution, confirmed by a higher span value and $Dv_{(50)}$ around 1 μm (Table 4.2). Both microfluidization and ultrasonication presented a monodisperse, unimodal distribution with a $Dv_{(50)}$ value in the submicron range, so each method is capable of preparing a formulation with small drug particle size. However, considering

the availability of in-line commercial scale-up equipment, we have chosen to pursue further studies using microfluidization. Similar results have been previously reported for phospholipid-stabilized nanodispersions of CoQ_{10} for intravenous administration forming supercooled unilamellar liposomes.[37] Nevertheless, the Fraunhofer theory applied in LD is limited only to cases when the particle size is greater than 0.5-2.0 μm (i.e., poor accuracy below one micron).[38, 39] Thus, DLS is included in further studies.

Once the manufacturing process was selected, Formulation A was processed to determine the influence relating the number of passes in the microfluidizer to drug particle size stability (Table 4.1). We can observe from LD results that, following preparation, all formulations presented particle size distribution in the submicron range (Figure 4.6). After 7 days, the formulations similarly presented larger particles regardless of the number of passes**.** We observed from the DLS results that increasing the number of passes above 50 does not appear to provide smaller hydrodynamic diameters or more monodisperse systems (Figure 4.7). A trough in particle size as function of number of passes has been previously reported and attributed to a secondary particle growth due to fusion or Ostwald ripening during repeated homogenization.[40] Nevertheless, no statistical difference was found for drug particle sizes between days 0 and 7 for any individual preparation with any different number of passes.

Reduction in number of passes and evaluation of different phospholipids were investigated using Formulation B (Table 4.1). Analysis using DLS show that drug particle sizes significantly decrease for increased number of microfluidization passes (up to 50 passes) for both lecithin and DPPC dispersions of CoQ_{10} (Figure 4.8). The DPPC formulation presented significantly smaller particle sizes than the lecithin dispersions of CoQ_{10} at the same microfluidization conditions (e.g. number of discrete passes), with Z-averages in the ranges of 50-120 nm and 120-170 nm, respectively. Although the DPPC

colloidal dispersion presented smaller PdI values than lecithin-stabilized formulations, both presented high polydispersity (PdI > 0.2). This result indicates that no more than 50 passes are needed to obtain formulations with small particle sizes; the final colloidal system will depend on the phospholipid utilized.

Once a small drug particle dispersion of CoQ_{10} was feasibly prepared, we investigated the capability of the Aeroneb Pro® device to steadily nebulize these formulations as well as the physicochemical properties of the aerosolized liquid influencing nebulization performance. As previously mentioned, intermittent mist can occur when vibrating-mesh nebulizers generate aerosols from suspended dosage forms. Therefore, formulations should be evaluated for a lack of intermittent mist, indicating aerosolization continuity throughout the nebulization event. In this study, we primarily used the Malvern Spraytec® to analyze transmission as a function of time in order to select dispersed formulations that are continuously aerosolized using the Aeroneb Pro® nebulizer. Alternatively, a method capable of evaluating change in concentration over time of nebulized droplets could also be used, as suggested by the recently published General Chapter <1601> of the United States Pharmacopoeia (USP) on the characterization of nebulizer products.[41] The ease of prescreening a number of formulations over a limited nebulization time with Malvern Spraytec® was instrumental in formulation selection.

Before setting up the Malvern Spraytec® with the “open bench” method, we attempted numerous times to perform these tests using the inhalation cell accessory provided by Malvern (Figure 4.9). In this system, a laser beam is projected from the left side of the instrument towards a detector positioned at the right side. In its trajectory, the laser beam crosses the inhalation cell coupled to this Spraytec®. At the rear of the inhalation cell setup a vacuum line is connected, while a nebulizer is positioned in front

of the inhalation cell. A set of tubes in the mid section of the inhalation cell creates an air sheath to help direct the aerosol droplets from the nebulizer towards the vacuum source. In order to best evaluate the nebulizer output of the dispersions, this setup was arranged with the inhalation cell in the horizontal position (90º angle) to measure aerosol generation as close as possible to the vibrating-mesh. The suction airflow rate was set to 30 L/min and the sheath airflow rate was set to 15 L/min (30 – 15 L/min = 15 L/min) to obtain a final airflow rate of 15 L/min. This airflow rate was selected to match that required to analyze nebulizer formulations in the Next Generation Impactor (NGI) for comparison reasons.[42]

However, a technique artifact could not be avoided due to the inhalation cell design. An inefficient air sheath was created in the Malvern Spraytec®, causing the aerosol cloud to "invade" the detector lens compartment, continuously increasing obscuration and consequently reducing transmission. During standard operation of the inhalation cell a HEPA membrane filter of 0.45 μm is positioned in-line with the vacuum source, both to avoid damaging the vacuum source and prevent potential exposure to the operator. However, in using the filter, the formulation gradually clogs the filter pores and a back pressure is created which overcomes the air sheath and directs the droplets towards the detection lens chamber. Once the inhalation cell windows are fogged the transmission values do not return to 100% and bogus data gives the appearance that the nebulizer operated uninterruptedly throughout the measurement. Despite testing different configurations and parameters (e.g. changing vacuum filter from membrane to cartridge type, changing suction level and sheath airflow rates, etc.), a feasible measurement using this setup was not possible. It was recognized that the amount of aerosol produced during each 15-minutes nebulization event was enormous when compared to pMDI and DPI devices, which the inhalation cell was primarily designed for. This accessory may be

more useful in characterizing aerosol generation from those other devices, and not for use with nebulizers for extended periods of time.

To overcome the technique artifact, we decided to use the "open bench" method. The position of the nebulizer reservoir was appropriately chosen to avoid vignetting (wide angle scattered light misses the detector field) while also avoiding recirculating droplets by positioning the air suction source properly for a continuous exhaustion of the generated droplets.[35, 43] The transmittograms presented in Figure 4.10 show a nebulization event of 15 minutes for Formulation C (Table 4.1). At the end of this duration the transmission values go back up to 100% for all formulations, indicating that the measurement was properly performed with no fogging of the detector lens. The three formulations presented a steady nebulization for the initial 5 minutes. After this time point, the transmission related to the formulation of the 10 pass runs were increased at a different rate than formulations of the 30 and 50 pass runs. To evaluate the nebulization performance of these formulations, the transmittogram was fitted to a linear regression in order to analyze the slopes of the rate curves. By comparing their slopes, we can infer about how steady a nebulization event was.

The slope values and TAO of Formulation C (Table 4.1) with different numbers of passes in the microfluidizer are presented in Figure 4.11. We observe a significantly lower slope value for formulations that were run at 10 passes compared to 30 and 50 passes; this is in agreement with the higher TAO values. These results indicate that Formulation C processed with 10 passes in the microfluidizer was able to present a steadier nebulization over time than if it was prepared with increased processing. Next, we evaluated the physicochemical properties of Formulation C with 10, 30 and 50 passes to identify how they may be influencing the nebulization performance of these dispersions of CoQ_{10}.

Upon analysis of the hydrodynamic size in the dispersions (Figure 4.12), we observe from LD results that the particle size appeared to be increasing slightly over time with most particles holding in the nanometric scale. When comparing formulations analyzed at day 0 for LD and DLS, we conclude that LD is not a suitable technique for the same reasons described earlier, based on the Fraunhofer theory. The DLS results then show that all formulations presented a Z-average of approximately 260 nm. After 7 days, $Dv_{(50)}$ is still below range of measurement for LD technique whereas Z-average did not vary significantly for the 30 and 50 passes. From the particle size distribution results we can conclude that the formulations with the higher number of passes were stable for about 1 week. PdI was between 0.2 and 0.3 following preparation and showed some level of polydispersity after 7 days.

The results indicate that a greater hydrodynamic diameter was formed for these lecithin dispersions (approximately 260 nm) than was formed with the previous formulation analyzed (Formulation B: 120-170 nm). These differences can be explained by the difference in electrolyte concentrations of the formulations. Addition of 0.9% w/v of sodium chloride to Formulation C serves two purposes: to provide normal physiological osmolarity and to reduce variability in aerosol generation from this active vibrating-mesh nebulizer.[21] Other than the reduced variability factor, Ghazanfari and coworkers have demonstrated increased aerosol output and smaller droplet sizes with solutions containing low ion concentrations. The low electrolyte content helps to overcome drop detachment resistance from the vibrating-mesh due to an improved electrical conductivity that works to suppress the high electrostatic charge of water,[44] which in turn favors aerosol generation. However, the addition of sodium chloride may also cause colloid instability, according to the Derjaguin-Landau-Verwey-Overbeek (DLVO) theory of interactions of electrolytes on phospholipid surfaces.[45] In this case,

a nonspecific adsorption based solely on electrostatic forces (no chemical interactions) may occur driven by the presence of monovalent cations (i.e. Na^+). A decrease in zeta potential caused by the presence of the ions increase the flocculation rate, which can be analyzed by turbidimetry.[45] In fact, based on visual observation, the addition of the aforementioned salt following microfluidization changed the dispersion color from dark orange to bright yellow. Despite extensive discussion concerning the mechanism of this colloid stability, current theories in colloid science are unable to fully explain this phenomenon.[46] Despite that, the differences in drug particle size in dispersion from Formulations B and C can be supported by DLVO theory. Drug particle size distribution of the aqueous dispersion alone does not appear to be influencing the nebulization performance, since the dispersions had similar diameters following preparation but different aerosolization behavior.

Analysis of zeta potential supports the dispersion stability previously discussed based on changes in drug particle size distribution over time. Increasing the number of passes increases both the surface tension and the module of zeta potential, which was statistically significant when comparing formulations processed with 10 or 50 microfluidization passes (Figure 4.13). When evaluating surface tension and zeta potential results together, Kawaguchi and coworkers hypothesized that a higher number of passes aids encapsulation.[47] Hence, less surfactant is available in "solution" than is needed to cause decrease in surface tension. The role of surface tension in aerosol generation from active vibrating-mesh nebulizers is still unclear.[21] No similarity has been found between the results of zeta potential and surface tension seen in Formulation C that correlates the different number of passes in the microfluidizer and their respective nebulization performance.

Finally, we evaluated the rheology of the dispersions. After plotting the shear stress as a function of shear rate, the results were fitted to their best rheological model. It was found that the Herschel-Bulkley was the model that best represented these three formulations:

$$\sigma = \sigma_y + \kappa \cdot \dot{\gamma}^n \qquad \text{(Equation 4.2)}$$

Where σ is shear stress, σ_y is yield stress, κ is consistency index or viscosity, γ is shear rate and n is flow index (n = 1: Newtonian fluid; n < 1: shear-thinning; n > 1: shear-thickening). Standard errors are 32.74 ± 3.58, 31.62 ± 2.04, 35.92 ± 3.57 for dispersions of CoQ_{10} prepared with 10, 30 and 50 microfluidization passes, respectively. The three elements of the Herschel-Bulkley model are presented in Figure 4.14. Although the values of each element are not statistically different, the similarity between the rheology results and the results of nebulization performance previously seen is more evident. Formulations of 30 and 50 passes presented a similar rheological behavior and nebulization performance, which were different from formulations of 10 passes. Interestingly, all formulations presented shear-thickening behavior (n > 1). It is well known that particle characteristics like size, size distribution, shape, charge, and the interactions between particles and the surrounding fluid play significant roles in the rheological behavior of these systems.[48] Therefore, it is not surprising that the rheological behavior of the formulations are more in agreement with the nebulization performance, since it considers the interactions of all the other physicochemical characteristics together due to interparticle forces acting on flow-induced structures.

To our knowledge, this is the first study investigating the capability of vibrating-mesh nebulizers to steadily nebulize dispersions in which fluid rheology is analyzed as

opposed to performing simpler kinematic viscosity measurements. Previous works have focused on the viscosity of the dispersion media *per se*, without considering the interactions between the dispersed particles with the surrounding fluid.[19, 49] The nebulizer used in this study (Aeroneb Pro®) functions by imparting a high vibration frequency (128 KHz) on a perforated membrane to generate the aerosol droplets. This high frequency mechanical stress is directly transferred to the liquid formulation. Therefore, analysis of rheology parameters at higher shear rates may better translate to what is actually occurring in the vicinity of the vibrating membrane. From the theory of rheology of suspensions, a shear thickening event may be expected at high shear rates depending on the particles' deformability, besides the aforementioned factors. In our studies, the upper limit of shear rate was established based on the hydrodynamic characteristics of the formulations. Increasing shear rates *ad infinitum*, although desirable for this purpose, is impossible in practice. Nevertheless, analysis of the rheological behavior of the dispersions based on flow index (shear thickening or shear thinning event) may dictate how the system will behave under the stress imposed to the drug particles and the surrounding fluid by the vibrating-mesh. Further studies investigating non-Newtonian fluids are warranted to better understand how rheology of dispersed systems can influence nebulization performance from vibrating-mesh nebulizers.

4.5. CONCLUSIONS

Aqueous colloidal dispersions of CoQ_{10} can be suitably produced using microfluidization, and formulations of this poorly-water soluble anticancer agent can be effectively nebulized using vibrating-mesh devices. Proper selection of phospholipids was found to be crucial since it profoundly influenced the final drug particle size.

Moreover, processing can further influence other physicochemical properties; increasing the number of microfluidization passes increased surface tension and the module of zeta potential. Evaluation of the 1:1 lecithin:CoQ_{10} formulation in conjunction with the active vibrating-mesh nebulizer Aeroneb Pro® showed that the nature of aerosolization event could be elucidated as either a continuous or intermittent process. By analysis of the aerosolization event, formulation performance of dispersed dosage forms can be effectively evaluated. Importantly, the rheological behavior of the dispersions appeared to best represent the interparticle interactions at the microscopic level in the vicinity of the vibrating membrane. Further studies are warranted to expand the understanding of how dosage forms behaving as non-Newtonian fluids can influence the droplet formation from nebulizers. This would help pave the way to promote development of other compounds with similar, poorly-water soluble properties for use in inhalation therapy.

4.6. TABLES

Formulation	Test	Phospholipids		Number of passes	Characterization
		Type(s)	Hydration		
A	Number of passes; stability	Lecithin	~ 1 hour, no stirring	20, 50, 70 and 100	Particle size distribution
B	Number of passes; type of phospholipids	Lecithin and DPPC	~ 1 hour, no stirring	10, 20, 30, 40 and 50	Particle size distribution
C*	Nebulization performance	Lecithin	Overnight, stirring	10, 30, and 50	Particle size distribution, surface tension, rheology, zeta potential, and TAO.

*0.9% w/v added to final formulation following processing with microfluidizer. DPPC: dipalmitoylphosphatidylcholine; TAO: Total Aerosol Output.

Table 4.1 – Formulations investigated for effect of processing parameters and type of phospholipids on the particle size distribution and nebulization performance.

Manufacturing Process	$Dv_{(50)}$ (µm)	Span Value
Shear Force	1.03	2.076
Microfluidization	0.63	0.367
Ultrasonication	0.71	0.459

Table 4.2 – $Dv_{(50)}$ and span values of dispersions prepared with different manufacturing processes.

4.7. FIGURES

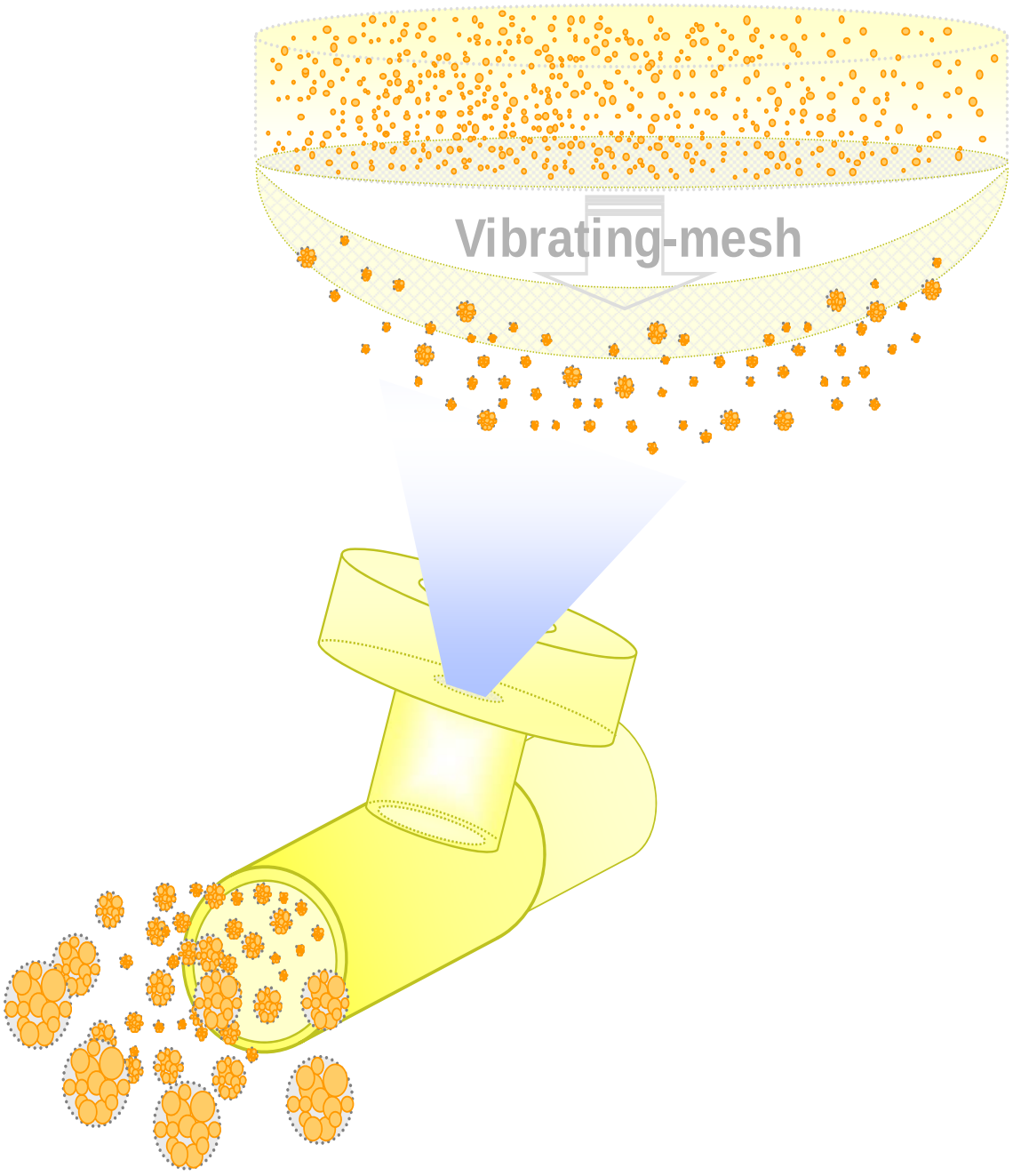

Figure 4.1 – Schematic diagram of aerosolization of CoQ_{10} dispersions using a vibrating-mesh nebulizer.

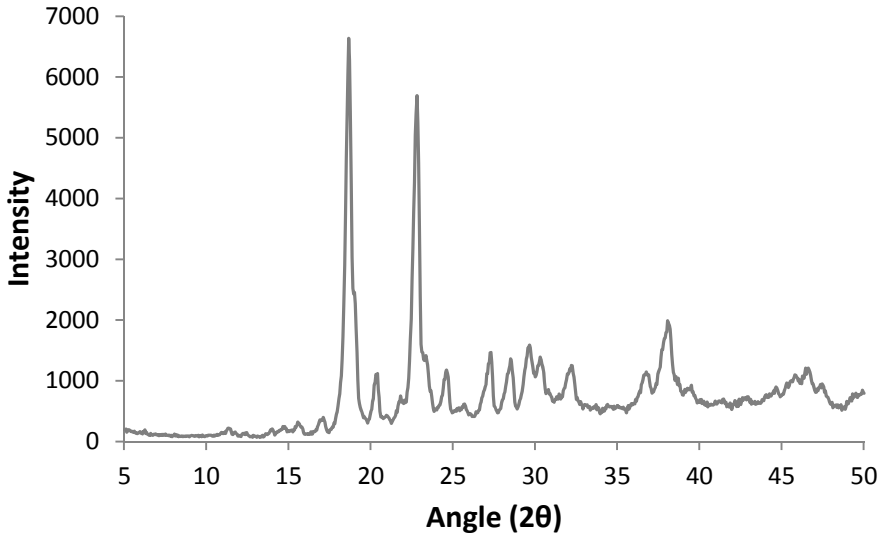

Figure 4.2 – X-Ray Diffraction pattern of bulk powder of CoQ_{10}.

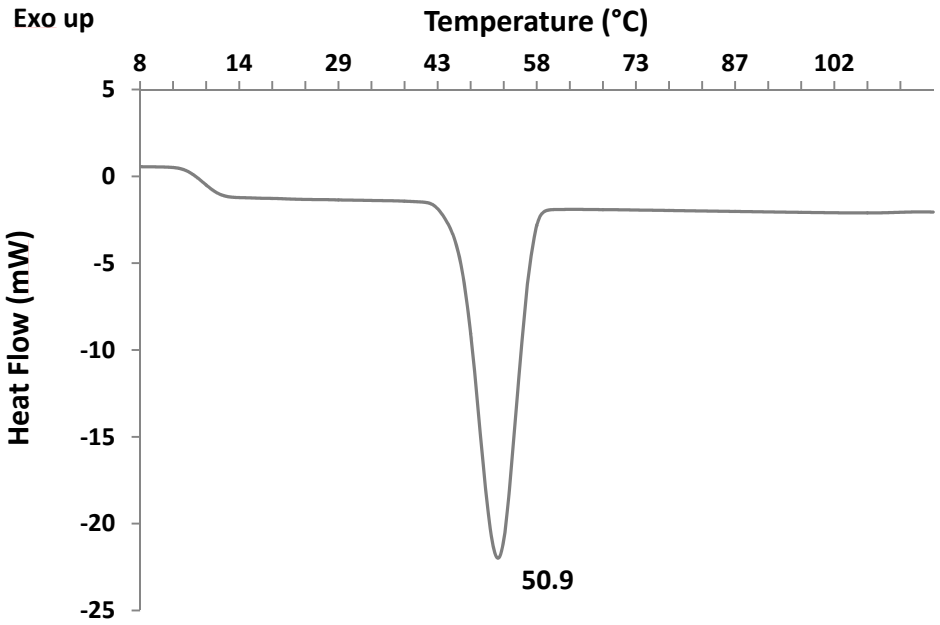

Figure 4.3 – Differential Scanning Calorimetry thermogram of bulk powder of CoQ_{10}.

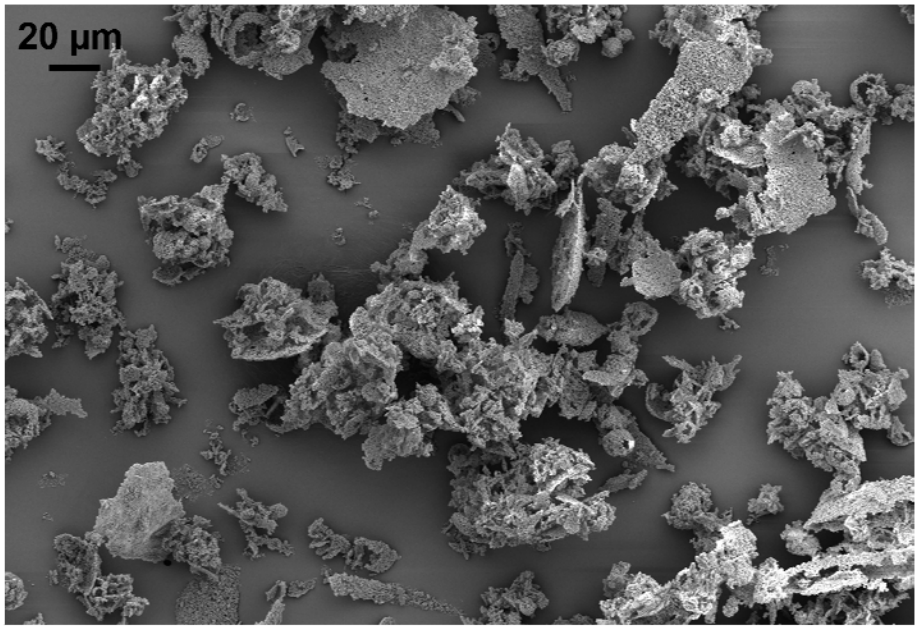

Figure 4.4 – Scanning Electron Microscopy picture of bulk powder of CoQ_{10}.

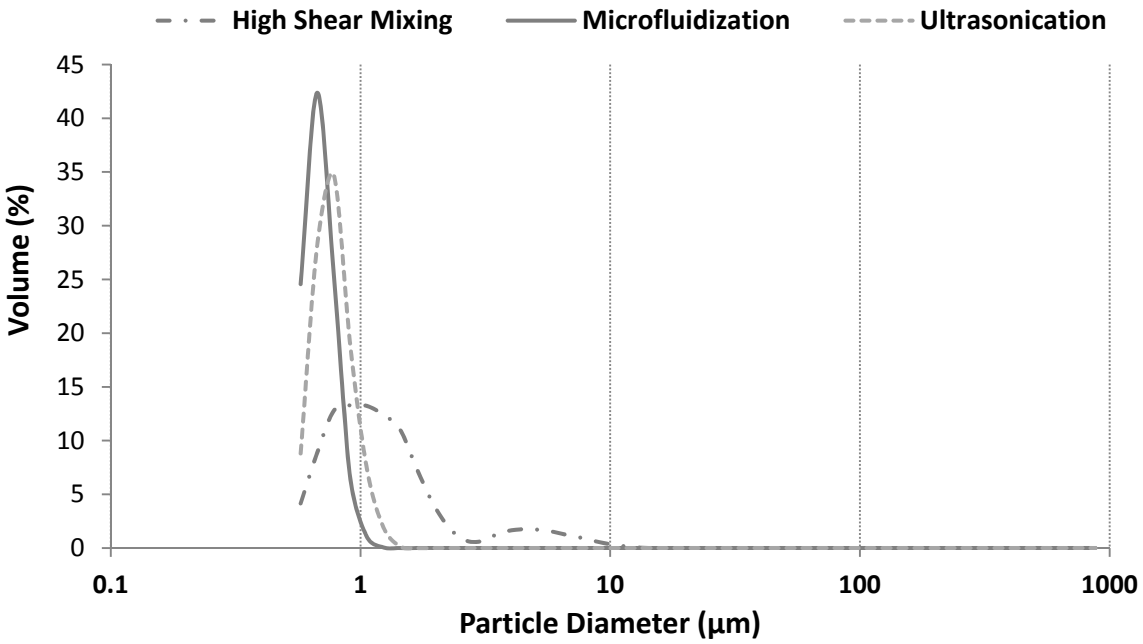

Figure 4.5 – Particle size distributions of CoQ_{10} dispersions prepared using different manufacturing processes.

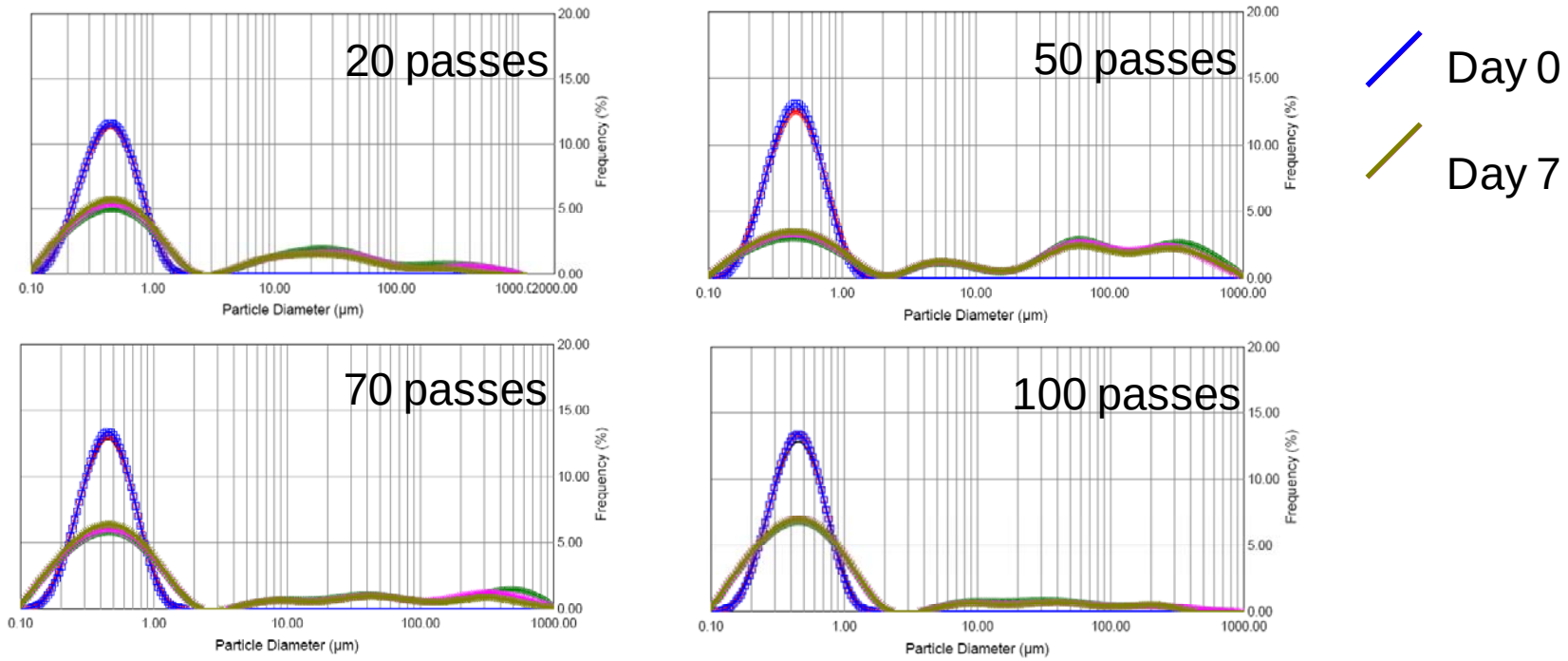

Figure 4.6 – Particle size distributions from Laser Diffraction technique of aqueous dispersions of CoQ_{10} following preparation in the microfluidizer and after 7 days (Formulation A, Table 4.1).

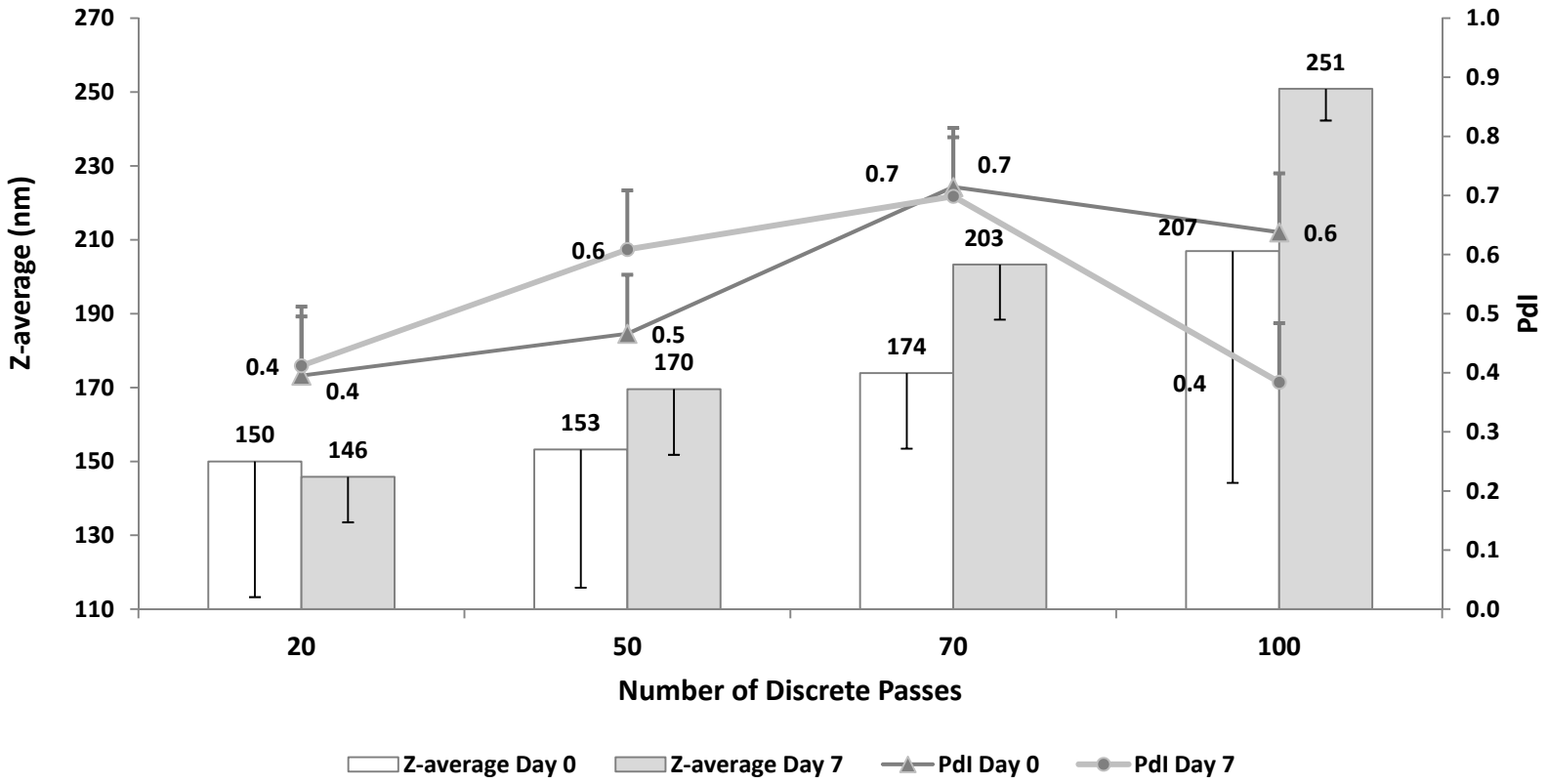

Figure 4.7 – Z-average and PdI values of aqueous dispersions of CoQ_{10} following preparation in the microfluidizer and after 7 days (Formulation A, Table 4.1). Statistical differences were not found for drug particle size distribution characteristics (Z-average and PdI) neither in formulations prepared with different number of microfluidization passes and analyzed following preparation nor when the same formulations were compared at days 0 and 7.

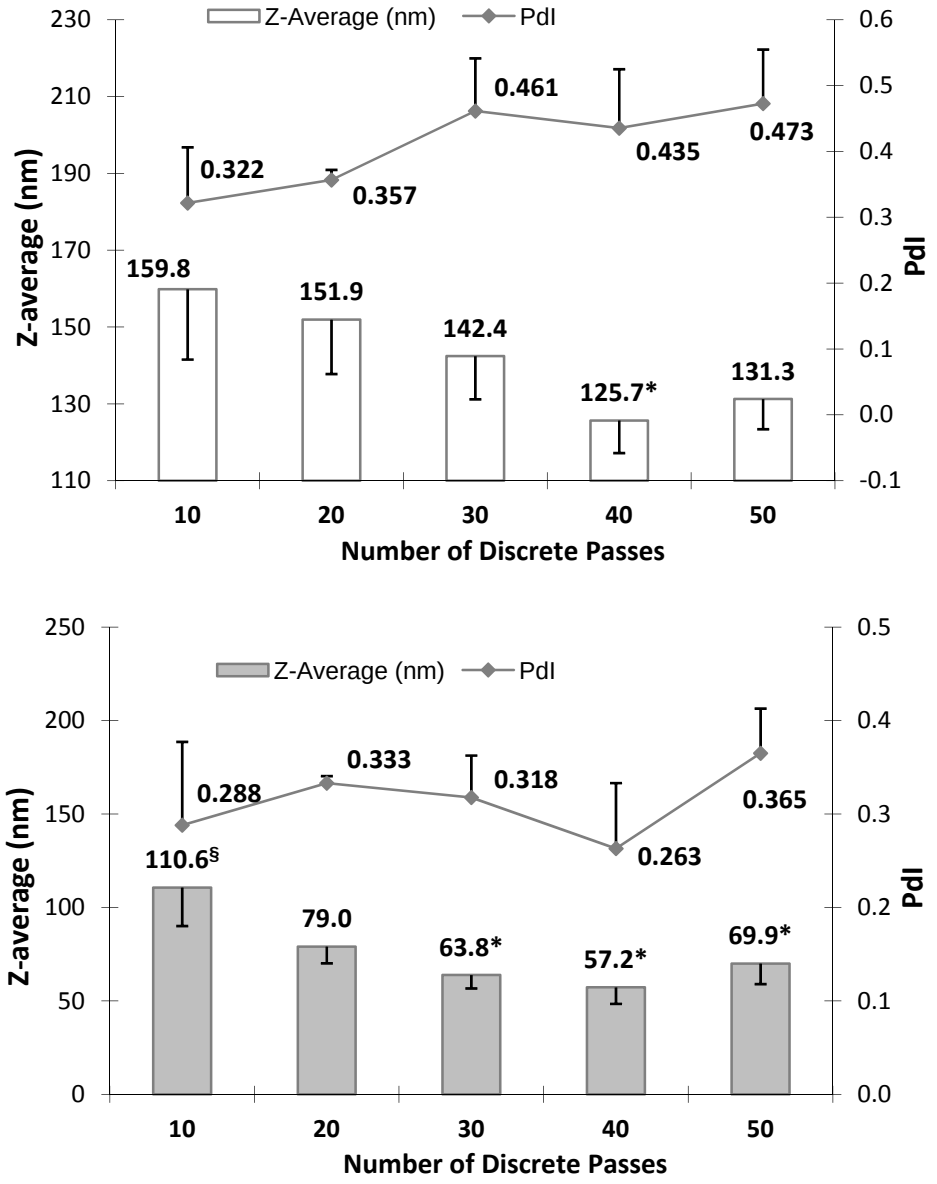

Figure 4.8 – Hydrodynamic diameters and polydispersity of aqueous dispersions of CoQ_{10} (Formulation B, Table 4.1) following preparation in the microfluidizer using lecithin (top) or DPPC (bottom). (* $P \leq 0.05$ when compared to 10 passes; § Not statistically different when compared to the lecithin dispersion prepared with same number of microfluidization passes)

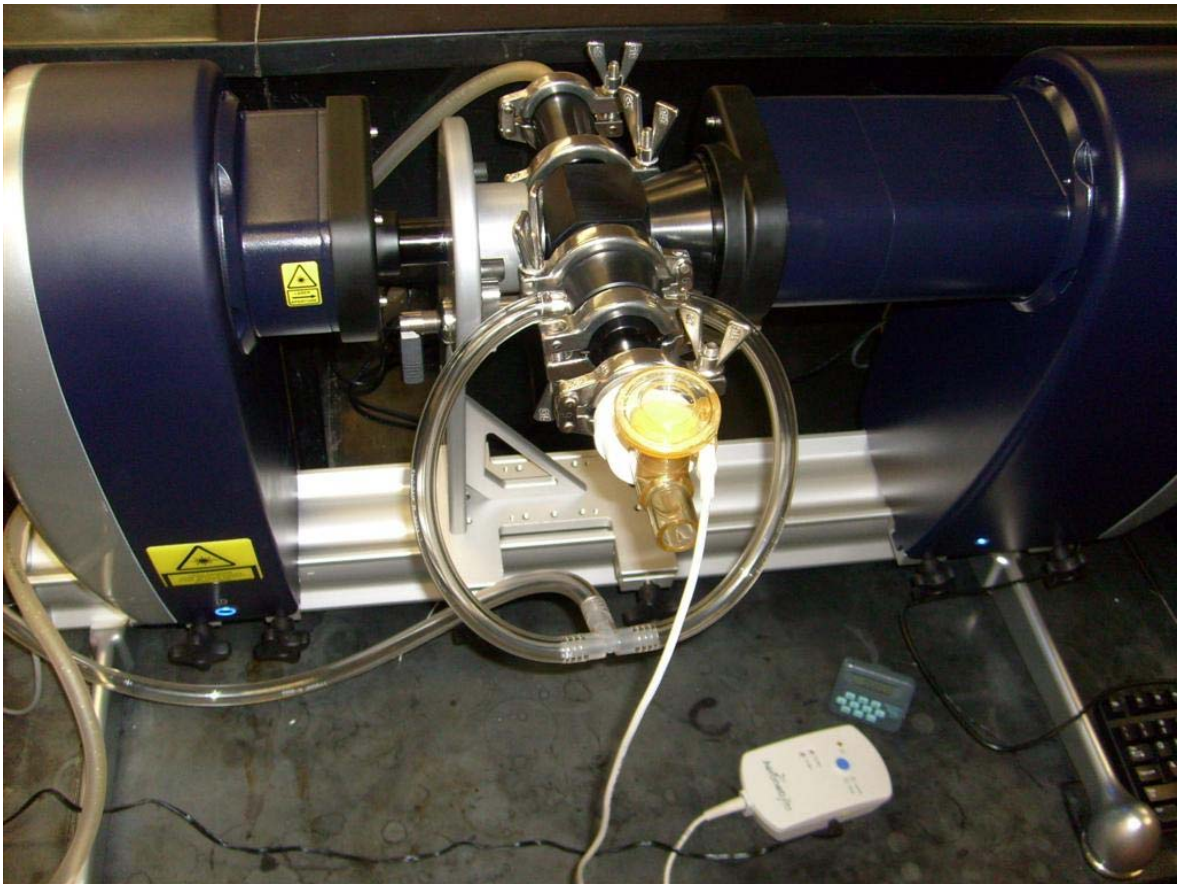

Figure 4.9 – Malvern Spraytec® coupled with inhalation cell.

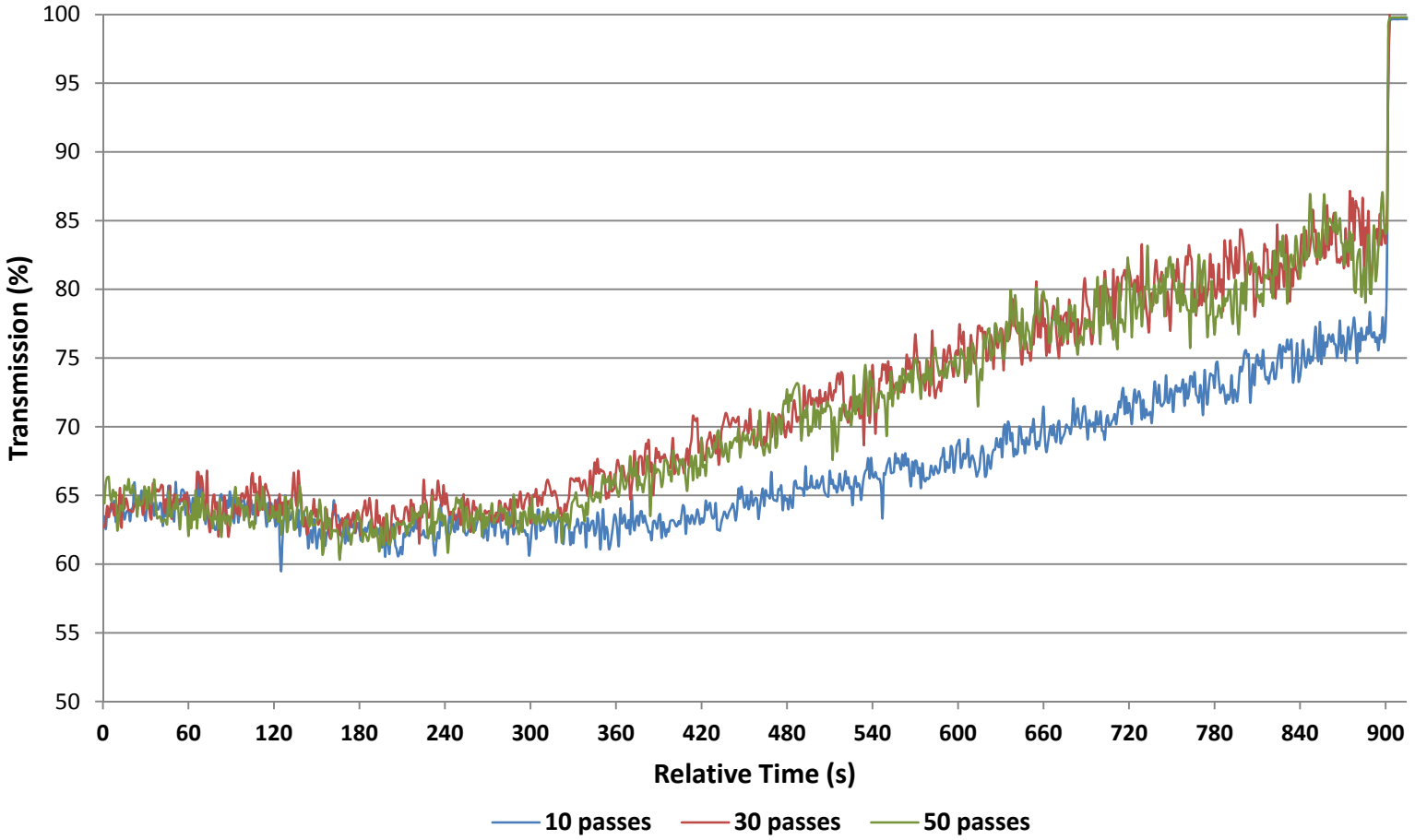

Figure 4.10 – Transmittograms of lecithin dispersions of CoQ_{10} (Formulation C, Table 4.1). Results are expressed as means (n = 3) of percentage transmission relative to nebulization of CoQ_{10} dispersions for15 minutes. The slope values from the linear regression analysis of the curves are evaluated as measurement of steadines in aerosol production.

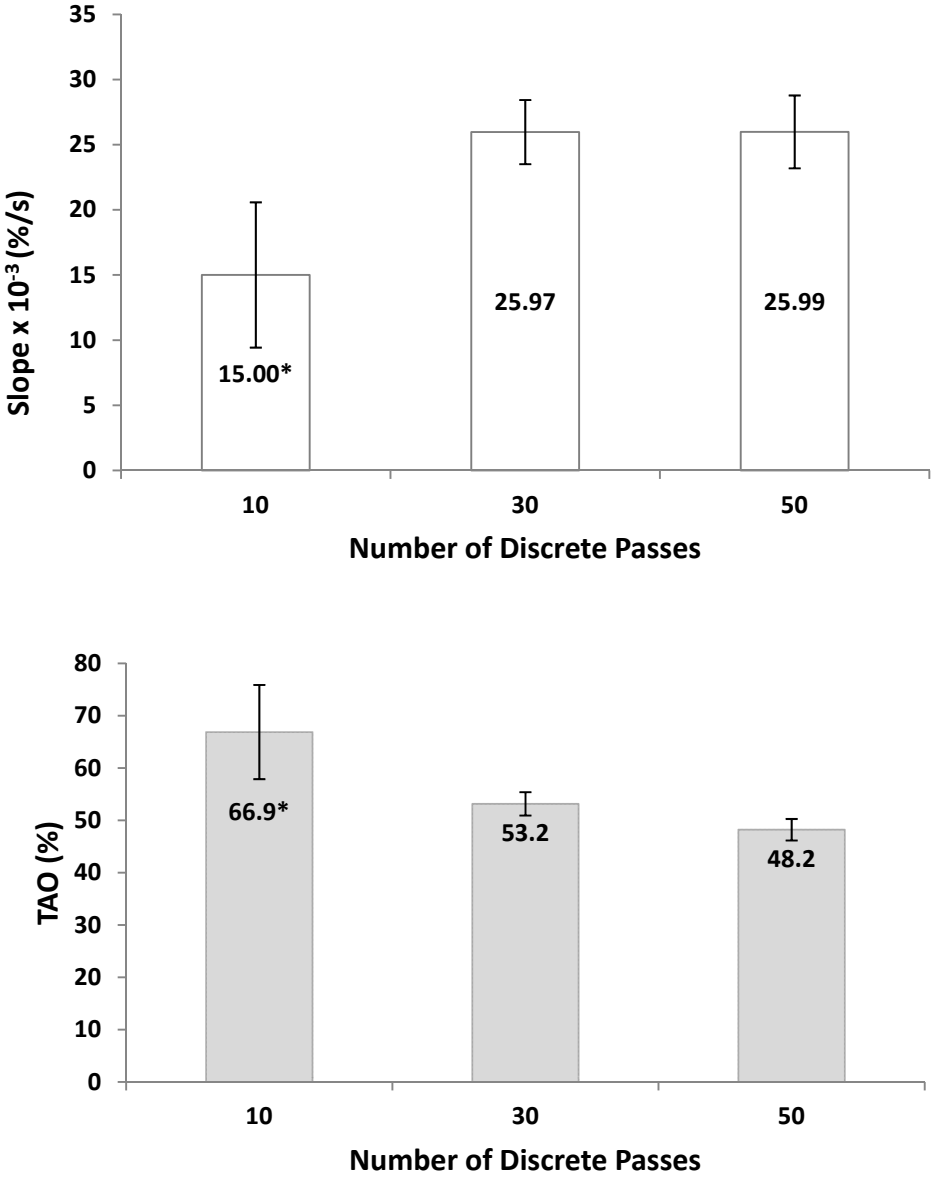

Figure 4.11 – Slope of transmittograms (top) and Total Aerosol Output (TAO – bottom) for nebulization of lecithin dispersions of CoQ_{10} (Formulation C, Table 4.1) during 15 minutes. (* $P \leq 0.05$ compared to other formulations)

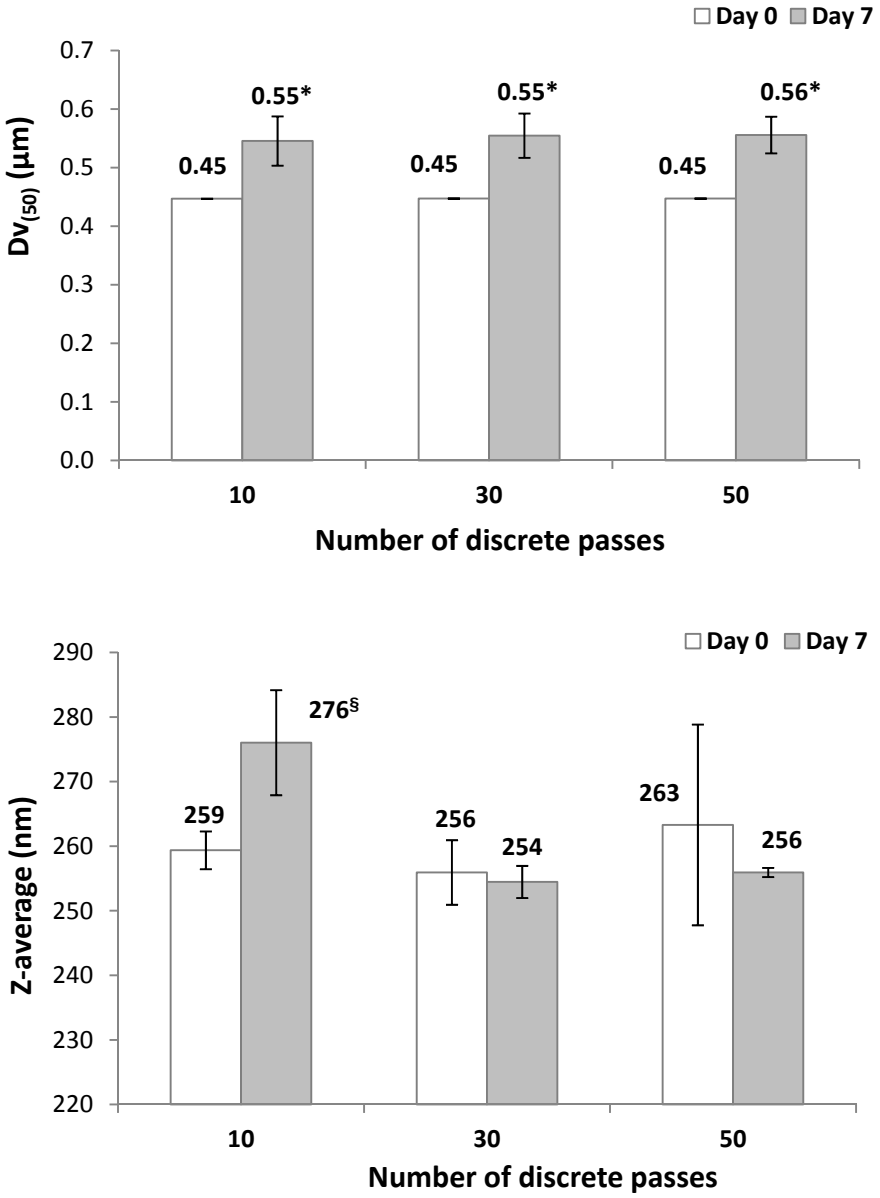

Figure 4.12 – Particle size distributions analyses of aqueous dispersions of CoQ10 (Formulation C, Table 4.1) following preparation in the microfluidizer using laser diffraction (left) and dynamic light scattering (right). (* $P \leq 0.05$ compared to formulations analyzed following preparation; § $P \leq 0.05$ compared to other formulations at day 7).

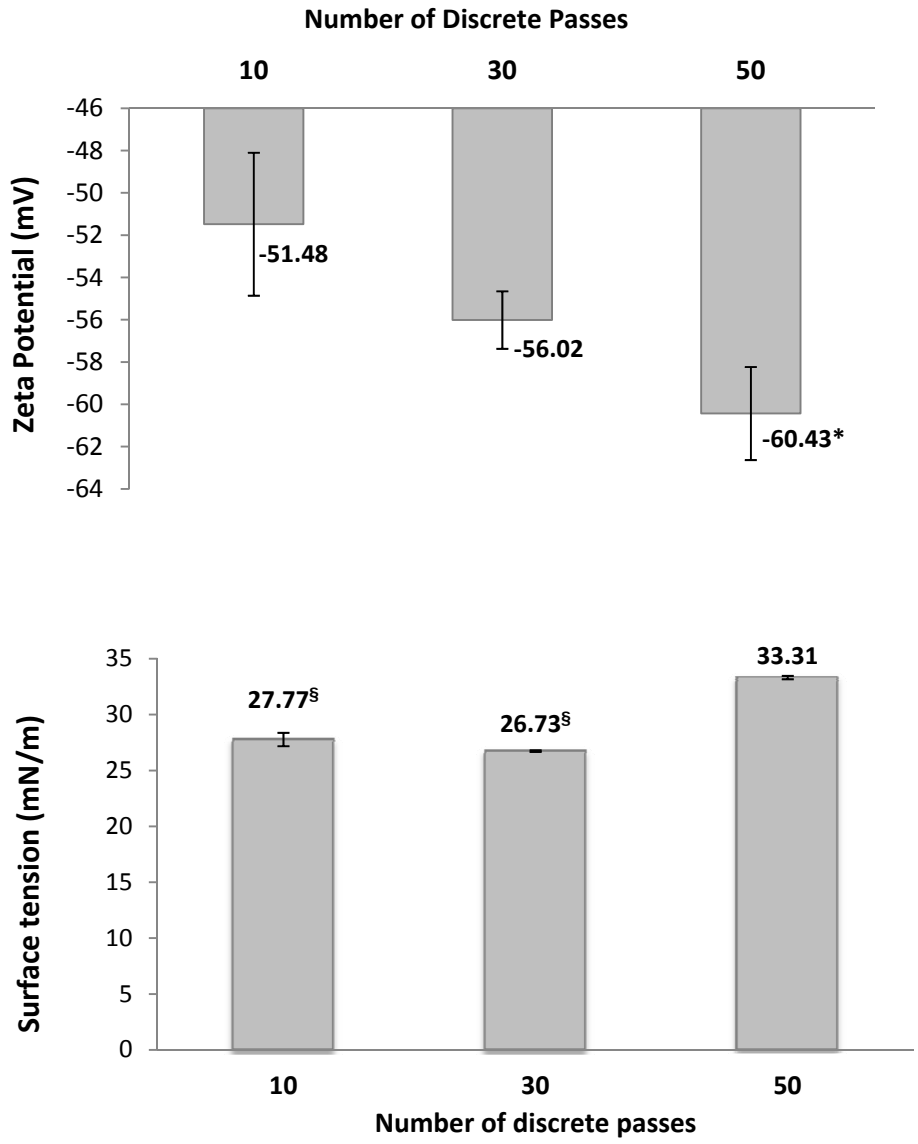

Figure 4.13 – Zeta potential and surface tension values related to formulations of CoQ_{10} processed at different number of microfluidization passes (Formulation C, Table 4.1). Columns and error bars represent means and standard errors, respectively (n = 10 for zeta potential and n = 5 for surface tension). The temperature during surface tension measurement was 25ºC. (* $P \leq 0.05$ when compared to 10 passes, § Not statistically different)

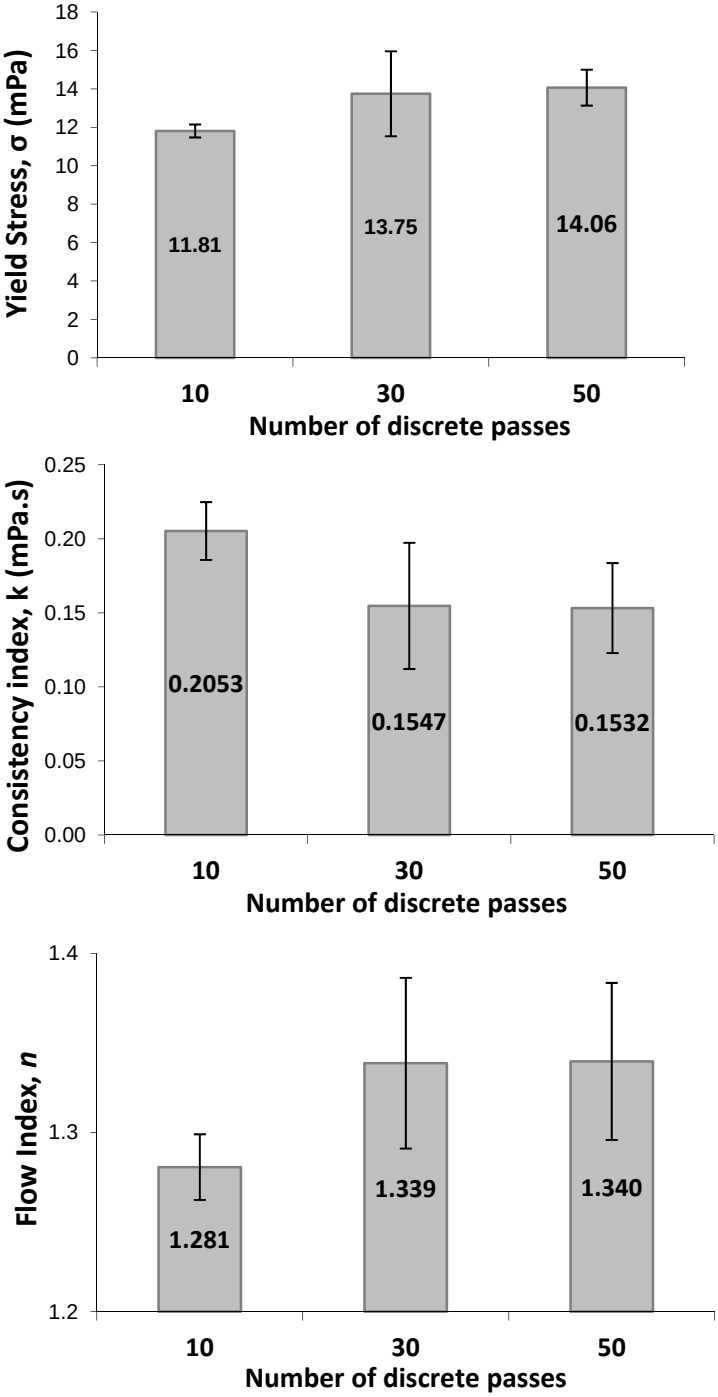

Figure 4.14 – Elements of Herschel-Bulkley model for aqueous dispersions of CoQ_{10} processed at different number of microfluidization passes (Formulation C, Table 4.1). No statistical differences were found.

4.8. REFERENCES

[1] Bhagavan HN, Chopra RK. Coenzyme Q10: Absorption, tissue uptake, metabolism and pharmacokinetics. Free Radic Res. 2006 May;40(5):445-53.

[2] Gurkan AS, Bozdag – Dundar, O. Coenzyme Q10. J Fac Pharm, Ankara. 2005;34(2):129-54.

[3] Dhanasekaran M, Ren J. The emerging role of coenzyme Q-10 in aging, neurodegeneration, cardiovascular disease, cancer and diabetes mellitus. Curr Neurovasc Res. 2005 Dec;2(5):447-59.

[4] Rusciani L, Proietti I, Rusciani A, Paradisi A, Sbordoni G, Alfano C, et al.. Low plasma coenzyme Q10 levels as an independent prognostic factor for melanoma progression. J Am Acad Dermatol. 2006;54(2):234-41.

[5] Folkers K, Brown R, Judy WV, Morita M. Survival of Cancer Patients on Therapy with Coenzyme Q10. Biochem Biophys Res Commun. 1993;192(1):241-5.

[6] Folkers K, Morita M, McRee J. The Activities of Coenzyme-Q(10) and Vitamin-B(6) for Immune-Responses. Biochem Biophys Res Commun. 1993 May;193(1):88-92.

[7] Brea-Calvo G, Rodríguez-Hernández Á, Fernández-Ayala DJM, Navas P, Sánchez-Alcázar JA. Chemotherapy induces an increase in coenzyme Q10 levels in cancer cell lines. Free Radic Biol Med. 2006;40(8):1293-302.

[8] Narain NR, Li J, Woan KV, Russell KJ, Ochoa MS, Persaud I, et al.. Coenzyme Q10 induces apoptosis in human melanoma cells. J Invest Dermatol. 2004;122(3):958.

[9] Pinto L, Sloan A, Persaud I, Narain NR. Normalization of BCL-2 Family Members in Breast Cancer by Coenzyme Q10. Ethn Dis. 2009 Sum;19(2):S17-S8.

[10] Narain NR, Li J, Russell KJ, Woan KV, He J, Persaud I, et al.. Coenzyme Q10 inhibits the proliferation of oncogenic cells while stabilizing growth in primary cells in vitro. J Invest Dermatol. 2004;122(3):167.

[11] Hertz N, Lister RE. Improved Survival in Patients with End-stage Cancer Treated with Coenzyme Q(10) and Other Antioxidants: a Pilot Study. J Int Med Res. 2009 Nov-Dec;37(6):1961-71.

[12] Ondarroa M, Sharma SK, Quinn PJ. Solvation properties of ubiquinone-10 in solvents of different polarity. Biosci Rep. 1986;6(9):783-96.

[13] McConville JT, Overhoff KA, Sinswat P, Vaughn JM, Frei BL, Burgess DS, et al.. Targeted high lung concentrations of itraconazole using nebulized dispersions in a murine model. Pharm Res. 2006 May;23(5):901-11.

[14] Tam JM, McConville JT, Williams RO, Johnston KP. Amorphous Cyclosporin Nanodispersions for Enhanced Pulmonary Deposition and Dissolution. J Pharm Sci. 2008 Nov;97(11):4915-33.

[15] Vaughn JM, McConville JT, Burgess D, Peters JI, Johnston KP, Talbert RL, et al.. Single dose and multiple dose studies of itraconazole nanoparticles. Eur J Pharm Biopharm. 2006;63(2):95-102.

[16] Elhissi AMA, Taylor KMG. Delivery of liposomes generated from proliposomes using air-jet, ultrasonic, and vibrating-mesh nebulisers. Journal of Drug Delivery Science and Technology. 2005;15(4):261-5.

[17] Elhissi AMA, Karnam KK, Danesh-Azari MR, Gill HS, Taylor KMG. Formulations generated from ethanol-based proliposomes for delivery via medical nebulizers. J Pharm Pharmacol. 2006;58(7):887-94.

[18] Elhissi AMA, Faizi M, Naji WF, Gill HS, Taylor KMG. Physical stability and aerosol properties of liposomes delivered using an air-jet nebulizer and a novel micropump device with large mesh apertures. Int J Pharm. 2007;334(1-2):62-70.

[19] Elhissi A, Gill H, Ahmed W, Taylor K. Vibrating-mesh nebulization of liposomes generated using an ethanol-based proliposome technology. J Liposome Res. 2011 Jun;21(2):173-80.

[20] Watts AB, McConville JT, Williams RO. Current therapies and technological advances in aqueous aerosol drug delivery. Drug Dev Ind Pharm. 2008;34(9):913-22.

[21] Ghazanfari T, Elhissi AMA, Ding Z, Taylor KMG. The influence of fluid physicochemical properties on vibrating-mesh nebulization. Int J Pharm. 2007;339(1-2):103-11.

[22] Carvalho TC, Peters JI, Williams III RO. Influence of particle size on regional lung deposition - What evidence is there? Int J Pharm. 2011;406(1-2):1-10.

[23] Bhagavan HN, Chopra RK. Plasma coenzyme Q10 response to oral ingestion of coenzyme Q10 formulations. Mitochondrion. 2007;7(Supplement 1):S78-S88.

[24] Boe J, Dennis JH, O'Driscoll BR. European Respiratory Society Guidelines on the use of nebulizers. Eur Respir J. 2001;18(1):228-42.

[25] Finer NN, Merritt TA, Bernstein G, Job L, Mazela J, Segal R. An Open Label, Pilot Study of Aerosurf (R) Combined with nCPAP to Prevent RDS in Preterm Neonates. Journal of Aerosol Medicine and Pulmonary Drug Delivery. 2010 Oct;23(5):303-9.

[26] Abdelrahim ME, Plant P, Chrystyn H. In-vitro characterisation of the nebulised dose during non-invasive ventilation. J Pharm Pharmacol. 2010 Aug;62(8):966-72.

[27] Rottier BL, van Erp CJP, Sluyter TS, Heijerman HGM, Frijlink HW, de Boer AH. Changes in Performance of the Pari eFlow (R) Rapid and Pari LC Plus (TM) during 6 Months Use by CF Patients. Journal of Aerosol Medicine and Pulmonary Drug Delivery. 2009;22(3):263-9.

[28] Pilcer G, Amighi K. Formulation strategy and use of excipients in pulmonary drug delivery. Int J Pharm. 2010;392(1-2):1-19.

[29] Bittar EE. Alveolar Surfactant. *Pulmonary biology in health and disease*. New York, NY, USA: Springer 2002:44-63.

[30] Ghodrat M. Lung surfactants. Am J Health Syst Pharm. 2006 Aug;63(16):1504-21.

[31] Taeusch HW, Lu K, Ramierez-Schrempp D. Improving pulmonary surfactants. Acta Pharmacol Sin. 2002 Oct;23:11-5.

[32] Wu YZ, Wang T. Soybean lecithin fractionation and functionality. J Am Oil Chem Soc. 2003 Apr;80(4):319-26.

[33] Wu YZ, Wang T. Phospholipid class and FA compositions of modified soybeans processed with two extraction methods. J Am Oil Chem Soc. 2003 Feb;80(2):127-32.

[34] Jin YL, Chen JY, Xu L, Wang PN. Refractive index measurement for biomaterial samples by total internal reflection. Phys Med Biol. 2006;51(20):N371-N9.

[35] Smart J, Berg, E., Nerbrink, O., Zuban, R., Blakey, D., New, M. TouchSpray™ Technology: Comparison of the Droplet Size Measured with Cascade Impaction and Laser Diffraction. In: Dalby RN, Byron, P. R., Peart, J., Farr, S. J., editor. Respiratory Drug Delivery VIII; 2002; Tucson, AZ, USA: Virginia Commonwealth University, Richmond, VA, USA; 2002. p. 525-8.

[36] Hintze J. NCSS and PASS. released January 29th, 2004 ed. Kaysville, UT, USA: Number Cruncher Statistical Systems 2001.

[37] Siekmann B, Westesen K. Preparation and Physicochemical Characterization of Aqueous Dispersions of Coenzyme Q_{10} Nanoparticles. Pharm Res. 1995;12(2):201-8.

[38] Shekunov BY, Chattopadhyay P, Tong HHY, Chow AHL. Particle size analysis in pharmaceutics: Principles, methods and applications. Pharm Res. 2007;24(2):203-27.

[39] Randall C. Particle Size Distribution. In: Brittain HG, ed. *Physical characterization of pharmaceutical solids*. New York, NY: M. Dekker 1995:157-86.

[40] Lasch J, Weissig V, Brandl M. Preparation of Liposomes. In: Torchilin VP, Weissig V, eds. *Liposomes: a practical approach*. 2nd edition ed. Oxford, UK: Oxford University Press 2003:3-29.

[41] USP. <1601> Products for Nebulization - Characterization Tests. 2011.

[42] Marple VA, Olson BA, Santhanakrishnan K, Roberts DL, Mitchell JP, Hudson-Curtis BL. Next generation pharmaceutical impactor: A new impactor for pharmaceutical inhaler testing. Part III. Extension of archival calibration to 15 L/min. J Aerosol Med-Depos Clear Eff Lung. 2004 Win;17(4):335-43.

[43] Mitchell JP, Nagel MW, Nichols S, Nerbrink O. Laser diffractometry as a technique for the rapid assessment of aerosol particle size from inhalers. J Aerosol Med-Depos Clear Eff Lung. 2006;19(4):409-33.

[44] Zhang G, David A, Wiedmann TS. Performance of the vibrating membrane aerosol generation device: Aeroneb micropump nebulizer (TM). J Aerosol Med-Depos Clear Eff Lung. 2007 Win;20(4):408-16.

[45] Washington C. Stability of lipid emulsions for drug delivery. Adv Drug Delivery Rev. 1996 Jul;20(2-3):131-45.

[46] Alfridsson M, Ninham B, Wall S. Role of Co-Ion specificity and dissolved atmospheric gas in colloid interaction. Langmuir. 2000 Dec;16(26):10087-91.

[47] Kawaguchi E, Shimokawa K, Ishii F. Physicochemical properties of structured phosphatidylcholine in drug carrier lipid emulsions for drug delivery systems. Colloids and Surfaces B-Biointerfaces. 2008;62(1):130-5.

[48] Barnes HA, Hutton JF, Walters K. Rheology of Suspensions. In: Walters K, ed. *An introduction to rheology*. Amsterdam, The Netherlands: Elsevier 1989:115-37.

[49] Packhaeuser CB, Lahnstein K, Sitterberg J, Schmehl T, Gessler T, Bakowsky U, et al.. Stabilization of Aerosolizable Nano-carriers by Freeze-Drying. Pharm Res. 2009 Jan;26(1):129-38.

Chapter 5: Prediction of *In Vitro* Aerosolization Profiles Based on Rheological Behaviors of Aqueous Dispersions of Coenzyme Q_{10}

Abstract

Coenzyme Q_{10} (CoQ_{10}) is a poorly-water soluble compound that is being investigated for the treatment of carcinomas. The final drug particle size in dispersions when using microfluidization preparation methods is highly influenced by the number of passes and type of phospholipid used in the process. The aim of the research work presented in this chapter is to investigate the feasibility of preparing phospholipid-stabilized dispersions of the anticancer agent for pulmonary delivery using a vibrating-mesh nebulizer. We determined the physicochemical properties and compared the nebulization performance of dispersions of CoQ_{10} prepared with dimyristoyl phosphatidylcholine (DMPC), dipalmitoyl phosphatidylcholine (DPPC), or distearoyl phosphatidylcholine (DSPC) to the formulation previously prepared with lecithin. The phospholipid formulations were characterized for drug particle size distribution in dispersion, zeta potential, surface tension, and rheology. An evaluation was performed on the aerosolization profile of the inhalation system triad: drug, excipients, and device, for nebulization performance (using laser diffractometry (LD) and gravimetrical analysis) and for the aerodynamic drug deposition of the formulations (using Next Generation Impactor – NGI). The Total Emitted Dose (TED) was characterized using both NGI and a Dose Uniformity Sampling Apparatus (DUSA) for Dry Powder Inhalers (DPIs) adapted for use with nebulizers. The hydrodynamic sizes of the drug particles in dispersion were primarily in the submicron range with the synthetic phospholipids presenting some larger particles. The lecithin dispersion presented a significantly large module of zeta potential (60 mV) while the synthetic phospholipids had values close to zero. The surface tension

of the formulations ranged in value from 26 to 46 mN/m. At high shear rates, DPPC, DMPC, and lecithin formulations of CoQ_{10} presented increased shear-thickening behavior. In addition, the formulations showed a decrease in mass and drug output over time within a 15-minute nebulization event, along with decreased aerodynamic and geometric sizes. The lecithin dispersion had the worst performance in terms of Fine Particle Dose (FPD), whilst the DPPC and DSPC dispersions showed similarly high FPDs. The results suggest that the rheological properties may be the determining factor in identifying potential formulations with a satisfactory aerosolization profile for the nebulization of dispersions.

5.1. INTRODUCTION

Aerosolization of dispersed formulations is expected to generate droplets containing variable drug concentration due to the heterogeneous nature of the dosage form. Therefore, it is crucial to characterize the formulations for *in vitro* drug deposition, which can be performed with cascade impactors.[1] Laser diffractometry (LD) can alternatively be used for this purpose when considering solution dosage forms. The non-homogeneous characteristic of dispersion systems may possibly give rise to droplets with heterogeneous concentrations of drug particles, deeming LD an unsuitable technique.[2-4] The United States Pharmacopoeia (USP) recommends the Next Generation Impactor (NGI) be used for this testing.[5] In addition, USP recommends an evaluation be performed of the delivered drug from the aerosol output.

The alveolar surfactant in humans is comprised 90% of phospholipids and 10% of neutral lipids.[6] Among the various types of phospholipids, phosphatidylcholine (PC) is predominant (76%). Among the different PC saturated and unsaturated fatty acid chains,

DPPC is the main component (81% of PC) with dimyristoyl phosphatidylcholine (DMPC) and distearoyl phosphatidylcholine (DSPC) each comprising 3% of PCs.[6] DPPC and DSPC are also present in the mixture of phospholipids that comprise the excipient soybean lecithin in widely varying concentrations depending on the source and extraction method.[7, 8]

In the previous chapter, we have defined high pressure homogenization (microfluidization) as a suitable manufacturing process to obtain a phospholipid-stabilized dispersion of Coenzyme Q_{10} (CoQ_{10}) with small drug particle size. The type of phospholipid used influenced drug particle size in dispersion. Processing formulations for more than 50 passes in the microfluidizer did not further decrease particle size (Chapter 4, Section 4.4). Lecithin was used as model excipient and dispersions of CoQ_{10} were also characterized for surface tension, zeta potential and rheology. Evaluation of nebulization performance (steady aerosolization over time) from an Aeroneb Pro® nebulizer using LD and gravimetrical analysis showed continuous aerosolization of CoQ_{10} dispersions for 15 minutes. The investigation suggests that the rheological behavior of the dispersions appears to play a role in the nebulization performance.

The aim of this study was to use synthetic phospholipids to prepare formulations of CoQ_{10} that can potentially provide improved nebulization performance, which would have the potential to deliver an improved Fine Particle Dose (FPD) of CoQ_{10} when compared to lecithin dispersions. We have chosen three synthetic phospholipids to stabilize these dispersions given their physiological occurrence in the lungs: DMPC, DPPC, and DSPC. They present 14, 16 and 18 carbons in their saturated fatty acid chains and molecular weights of 678, 734, and 790 g/mol, respectively. Besides the characterization tests performed in our previous study, the formulations were further characterized for *in vitro* drug deposition using NGI and Total Emitted Dose (TED) using

both NGI and a Dose Uniformity Sampling Apparatus (DUSA) for Dry Powder Inhalers (DPIs) adapted for nebulizers. The results were thoroughly analyzed in conjunction with the nebulization performance tests for continuous aerosolization and for identifying the physicochemical properties governing the mechanism of aerosol generation of dispersed systems of CoQ_{10} from the micropump nebulizer. We confirmed our previous results by demonstrating that rheology of dispersions plays a significant role in the hydrodynamics of aerosol production using active vibrating-mesh nebulizer.

5.2. MATERIALS AND METHODS

5.2.1. Materials

Coenzyme Q_{10} was supplied by Asahi Kasei Corp. (Tokyo, Japan). Lecithin (granular, NF) was purchased from Spectrum Chemical Mfg. Corp. (Gardena, CA, USA). Genzyme Pharmaceuticals (Liestal, Switzerland) provided 1,2-dimyristoyl-sn-glycero-3-phosphocholine (DMPC), 1,2-dipalmitoyl-sn-glycero-3-phosphocholine (DPPC), and 1,2-distearoyl-sn-glycero-3-phosphocholine (DSPC). DMPC was also purchased from Lipoid GmbH (Ludswighafen, Germany). Sodium chloride (crystalline, certified ACS) was acquired from Fisher Chemical (Fisher Scientific, Fair lawn, NJ, USA) and the deionized water was obtained from a central reverse osmosis/demineralizer system commonly found in research laboratories. Hexane and ethanol 200 proof were purchased from Sigma-Aldrich (St. Louis, MO, USA) and methanol from Fisher Chemical (Fisher Scientific, Fair lawn, NJ, USA), all of which were from HPLC grade. The external filter for NGI testing (glass fiber, GC50, 75 mm) and the filter for DUSA (glass fiber, AP40, 47 mm) testing were purchased from Advantec MFS Inc. (Dublin, CA, USA) and from Millipore (Billerica, MA, USA), respectively. Syringes (1 mL) and syringe filters

(hyperclean, 17 mm, 0.45 µm, PTFE) were obtained from Becton Dickinson (Franklin Lakes, NJ, USA) and Thermo Scientific (Bellefonte, PA, USA), respectively.

5.2.2. Formulation

Formulations (100 mL) were prepared using hot high pressure homogenization to determine the effect of the type of phospholipid on the aerosolization profile – nebulization performance and *in vitro* drug deposition of particles for pulmonary delivery. We have chosen 2.5% w/w to be the maximum phospholipid concentration in our formulations, the same concentration as is in the approved drug product Survanta® (Abbott Laboratories, Abbott Park, IL, USA). During preliminary studies (see Appendix B), it was found that the maximum nominal drug loading that could be achieved with formulations not presenting intermittent mist within a 15-minute nebulization event using the Aeroneb Pro® nebulizer was 4% w/w. Therefore, formulations with synthetic phospholipids were prepared at a drug-to-lipid ratio of 4:2.5.

Following overnight hydration while stirring, a phospholipid dispersion containing 2.5% w/w of phospholipid (DMPC, DPPC, or DSPC) in water was added to the molten CoQ_{10} (4% w/w) at 55 °C. The formulation was then predispersed using high shear mixing with an Ultra-Turrax® TP 18/10 Homogenizer with 8 mm rotor blade (IKA-Werke GmbH, Staufen, Germany) for 5 minutes at 20,000 rpm. Subsequently, each formulation was passed 50 times through an M-110P Bench-top Microfluidizer® (Microfluidics, Newton, MA, USA) at approximately 30,000 psi while maintaining a temperature between 55 and 65 °C. Following microfluidization, 0.9% w/v of sodium chloride was added to the final formulation for reasons outlined in the previous chapter (Section 4.4).

The particle size distributions of the formulations were then analyzed using Laser Diffraction (LD) and/or Dynamic Light Scattering (DLS). The surface tension, zeta potential and rheology were also evaluated. For nebulization performance, aerosol output generated from an Aeroneb Pro® nebulizer (Aerogen, Galway, Ireland) was analyzed using LD and gravimetrical analysis. *In vitro* drug deposition was evaluated using a NGI while the TED was analyzed from both the NGI results and from measurement using a Dose Uniformity Sampling Apparatus (DUSA). Besides the characterization and nebulization performance presented in the previous chapter, the *in vitro* drug deposition of lecithin dispersion of CoQ_{10} (drug-to-lipid ratio: 1:1) passed 50 times through the Microfluidizer® was prepared and analyzed. This was evaluated against the synthetic phospholipid formulations (DMPC, DPPC, or DSPC dispersions of CoQ_{10}). Details of the preparation, characterization and evaluation of nebulization performance of the lecithin dispersion are presented in the previous chapter. Testing was performed immediately following preparation, except for stability of drug particle size in the dispersions in which the samples were tested 7 days after preparation.

5.2.3. Characterization

5.2.3.1. Particle Size Distribution

Particle size distribution testing of the dispersed formulations was performed with LD using a wet sample dispersion unit stirring at 1,000 rpm coupled to a Malvern Spraytec® (Malvern Instruments, Worcestershire, UK) equipped with a 300 mm lens. The dispersed formulations were added to distilled water (dispersant) until approximately 5% obscuration was attained. The internal phase and dispersant refractive indexes were 1.45 and 1.33, respectively, based on reports related to lecithin in the literature[9]. A timed

measurement was performed for 45 seconds with 1 second sampling periods (a total of 45 data acquisition periods). Results are presented as $Dv_{(X)}$ and span, where X is the cumulative percentile of particles under the referred size (e.g. $Dv_{(50)}$ corresponds to the median volume of the particles). Span is the measurement of particle size distribution calculated as $[Dv_{(90)} - Dv_{(10)}]/Dv_{(50)}]$. Therefore the higher the span, the more polydisperse the particle size distribution was.

In addition, the nanoparticle hydrodynamic diameter of the dispersed formulations was characterized with DLS using a Malvern Zetasizer Nano ZS® (Malvern Instruments, Worcestershire, UK) at 25°C and pre-equilibrated for 2 minutes. The intercept of the correlation function was between 0.5 and 1.0. Distilled water was used for dilution of the dispersions whenever needed.

5.2.3.2. Surface Tension

Surface tension testing was performed using a TA.XT.plus Texture Analyzer (Texture Technologies, Scarsdale, NY, USA) from the maximum pull on a disk as described in Chapter 3. Briefly, the container and glass disk probe were thoroughly degreased, cleaned with ethanol and allowed to dry. The probe was attached to the texture analyzer arm, and lowered until the bottom surface of the probe contacted the surface of the liquid formulation contained in the reservoir. The temperature of the liquid was measured and recorded. At the start of testing, the probe was raised from the surface of the liquid at a constant speed (0.05 mm/s) for 10 mm, while the texture analyzer registered at 5 points per second the force exerted as a function of either time or distance. Using the maximum (detachment) force the surface tension was calculated using the equation below:

$$\frac{X}{k} = 0.0408687 + 6.20312 \cdot \left(\frac{X^3}{V}\right) - 0.0240752 \cdot \left(\frac{X^3}{V}\right)^2 \qquad \text{(Equation 5.1)}$$

Where X is probe radius, V is volume and k is the meniscus coefficient. For more details, see Chapter 3. The density values used to calculate surface tension were assumed to be the same as the density of water at the measurement temperature.

5.2.3.3. Zeta Potential

Electrophoretic light scattering was used to perform zeta potential testing with a Malvern Zetasizer Nano ZS® (Malvern Instruments, Worcestershire, UK). The samples were analyzed at a constant temperature of 25°C and constant (neutral) pH. Samples were diluted with distilled water, obtaining conductivity values ranging from 400 to 1400 µS/cm. Each sample was analyzed in triplicate and subjected to 10 to 100 runs each measurement, with automatic optimization of attenuation and voltage selection.

5.2.3.4. Rheology

Rheological behavior of the dispersed formulations were tested using a AR-G2 rheometer (TA Instruments, New Castle, DE, USA) equipped with a cone-and-plate geometry (cone diameter: 40 mm; truncation: 54 µm). Zero-gap and rotational mapping were performed prior to testing. All measurements were executed with fresh sample dispersion at a constant temperature of 25°C with no pre-shear. Excess sample around the edge of the probe was trimmed and water was added to the solvent trap compartment. The samples were measured at the steady state flow step over a range of shear rates (from 1000 to as low as 0.01 s^{-1}) decreasing logarithmically (5 points per decade). The lower

and upper limits of shear rate were determined, respectively, by the instrument sensitivity and hydrodynamic limitations (high probe speed will cause the liquid sample to spill away from the measurement zone) for each formulation. The sample period was 20 seconds and considered in equilibrium after 2 consecutive analyses within 5% tolerance, not exceeding a maximum measurement time of 2 minutes. The results were evaluated using Rheology Advantage Data Analysis software (TA Instruments, New Castle, DE, USA).

5.2.3.5. Nebulization Performance

Based on previous experience, the performance of vibrating-mesh nebulizers can be affected by mesh clogging, resulting in variable aerosol emission (i.e. intermittent mist), since this formulation is a dispersed system.[10] To analyze the nebulization performance of these formulations, the changes in transmission over time were evaluated from LD technique measurements. The nebulization performance of the dispersions was evaluated using the "open bench" method with a Malvern Spraytec® instrument (Malvern Instruments, Worcestershire, UK) equipped with 300 mm lens.[11] The nebulizer reservoir was positioned with the vibrating mesh located 25 mm above the upper edge of the laser beam at a distance of 25 mm between the lens and the center of the aerosol cloud. Air suction was positioned 10 cm beneath the laser beam. The device and air suction apparatus positions were not disturbed throughout the entire measurement period. The internal phase and dispersant refractive indexes were 1.33 (water) and 1.00 (air), respectively. Formulation (10 mL) was added to the nebulizer reservoir. At the start of nebulization, aerosol characteristics were continuously measured every second for 15

minutes. The slope of the transmission-time curves (transmittograms) were considered when comparing the different phospholipid formulations.

In addition, the Total Aerosol Output (TAO) was gravimetrically measured for each of the formulations studied. Before aerosolization, the nebulizer was weighed after each formulation was dispensed into the reservoir. The remaining formulation in the nebulizer reservoir was re-weighed after undergoing 15 minutes of nebulization. The difference in weight before and after nebulization results in the calculated TAO. The weight of the nebulizer mouthpiece was not considered during the measurements.

Importantly, neither transmittogram nor TAO provide information regarding drug output from the nebulizer. Information is limited solely to total mass output (droplets emitted over time). In the aerosolization of these dispersions, droplets not containing drug particles (empty droplets) are potentially generated. However, our purpose with this test is to investigate the capability of the Aeroneb Pro® nebulizer to continuously and steadily aerosolize the aqueous dispersions of CoQ_{10} over time. Intermittent mist can be identified in the transmittograms while TAO elucidates the magnitude of total mass being aerosolized. Saline solution (12 mL of 0.9% w/v NaCl in water) was used as the control.

5.2.3.6. In vitro *Aerodynamic Deposition*

To evaluate *in vitro* aerosol deposition, we have designed the study as follows. Within a 15-minute nebulization event, the first and last 15 seconds (herein called initial and final sections or phases) of aerosol generation were collected using NGI or DUSA for DPI (both from Copley Scientific, Nottingham, UK). This design helps in determining whether the slope in transmission, previously observed for lecithin formulations and related to TAO (Chapter 4, Section 4.3), translates into similar drug mass output.

To measure the aerodynamic properties of the formulations, the NGI was set up with airflow of 15 L/min and the drug collected from the induction port, the seven stages of the cascade impactor, the micro-orifice collector (MOC) and the external filter was analyzed using High Performance Liquid Chromatography (HPLC). The sum of the masses in each of the mentioned compartments of the NGI hardware setup provides the TED measured from the NGI. The mass deposited in each stage is also used to determine the deposition pattern and to calculate the Mass Median Aerodynamic Diameter (MMAD) as described in the General Chapter <601> of the USP.[12] This parameter is the equivalent droplet size in which half (50%) of the droplets are smaller and the other half are larger than the specified cutoff diameter, based on the drug amount deposited in different stages of the NGI. Commonly, the Geometric Standard Deviation (GSD) is reported to indicate the dispersity droplet size distribution around the MMAD. The FPD was calculated from the sum of drug mass deposited on impaction Stages 3 through 7, MOC and external filter (aerodynamic cutoff diameter below 5.39 μm). Finally, the Fine Particle Fraction (FPF) was calculated by dividing FPD by TED from NGI, as described above. Since our objective herein was to perform a comparative analysis of the different dispersions of CoQ_{10}, it was decided not to refrigerate the NGI equipment prior to analysis, as was recently recommended.[5, 13] Therefore, an underestimation of MMAD values may have occurred due to droplet evaporation.

During the NGI analysis, losses may occur during drug collection due to deposition in inner compartments between stages of the cascade impactor or in the nebulizer mouthpiece. Therefore, mass balance is recommended to be performed. During preliminary studies, it was observed that a 15-minute aerosol generation from dispersions prepared with synthetic phospholipids caused high amounts of formulation to accumulate in the nebulizer mouthpiece. For this reason, mass balance from NGI analysis was

deemed inappropriate at the final phase of each nebulization period due to the accumulated drug in the nebulizer mouthpiece. To certify that an acceptable mass recovery during the analysis of TED from NGI was being achieved, we evaluated the TED from an adapted DUSA (Figure 5.1). In the DUSA testing, the aerosol was deposited directly onto a glass fiber filter, positioned on one end of the DUSA, which was connected to a vacuum pump. The nebulizer mouthpiece was positioned onto the opposite end, and directly connected to the DUSA using a silicone adapter. TED was determined from the drug amount collected in the glass fiber filter and from the internal walls of the DUSA, which was analyzed using HPLC generated data following a timed nebulization. TED values from NGI and DUSA methods should not have varied significantly, thus ensuring a satisfactory mass balance.

To further analyze the dose that may potentially be delivered to the lungs, the FPD results were extrapolated from 15-second measurements to calculate an estimated total delivered drug (estimated total FPD or FPD_{et}) within a 15-minute period as follows:

$$FPD_{et} = \sum_{i=2}^{n} FPD_{i-1} + \left(\frac{FPD_n - FPD_{i-j}}{n-1}\right) \qquad \text{(Equation 5.2)}$$

Where i is an integer number representing 15-second intervals, referring to the time duration of NGI and TED analyses. The j value is the subsequent integer number smaller than i and n is the number of 15-second fractions within a 15-minute nebulization period (n = 60).Based on FPD_{et}, the rate of delivery of the Fine Particle Dose (FPD_r) was also calculated.

5.2.3.7. HPLC Analysis of CoQ_{10}

This method was adapted from the previously developed method presented in the Appendix A. The Waters HPLC and column system (Waters Co., Milford, MA, USA) connected with UV detection consisted of a 1525 binary pump, a 717 autosampler, a 2487 dual λ absorbance detector, set at 275 nm, and a Symmetry® RP-C8 column (3.9 x 150 mm, 5 µm) connected to Symmetry® C8 guard column (3.9 x 20 mm, 5 µm). The mobile phase consisted of methanol:hexane at 97:3 (v/v) and was eluted at a flow rate of 1.0 mL/min. Stock solution of CoQ_{10} was initially dissolved in hexane:ethanol at a ratio of 2:1 (v/v) and subsequently diluted with the mobile phase to obtain the desired concentrations. The linearity range was determined by injecting 50 µL of samples at a controlled temperature of 40 ºC. Chromatogram peaks were acquired within run time of 9 minutes and the peak areas were used to determine curve linearity.

All samples were collected from NGI and DUSA testing with ethanol, with the exception of drug collection from the NGI plates (Stages 1 through 7 and MOC) for analysis of lecithin dispersions. Due to the low solubility of the formulation in ethanol, a mixture of hexane:ethanol 2:1 v/v was used instead. The samples collected in glass fiber filters (external filter in NGI and filter from DUSA) were vortexed for 30 seconds prior to filtering with 0.45 µm syringe filters. The mobile phase was used for sample dilution.

5.2.4. Statistical Analysis

The data is expressed as mean ± standard deviation with the exception of surface tension, which was expressed as mean ± standard error. For rheology studies, standard errors were provided by the software used to analyze the best fit of the results to the rheological models. Samples were analyzed at least in triplicate and evaluated for statistical differences with One-Way ANOVA for significance when $p < 0.05$ using

NCSS/PASS software Dawson edition.[14] *Post hoc* comparisons were performed to identify statistically significant differences among groups using Tukey-Kramer method. A paired *t-test* was performed to analyze statistical differences ($p < 0.05$) within the same nebulization event for different formulations and to compare TED methods: specific phases for each formulation for NGI versus DUSA methods.

5.3. RESULTS AND DISCUSSION

In this study, we used synthetic phospholipids (DMPC, DPPC, and DSPC) to prepare formulations of CoQ_{10} and compared the results with the previously investigated lecithin formulation (Chapter 4). Soybean lecithin is a mixture of different types of phospholipids, with concentrations varying widely depending on the source and extraction method.[7, 8] We also extended the investigation to further than the capability of the device to generate aerosol uninterruptedly. Since it is a dispersed system, the aerosolization of this dosage form may generate droplets from the device that may contain different drug amounts. Therefore, we evaluated the aerodynamic properties of the formulation using a cascade impactor based on the drug amount deposited in each stage of the NGI apparatus. Furthermore, we investigated the TED based on drug collected in a filter delivered directly from the nebulizer mouthpiece. The nebulization performance in conjunction with the aerodynamic properties can provide a basis for the comparison of the inhalable potential of the formulations. It also allows us to identify which physicochemical properties favor an effective drug emission of the CoQ_{10} dispersions from the Aeroneb Pro® nebulizer.

The HPLC method has shown linearity in the concentration range of CoQ_{10} from 100 ng/mL to 10 µg/mL, with a correlation coefficient (r^2) of 0.9997. Extraction of filters

spiked with CoQ_{10} and the phospholipids did not appear to interfere with the CoQ_{10} peak, which was eluted at approximately 6.6 minutes.

Upon observation of the hydrodynamic size in the dispersions (Figure 5.2 and Table 5.1), it was observed from the LD results that the drug particle size of the lecithin formulation was mostly in the submicron range. Synthetic phospholipid formulations presented some larger particles, although analysis of $Dv_{(X)}$ and span does not present statistical differences among formulations (except for $Dv_{(10)}$ of DMPC and DSPC dispersions). Further analysis of drug particle size distribution using DLS shows that lecithin dispersions presented larger nanoparticles with a higher polydispersity than any other formulation (Figure 5.3). Among synthetic phospholipids, the DSPC dispersion presented the largest drug nanoparticles while the DMPC formulation presented the most monodisperse profile. Following processing, the synthetic phospholipids presented some microparticles, although the population of particles in the nanometric scale was primarily smaller than drug particles that were produced from lecithin dispersions of CoQ_{10}.

The module of zeta potential of lecithin dispersion of CoQ_{10} was significantly higher than that which was found for the formulations prepared with synthetic phospholipids (Figure 5.4). The mixture of different types of phospholipids at various concentrations depending on the source and extraction method[7, 8] that comprises soybean lecithin is known to provide widely variable zeta potential values for dispersions.[15] Nonetheless, the zeta potential values of synthetic phospholipids that were close to zero may be attributed to the presence of sodium chloride in the formulations. Increase in ionic strength at neutral pH greatly increases the zeta potential of negatively charged phospholipids like DMPC, DPPC, and DSPC.[16]

We have previously found that an increased number of passes in the microfluidizer causes a decrease in surface tension, possibly due to a more efficient

encapsulation. In this study, all dispersions were processed 50 times in the high pressure homogenizer. Hence, less surfactant is available in "solution" than is needed to cause a decrease in surface tension. Among synthetic phospholipids, a significant increase in surface tension was observed in this study which followed an increase in the number of carbons in the acyl chains of the phospholipids used to prepare the formulations. As was previously discussed, the formulations were designed to have the same amount of DMPC, DPPC, and DSPC at 2.5% w/w. With a different number of carbons in each respective acyl chain, the molecular weights vary slightly. Consequently, the molar concentrations of the phospholipids in the dispersions were 36.9, 34.1 and 31.6 mM, respectively. The structure of phospholipids in water dispersions depended directly on the number of phospholipid molecules.[17] Therefore, the differences in surface tension can be explained by the number of phospholipid molecules available in "solution" to cause a decrease in surface tension at a constant temperature.[18] Interestingly, the surface tension of the CoQ_{10} dispersion prepared with lecithin, comprised of a mixture of phospholipids, falls between the DMPC and DSPC values (Figure 5.5).

It is well known that particle characteristics like size, size distribution, shape, charge, deformability, and the interactions between particles and the surrounding fluid play significant roles in the rheological behavior of dispersed systems.[19] To evaluate the rheology of the dispersions, we plotted shear stress as a function of shear rate and fit the results to the best rheological model. It was determined that the Herschel-Bulkley was the model that best represented most of the formulations:

$$\sigma = \sigma_y + \kappa \cdot \dot{\gamma}^n \qquad \text{(Equation 5.3)}$$

Where σ is shear stress, σ_y is yield stress, κ is consistency coefficient (or Non-Newtonian viscosity), $\dot{\gamma}$ is shear rate and n is flow index (n = 1: Newtonian fluid; n < 1: shear-thinning; n > 1: shear-thickening). The Power Law model is similar to Herschel-Bulkley, except that it does not present yield stress value. Standard errors are 35.92 ± 3.57, 9.83 ± 0.17, 10.27 ± 0.35, 21.15 ± 8.17 for lecithin, DMPC, DPPC and DSPC dispersions, respectively. The three elements of the Herschel-Bulkley model are presented in Figure 5.6. DSPC dispersion of CoQ_{10} was governed by Power Law and therefore did not present yield stress. Despite that, the yield stresses of the formulations are shown to be statistically different but no trend can be found. DSPC formulation had a significantly higher Non-Newtonian viscosity than the other analyzed samples, possibly due to its evident shear-thinning behavior (n < 1). Most interestingly, the flow index results indicated that DPPC, DMPC, and lecithin dispersions respectively presented increasing shear-thickening behavior (n > 1).

We further analyzed the rheology by holding shear rate and viscosity as the independent and dependent variables, respectively, in order to fit the results to the general flow curve of aqueous dispersions (Figure 5.7Figure 5.). Graphical representations are presented in Figure 5.8, which clearly shows the accentuated shear-thinning event previously mentioned for DSPC formulation. Relevant equations related to these models are shown in Table 5.2. By fitting these curves to the rheological models, we found that the formulations presented rather different behavior (Table 5.3). Standard errors are 93.49 ± 8.60, 43.27 ± 10.55, 41.34 ± 8.57, 16.00 ± 4.74 for lecithin, DMPC, DPPC and DSPC dispersions, respectively.

The lecithin formulation of CoQ_{10} fits to the Sisko model, indicating that the investigated shear rate range falls within the mid-to-high shear-rate range related to the general flow curve of dispersions. This is confirmed by the extremely small characteristic

time seen in Table 5.3 and the curve shape at higher shear rates shown in Figure 5.8. Moreover, this result confirms the shear-thickening behavior presented from the evaluation of the Herschel-Bulkley model (Figure 5.6). From all formulations studied only the lecithin dispersion presented thixotropic behavior. This indicates a time-dependent change following interruption of shear stress (in this case, shear-thinning event) during structure recovery from the shear-thickening behavior presented by this dispersion in the shear rate range studied. Therefore, all other formulations analyzed promptly recover to their initial state at cessation of shear stress.

The DMPC and DPPC dispersions fit to the Cross model, thus both zero-rate and infinite-rate viscosities are presented. Characteristic times however differ greatly, with the lowest value shown for the DMPC formulation. This indicates that, similarly to lecithin dispersion, the DMPC formulation falls towards the upper range of shear rate related to the general flow curve of dispersions (Table 5.3), explaining the second Newtonian plateau (3.66 cP) being greater than the first Newtonian zone (1.13 cP). Therefore, the rheological behavior of the DMPC dispersion is closer to the Sisko than the Cross model. For this reason, both lecithin and DMPC dispersions present rate index (or Cross rate constant) values above unity, reflecting the absence of the power law region in the shear rate range investigated. When the viscosity within this specific range is appropriately extending from the first to the second Newtonian zone, $1 - m$ is close to the rate index n.[20-22] Inarguably, the shear-thickening behavior is evident from the curve shape at higher shear rates (Figure 5.8). The larger characteristic time of the DPPC formulation indicates that the curve falls more towards the lower range of shear rates and therefore supports the infinite-rate viscosity being smaller than the zero-rate viscosity. The Cross rate constant is close to unity, which indicates a degree of shear-thinning behavior in the power law region. Observation of the curve shape of DPPC dispersion in

Figure 5.8 supports these findings and the relatively low degree of shear-thickening behavior presented in the Herschel-Bulkley model (Figure 5.6). This relatively low degree of shear-thickening behavior, when compared to lecithin and DMPC formulations, can be attributed to differences in rheology at higher shear rates.

The rheological behavior of the DSPC dispersion fits to the Williamson model. The statistically significant higher characteristic time in conjunction with the flow curve shape of this dispersion indicate that the shear rate range investigated falls within the low-mid shear rate range of the general flow curve of dispersions (Figure 5.8). The rate index value reflects the shear-thinning behavior at the power law region (Table 5.3).

As mentioned in the previous chapter, it is important to investigate the capability of vibrating-mesh nebulizers to continuously and steadily aerosolize dispersions, with concomitant analysis of fluid rheology as opposed to simpler kinematic viscosity measurements. Previous works have focused on the viscosity of the dispersion media *per se*, regardless of the interactions between the dispersed particles within the surrounding fluid.[23, 24] As described in Chapter 1, the nebulizer used in this study (Aeroneb Pro®) functions by imparting a high vibration frequency (128 KHz) on a perforated plate to generate the aerosol droplets. This high frequency mechanical stress is directly transferred to the liquid formulation. Therefore, analysis of rheology parameters at higher shear rates may better translate to what is actually occurring in the vicinity of the vibrating membrane.

The Aeroneb Pro® nebulizer has previously demonstrated its ineffectiveness to produce aerosols from solutions that have viscosities higher than approximately 2-3 cP, depending on other physicochemical properties of the liquid (i.e. surface tension).[25] Notably, the viscosities of lecithin, DMPC, and DPPC formulations investigated in this study at high shear rates may be considered sufficiently low to provide continuous

nebulization. The infinity-rate viscosity of DSPC dispersion was not identified within the shear rate range studied. Since the hydrodynamic characteristics of this specific formulation allowed for further analysis expanding the upper range of shear rate to 3000 s^{-1}, an infinite-rate viscosity of approximately 1 cP was observed following the Cross model. Therefore, all formulations were expected to be nebulized using this active vibrating-mesh nebulizer.

We acknowledge that some standard error values obtained from fitting the results to rheological models are rather high. These high values may be attributed to a limited shear rate range studied using this experimental design. Further evaluation of rheological behavior at lower shear rates using creep tests could be accomplished, and by superimposing the results to this data could help to provide lower standard errors.[21] However, our interest in this study lies in the formulation behavior at higher shear rates. It is also recognized that a direct correlation between the rotational shear rate that was applied during rheology tests and the vertical membrane oscillation during nebulization is improbable. Nonetheless, an understanding of the formulation reaction to the stress applied should give valuable information as to what can be expected from the active membrane nebulization of such dispersions.

To compare the nebulization performance of the formulations, we set up the Malvern Spraytec® with the "open bench" method as described in the previous chapter. The transmittograms presented in Figure 5.9 show a nebulization event of 15 minutes. At the end of this duration the transmission values go back up to 100% for all formulations. This result indicates that the measurement was properly performed with no fogging of the detector lens. To evaluate the nebulization performance of these formulations, the generated transmittograms were fitted to a linear regression in order to analyze the slopes of the curves. By comparing their slopes, it can be inferred how steady a given

nebulization event was. The slopes of the transmittograms and the TAO results are presented in Figure 5.10. Aerosolization of saline (control) has shown to be steady over time, which is indicated by a slope close to zero and the highest TAO. This confirms the feasibility of delivering solutions with this type of nebulizer. The lecithin formulation presented a steady nebulization for the initial 5 minutes (300 seconds), followed by an increase in transmission after this time point. Interestingly, the DMPC dispersion presented a transmission profile with a pattern opposite to the one displayed with the lecithin formulation of CoQ_{10}. At the start of nebulization, a slight slope can be observed for up to about 8 minutes (480 seconds) followed by steady nebulization to the end of the testing period. DPPC and DSPC dispersions presented a very shallow slope throughout the whole nebulization event.

The lecithin dispersion of CoQ_{10} presented a low TAO that was not statistically different from DMPC formulation, and the highest slope. On the other hand, although DPPC and DSPC formulations presented similar slopes (not statistically different), the TAO from DSPC showed a higher mass output than that which was shown for the DPPC, despite both being steadily nebulized. These findings indicate the importance of analyzing the slope of the transmittograms in conjunction with the mass output (or TAO). The DSPC formulation presented the best results among the aqueous dispersions of CoQ_{10}, exhibiting a low slope value and the highest TAO among the phospholipid dispersions. In summary, the respective order of increasing nebulization performance of CoQ_{10} was:

Lecithin < DMPC < DPPC < DSPC

These findings can be evaluated concomitantly with the respective rheological behavior of the formulations at higher shear rates. It is apparent when looking at the curve shapes (Figure 5.8) that, at high shear rates, lecithin and DMPC dispersions present the characteristic shear-thickening behavior following the second Newtonian plateau of the general flow curve of dispersions. This is confirmed by their low respective characteristic times. The occurrence of shear-thickening following the shear-thinning event happens due to an arrangement instability following the two-dimensional layering of the fluid. Being above a critical shear stress causes the random arrangement of particles, resulting therefore in an increase in viscosity.[19] This consequent random arrangement of the dispersed particles may be the cause of limitation to a steady nebulization performance presented by these two formulations. On the other hand, the high characteristic times and shear-thinning behavior at the power law region presented mainly by DSPC and to a lesser extent DPPC dispersions at high shear rates may explain an improved nebulization performance of these formulations. These results suggest that a high characteristic time corresponding to a shear-thinning behavior at high shear rates may favor the nebulization performance, while shear-thickening (low characteristic time) has the counter effect. Therefore, these results suggest that the rheological behavior at high shear rates may be directly related to the nebulization performance of the dispersions.

However, the mass output may not be correlated to drug emission in the case of nebulization of dispersions, as was previously discussed. To verify drug aerosolization and to gain understanding of the aerodynamic properties, the *in vitro* deposition of the phospholipid formulations of CoQ_{10} was analyzed using NGI and adapted DUSA. Analysis of drug deposition at initial and final time fractions of the 15-minute

nebulization period allowed for an evaluation of this data in conjunction with the nebulization performance previously discussed.

The TED of lecithin, DMPC, DPPC and DSPC formulations are presented in Figure 5.11. The lecithin dispersion of CoQ_{10} presented a statistically significant decrease in drug aerosolization comparing initial and final phases of nebulization period, following both NGI and DUSA analysis. This difference in drug amount emitted at the beginning and at the end of the nebulization confirms that the slope ($25.99 \times 10^{-3} \pm 2.80 \times 10^{-3}$ %/s) observed in the results from nebulization performance using LD is not only related to decreased mass output, but also to the amount of drug being aerosolized. Overall, the lecithin dispersion also presented a significantly smaller TED both at the initial and final phases when compared to the synthetic phospholipid formulations.

Following NGI analysis, no statistical difference was found within the same nebulization event for the dispersions prepared with synthetic phospholipids. However, the DMPC dispersion presented a significantly smaller TED within the same nebulization event following the DUSA method. It is more appropriate in this case to consider the TED results related to DUSA since the droplets containing the drug are directly deposited in a filter, while the TED from the NGI analysis may have losses associated with the NGI apparatus. Nevertheless, a satisfactory mass balance was reached, since no statistical difference was found when comparing each phase from each formulation for the two methods to determine TED. Again, the slope result ($16.06 \times 10^{-3} \pm 2.88 \times 10^{-3}$ %/s) from nebulization performance testing of DMPC dispersion is in agreement with the difference in drug amount being aerosolized within the same 15-minute nebulization period. DPPC and DSPC dispersions of CoQ_{10} aerosolized approximately equal amounts in both phases of nebulization. These results demonstrate the steadiness of nebulizing these formulations

as seen during nebulization performance testing which presented small linear regression slope values.

In addition to testing the capacity of vibrating-mesh nebulizers to continuously aerosolize these dispersions, it should also be observed that the droplets containing drug particles present aerodynamic properties that allow CoQ_{10} delivery to the lungs. These aerodynamic properties can be seen in Figures 5.12 and 5.13, where the deposition patterns of the studied formulations are presented. Interestingly, the lecithin formulation presented a higher droplet size related to drug mass fraction deposited at the initial phase of nebulization than at the final section (Figure 5.12). The DMPC formulation presented a similar pattern to the lecithin formulation, but to a much smaller degree. Formulations of DPPC and DSPC had a more balanced droplet size throughout the 15-minute nebulization event. As for drug amount deposited (as opposed to drug fraction), it is clear from Figure 5.13 that the overall deposition of lecithin formulation was low both at the initial and final phases when compared to the other formulations, as previously seen with the TED results. Among the three synthetic phospholipids studied, the DMPC formulation presented the lowest deposition, with agreement of the TAO and TED results. Formulations of DPPC and DSPC had high drug amounts deposited while maintaining the aerodynamic properties throughout the 15-minute nebulization event.

To further compare the aerodynamic properties of the aerosolized dispersions, the MMADs and GSDs are presented in Figure 5.14. The MMAD and GSD values at the initial phase are similar when comparing all of the formulations. At the end of nebulization, these values were quite variable at different degrees, indicating that the aerosolization process had a different impact on the size of the emitted droplet containing drug nanoparticles depending on the type of phospholipid used to disperse CoQ_{10}. Remarkably, it appears that the changes seen within the same nebulization event for

lecithin and DMPC dispersions through the slope from the transmittogram results (Figure 5.10) are reflected not only in the amount of drug being aerosolized, as observed in the TED results (Figure 5.11), but also on the aerodynamic properties shown in their *in vitro* NGI deposition profiles (Figures 5.12 and 5.13). As the nebulization progresses, the droplets aerosolized become smaller and decrease in quantity.

By analyzing the fine particles (with aerodynamic sizes below 5.39 μm), we can acquire a better understanding of the drug output that may potentially be deposited into the lungs. Figure 5.15 shows the FPD_{et} and FPF values for the formulations of CoQ_{10} studied. The FPF appears to increase over time for all of the dispersions aerosolized with the Aeroneb Pro® nebulizer, confirming that the droplet sizes are decreasing as a result of the nebulization process. As seen with the MMAD differences obtained at initial and final phases of aerosolization of lecithin dispersions of CoQ_{10}, the FPD of this formulation drastically changes over time within the same nebulization event. Moreover, the MMAD values of aerosolized DMPC dispersions are significantly shown to decrease, while the FPD is not statistically different. The DPPC formulation presents a steady nebulization performance and, consequently, similar TED values within the nebulization event, as previously shown. Although the MMAD values are not statistically different, it can be observed from the FPD results that the DPPC formulation presents a significantly higher amount of drug particles that are aerosolized by the end of the nebulization period. A similar behavior was observed for the DSPC dispersion of CoQ_{10}, but this fell short from the value of statistical significance ($P = 0.08$). In general, these findings confirm that the aerodynamic size of the aerosolized dispersions decreased over time within the same nebulization event.

Figure 5.16 shows that the geometric sizes of the droplets containing CoQ_{10} particles also decrease over time, more so for lecithin and DMPC dispersions. Aerosols

of DPPC and DSPC formulations presented a steadier droplet size within the 15-minute nebulization period, which were more similar to the saline (control). The discrepancy in aerodynamic and geometric sizes may be attributed to the different testing setups as discussed in a previous study.[26] The "open bench" method using LD technique evaluates the volume-based geometric sizes as soon as the droplets are generated from the vibrating-mesh. On the other hand, larger particles are excluded from MMAD calculation due to inertial impaction of droplets onto the nebulizer mouthpiece adapted to the aerosol generating vibrating-mesh and onto the induction port attached to the NGI setup.

We have observed unprecedentedly high doses with the potential to reach the lungs based on FPD, results presented in Table 5.4, with DPPC and DSPC formulations presenting the highest values. These doses are approximately 10 to 40 times greater than itraconazole nanodispersions previously aerosolized using the same type of nebulizer (vibrating-mesh device) and as much as 280 times greater than previous aerosolization of budesonide suspension (Pulmicort Respule®, AstraZeneca, UK) using a Sidestream® PortaNeb® jet nebulizer (Medic-Aid Ltd., UK).[27-29] Most importantly, the experimental design in the present study allows for verifying further whether there was a burst or a steady aerosol generation throughout the desired 15-minute nebulization event.

Further studies are warranted to verify the effective drug loading, which we anticipate to be somewhat different from the nominal drug concentration. During hot high pressure homogenization, water evaporation may occur. In addition, the small volume of formulation prepared (100 mL) may allow for drug loss deposited in the internal walls of the container of the manufacturing equipment. Moreover, stability studies of the formulations should be performed.

The changes identified in nebulization performance of CoQ_{10} within a nebulization event using LD technique have been confirmed by the changes in aerodynamic properties of these formulations. Most importantly, the rheological behavior of these dispersions was in agreement with the capacity of the active vibrating-mesh nebulizer used in this study to steadily nebulize phospholipid-stabilized formulations of CoQ_{10}. It is well known that the concentration of dispersions has a significant role in determining the critical shear rate at which the shear thickening event post-second Newtonian plateau starts to happen.[19] Thus, the knowledge of rheology of dispersions may be used in future studies to identify the maximum drug loading based on this critical shear rate while still maintaining satisfactory nebulization performance. The aerosol generation from nebulizers occurs through an applied stress (i.e. air jet stream, ultrasonic force, vibrating-mesh, etc.) into or onto the bulk liquid formulation. Therefore, rheological studies of dispersions together with the analysis of nebulization performance using LD technique may greatly favor the formulation development of poorly-water soluble drugs for inhalation therapy using nebulizers. Nonetheless, special attention should be given to the functioning mechanism of the different types of nebulizers as described in Chapter 1 and how it may be related to the shear stress applied in the rheological studies.

5.4. CONCLUSIONS

Despite the similarities between the chemical structures of the excipients, the formulations of CoQ_{10} prepared with different phospholipids presented very different physicochemical properties which were holistically analyzed using the rheology of the dispersions. Evaluation of the non-Newtonian behavior at higher shear rates may indicate

the aerosolization profile (nebulization performance and *in vitro* drug deposition) of these formulations. Formulations of CoQ_{10} presenting low characteristic time (lecithin and DMPC) and therefore shear-thickening behavior at high shear rates presented a continuous, but not steady, nebulization performance. Decreased mass and drug output as well as decreased aerodynamic and geometric droplet sizes were also significant for these dispersions within the same 15-minute nebulization event. On the other hand, formulations presenting high characteristic time (DPPC and DSPC) and therefore a slight shear-thickening behavior or shear-thinning characteristic of power law region at high shear rates presented a steady nebulization performance. This was followed by a steady mass and drug output while maintaining the aerodynamic and geometric droplet sizes within the same nebulization event. The experimental design presented in this study may be a useful predictive tool to identify formulations with potential to deliver poorly-water soluble drugs as colloidal systems when aerosolized using vibrating-mesh nebulizers. Nonetheless, these findings warrant *in vivo* studies to determine the amount of CoQ_{10} that can be successfully aerosolized and deposited into animal lungs.

5.5. TABLES

Formulation	$Dv_{(10)}$ (µm)	$Dv_{(50)}$ (µm)	$Dv_{(90)}$ (µm)
Lecithin	0.24 ± 0.00	0.45 ± 0.00	0.81 ± 0.00
DMPC	0.21 ± 0.01*	0.81 ± 0.14	37.84 ± 27.25
DPPC	0.22 ± 0.01	0.85 ± 0.10	36.30 ± 34.26
DSPC	0.25 ± 0.02*	2.41 ± 1.93	97.24 ± 103.06

Results are expressed as means ± standard deviations (n = 3). * $P < 0.05$ following Tukey-Kramer test.

Table 5.1 – CoQ_{10} particle sizes in aqueous dispersions of phospholipid formulations represented as $Dv_{(10)}$, $Dv_{(50)}$, and $Dv_{(90)}$ values.

Model	Equation
Cross	$\frac{\eta - \eta_\infty}{\eta_0 - \eta_\infty} = \frac{1}{(1 + (K \cdot \dot{\gamma})^m)}$
Sisko	$\eta = \eta_\infty + K \cdot \dot{\gamma}^{n-1}$
Williamson	$\eta = \frac{\eta_0}{(1 + (K \cdot \dot{\gamma})^n)}$

η_0 and η_∞ are the asymptotic values of viscosity at very low (zero-rate viscosity) and very high (infinite-rate viscosity) shear rates; *K* is the characteristic time (the lower the value, the further to the right the curve lies); *m* is a dimensionless constant indicating rheological behavior (viscosity as a function of shear rate) in the shear thinning region where m = 0 refers to Newtonian behavior and increasing values tending to unity corresponds to increasing shear thinning behavior; *n* is the power-law index and values below and above unity represent shear-thinning and shear thickening events, respectively; and $\dot{\gamma}$ is shear rate.

Table 5.2 - Rheological models and their respective equations applied in this study.

Formulation	Model	Zero-rate viscosity (mPa.s)[§]	Infinite-rate viscosity (mPa.s)	Characteristic time (s)	Rate index (n) or Cross rate constant (m)	Thixotropy (Pa/s)	Normalized Thixotropy (s^{-1})
Lecithin	Sisko	N/A	0.95 ± 0.01	$8.60x10^{-4}$± $14.9x10^{-4}$	23.35 ± 1.90*	85.48 ± 0.79	$16.92x10^{-4}$± $0.31x10^{-4}$
DMPC	Cross	1.13 ± 0.01	3.66 ± 3.11	$9.06x10^{-4}$ ± $5.38x10^{-4}$	2.59 ± 0.52	Zero	Zero
DPPC	Cross	5.31 ± 0.96	1.61 ± 0.01	0.51 ± 0.03	0.70 ± 0.05	Zero	Zero
DSPC	Williamson	621.17 ± 446.30	N/A	15.19 ± 11.12*	0.54 ± 0.10	Zero	Zero

Results are expressed as means ± standard deviations (n = 3). N/A: not applicable when referred to this rheological model (compare to equations in table 2). [§] Groups are statistically different but *post hoc* test was unable to distinguish differences among groups. * $P < 0.05$ when compared to other formulations.

Table 5.3 – General flow curve data of CoQ_{10} dispersions.

Formulation	FPD_{et} (mg)	FPD_r (µg/min)
Lecithin	24.84	1656
DMPC	126.30	8420
DPPC	168.36	11224
DSPC	173.79	11586

Table 5.4 – Estimated total (FPD_{et}) and rate of delivery (FPD_r) of fine particle doses from aqueous dispersions of CoQ_{10} containing different phospholipids.

5.6. FIGURES

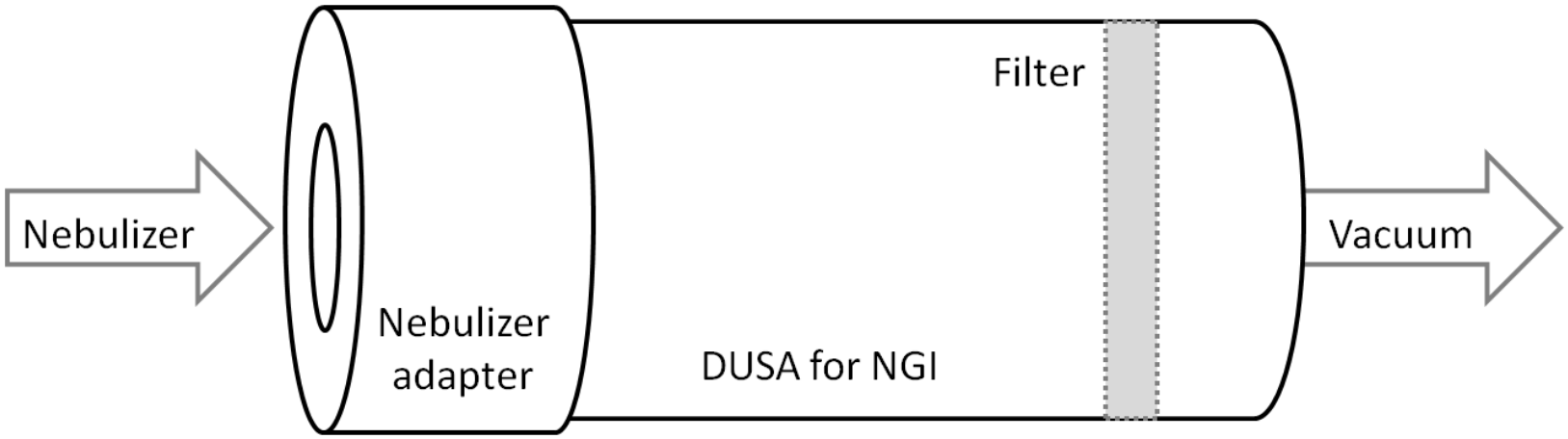

Figure 5.1 – Schematic diagram of Dose Uniformity Sampling Apparatus (DUSA) for Dry Powder Inhalers (DPIs) adapted for nebulizers.

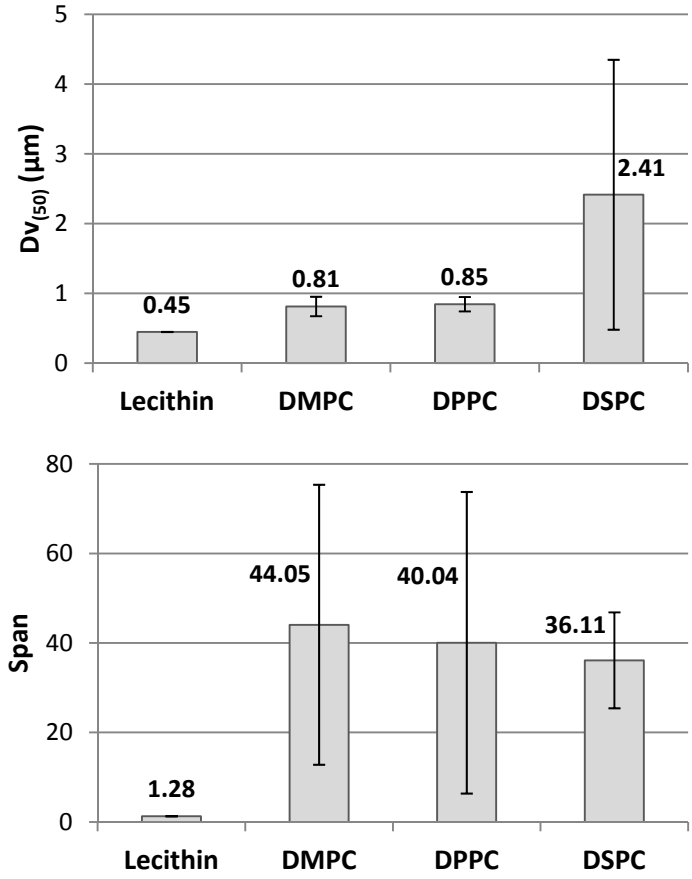

Figure 5.2 – Particle size distributions from laser diffraction technique of aqueous dispersions of CoQ_{10} following 50 passes in the Microfluidizer®. Results are expressed as means ± standard deviations (n = 3). Some standard deviations are too small to be visible.

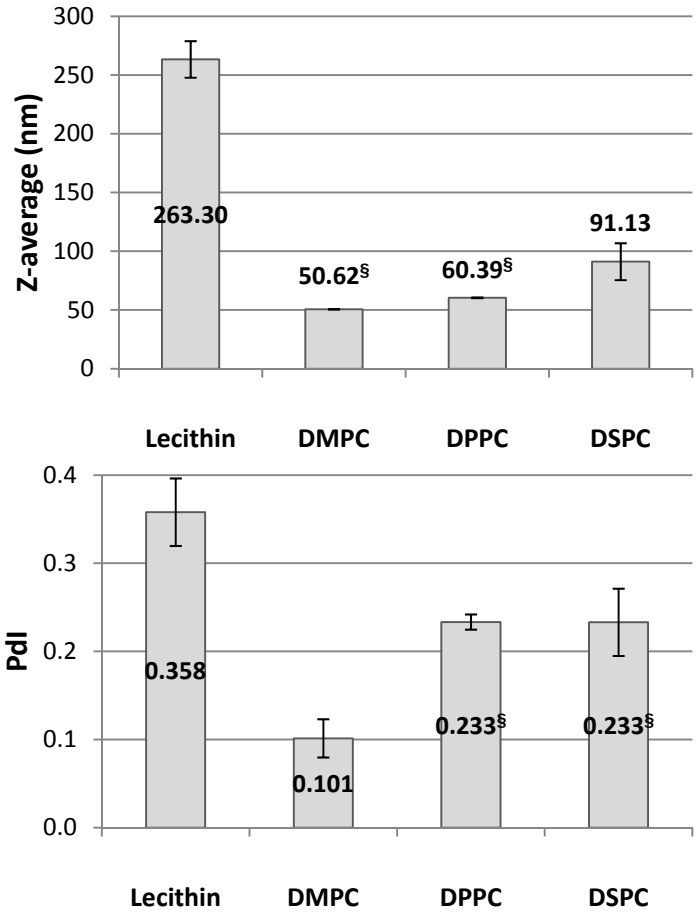

Figure 5.3 – Z-average and PdI values of aqueous dispersions of CoQ_{10} following 50 passes in the microfluidizer. Results are expressed as means ± standard deviations (n = 3). Some standard deviations are too small to be visible (n = 3). § Not statistically different.

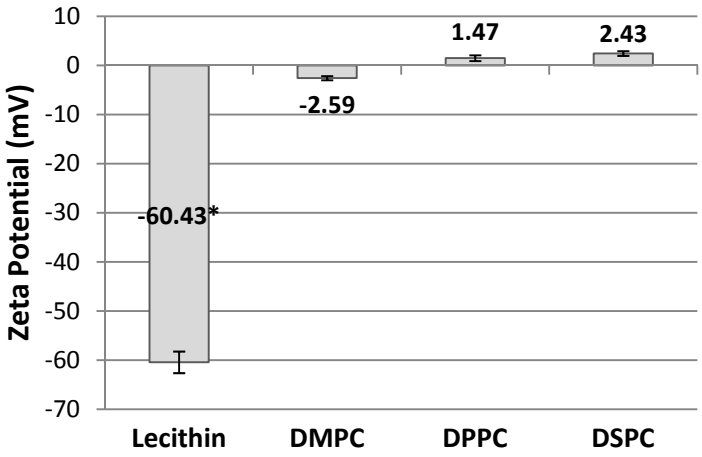

Figure 5.4 – Zeta potential of CoQ_{10} dispersions. Results are expressed as means ± standard deviation (n = 3).* $P < 0.05$ when compared to synthetic phospholipids.

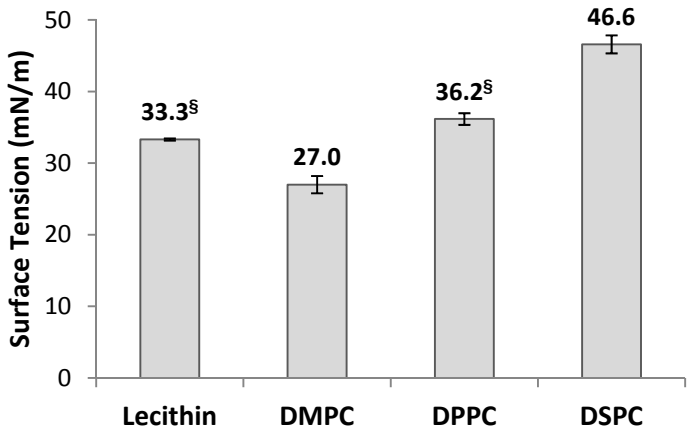

Figure 5.5 – Surface tension of CoQ_{10} dispersions. Results are expressed as means ± standard error ($n \geq 5$). The temperature values during measurement were 25ºC, 25ºC, 19ºC and 17ºC, respectively. § Not statistically different.

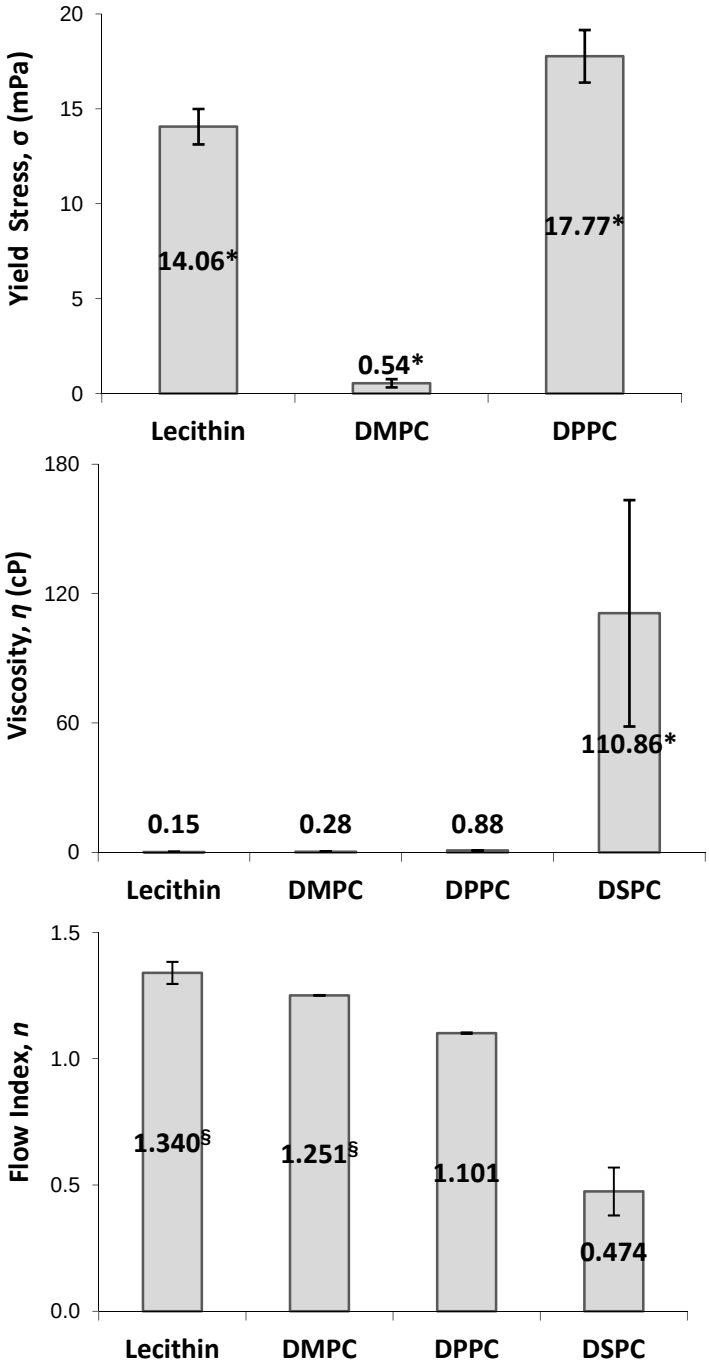

Figure 5.6 – Elements of Herschel-Bulkley model for aqueous dispersions of CoQ_{10}, expressed as means ± standard deviations (n = 3). Yield stress of DSPC formulation is not presented because it follows Power Law model. Some standard deviations are too small to be visible. * $P < 0.05$. § Not statistically different.

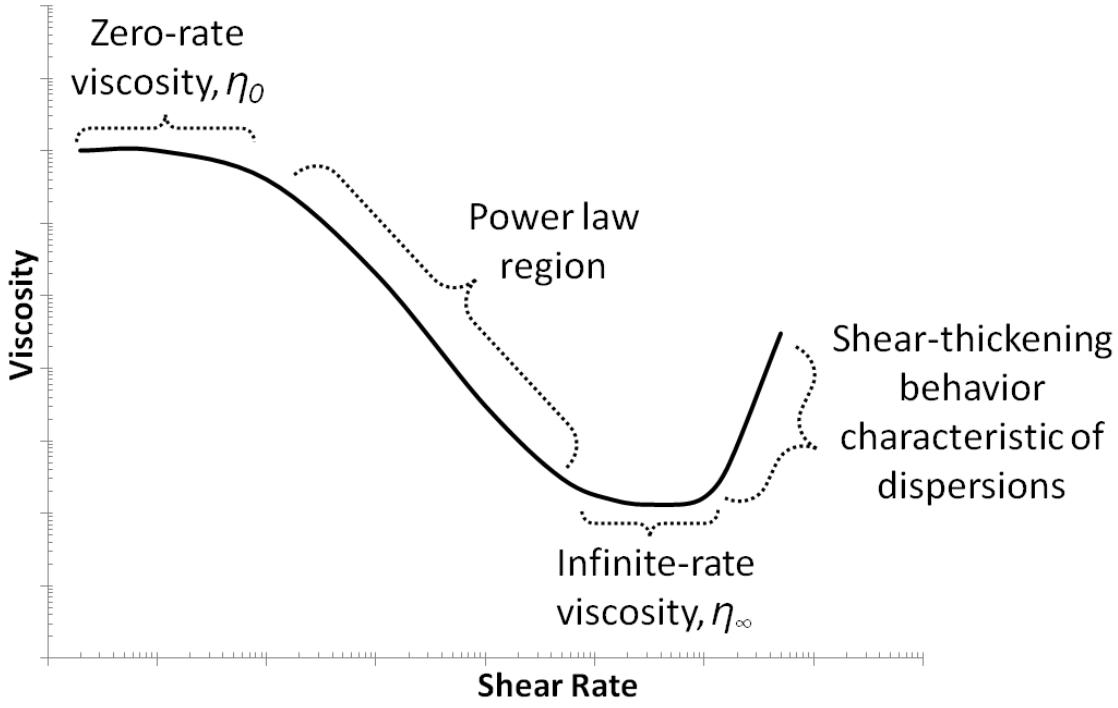

Figure 5.7 – General flow curve of aqueous dispersions. Adapted from ref. [19].

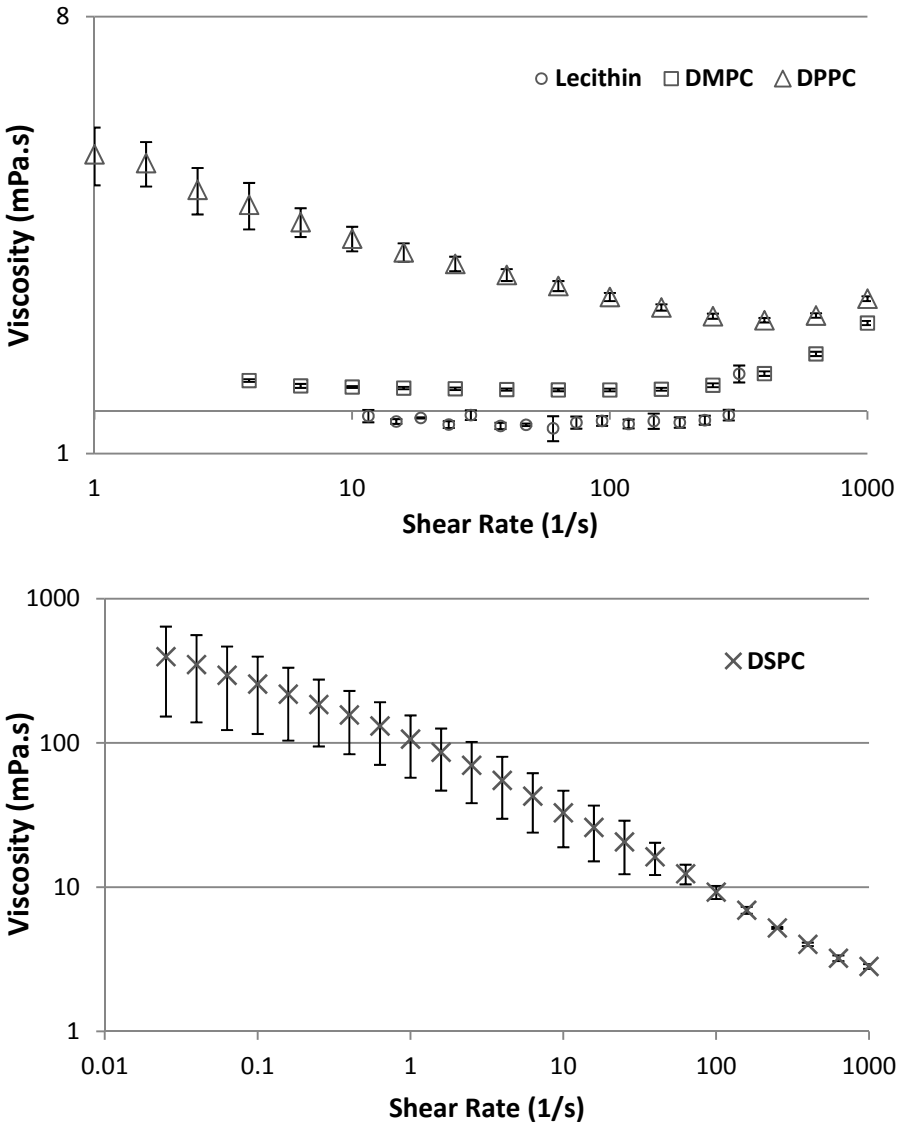

Figure 5.8 – Rheological behavior of CoQ_{10} dispersions. Graphs presented in different scales are expressed as means ± standard deviations (n = 3).

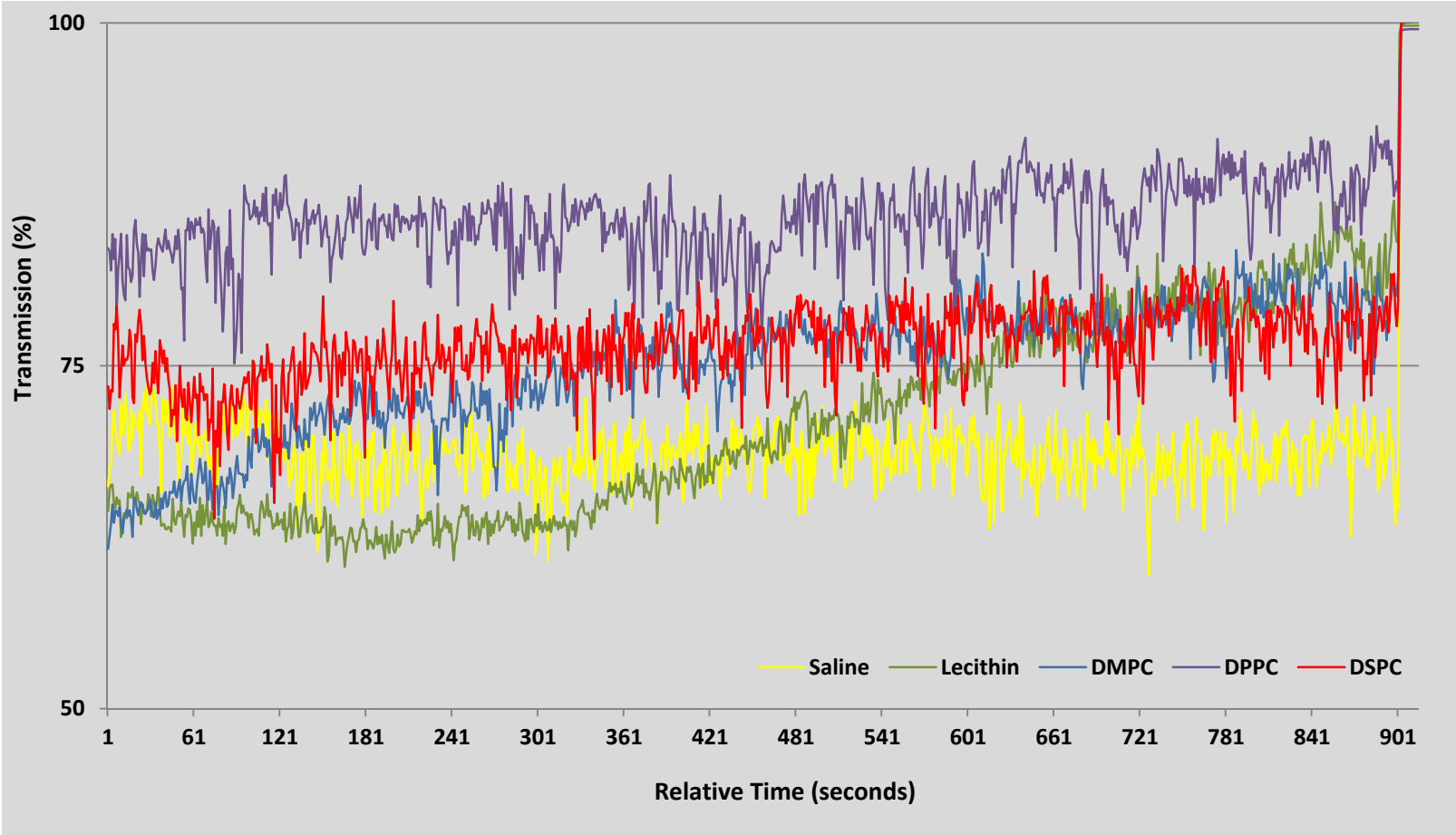

Figure 5.9 – Transmittograms of saline (control) and lecithin, DMPC, DPPC and DSPC dispersions of CoQ_{10}. Results are expressed as means (n = 3) of percentage transmission relative to nebulization of CoQ_{10} dispersions for15 minutes. The slope values from the linear regression analysis of the curves are evaluated as measurement of steadines in aerosol production.

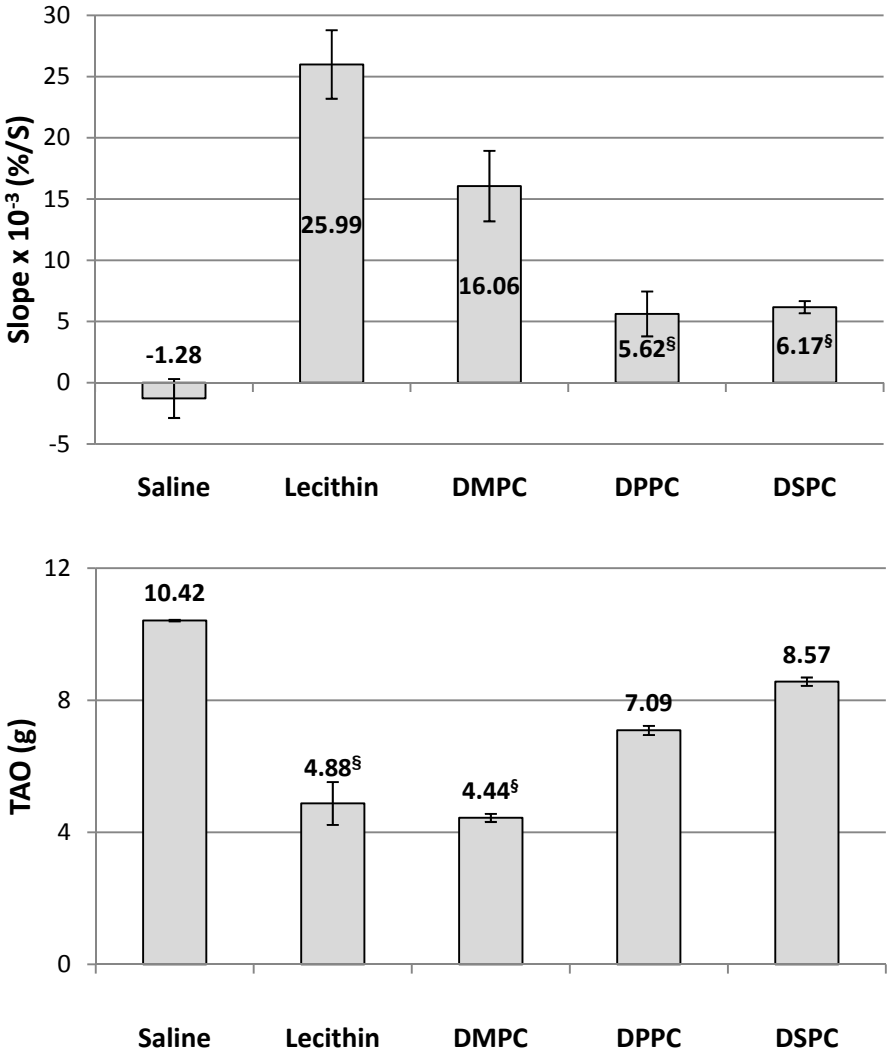

Figure 5.10 – Slope of transmittograms (top) and Total Aerosol Output, TAO (bottom), expressed as means ± standard deviations (n = 3) relative to nebulization of CoQ_{10} dispersions for15 minutes. § Not statistically different.

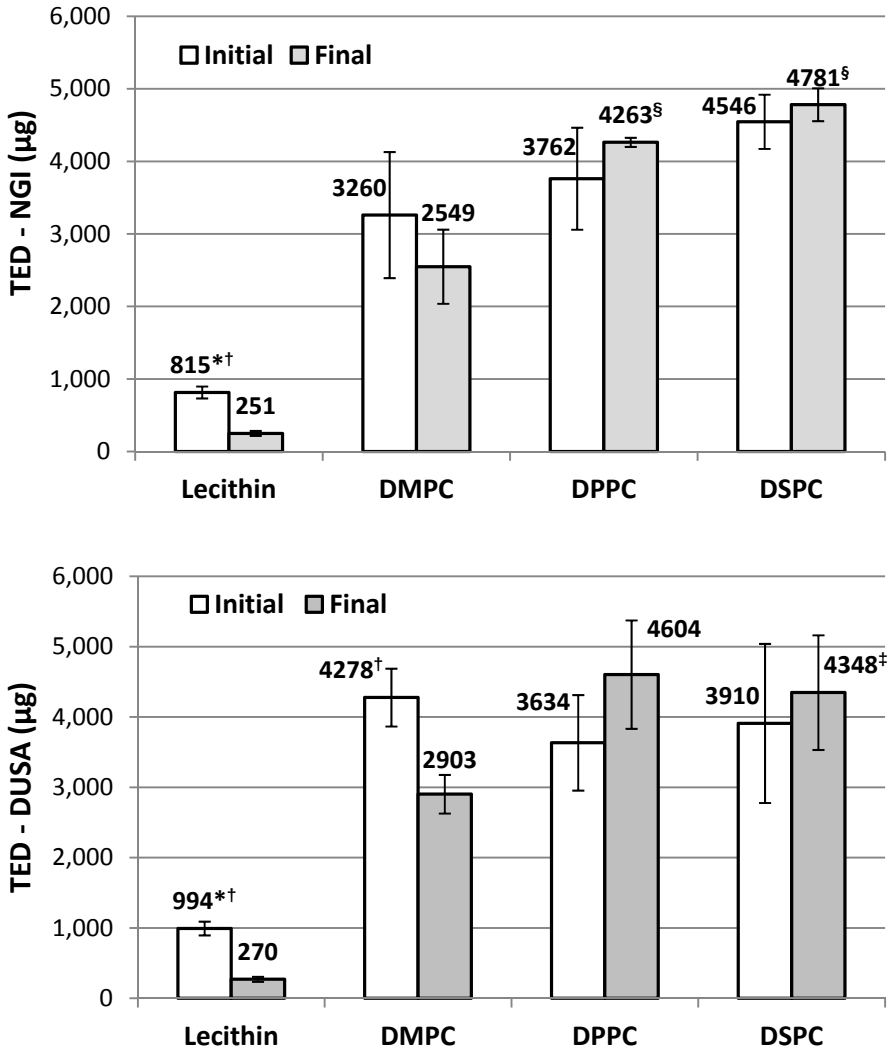

Figure 5.11 – TED from NGI (top) and from DUSA for DPI adapted for nebulizers (bottom) of dispersions of CoQ_{10}. Results are expressed as means ± standard deviations (n = 3) of total drug deposited within a 15 second period at initial and final phases of a 15-minute nebulization event. TED: Total Emitted Dose; DUSA: Dose Uniformity Sampling Unit; DPI: Dry Powder Inhaler. * $P < 0.05$ when compared to synthetic phospholipids. † $P < 0.05$ within nebulization event. § Not statistically different compared to each other. ‡ Not statistically different compared to other synthetic phospholipids.

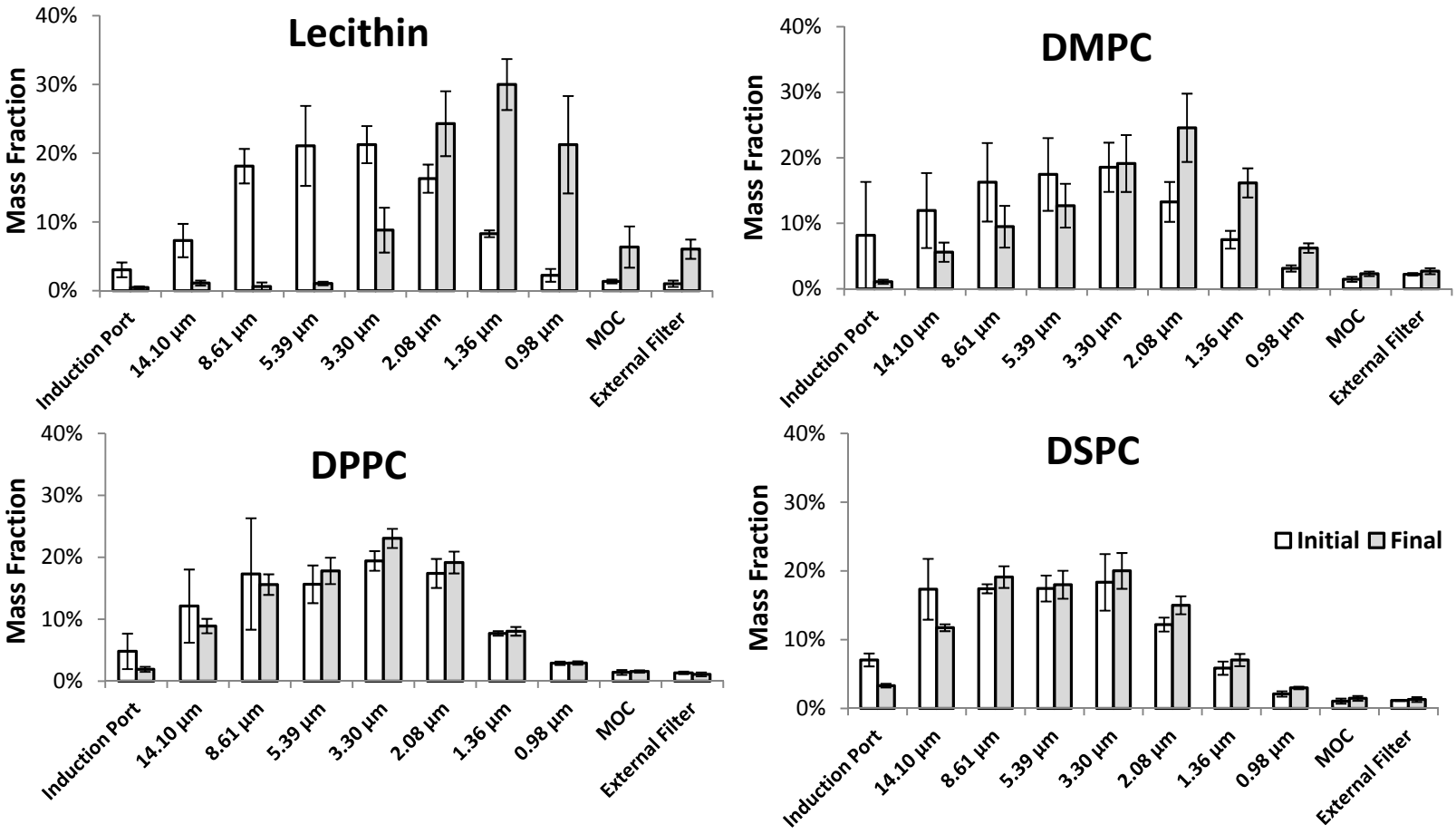

Figure 5.12 – *In vitro* deposition profiles of lecithin, DMPC, DPPC and DSPC dispersions of CoQ_{10} at a flow rate of 15 L/min using an Aeroneb Pro® nebulizer. Results are expressed as means ± standard deviations (n = 3) of the percentage of total drug deposited within a 15-second period at initial and final phases of a 15-minute nebulization event.

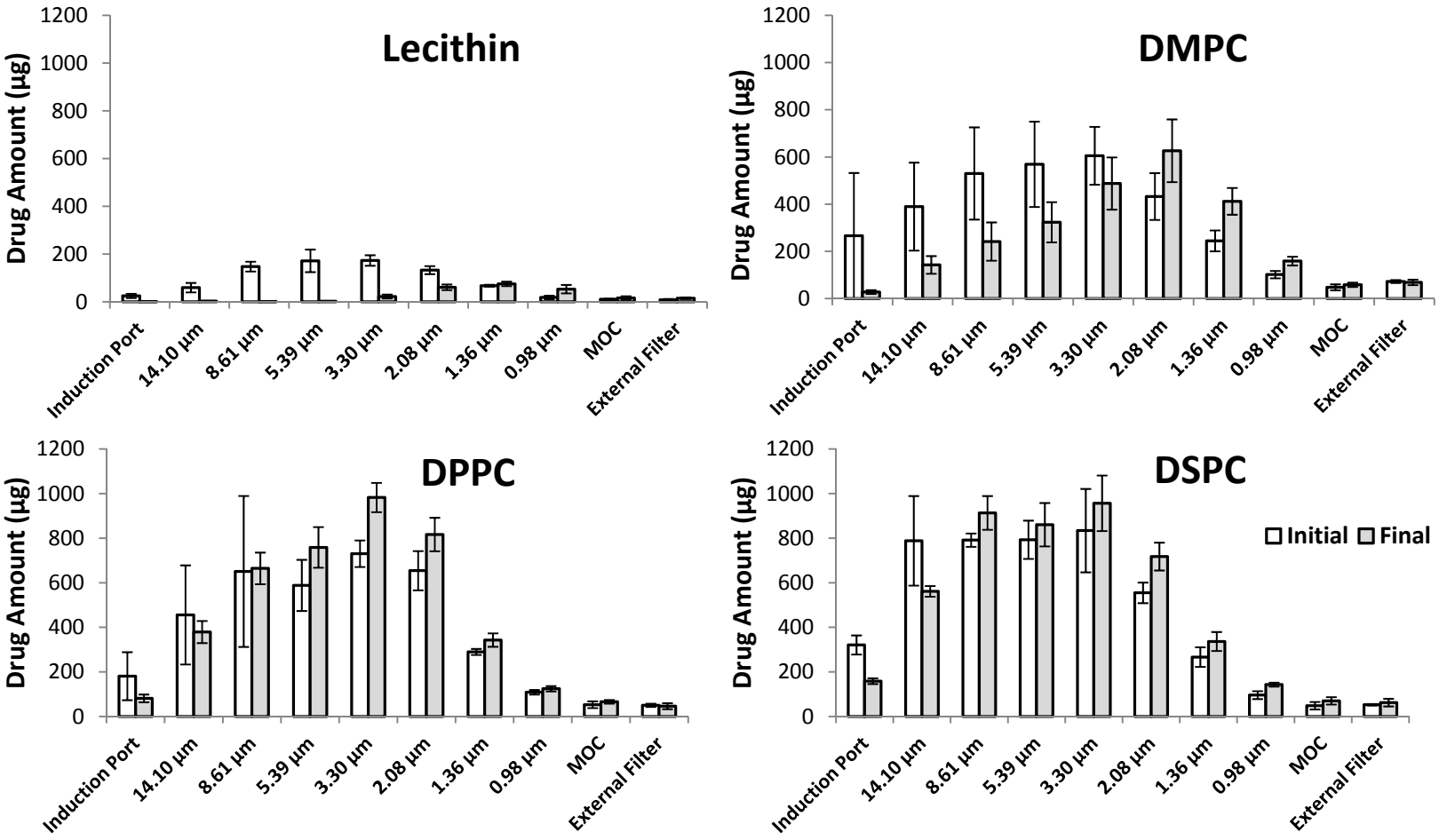

Figure 5.13 – *In vitro* deposition profiles of lecithin, DMPC, DPPC and DSPC dispersions of CoQ_{10} at a flow rate of 15 L/min using an Aeroneb Pro® nebulizer. Results are expressed as means ± standard deviations (n = 3) of the drug amount deposited within a 15-second period at initial and final phases of a 15-minute nebulization event.

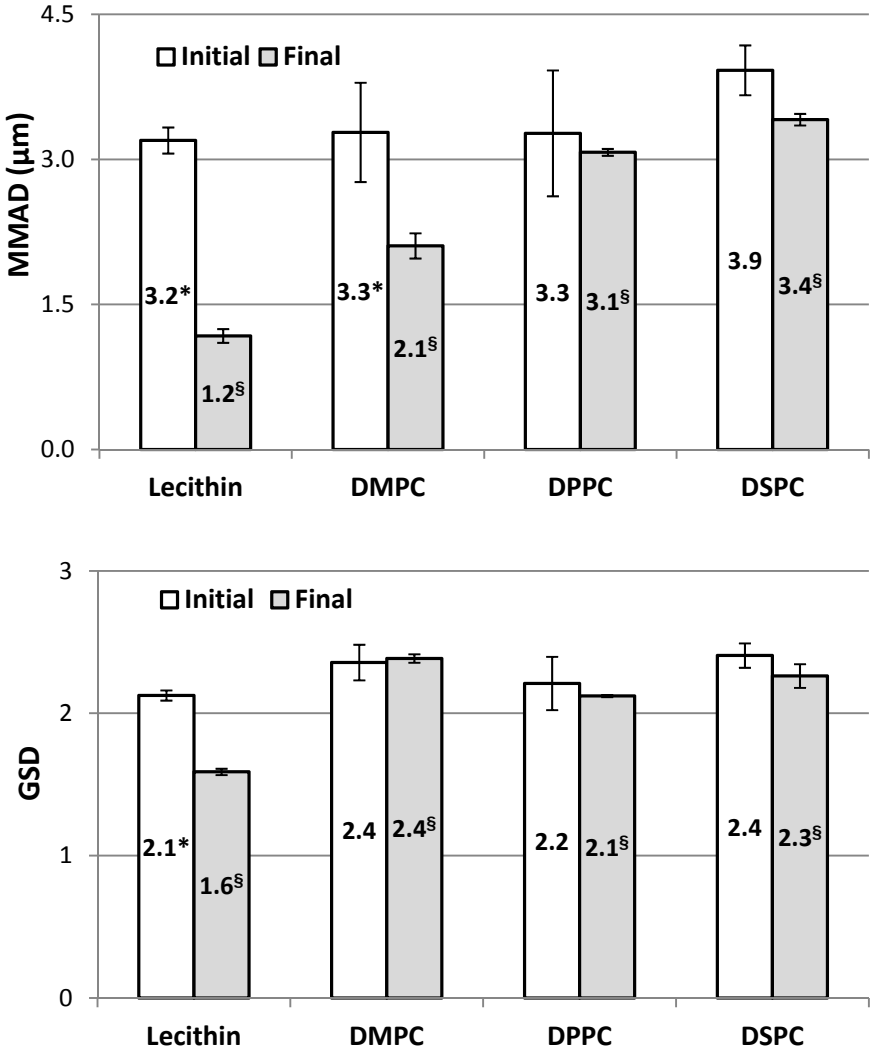

Figure 5.14 – Aerodynamic properties of lecithin, DMPC, DPPC and DSPC dispersions of CoQ_{10} at a flow rate of 15 L/min using an Aeroneb Pro® nebulizer. Results are expressed as means ± standard deviations (n = 3) of MMAD or GSD within a 15-second period at initial and final phases of a 15-minute nebulization event. * $P < 0.05$ within nebulization event. § $P < 0.05$ when compared to each other.

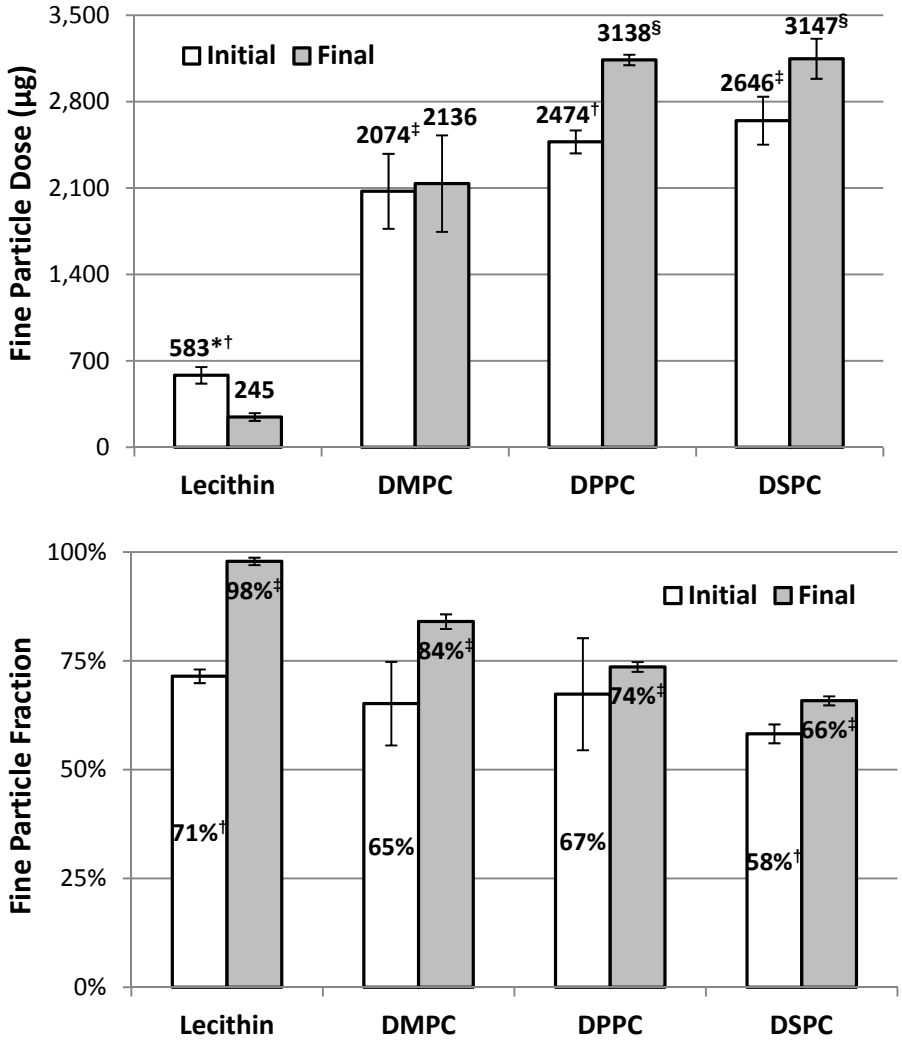

Figure 5.15 – Estimated total dose (FPD_{et}) and fraction (FPF) of aerosolized fine particles from lecithin, DMPC, DPPC and DSPC dispersions of CoQ_{10} at a flow rate of 15 L/min using an Aeroneb Pro® nebulizer. Results are expressed as means ± standard deviations (n = 3) related to a 15-second period at initial and final phases of a 15-minute nebulization event. * $P < 0.05$ when compared to synthetic phospholipids. † $P < 0.05$ within nebulization event. § Not statistically different compared to each other. ‡ $P < 0.05$ when compared to each other.

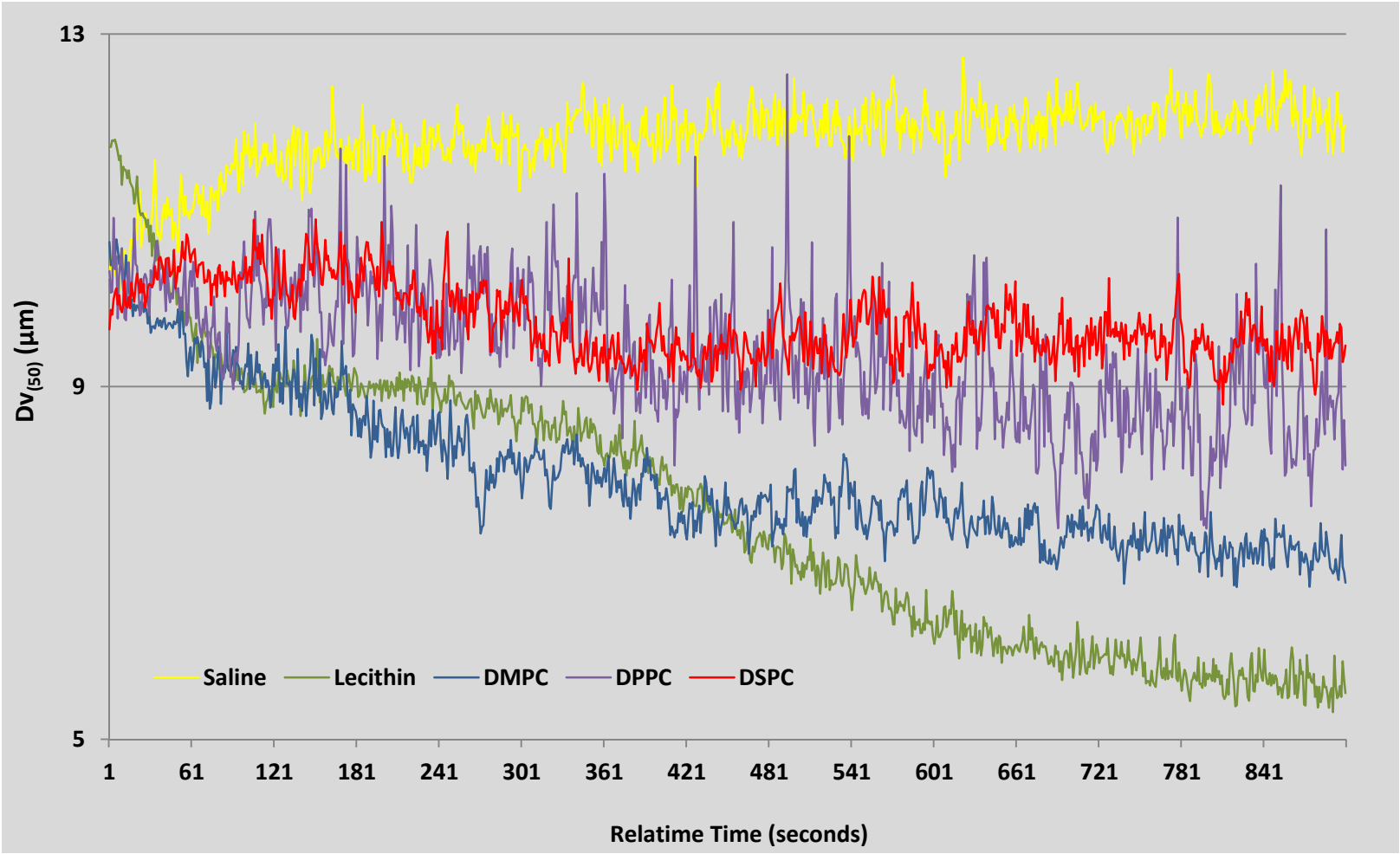

Figure 5.16 – Average $Dv_{(50)}$ of CoQ_{10} dispersions aerosolized using Aeroneb Pro® nebulizer for 15 minutes (n = 3).

5.7. REFERENCES

[1] Mitchell JP, Nagel MW. Cascade impactors for the size characterization of aerosols from medical inhalers: Their uses and limitations. J Aerosol Med-Depos Clear Eff Lung. 2003;16(4):341-+.

[2] Mitchell JP, Tservistas M. Laser diffractometry and cascade impaction for nebulizer product characterization. Pharmeuropa Scientific Notes. 2006;2006(2):49-52.

[3] Mitchell JP, Nagel MW, Nichols S, Nerbrink O. Laser diffractometry as a technique for the rapid assessment of aerosol particle size from inhalers. J Aerosol Med-Depos Clear Eff Lung. 2006;19(4):409-33.

[4] Mitchell J, Bauer R, Lyapustina S, Tougas T, Glaab V. Non-impactor-Based Methods for Sizing of Aerosols Emitted from Orally Inhaled and Nasal Drug Products (OINDPs). AAPS PharmSciTech. 2011;12(3):965-88.

[5] USP. <1601> Products for Nebulization - Characterization Tests. 2011.

[6] Bittar EE. Alveolar Surfactant. *Pulmonary biology in health and disease*. New York, NY, USA: Springer 2002:44-63.

[7] Wu YZ, Wang T. Soybean lecithin fractionation and functionality. J Am Oil Chem Soc. 2003 Apr;80(4):319-26.

[8] Wu YZ, Wang T. Phospholipid class and FA compositions of modified soybeans processed with two extraction methods. J Am Oil Chem Soc. 2003 Feb;80(2):127-32.

[9] Jin YL, Chen JY, Xu L, Wang PN. Refractive index measurement for biomaterial samples by total internal reflection. Phys Med Biol. 2006;51(20):N371-N9.

[10] Rottier BL, van Erp CJP, Sluyter TS, Heijerman HGM, Frijlink HW, de Boer AH. Changes in Performance of the Pari eFlow (R) Rapid and Pari LC Plus (TM) during 6 Months Use by CF Patients. Journal of Aerosol Medicine and Pulmonary Drug Delivery. 2009;22(3):263-9.

[11] Smart J, Berg, E., Nerbrink, O., Zuban, R., Blakey, D., New, M. TouchSpray™ Technology: Comparison of the Droplet Size Measured with Cascade Impaction and Laser Diffraction. In: Dalby RN, Byron, P. R., Peart, J., Farr, S. J., editor. Respiratory Drug Delivery VIII; 2002; Tucson, AZ, USA: Virginia Commonwealth University, Richmond, VA, USA; 2002. p. 525-8.

[12] USP. <601> Aerosols, Nasal Sprays, Metered-Dose Inhalers, and Dry Powder Inhalers. In: Pharmacopoeia US, ed. 2010.

[13] Berg E, Svensson JO, Asking L. Determination of nebulizer droplet size distribution: A method based on impactor refrigeration. J Aerosol Med-Depos Clear Eff Lung. 2007;20(2):97-104.

[14] Hintze J. NCSS and PASS. released January 29th, 2004 ed. Kaysville, UT, USA: Number Cruncher Statistical Systems 2001.

[15] Imura T, Otake K, Hashimoto S, Gotoh T, Yuasa M, Yokoyama S, et al.. Preparation and physicochemical properties of various soybean lecithin liposomes using supercritical reverse phase evaporation method. Colloids and Surfaces B-Biointerfaces. 2003 Feb;27(2-3):133-40.

[16] Makino K, Yamada T, Kimura M, Oka T, Ohshima H, Kondo T. Temperature-Induced and Ionic Strength-Induced Conformational Changes in the Lipid Head Group Region of Liposomes as Suggested by Zeta-Potential Data. Biophys Chem. 1991 Nov;41(2):175-83.

[17] Shinoda W, DeVane R, Klein ML. Zwitterionic Lipid Assemblies: Molecular Dynamics Studies of Monolayers, Bilayers, and Vesicles Using a New Coarse Grain Force Field. J Phys Chem B. 2010 May;114(20):6836-49.

[18] Lee S, Kim DH, Needham D. Equilibrium and dynamic interfacial tension measurements at microscopic interfaces using a micropipet technique. 2. Dynamics of phospholipid monolayer formation and equilibrium tensions at water-air interface. Langmuir. 2001 Sep;17(18):5544-50.

[19] Barnes HA, Hutton JF, Walters K. Rheology of Suspensions. In: Walters K, ed. *An introduction to rheology*. Amsterdam, The Netherlands: Elsevier 1989:115-37.

[20] Rao MA. Flow and Functional Models for Rheological Properties of Fluid Foods. In: Rao MA, ed. *Rheology of fluid and semisolid foods: principles and applications*. 2nd ed. New York, NY: Springer 2007:27-58.

[21] Giboreau A, Cuvelier G, Launay B. Rheological Behaviour of Three Biopolymer/Water Systems, with Emphasis on Yield Stress and Viscoelastic Properties. J Texture Stud. 1994;25(2):119-38.

[22] Launay B, Doublier JL, Cuvelier G. Flow Properties of Aqueous Solutions and Dispersions of Polysaccharides. In: Mitchell JR, Ledward DA, eds. *Functional Properties of Food Macromolecules*. London ; New York, N.Y: Elsevier Applied Science Publishers 1986:1-78.

[23] Packhaeuser CB, Lahnstein K, Sitterberg J, Schmehl T, Gessler T, Bakowsky U, et al.. Stabilization of Aerosolizable Nano-carriers by Freeze-Drying. Pharm Res. 2009 Jan;26(1):129-38.

[24] Elhissi A, Gill H, Ahmed W, Taylor K. Vibrating-mesh nebulization of liposomes generated using an ethanol-based proliposome technology. J Liposome Res. 2011 Jun;21(2):173-80.

[25] Ghazanfari T, Elhissi AMA, Ding Z, Taylor KMG. The influence of fluid physicochemical properties on vibrating-mesh nebulization. Int J Pharm. 2007;339(1-2):103-11.

[26] Watts AB, Cline AM, Saad AR, Johnson SB, Peters JI, Williams RO. Characterization and pharmacokinetic analysis of tacrolimus dispersion for nebulization in a lung transplanted rodent model. Int J Pharm. 2010;384(1-2):46-52.

[27] Tam JM, McConville JT, Williams RO, Johnston KP. Amorphous Cyclosporin Nanodispersions for Enhanced Pulmonary Deposition and Dissolution. J Pharm Sci. 2008 Nov;97(11):4915-33.

[28] McConville JT, Overhoff KA, Sinswat P, Vaughn JM, Frei BL, Burgess DS, et al.. Targeted high lung concentrations of itraconazole using nebulized dispersions in a murine model. Pharm Res. 2006 May;23(5):901-11.

[29] Bouwman AM, Heijstra MP, Schaefer NC, Duiverman EJ, LeSouef PN, Devadason SG. Improved efficiency of budesonide nebulization using surface-active agents. Drug Delivery. 2006 Sep-Oct;13(5):357-63.

Chapter 6: Pulmonary Deposition and Systemic Distribution in Mice of Inhalable Formulations of Coenzyme Q_{10}

Abstract

Coenzyme Q_{10} (CoQ_{10}) is a poorly-water soluble compound that is being investigated for the treatment of carcinomas. *In vitro* deposition studies of the aerodynamic properties of dispersions prepared with synthetic phospholipids have shown that high doses of this anticancer agent may potentially be delivered to the lungs. The aim of the research presented in this chapter was to investigate systemic distribution along with lung and nasal depositions in mice following single-dose pulmonary delivery of CoQ_{10} formulations prepared with synthetic phospholipids. An Aeroneb Pro® vibrating-mesh nebulizer was used to generate aerosols into a nose-only inhalation chamber. Following calculation of the estimated dose delivered, the drug concentration in the blood plasma, lung tissue, and nasal cavity was analyzed. The estimated doses delivered were 166.2, 229.1 and 226.9 mg/kg of mouse body weight for DMPC, DPPC, and DSPC dispersions of CoQ_{10}, respectively. For up to 48 hours, high drug concentrations were found in the lungs while no quantifiable levels of CoQ_{10} were observed in the blood plasma. The drug deposition in the nasal cavity up to one hour post dosing was lower than that which was measured in the lungs. These findings suggest that exogenous CoQ_{10} clears slowly from mouse lungs when high amounts are delivered.

6.1. INTRODUCTION

In the work described in earlier chapters, the feasibility of preparing phospholipid-stabilized dispersions for potential pulmonary delivery has been explored. By direct administration to the lung, it was anticipated that high doses of this anticancer agent could be deposited using an Aeroneb Pro® vibrating-mesh nebulizer. We had also

discussed the influence of the physicochemical properties of the dispersions of CoQ_{10} on the aerosolization profile. As described in the previous chapter, the rheology of dispersions at high shear rates may be indicative of the aerosolization profile (nebulization performance and *in vitro* drug deposition). Dipalmitoyl phosphatidylcholine (DPPC) and distearoyl phosphatidylcholine (DSPC) dispersions were shown to demonstrate continuous and steady aerosolization over time. Each dispersion displayed comparably high amounts of respirable doses of CoQ_{10}, exhibiting potential to be delivered effectively to the deep lungs. The dimyristoyl phosphatidylcholine (DMPC) dispersion showed a lower Fine Particle Dose (FPD) comparatively to the other synthetic phospholipids, but a significantly higher FPD compared with the lecithin formulation.

The aim of the study presented in this chapter was to evaluate the *in vivo* systemic distribution, lung, and nasal depositions in mice following pulmonary delivery of CoQ_{10} formulations prepared with synthetic phospholipids. Three synthetic phospholipids were selected to stabilize these dispersions because of their physiological occurrence in the lungs, these were: DMPC, DPPC and DSPC. Due to the low *in vitro* deposition profile of the model excipient lecithin, compared with those displayed with the synthetic phospholipids, the lecithin formulation was not selected for use in the animal study. The animal dosing apparatus consisted of a nose-only inhalation chamber with aerosol generated from an Aeroneb Pro® vibrating-mesh nebulizer.[1-3] A high and sustained dose of CoQ_{10} into the mice's lungs was achieved, which varied from 1.8 to 3.0% of the theoretical exposure.

6.2. MATERIALS AND METHODS

6.2.1. Materials

CoQ_{10} was supplied by Asahi Kasei Corp. (Tokyo, Japan). Genzyme Pharmaceuticals (Liestal, Switzerland) provided 1,2-dimyristoyl-sn-glycero-3-phosphocholine (DMPC), 1,2-dipalmitoyl-sn-glycero-3-phosphocholine (DPPC), and 1,2-distearoyl-sn-glycero-3-phosphocholine (DSPC). DMPC was also obtained from Lipoid GmbH (Ludswighafen, Germany). Sodium chloride (crystalline, certified ACS) was acquired from Fisher Chemical (Fisher Scientific, Fair lawn, NJ, USA) and the deionized water was obtained from a central reverse osmosis/demineralizer system commonly found in research laboratories. Mouse restraint tubes (item E2QY-PC), anterior nose inserts (item E2TE-N) and posterior holders (item E2TA-N) were purchased from Battelle Toxicology Northwest (Richland, WA, USA). A fan (12V, 0.10A, model OD4020-12HB) was purchased from Knight Electronics (Dallas, TX, USA). HPLC grade hexane and ethanol 200 proof were purchased from Sigma-Aldrich (St. Louis, MO, USA). Syringes (1 mL) and needles (gauges 21G1 and 23G1) were obtained from Becton Dickinson (Franklin Lakes, NJ, USA). Heparinized tubes (1.3 mL microtubes Lithium Heparin (LH) with screw cap closure, product no. 41.1393.105) were purchased from Sarstedt AG & Co. (Numbrecht, Germany). Microcentrifuge tubes (1.5 mL, clear, RNase/DNase free, BL3152) were obtained from Bio-Link Scientific, LLC (Wimberley, TX, USA).

6.2.2. Formulation

Formulations were prepared using high pressure homogenization as described in the previous chapter. In brief, following overnight hydration while stirring, a

phospholipid dispersion containing 2.5% w/w of phospholipids (DMPC, DPPC, or DSPC) in water was added to the molten CoQ_{10} (4% w/w) at 55 °C. The formulation was then predispersed, using an Ultra-Turrax® TP 18/10 Homogenizer with 8 mm rotor blade, by high shear mixing (IKA-Werke, Staufen, Germany) for 5 minutes at 20,000 rpm. Subsequently, the formulation was passed 50 times through a M-110P "Plug-and-Play" Bench-top Microfluidizer® (Microfluidics, Newton, MA USA) at approximately 30,000 psi while maintaining the temperature between 55 and 65 °C. Following microfluidization, 0.9% w/v of sodium chloride was added to the final formulation. A formulation for the control group was similarly prepared using DPPC in absence of drug (CoQ_{10} was not added).

6.2.3. Pulmonary Delivery to Mice

The protocol for this animal study was approved by the Institutional Animal Care and Use Committee (IACUC) at the University of Texas at Austin, Austin, TX. Animals were caged in groups of 4, and maintained on a normal rodent chow diet with free access to water. A nose-only chamber apparatus capable of dosing six mice at a time was assembled according to Figure 6.1.[1-3] Prior to dosing, CD-1® IGS ICR mice (Charles River Laboratories International, Inc., Wilmington, MA, USA) were individually acclimatized for approximately 10 minutes per day for 3 days into restraint tubes, restricted by an anterior nose insert and a posterior holder. The dosing apparatus was placed inside a fume hood to collect escaping aerosol containing drug. To avoid influence from the airflow provided by the fume hood, an erlenmeyer container was placed at the end of the tubing system (as an air buffer). The airflow rate was set to 1 L/min to ensure proper drug aerosolization into the nose-only chamber (internal volume: 230 mL;

diameter: 3.8 cm; length: 20.3 cm) using an Aeroneb Pro® vibrating-mesh nebulizer (Aerogen, Galway, Ireland). Following preparation, all formulations (saline control, DMPC, DPPC, or DSPC) were dosed for 15 minutes to mice weighing from 23 to 33g each, at time of dosing. Each single-dose studied group consisted of thirty-six male animals. At each time point (0.5, 1, 3, 8, 24, and 48 hours after the end of the aerosolization event) six animals randomly selected from different dosing events of the same formulation were sacrificed by narcosis with carbon dioxide. As part of the collection process, blood was withdrawn by cardiac puncture, lungs were harvested, and a nasal wash was performed. The samples were extracted for analysis with liquid chromatography coupled with tandem mass spectrometry (LC/MS/MS).

6.2.3.1. Estimated Dose

To estimate the dose to which mice were exposed during this study, it was assumed that the nose-only chamber gradually fills with the aerosol containing CoQ_{10}. Therefore, the drug concentration steadily increases until it reaches a plateau. At steady-state, it is also assumed that the rate of drug entering the chamber is equal to the rate of drug leaving the chamber (dC/dt=0). Therefore, the following equation can be used to measure the drug concentration inside the chamber at any given time:

$$C = \frac{FPD_r}{F} \cdot \left(1 - e^{-\lambda \cdot t}\right) \qquad \text{(Equation 6.1)}$$

Where C is the drug concentration, FPD_r is the rate of delivery of the Fine Particle Dose (the amount of particles with aerodynamic cutoff diameter below 5.39 μm per minute) as determined in the previous chapter, F is the airflow rate, λ is the chamber

air-change rate and *t* is any given time within the nebulization period. The chamber air-change rate, λ, can be determined based on the airflow rate and on the chamber internal volume, *V*, as follows:

$$\lambda = \frac{F}{V} \qquad \text{(Equation 6.2)}$$

Based on these assumptions, the following equation describes the estimated dose delivered to mice:

$$Estimated\ Dose\ = RMV \cdot \frac{FPD_T}{F} \cdot \left\{ t' + \frac{V}{F} \cdot \left[\left(e^{-\lambda \cdot t'} \right) - 1 \right] \right\} \qquad \text{(Equation 6.3)}$$

Where *RMV* is the species-specific Rate Minute Volume and *t'* is the duration of the nebulization event. The estimated dose as calculated above can then be normalized by the animal body weight, *W (g)*. RMV is calculated as previously reported:[4]

$$RMV = 4.19 \cdot W^{0.66} \qquad \text{(Equation 6.4)}$$

6.2.4. Analysis of CoQ_{10} Levels in Lung Tissue, Blood Plasma, and Nasal Cavity

The analyses were performed according to an internal protocol from Berg Diagnostics (Natick, MA, USA). Briefly, the method was validated in the drug concentration range of 0.1 to 600 µg/mL. Following liquid extraction, CoQ_{10} levels were determined using liquid chromatography coupled with tandem mass spectrometry (LC-MS/MS).

Following harvesting of the mice's lungs, the tissue was weighed (wet weight) and subsequently frozen in dry ice, where it was kept until transference to a -80ºC refrigerator for storage prior to analysis. Following sample thawing at time of analysis, lung tissue (50 ± 1.5 mg) was weighed and subsequently homogenized with Dulbecco's Phosphate Buffer Saline (dPBS). Homogenate (100 μL) and internal standard were added to isopropanol (IPA) and the sample vortexed. Following centrifugation, the supernatant (100 μL) was added to another tube containing IPA. The sample was vortexed again and transferred to LC-MS/MS vial for analysis.

Following cardiac puncture, approximately 1 mL of mice blood was collected in heparinized tubes and kept in ice bath until centrifugation for 10 minutes at 7000g. The supernatant was then transferred to 1.5 mL microcentrifuge tubes and kept refrigerated at -80ºC until analysis, which was similar to the described procedure for lung tissue.

To evaluate the amount of drug deposited into the nasal cavity, a solvent wash was performed. The mice nasal cavity was directly accessed from the posterior portion of the hard palate by inserting a needle into the mice nasopharynx and flushing the nasal fossa with hexane:ethanol 2:1 (v/v). The solvent was collected into a scintillation vial from the anterior (frontal) portion of the nose and subsequently allowed to dry at room temperature. The sample was then re-suspended and injected into LC-MS/MS.

6.2.5. Statistical Analysis

Samples were tested for normality using the Shapiro Wilk test ($p < 0.05$) and outliers were excluded from the data analysis. The data is expressed as mean ± standard deviation. Pharmacokinetic parameters were determined using Microsoft Office Excel 2007 software (Redmond, WA) with the add-in program PKSolver.[5] Statistical analysis

was performed using NCSS/PASS software Dawson edition.[6] At each time point, lung tissue samples were analyzed for statistical differences among different groups with One-Way ANOVA for significance ($p < 0.05$). The same analysis was performed for nasal wash samples, with additional *post hoc* multiple comparison tests performed to identify statistically significant differences between treated and control groups using Dunnett's method ($p < 0.05$). A paired *t-test* was performed to analyze statistical differences ($p < 0.05$) within the same treatment group for changes in drug deposition in the nasal cavity over time.

6.3. RESULTS AND DISCUSSION

The drug concentration in the blood plasma and lung deposition profile of the CoQ_{10} dispersions that were previously developed have been determined over time in this study. The investigation has also been extended to determine the drug deposition in the nasal cavity following inhalation. Using an Aeroneb Pro® nebulizer to generate aerosol into a nose-only inhalation chamber, mice were dosed for 15 minutes with control, DMPC, DPPC, and DSPC formulations. The dose delivered to the mice's lungs was estimated based on the FPD_r values as was determined during the *in vitro* characterization of drug deposition using the Next Generation Impactor (NGI), described in the previous chapter.

Figure 6.2 shows the calculated drug concentration-time profile within the nose-only chamber. The plateau is reached at 3.0 minutes and the concentration at steady-state, C_{SS}, is equal to FPD_r since the airflow rate during this experiment was 1 L/min (Table 6.1). The chamber air-change rate was 4.35 min^{-1}. The estimated doses delivered to mice of aerosolized DMPC, DPPC, and DSPC dispersions of CoQ_{10} for 15 minutes increases

in this respective order (Figure 6.3). When normalized to the body weight of animals, similar estimated doses were delivered to mice receiving either DPPC or DSPC formulations. These doses of CoQ_{10} were found to be greater than when the mice were dosed with the DMPC dispersion.

The drug concentration in plasma was below the quantitative level (0.1 μg/mL) for all studied groups at every time point. The baseline concentration of CoQ_{10} in mice blood plasma is approximately 0.1 μmol/L (86 ng/mL).[7-9] In the lungs, the drug concentration was also below the quantitative level for the control group at every time point investigated. It is evident from Figure 6.4 that CoQ_{10} stays in the lungs at relatively high concentrations for up to 48 hours. The mechanism by which CoQ_{10} could be absorbed through the lung epithelium is unknown, but it is known that CoQ_{10} is dependent on multiple carrier-mediated transport mechanisms for absorption through the gastrointestinal tract.[10] In the GI tract, chylomicrons sequester exogenous CoQ_{10} and transfer it to the liver prior to systemic distribution mediated by very low density lipoproteins (VLDL). Despite the lipophilicity of CoQ_{10}, it is believed that passive diffusion is only part of a more complex absorption process involving an additional active and facilitated transport phenomena.[10] The small amount of translocation of the drug from the lungs to the systemic circulation may be in part due to this low permeability. In addition, the dispersions are formulated in the nano-size range. The stealthiness of particles below 0.2-0.5 μm to alveolar macrophages has been extensively reviewed.[11-13] In addition to size, other physicochemical properties of the drug may influence the translocation of nanoparticles across the air-blood barrier; such as particle material, *in vivo* solubility, and binding affinity to cell membranes (e.g. through surface charge and structure).[14, 15] The solubility of CoQ_{10} in water at 20ºC is less than 5 μg/mL.[16] It has been previously shown that phospholipids induce migration of

insoluble particles to the lung periphery of rodents.[17] Therefore, the presence of phospholipids in these formulations may have also caused a greater lung peripheral distribution of the drug nanoparticles. The translocation of insoluble nanoparticles across the air-blood barrier is known to be minimal compared to the long term clearance from the alveoli up to the mucociliary escalator and into the GI tract, which may take weeks.[11, 14] A significant spreading of drug towards the lung periphery due to the presence of phospholipids in the formulations investigated in this study may help in explaining why the clearance of CoQ_{10} from the lungs was not detected after 48 hours and similarly why the drug levels in the plasma were below the quantitative limit.

Additionally, since the drug clearance from the lungs was not significant in the time period studied, the elimination constants and half-lives could not be determined for the nebulized formulations of CoQ_{10} in this study. Other pharmacokinetic parameters are presented in Table 6.2. The lung deposition profiles of aqueous dispersions of CoQ_{10} using different phospholipids presented relatively similar results. The C_{max} ranged from 604.0 to 791.3 μg/g of wet lung tissue, and was observed 1 hour (t_{max}) post dosing for all treated groups. These values translate to approximately 4.0 to 5.0 mg/kg of mouse body weight and correspond to 1.8 to 3.0% of the theoretical exposure dose (Figure 6.5). The $AUC_{0\text{-}48}$ results were surprisingly different; with the DMPC formulation of CoQ_{10} presenting the highest value regardless of whether the smallest estimated dose that the mice were exposed to was presented. Although DPPC and DSPC dispersions of CoQ_{10} presented high estimated dose, their C_{max} and $AUC_{0\text{-}48}$ values varied widely. No statistical differences were found in drug concentration at the same time point among the treated groups (Figures 6.4 and 6.5).

The drug deposition in the nasal cavity was lower than that which was measured in the lungs (Figure 6.6), not exceeding an average of 1.7 mg/kg of mouse body weight

among the treated groups. Only the DPPC group demonstrated a statistically significant decreasing trend for the first two time points investigated. A small amount of CoQ_{10} was observed in the control group, possibly from an endogenous source. Finally, all mice were alive and presenting healthy signs 48 hours after the end the nebulization event. This demonstrates the safety of delivering high amounts of exogenous CoQ_{10} to the lungs.

In the previous chapter, unprecedentedly high doses with potential to reach the lungs based on FPD_{et} results was predicted, with DPPC and DSPC formulations presenting the highest values. These doses are approximately 10 to 40 times greater than itraconazole nanodispersions previously aerosolized using the same type of nebulizer (vibrating-mesh device) and as much as 280 times greater than previous aerosolization of a budesonide suspension (Pulmicort Respule®, AstraZeneca, UK) using a Sidestream® PortaNeb® jet nebulizer (Medic-Aid Ltd., UK).[1, 18, 19] In this study, it was verified that the high doses that mice were exposed to translate into an improved drug deposition into the mice's lungs. C_{max} values of CoQ_{10} were as much as 75-fold and 165-fold higher than previous studies using the same nebulizer to deliver dispersions of cyclosporine A and itraconazole, respectively.[1, 18, 20] This is a significant improvement in deliverance of high amounts of drug to the lungs, considering that the estimated doses in this present study were not proportionally higher to the same extent when comparing to previous reports. We believe that the *in vitro* methods utilized in the experimental design to screen appropriate formulations with optimized potential to deliver high drug amounts to the lungs were essential in achieving these results.

6.4. CONCLUSIONS

Following a single-dose pulmonary delivery, the drug concentration in the blood plasma was below the quantitative level of the validated method and high drug concentrations remained in the lungs for up to 48 hours. The deposition in the nasal cavity was lower than that which was measured in the mice's lungs. The C_{max} and $AUC_{0\text{-}48}$ values were not directly related to the estimated doses at which mice were exposed to during nebulization of CoQ_{10} formulations. The findings in this *in vivo* study indicate that high amounts of exogenous CoQ_{10} can be successfully aerosolized and deposited into the lungs of rodents in a nose-only inhalation chamber. Further studies comprising analysis at longer time points are warranted to determine the elimination rate from lung tissue.

Acknowledgements

We thank Dr. Thomas Leach at MedImmune for his contribution with the calculation of the estimated doses exposed to animals. We also would like to extend this acknowledgement to the staff at the Animal Resource Center (ARC) at The University of Texas at Austin, Austin, TX, for the support given in this animal study, and to Nikunj Tanna and Dr. Shen Luan from Berg Diagnostics for the samples bioanalyses.

6.5. TABLES

Formulation	FPD_r (mg/min)	Mouse weight (g)	RMV (mL/min)	Estimated Dose	
				After 15 minutes of nebulization (mg)	Normalized to body weight (mg/kg)
DMPC	8.420	28.8 ± 1.4	38.50	4.787	166.2
DPPC	11.224	26.1 ± 1.5	36.07	5.980	229.1
DSPC	11.586	29.5 ± 2.0	39.11	6.693	226.9

Results of mouse weight are expressed as mean ± standard deviations (n = 36 per group). *FPD_r* is the rate of delivery of the Fine Particle Dose (the amount of particles with aerodynamic cutoff diameter below 5.39 μm per minute) and *RMV* is the Rate Minute Volume calculated based on 10 mL/kg at 120 breaths per minute.[21]

Table 6.1 – Estimated doses delivered to mice during nebulization of CoQ_{10} dispersions.

Pharmacokinetic Parameter	DMPC	DPPC	DSPC
C_{max} (μg/g wet tissue)	777.7	604.0	791.3
t_{max} (h)	1	1	1
$AUC_{0\text{-}48}$ (mg·h/g)	28.228	21.144	26.830

Table 6.2 – Pharmacokinetic parameters for lung deposition of a single-dose of CoQ_{10} following 15 minutes of nebulization of phospholipid-stabilized dispersions to mice based on non-compartmental analysis of tissue concentration versus time.

6.6. FIGURES

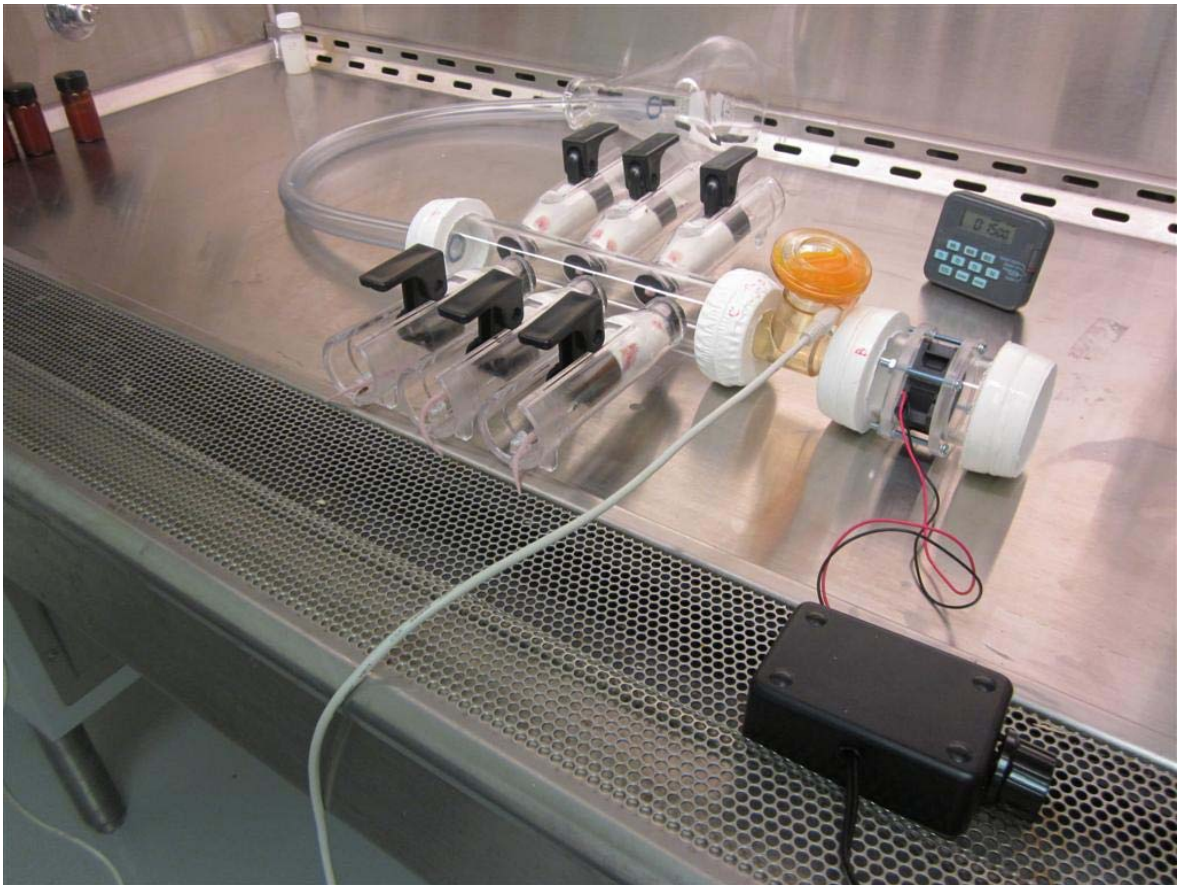

Figure 6.1 – Nose-only dosing apparatus used to aerosolize CoQ_{10} to mice. Six mice are individually restrained in a tube, exposing their noses to the chamber. The nebulizer is positioned between the chamber and the fan that will provide sufficient airflow to fill the chamber with the drug aerosol. The tubing system is open to avoid drug recirculation.

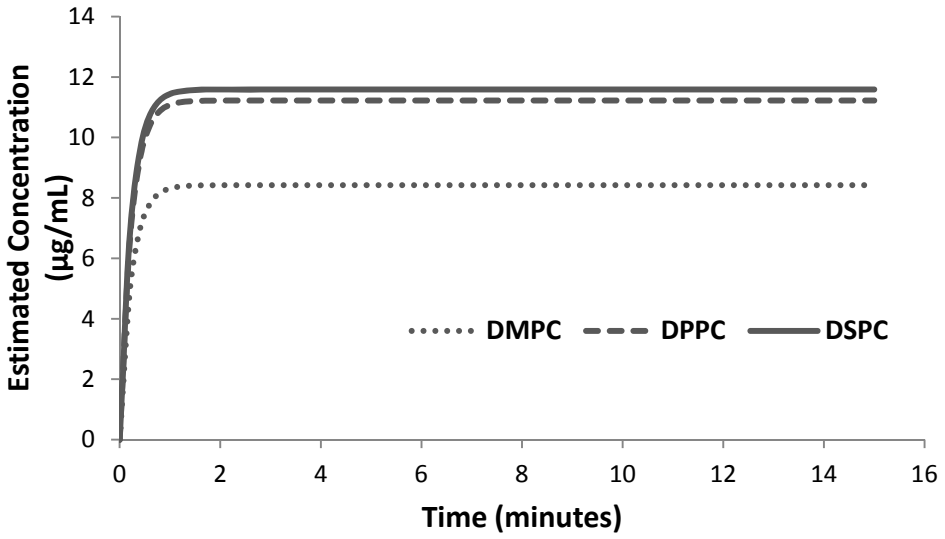

Figure 6.2 – Estimated drug concentration-time profiles of CoQ_{10} inside the nose-only inhalation chamber.

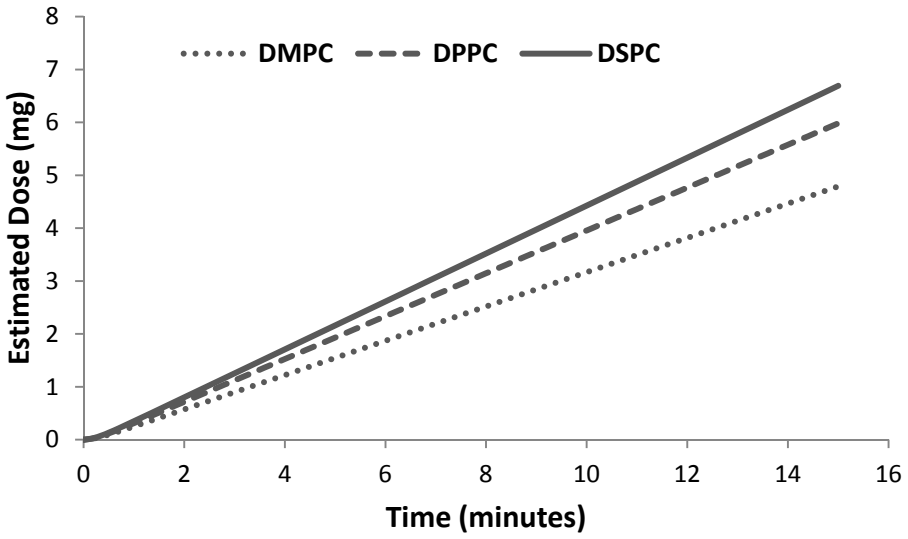

Figure 6.3 – Cumulative estimated doses of CoQ_{10} from synthetic phospholipid formulations aerosolized to mice into a nose-only inhalation chamber during 15 minutes.

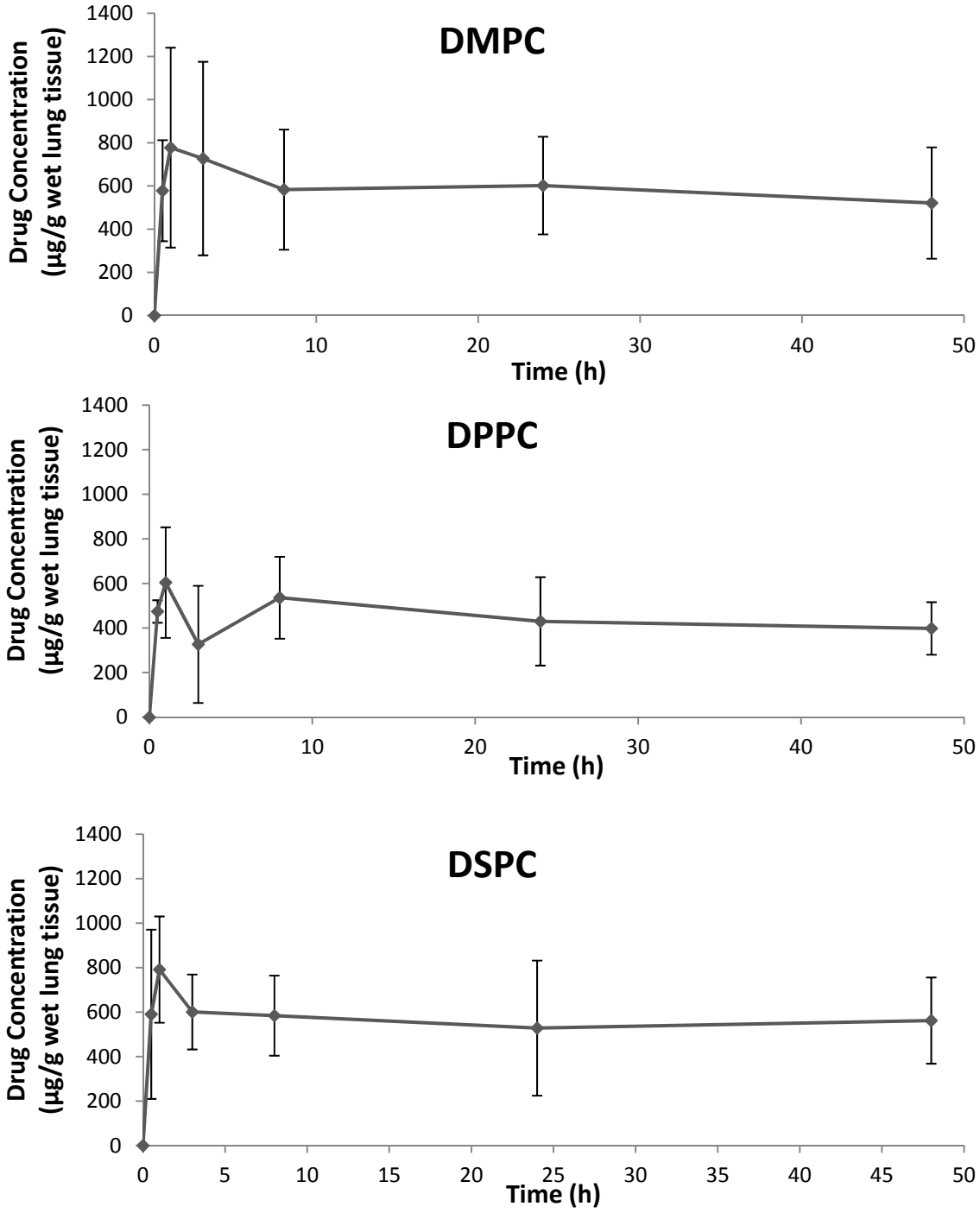

Figure 6.4 – Mean lung concentrations normalized to wet lung tissue of CoQ_{10} from synthetic phospholipid dispersions following aerosolization to mice into a nose-only inhalation chamber during 15 minutes. Error bars indicate standard deviation (n = 6).

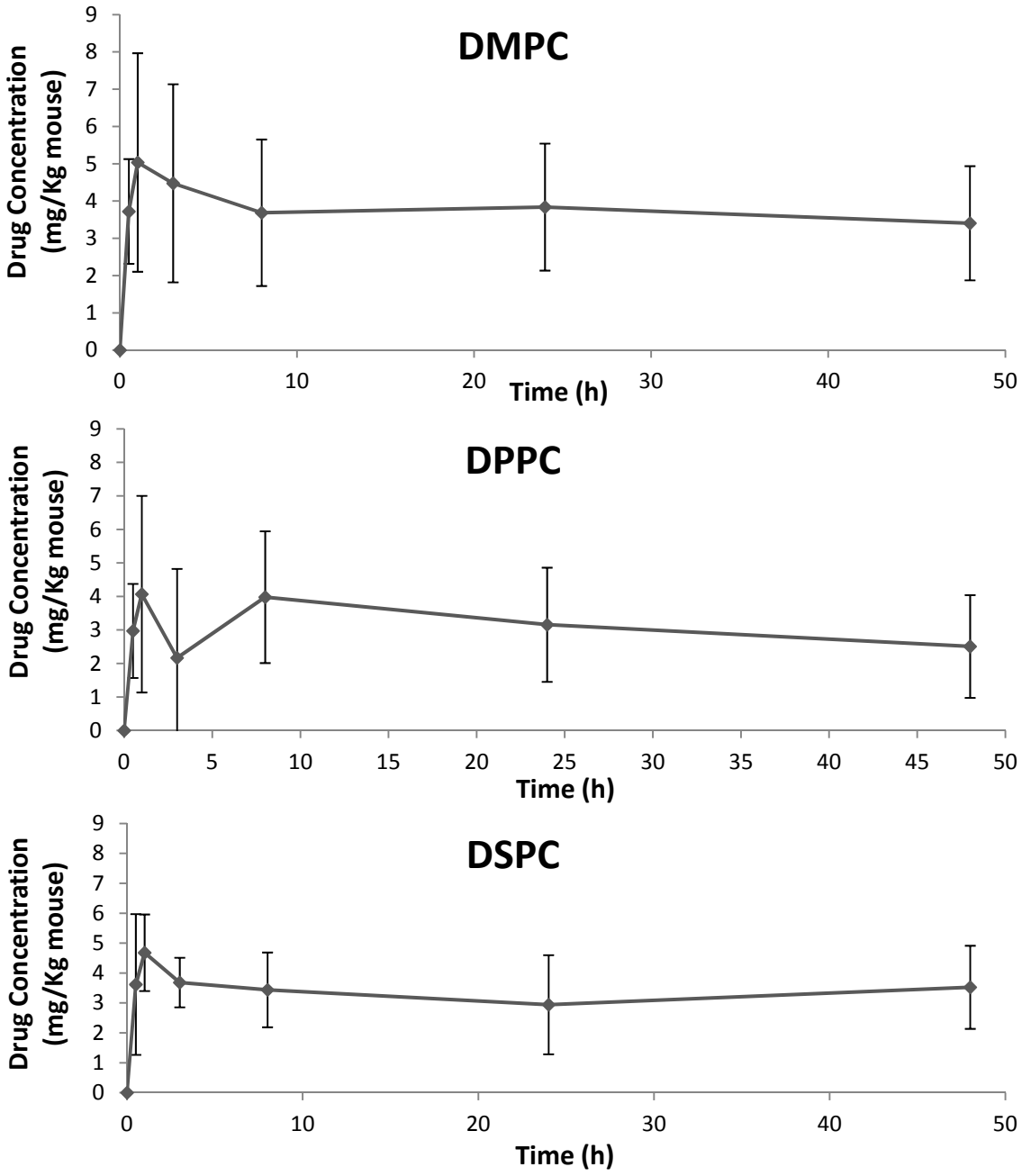

Figure 6.5 – Mean lung concentrations normalized to animal body weight of CoQ_{10} from synthetic phospholipid dispersions following aerosolization to mice into a nose-only inhalation chamber during 15 minutes. Error bars indicate standard deviation (n = 6).

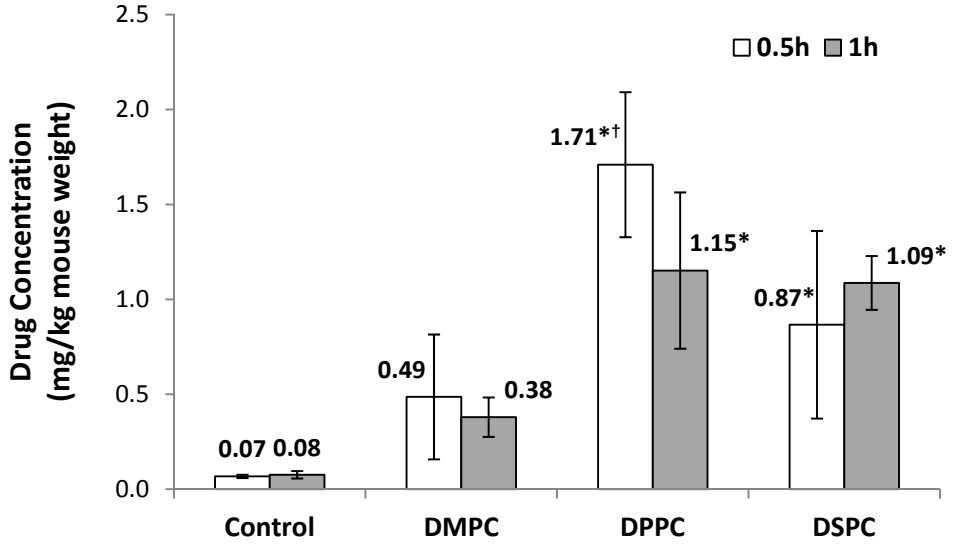

Figure 6.6 – Deposition of CoQ_{10} in the nasal cavity of mice 0.5 and 1 hour post 15-minute nebulizer dosing. Results are expressed as means ± standard deviations (n = 6). * $P < 0.05$ when compared to control group. † $P < 0.05$ when compared within the same group.

6.7. REFERENCES

[1] Tam JM, McConville JT, Williams RO, Johnston KP. Amorphous Cyclosporin Nanodispersions for Enhanced Pulmonary Deposition and Dissolution. J Pharm Sci. 2008 Nov;97(11):4915-33.

[2] Tolman JA, Nelson NA, Son YJ, Bosselmann S, Wiederhold NP, Peters JI, et al.. Characterization and pharmacokinetic analysis of aerosolized aqueous voriconazole solution. Eur J Pharm Biopharm. 2009;72(1):199-205.

[3] Tolman JA, Wiederhold NP, McConville JT, Najvar LK, Bocanegra R, Peters JI, et al.. Inhaled Voriconazole for Prevention of Invasive Pulmonary Aspergillosis. Antimicrob Agents Chemother. 2009;53(6):2613-5.

[4] McMahon TA, Brain, JD, Lemott, S. Species differences in aerosol deposition. Inhaled Particles IV. 1977;International Symposium of The British Occupational Hygiene Society(1):23-33.

[5] Zhang Y, Huo M, Zhou J, Xie S. PKSolver: An add-in program for pharmacokinetic and pharmacodynamic data analysis in Microsoft Excel. Comput Methods Programs Biomed. 2010;99(3):306-14.

[6] Hintze J. NCSS and PASS. released January 29th, 2004 ed. Kaysville, UT, USA: Number Cruncher Statistical Systems 2001.

[7] Witting PK, Pettersson K, Letters J, Stocker R. Anti-atherogenic effect of coenzyme Q10 in apolipoprotein E gene knockout mice. Free Radic Biol Med. 2000;29(3-4):295-305.

[8] Thomas SR, Leichtweis SB, Pettersson K, Croft KD, Mori TA, Brown AJ, et al.. Dietary cosupplementation with vitamin E and coenzyme Q(10) inhibits atherosclerosis in apolipoprotein E gene knockout mice. Arterioscler Thromb Vasc Biol. 2001;21(4):585-93.

[9] Lonnrot K, Alho H, Holm P, Lagerstedt A, Huhtala H. The effects of lifelong ubiquinone Q10 supplementation on the Q9 and Q10 tissue concentrations and life span of male rats and mice. IUBMB Life. 1998;44(4):727-37.

[10] Palamakula A, Soliman M, Khan MMA. Regional permeability of coenzyme Q10 in isolated rat gastrointestinal tracts. Pharmazie. 2005 Mar;60(3):212-4.

[11] Todoroff J, Vanbever R. Fate of nanomedicines in the lungs. Curr Opin Colloid Interface Sci. 2011 Jun;16(3):246-54.

[12] Geiser M, Rothen-Rutishauser B, Kapp N, Schurch S, Kreyling W, Schulz H, et al.. Ultrafine particles cross cellular membranes by nonphagocytic mechanisms in lungs and in cultured cells. Environ Health Perspect. 2005 Nov;113(11):1555-60.

[13] Geiser M. Update on Macrophage Clearance of Inhaled Micro- and Nanoparticles. Journal of Aerosol Medicine and Pulmonary Drug Delivery. 2010 Aug;23(4):207-17.

[14] Geiser M, Kreyling WG. Deposition and biokinetics of inhaled nanoparticles. Part Fibre Toxicol. 2010 Jan;7:17.

[15] Takenaka S, Karg E, Kreyling WG, Lentner B, Moller W, Behnke-Semmler M, et al.. Distribution pattern of inhaled ultrafine gold particles in the rat lung. Inhal Toxicol. 2006 Sep;18(10):733-40.

[16] Ondarroa M, Sharma SK, Quinn PJ. Solvation properties of ubiquinone-10 in solvents of different polarity. Biosci Rep. 1986;6(9):783-96.

[17] Ganguly S, Moolchandani V, Roche JA, Shapiro PS, Somaraju S, Eddington ND, et al.. Phospholipid-Induced In Vivo Particle Migration to Enhance Pulmonary Deposition. Journal of Aerosol Medicine and Pulmonary Drug Delivery. 2008;21(4):343-50.

[18] McConville JT, Overhoff KA, Sinswat P, Vaughn JM, Frei BL, Burgess DS, et al.. Targeted high lung concentrations of itraconazole using nebulized dispersions in a murine model. Pharm Res. 2006 May;23(5):901-11.

[19] Bouwman AM, Heijstra MP, Schaefer NC, Duiverman EJ, LeSouef PN, Devadason SG. Improved efficiency of budesonide nebulization using surface-active agents. Drug Delivery. 2006 Sep-Oct;13(5):357-63.

[20] Vaughn JM, McConville JT, Burgess D, Peters JI, Johnston KP, Talbert RL, et al.. Single dose and multiple dose studies of itraconazole nanoparticles. Eur J Pharm Biopharm. 2006;63(2):95-102.

[21] Mechanics of Respiration. In: Ruckebusch Y, Phaneuf LP, Dunlop R, eds. *Physiology of Small and Large Animals*. Philadelphia, PA: B.C. Decker, Inc. 1991:53-64.

Chapter 7: Summary, Conclusions and Recommendations

In the research work presented in this dissertation, a suitable formulation for pulmonary delivery of Coenzyme Q_{10} (CoQ_{10}) for the purpose of treating lung malignancies was successfully developed and tested *in vitro* and *in vivo*. In this chapter, a summary of each research project is presented, along with the conclusions obtained from them and recommendations deemed appropriate for future studies based on these conclusions.

Initially, an analytical method to accurately, precisely and reproducibly measure the surface tension of liquids was developed. As earlier indicated, this interfacial phenomenon had previously been demonstrated to have an influence on the aerosolization profile of liquids from nebulizer devices. As described in Chapter 3, a glass disk probe was manufactured and connected to the arm of a texture analyzer instrument. From the measurement of the detachment force of the probe from the surface of a bulk liquid, the calculation of surface tension was extrapolated using the theory of the maximum pull on a rod. The maximum pull on rod a theory was applied in a novel way to describe the mechanism presented in this work, for the maximum pull on a disk. Results within 5% of the literature values were obtained, for standard solutions, and it was also found that the accuracy of this method may be related to the probe diameter used to measure the detachment force from the bulk liquid surface. For this reason, further studies are warranted to test glass disk probes with different dimensions in order to achieve even more accurate results when compared to literature values for standard solutions. Also, it is suggested that a method optimization may be done by reducing the sample volume to a minimum while maintaining the infinite interface conditions, which

is related to the probe diameter and the liquid surface free from wall interference. Regardless of this being a non-destructive test, a small volume of samples may be required in cases where liquids containing expensive ingredients (i.e. active pharmaceutical ingredients, excipients, etc.) may be need to be evaluated in order to lower costs. Nevertheless, the present method has shown satisfactory results, and was used to analyze the surface tension of formulations of CoQ_{10} presented in this work.

In Chapter 4, soybean lecithin, a mixture of phospholipids, was initially used as a model excipient to allow for the determination of a suitable manufacturing process in order to acquire an aqueous submicron dispersion of CoQ_{10}. High shear mixing and ultrasonication were also evaluated in the manufacturing process, but high pressure homogenization was ultimately selected given the satisfactory results obtained. This high pressure homogenization was also deemed appropriate with a potential for scale up capabilities. To achieve an optimized number of passes in the microfluidization system, formulations of CoQ_{10} stabilized with lecithin (1:1 w/w) were analyzed for particle size distribution using laser diffraction (LD) and dynamic light scattering (DLS), surface tension according to the method previously described, zeta potential, and rheological behavior. Formulations prepared with dipalmitoylphosphatidylcholine (DPPC) were also analyzed at the same (1:1) drug-to-lipid ratio. These physicochemical properties were then considered in terms of nebulization performance of the CoQ_{10} dispersions as aerosolized by an Aeroneb Pro® vibrating-mesh nebulizer. Previous studies had shown that this type of nebulizer can have the pores of the mesh clogged and consequently present variable aerosol output results. To ensure continuous and steady aerosol generation from the dispersed phospholipid containing formulations, the nebulization performance was investigated using LD to analyze the percentage transmission over time (transmittogram) related to aerosol output. It was found that the physicochemical

properties and the nebulization performance of the formulations varied according to the different phospholipids used to stabilize the dispersions. It was also found that 50 passes would be a satisfactory processing protocol to attain aqueous submicron dispersions of CoQ_{10} with continuous nebulization capabilities for 15 minutes at this drug-to-lipid ratio, regardless of the type of phospholipids utilized in the formula preparation. The results suggested that the rheological behavior of the CoQ_{10} formulations could be used to help explain the aerosolization profiles.

Considering these findings, the synthetic phospholipids dimyristoyl-, dipalmitoyl- and distearoyl- phosphatidylcholines (DMPC, DPPC, and DSPC, respectively) were used for stabilizing the dispersions of CoQ_{10} described in Chapter 5. Their physicochemical properties and nebulization performances were compared to the lecithin formulation previously investigated in Chapter 4. Since the LD technique employed to analyze nebulization performance was able to analyze the aerosol in terms of mass output and not drug output, the formulations of CoQ_{10} were investigated for their aerodynamic deposition profiles and emitted doses. The slope of the transmittogram was compared to drug output at initial and final 15-second periods in a 15-minute nebulization event in the cascade impactor tests. It was found that higher slopes corresponded to decreased mass and drug output as well as reduced droplet sizes over time. Formulations of CoQ_{10} stabilized with DPPC and DSPC presented a similar aerosol profile, emitting high amounts of drug with potential to reach the lungs following nebulization. The DMPC dispersion presented an intermediate result compared to that of the other synthetic phospholipids and lecithin formulations. From the physicochemical properties investigated, the rheology of the formulations was indicative of aerosolization profile since DMPC and lecithin formulations both presented shear-thickening behavior at high shear rates. The applied stress in this experimental design may parallel the high frequency

of vibrating-mesh from the nebulizer used. Formulations of CoQ_{10} prepared with DPPC and DSPC presented a steady profile within the 15-minute nebulization period. Nevertheless, additional studies are necessary to determine the state matter of the drug particles in these dispersions, for instance, through differential scanning calorimetry. Further elucidation of drug encapsulation may be obtained through cryo-electron microscopy. In addition, the drug concentrations presented in this research project are nominal values. Therefore, evaluations of drug loading and manufacturing robustness are worthy of further investigation, including an analysis of particle size distribution and drug concentration prior to the microfluidization process. Stability of formed dispersions of CoQ_{10} to the nebulization process is suggested to be considered as well as evaluation of performance of different types of nebulizers to aerosolize these formulations.

Finally in Chapter 6, the drug deposition in the pulmonary airways was evaluated in mice that were exposed for 15 minutes by restraining them in a nose-only inhalation chamber and subjecting them to aerosols of CoQ_{10} prepared with DMPC, DPPC, and DSPC. While CoQ_{10} levels were below the quantitative limit in the blood plasma and in a DPPC-containing saline control group for up to 48 hours, the drug deposition in the lungs achieved high doses within this time interval for all treated groups. C_{max} and $AUC_{0\text{-}48}$ values reached 791 µg/g and 26.8 mg·h/g of lung tissue, respectively, at 1 hour after the end of pulmonary administration using an Aeroneb Pro® vibrating-mesh nebulizer. Proportionally to animal body weight, the concentration of drug found in the nasal cavity was lower than in the lungs. In conclusion, high levels of CoQ_{10} were determined in the lungs after 48 hours. The determination of the time to completely clear the drug from the lungs is an investigation warranted for future studies, which could be designed for a larger animal (e.g. rats) in order to compare differences in lung deposition of these dispersions of CoQ_{10}. The formulations presented in this dissertation were manufactured

for immediate use following preparation. Therefore, further studies to identify formulation stability at different temperatures are necessary to move forward into further preclinical and clinical studies.

The work presented in this dissertation shows that evaluation of aerosol output using a LD technique may favor rapid screening of formulations that have potential for pulmonary delivery. Following the selection of suitable candidates, analysis of aerodynamic deposition profiles must be performed to determine the drug output from the aerosol generated from these formulations. By evaluating continuous aerosol output from a nebulizer it was demonstrated that investigation of the rheology of dispersions may be useful in predicting the overall nebulization performance of formulations for use with vibrating-mesh nebulizers. This may be especially important in the formulation development process for the inhalation therapy of poorly-water soluble compounds, where colloidal systems may be involved.

In a broader sense, this work presents a novel method used in order to measure the surface tension of liquids. This new method of surface tension evaluation could be applied in a variety of settings, including the paint and cosmetic industries, in addition to the food and pharmaceutical industries.

Lastly, this body of work is an important proof-of-concept to demonstrate the delivery of high amounts of exogenous CoQ_{10} to the lungs via inhalation. It is hoped that further studies can build on the understanding of nebulization performance as well as the mouse deposition studies to the future development of therapies to treat lung carcinomas, either as primary or supportive care.

Appendices

APPENDIX A: LOW CONCENTRATION RANGE DETERMINATION OF COENZYME Q_{10} USING HIGH PERFORMANCE LIQUID CHROMATOGRAPHY (HPLC)

A.1. Introduction

Coenzyme Q_{10} (CoQ_{10}) is a lipophilic drug that is being evaluated for the treatment of certain diseases related to the mitochondrial function. Preclinical and clinical studies require the determination of small amounts of this compound in different biological fluids and tissues. Currently, there are many analytical methods of HPLC with ultraviolet (UV) detectors available to determine CoQ_{10}. However, for high sensitivity analysis, more sophisticated and complex methods are required, such as: HPLC followed by chemical reactions, HPLC with electrochemical detectors (ECD) and liquid chromatography-triple quadrupole (tandem) mass spectrometry (LC – MS/MS). Among the parameters for validation of HPLC methods are accuracy, precision, range, linearity and limits of detection (LOD) and quantification (LOQ). Signal-to-noise (S/N) ratio is a quick and simple method to determine LOD and LOQ, which are essential when analyzing low concentration of drugs.

A.2. Purpose

The aim of this study was to develop an analytical method with improved sensitivity to determine CoQ_{10} using reverse-phase high performance liquid chromatography.

A.3. Methods

The Waters HPLC and column system consisted of a 1525 binary pump, a 717 autosampler, a 2487 dual λ absorbance detector, set at 275 nm, and a Symmetry RP-C8 column 5 µm (3.9 x 150 mm) connected to Symmetry C8 guard column 5 µm (3.9 x 20 mm). The mobile phase (MP) consisted of Methanol:Hexane at 97:3 (v/v). Stock solution of pure CoQ_{10} was initially dissolved in Hexane:Ethanol (diluent) at a ratio of 2:1 (v/v) and subsequently diluted with the mobile phase to obtain the desired concentration. Limit of Detection (LOD), Limit of Quantification (LOQ) and linearity (3-interday curves) were determined by injecting 50 µL samples at a controlled temperature of 30ºC. Chromatogram peaks were acquired within run time of 11 minutes at a flow rate of 1.0 mL/min. Area and height of peaks were used to determine curve linearity. LOD and LOQ were defined by signal-to-noise (S/N) ratio calculations according to method from the European Pharmacopoeia, with minimum acceptable values of 3 and 10, respectively. Concentration points were 10, 25, 37.5 and 50 ng/mL (n = 6).

For mobile phase preparation, solvents were filtered prior to use through 0.45 µm nylon membrane filters and sparged for 10 minutes with helium gas. For preparation of stock and working standard solutions (500 µg/mL), 12.5 mg of CoQ_{10} was accurately weighed in a 25 mL amber volumetric flask and dissolved in hexane-ethanol (2:1 v/v). Subsequently, this stock standard solution was diluted with MP to 10 µg/mL. To avoid light degradation of the API, standard solutions were kept in amber containers during drug manipulation. Working standard solutions were prepared by transferring suitable aliquots of stock solution to transparent tubes and diluted to final concentration with MP. Finally, the working standard solutions were transferred to polypropylene conical containers and placed them in amber HPLC vials for analyses.

A.4. Results

The retention time (RT) of CoQ_{10} was determined as approximately 8 minutes and injection of blank sample (diluent) shown not to interfere in peak determination at 275 nm. Temperature control was observed to be essential to obtain symmetric peaks at lower concentrations. LOD and LOQ were defined as 10 ng/mL (n = 6; S/N ratio = 6.0; SD = 0.6; RSD = 10.5%) and 25 ng/mL (n = 6; S/N ratio = 12.6; SD = 1.3; RSD = 10.1%); respectively. The curve linearities were obtained using height or area of the chromatogram peaks in the range of 25 to 2500 ng/mL with $r^2 \geq 0.9999$ (n=3 for each concentration).

A.5. Conclusion

The method can be used as an alternative to more complex and expensive methods for analysis of CoQ_{10} in small concentrations. The ease of sample preparation and small retention time allows for a quick analysis. The possibility of using either the area or the height of chromatogram peaks gives more flexibility to adapt this method to different applications. Further studies on extraction of CoQ_{10} from biological materials, stability, and internal standard selection are needed to define the role of this method. This study provides an alternative and suitably stable method to determine CoQ_{10} at very low concentrations using an economically viable RP-HPLC system.

APPENDIX B: DETERMINATION OF APPROPRIATE COENZYME Q_{10} CONCENTRATION IN PHOSPHOLIPID-STABILIZED DISPERSIONS FOR CONTINUOUS VIBRATING-MESH NEBULIZATION.

B.1. Introduction

Coenzyme Q_{10} (CoQ_{10}) is a poorly-water soluble compound that is being studied for the treatment of lung malignancies. The phospholipid concentration in the drug product Survanta® is 2.5% w/w, which is the same concentration that we have chosen to use when stabilizing phospholipid dispersions of CoQ_{10} prepared using microfluidization. Aeroneb Pro® micropump device is a vibrating-mesh nebulizer that is capable of aerosolizing dispersed system but that has been reported to present variable aerosolization due to clogging of mesh pores.

B.2. Purpose

The purpose of the preliminary study presented in this appendix is to establish a maximum nominal drug loading to phospholipid-stabilized dispersions of CoQ_{10} while maintaining continuous vibrating-mesh nebulization.

B.3. Methods

The preparation of the formulations is described in detail as in Formulation C of Chapter 4, Section 4.3.4, Table 4.1. In particular, the formulations investigated in this study were prepared with 50 microfluidization discrete passes using 2.5% w/w of dimyristoyl phosphatidylcholine (DMPC) and 7.5%, 7.0%, 6.0%, 5.0%, or 4.0% w/w of CoQ_{10}. The dispersions were then aerosolized no later than one day after preparation

using an Aeroneb Pro® nebulizer for 15 minutes. The aerosolization profile was monitored via analysis of Total Aerosol Output (TAO) and using laser diffraction with a Malvern Spraytec® coupled with an inhalation cell as described in Chapter 4, Section 4.4.

B.4. Results and Discussion

The nebulization performances of the DMPC-stabilized formulations of CoQ_{10} are presented in Figure B.1. It can be observed that as the drug concentration decreases, the aerosolization becomes more continuous. The TAO values for decreasing drug concentrations are, respectively, 1.25g (12.4%), 1.62g (16.1%) and 2.15g (21.4%). The TAO results are in agreement with the analysis of nebulization performance from laser diffraction, with increasing values as the drug concentrations decrease. The transmission values do not return to 100% at the end of nebulization, due to the reasons described in Section 4.4 of Chapter 4. Although a formulation containing 5% w/w of CoQ_{10} was prepared, the analysis using laser diffraction could not be performed appropriately due to this technique artifact. Based on visual observation, it was determined that this drug concentration was not suitable for continuous aerosolization of the CoQ_{10} dispersion because of generation of intermittent mist during nebulization. For the 4.0% w/w CoQ_{10} formulation, this intermittence was only observed at the end phase of nebulization, therefore being chosen as the appropriate nominal drug concentration.

B.5. Conclusion

The nominal concentration of 4% w/w of CoQ_{10} was determined to be the appropriate drug loading for continuous aerosolization with the Aeroneb Pro® nebulizer as established using DMPC at 2.5% w/w to stabilize the dispersions.

B.6. Figures

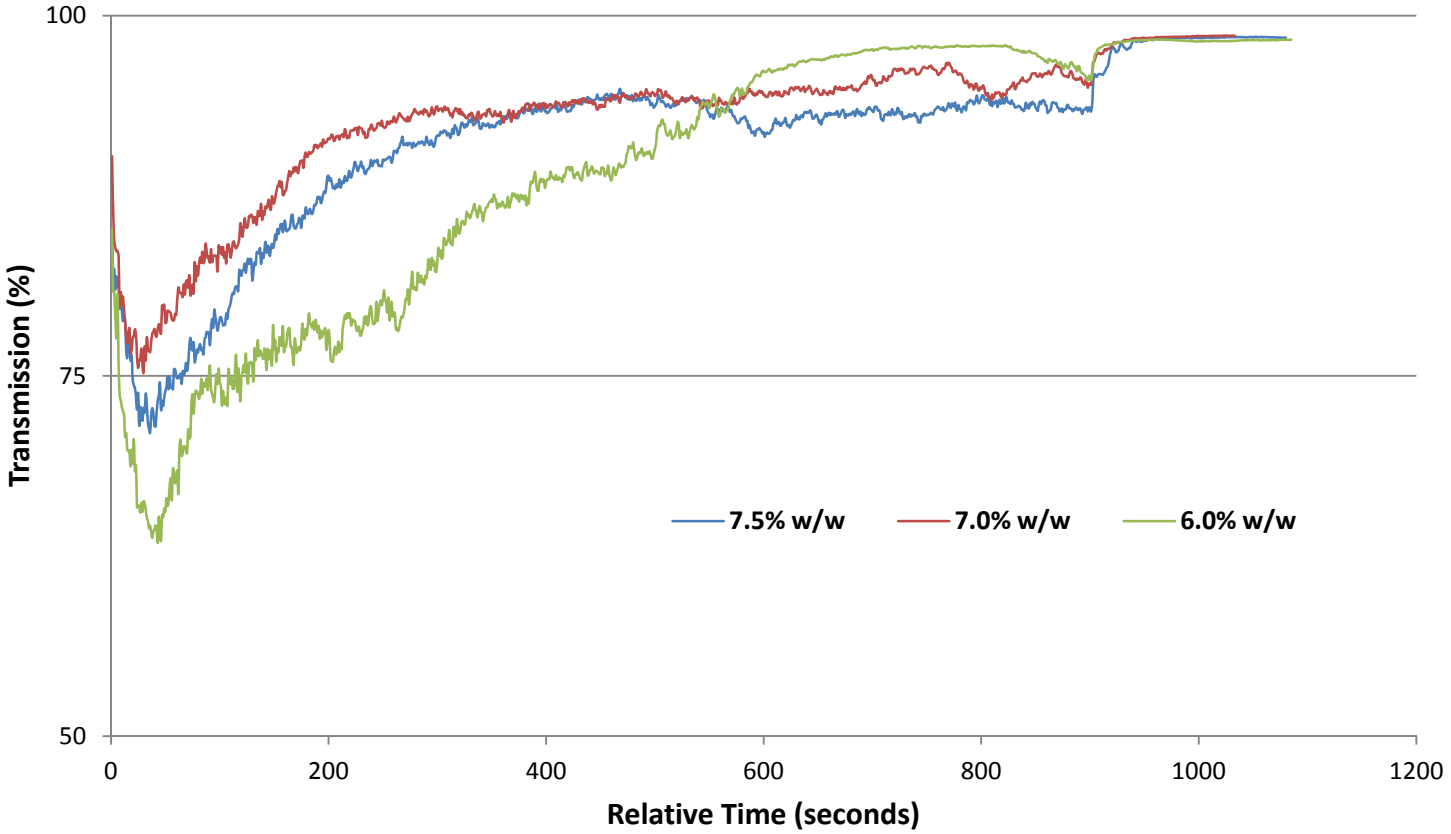

Figure B.1 – Transmittograms of aerosolization of DMPC-stabilized dispersions with different concentrations of CoQ_{10}.

Bibliography

(02/05/2010). "Physician Data Query (PDQ): Non-Small Cell Lung Cancer Treatment (health professional version)." Retrieved 02/22/2010, from http://www.cancer.gov/cancertopics/pdq/treatment/non-small-cell-lung/healthprofessional.

(07/01/2009). "Physicians Data Query (PDQ): Small Cell Lung Cancer Treatment (health professional version)." Retrieved 02/22/2010, from http://www.cancer.gov/cancertopics/pdq/treatment/small-cell-lung/healthprofessional.

(2007). Cancer Facts & Figures 2007, American Cancer Society.

(2008). Cancer Facts & Figures 2008, American Cancer Society.

(2009). Cancer Facts & Figures 2009, American Cancer Society.

(2010). American Hospital Formulary Service (AHFS) Drug Information® 2010. G. K. McEvoy. Bethesda, MD, American Society of Health-System Pharmacists, Inc.: 902-1260.

(2010). Surface Tension of Aqueous Mixtures. CRC handbook of chemistry and physics, 90th edition (Internet Version 2010). D. R. Lide. Boca Raton, FL, CRC Press/Taylor and Francis: 6-131.

Abdelrahim, M. E., P. Plant, et al.. (2010). "In-vitro characterisation of the nebulised dose during non-invasive ventilation." Journal of Pharmacy and Pharmacology 62(8): 966-972.

Al Hebshi, A. and A. Al Hadab (2008). "An overview of radiation therapy in the treatment of non-small-cell lung cancer." Annals of Thoracic Medicine 3(6): S89-S96.

Albasarah, Y. Y., S. Somavarapu, et al.. (2010). "Stabilizing protein formulations during air-jet nebulization." International Journal of Pharmaceutics 402(1-2): 140-145.

Alberg, A. J. and J. M. Samet (2003). "Epidemiology of lung cancer." Chest 123(1): 21S-49S.

Alfridsson, M., B. Ninham, et al.. (2000). "Role of Co-Ion specificity and dissolved atmospheric gas in colloid interaction." Langmuir 16(26): 10087-10091.

Alvarez, M., J. Friend, et al.. (2008). "Rapid generation of protein aerosols and nanoparticles via surface acoustic wave atomization." Nanotechnology 19(45).

Alvarez, M., J. R. Friend, et al.. (2008). "Surface vibration induced spatial ordering of periodic polymer patterns on a substrate." Langmuir 24(19): 10629-10632.

Alvarez, M., L. Y. Yeo, et al.. (2009). "Rapid production of protein-loaded biodegradable microparticles using surface acoustic waves." Biomicrofluidics 3(1).

Amani, A., P. York, et al.. (2010). "Evaluation of a Nanoemulsion-Based Formulation for Respiratory Delivery of Budesonide by Nebulizers." Aaps Pharmscitech 11(3): 1147-1151.

Amirav, I., M. T. Newhouse, et al.. (2010). "Factors that affect the efficacy of inhaled corticosteroids for infants and young children." Journal of Allergy and Clinical Immunology 125(6): 1206-1211.

Anderson, P. (2006). "Use of Respimat Soft Mist inhaler in COPD patients." International journal of chronic obstructive pulmonary disease 1(3): 251-9.

Ari, A., O. T. Atalay, et al.. (2010). "Influence of Nebulizer Type, Position, and Bias Flow on Aerosol Drug Delivery in Simulated Pediatric and Adult Lung Models During Mechanical Ventilation." Respiratory Care 55(7): 845-851.

Arzhavitina, A. and H. Steckel (2010). "Surface active drugs significantly alter the drug output rate from medical nebulizers." Int J Pharm 384(1-2): 128-36.

Atkins, P. J., N. P. Barker, et al.. (1992). Drugs and the Pharmaceutical Sciences. Pharmaceutical Inhalation Aerosol Technology. A. J. Hickey. New York, New York, USA., Marcel Dekker, Inc. 54: 155-185.

Avdeef, A. (2003). Absorption and drug development: solubility, permeability and charge state. Hoboken, NJ, John Wiley & Sons, Inc.

Azarmi, S., X. Tao, et al.. (2006). "Formulation and cytotoxicity of doxorubicin nanoparticles carried by dry powder aerosol particles." International Journal of Pharmaceutics 319(1-2): 155-161.

Baker, G. L., A. Gupta, et al.. (2008). "Inhalation toxicity and lung toxicokinetics of C-60 fullerene nanoparticles and microparticles." Toxicological Sciences 101(1): 122-131.

Balashazy, I., B. Alfoldy, et al.. (2007). "Aerosol drug delivery optimization by computational methods for the characterization of total and regional deposition of

therapeutic aerosols in the respiratory system." Current Computer-Aided Drug Design 3(1): 13-32.

Ballo, M. T., M. I. Ross, et al.. (2006). "Combined-modality therapy for patients with regional nodal metastases from melanoma." International Journal of Radiation Oncology Biology Physics 64(1): 106-113.

Bansal, K., M. K. Rawat, et al.. (2009). "Development of Satranidazole Mucoadhesive Gel for the Treatment of Periodontitis." Aaps Pharmscitech 10(3): 716-723.

Barnes, H. A., J. F. Hutton, et al.. (1989). Rheology of Suspensions. An introduction to rheology. K. Walters. Amsterdam, The Netherlands, Elsevier. 3: 115-137.

Barry, P. W. and C. O'Callaghan (1999). "An in vitro analysis of the output of budesonide from different nebulizers." Journal of Allergy and Clinical Immunology 104(6): 1168-1173.

Beck-Broichsitter, M., J. Gauss, et al.. (2009). "Pulmonary drug delivery with aerosolizable nanoparticles in an ex vivo lung model." International Journal of Pharmaceutics 367(1-2): 169-178.

Bendstrup, K. E., M. T. Newhouse, et al.. (1999). "Characterization of heparin aerosols generated in jet and ultrasonic nebulizers." Journal of Aerosol Medicine-Deposition Clearance and Effects in the Lung 12(1): 17-25.

Berg, E., J. O. Svensson, et al.. (2007). "Determination of nebulizer droplet size distribution: A method based on impactor refrigeration." Journal of Aerosol Medicine-Deposition Clearance and Effects in the Lung 20(2): 97-104.

Berg, E. B. and R. J. Picard (2009). "In Vitro Delivery of Budesonide From 30 Jet Nebulizer/Compressor Combinations Using Infant and Child Breathing Patterns." Respiratory Care 54(12): 1671-1678.

Berger, W., U. Setinek, et al.. (2005). "Multidrug resistance markers P-glycoprotein, multidrug resistance protein 1, and lung resistance protein in non-small cell lung cancer: prognostic implications." Journal of Cancer Research and Clinical Oncology 131(6): 355-363.

Berlinski, A. and J. B. Hayden (2010). "Optimization of a Procedure Used to Measure Aerosol Characteristics of Nebulized Solutions Using a Cooled Next Generation Impactor." Journal of Aerosol Medicine and Pulmonary Drug Delivery 23(6): 397-404.

Bernardin, J. D., I. Mudawar, et al.. (1997). "Contact angle temperature dependence for water droplets on practical aluminum surfaces." International Journal of Heat and Mass Transfer 40(5): 1017-1033.

Berridge, M. S., D. L. Heald, et al.. (2003). "Imaging studies of biodistribution and kinetics in drug development." Drug Development Research 59(2): 208-226.

Berridge, M. S., Z. Lee, et al.. (2000). "Pulmonary distribution and kinetics of inhaled [C-11]triamcinolone acetonide." Journal of Nuclear Medicine 41(10): 1603-1611.

Berridge, M. S., Z. H. Lee, et al.. (2000). "Regional distribution and kinetics of inhaled pharmaceuticals." Current Pharmaceutical Design 6(16): 1631-1651.

Bhagavan, H. N. and R. K. Chopra (2006). "Coenzyme Q10: Absorption, tissue uptake, metabolism and pharmacokinetics." Free Radical Research 40(5): 445-453.

Bhagavan, H. N. and R. K. Chopra (2007). "Plasma coenzyme Q10 response to oral ingestion of coenzyme Q10 formulations." Mitochondrion 7(Supplement 1): S78-S88.

Bhavna, F. J. Ahmad, et al.. (2009). "Nano-salbutamol dry powder inhalation: A new approach for treating broncho-constrictive conditions." European Journal of Pharmaceutics and Biopharmaceutics 71(2): 282-291.

Bittar, E. E. (2002). Alveolar Surfactant. Pulmonary biology in health and disease. New York, NY, USA, Springer: 44-63.

Boe, J., J. H. Dennis, et al.. (2001). "European Respiratory Society Guidelines on the use of nebulizers." European Respiratory Journal 18(1): 228-242.

Bouyssou, T., P. Casarosa, et al.. (2010). "Pharmacological Characterization of Olodaterol, a Novel Inhaled beta(2)-Adrenoceptor Agonist Exerting a 24-Hour-Long Duration of Action in Preclinical Models." Journal of Pharmacology and Experimental Therapeutics 334(1): 53-62.

Boyd, B., P. Noymer, et al.. (2004). "Effect of gender and device mouthpiece shape on bolus insulin aerosol delivery using the AER(x) pulmonary delivery system." Pharmaceutical Research 21(10): 1776-1782.

Brand, P., K. Haussinger, et al.. (1999). "Intrapulmonary distribution of deposited particles." Journal of Aerosol Medicine-Deposition Clearance and Effects in the Lung 12(4): 275-284.

Brea-Calvo, G., Á. Rodríguez-Hernández, et al.. (2006). "Chemotherapy induces an increase in coenzyme Q10 levels in cancer cell lines." Free Radical Biology and Medicine 40(8): 1293-1302.

Bridges, P. A. and K. M. G. Taylor (2000). "An investigation of some of the factors influencing the jet nebulisation of liposomes." International Journal of Pharmaceutics 204(1-2): 69-79.

Brown, R. A. and L. S. Schanker (1983). "ABSORPTION OF AEROSOLIZED DRUGS FROM THE RAT LUNG." Drug Metabolism and Disposition 11(4): 355-360.

Bummer, P. M. (2005). Interfacial Phenomena. Remington: The Science and Practice of Pharmacy. R. Hendrickson. Baltimore, MD, Lippincott Williams & Wilkins: 280-292.

Butterweck, G., G. Vezzu, et al.. (2001). "In vivo measurement of unattached radon progeny deposited in the human respiratory tract." Radiation Protection Dosimetry 94(3): 247-250.

Cantrell, C. L., S. G. Franzblau, et al.. (2001). "Antimycobacterial plant terpenoids." Planta Medica 67(8): 685-694.

Carroll, N., J. Elliot, et al.. (1993). "THE STRUCTURE OF LARGE AND SMALL AIRWAYS IN NONFATAL AND FATAL ASTHMA." American Review of Respiratory Disease 147(2): 405-410.

Carstens, M. G., P. de Jong, et al.. (2008). "The effect of core composition in biodegradable oligomeric micelles as taxane formulations." European Journal of Pharmaceutics and Biopharmaceutics 68(3): 596-606.

Carvalho, T. C., M. Horng, et al.. (2010). Measurement of Surface Tension of Liquids using a Texture Analyzer. AAPS PharmSci.

Carvalho, T. C., J. I. Peters, et al.. (2011). "Influence of particle size on regional lung deposition - What evidence is there?" International Journal of Pharmaceutics 406(1-2): 1-10.

CEN (2007). Respiratory therapy equipment - Part 1: Nebulizing systems and their components. E. C. f. Standardization, BSI. BS EN 13544-1:2007+A1:2009.

Chan, H. K., E. Daviskas, et al.. (1999). "Deposition of aqueous aerosol of technetium-99m diethylene triamine penta-acetic acid generated and delivered by a novel system (AER(x)) in healthy subjects." European Journal of Nuclear Medicine 26(4): 320-327.

Chan, H. K., S. Eberl, et al.. (2002). "Changes in lung deposition of aerosols due to hygroscopic growth: A fast SPECT study." Journal of Aerosol Medicine-Deposition Clearance and Effects in the Lung 15(3): 307-311.

Chan, J. G. Y., P. C. L. Kwok, et al.. (2011). "Mannitol Delivery by Vibrating Mesh Nebulisation for Enhancing Mucociliary Clearance." Journal of Pharmaceutical Sciences 100(7): 2693-2702.

Chang, L. Q. and M. J. Pikal (2009). "Mechanisms of Protein Stabilization in the Solid State." Journal of Pharmaceutical Sciences 98(9): 2886-2908.

Charvat, A., A. Bogehold, et al.. (2006). "Time-resolved micro liquid desorption mass spectrometry: Mechanism, features, and kinetic applications." Australian Journal of Chemistry 59(2): 81-103.

Chattopadhyay, P., B. Y. Shekunov, et al.. (2007). "Production of solid lipid nanoparticle suspensions using supercritical fluid extraction of emulsions (SFEE) for pulmonary delivery using the AERx system." Advanced Drug Delivery Reviews 59: 444-453.

Chattopadhyay, S., L. B. Modesto-Lopez, et al.. (2010). "Size Distribution and Morphology of Liposome Aerosols Generated By Two Methodologies." Aerosol Science and Technology 44(11): 972-982.

Chen, F., T. Fujinaga, et al.. (2009). "Clinical features of surgical resection for pulmonary metastasis from breast cancer." Ejso 35(4): 393-397.

Cheng, Y. S., H. Irshad, et al.. (2008). "Lung Deposition of Droplet Aerosols in Monkeys." Inhalation Toxicology 20(11): 1029-1036.

Chimote, G. and R. Banerjee (2009). "Evaluation of antitubercular drug-loaded surfactants as inhalable drug-delivery systems for pulmonary tuberculosis." Journal of Biomedical Materials Research Part A 89A(2): 281-292.

Chimote, G. and R. Banerjee (2010). "In Vitro Evaluation of Inhalable Isoniazid-Loaded Surfactant Liposomes as an Adjunct Therapy in Pulmonary Tuberculosis." Journal of Biomedical Materials Research Part B-Applied Biomaterials 94B(1): 1-10.

Chou, A. J., M. D. Bell, et al.. (2007). "Phase Ib/IIa study of sustained release lipid inhalation targeting cisplatin by inhalation in the treatment of patients with relapsed/progressive osteosarcoma metastatic to the lung." J Clin Oncol (Meeting Abstracts) 25(18_suppl): 9525.

Chow, A. H. L., H. H. Y. Tong, et al.. (2007). "Particle engineering for pulmonary drug delivery." Pharmaceutical Research 24(3): 411-437.

Christian, S. D., A. R. Slagle, et al.. (1998). "Inverted vertical pull surface tension method." Langmuir 14(11): 3126-3128.

Chrystyn, H. (2001). "Methods to identify drug deposition in the lungs following inhalation." British Journal of Clinical Pharmacology 51(4): 289-299.

Cipolla, D. C., Boyd, B., Evans, R.M., Warren, S., Taylor, G., Farr, S.J. (2000). Bolus Administration of INS365: Studying the Feasibility of Delivering High Doses of Drugs Using the AERx Pulmonary Delivery System. Respiratory Dru Delivery VII, Tarpon Springs, FL, USA, Serentec Press, Raleigh, NC, USA.

Clark, A., M. C. Kuo, et al.. (2008). "A comparison of the pulmonary bioavailability of powder and liquid aerosol formulations of salmon calcitonin." Pharmaceutical Research 25(7): 1583-1590.

Clear, N., Ticehurst, M., Clarke, J., Miller, P., Shepherd, M. (2004). "Electrohydrodynamic Aerosol Drug Delivery: Experience in Early Clinical Development." Journal of Aerosol Medicine 17(1): 95-95.

Coates, A. L., O. Denk, et al.. (2011). "Higher Tobramycin Concentration and Vibrating Mesh Technology Can Shorten Antibiotic Treatment Time in Cystic Fibrosis." Pediatric Pulmonology 46(4): 401-408.

Coates, A. L., M. Green, et al.. (2008). "Rapid pulmonary delivery of inhaled tobramycin for pseudomonas infection in cystic fibrosis: A pilot project." Pediatric Pulmonology 43(8): 753-759.

Coates, A. L., K. Leung, et al.. (2011). "Testing of Nebulizers for Delivering Magnesium Sulfate to Pediatric Asthma Patients in the Emergency Department." Respiratory Care 56(3): 314-318.

Coates, A. L., C. F. MacNeish, et al.. (1997). "The choice of jet nebulizer, nebulizing flow, and addition of albuterol affects the output of tobramycin aerosols." Chest 111(5): 1206-1212.

Corren, J. and D. R. Tashkin (2003). "Evaluation of efficacy and safety of flunisolide hydrofluoroalkane for the treatment of asthma." Clinical Therapeutics 25(3): 776-798.

Cory J. Hitzman, W. F. E. T. S. W. (2006). "Development of a respirable, sustained release microcarrier for 5-fluorouracil II: In vitro and in vivo optimization of lipid coated nanoparticles." Journal of Pharmaceutical Sciences 95(5): 1127-1143.

Crowder, T. M., J. A. Rosati, et al.. (2002). "Fundamental effects of particle morphology on lung delivery: Predictions of Stokes' law and the particular relevance to dry powder inhaler formulation and development." Pharmaceutical Research 19(3): 239-245.

Cryan, S.-A., N. Sivadas, et al.. (2007). "In vivo animal models for drug delivery across the lung mucosal barrier." Advanced Drug Delivery Reviews 59(11): 1133-1151.

Dahlstrom, K., L. Thorsson, et al.. (2003). "Systemic availability and lung deposition of budesonide via three different nebulizers in adults." Annals of Allergy, Asthma & Immunology: Official Publication of the American College of Allergy, Asthma, & Immunology 90(2): 226-232.

Dailey, L. A., T. Schmehl, et al.. (2003). "Nebulization of biodegradable nanoparticles: impact of nebulizer technology and nanoparticle characteristics on aerosol features." Journal of Controlled Release 86(1): 131-144.

Dalby, R., M. Spallek, et al.. (2004). "A review of the development of Respimat((R)) Soft Mist (TM) Inhaler." International Journal of Pharmaceutics 283(1-2): 1-9.

Darquenne, C. and G. K. Prisk (2008). "Deposition of inhaled particles in the human lung is more peripheral in lunar than in normal gravity." European journal of applied physiology 103(6): 687-95.

Davies, A. M., P. N. Lara, et al.. (2004). "Treatment of extensive small cell lung cancer." Hematology-Oncology Clinics of North America 18(2): 373-385.

Davies, D. N., M. Pollard, et al.. (2011). Liquid formations for electrohydrodymanic spraying containing polymer and suspended particles. USPTO. USA, Battelle Memorial Institute, Columbus, OH (US): 25.

Davis, S. S., J. G. Hardy, et al.. (1992). "GAMMA-SCINTIGRAPHY IN THE EVALUATION OF PHARMACEUTICAL DOSAGE FORMS." European Journal of Nuclear Medicine 19(11): 971-986.

Davison, S., J. Thipphawong, et al.. (2005). "Pharmacokinetics and acute safety of inhaled testosterone in postmenopausal women." Journal of Clinical Pharmacology 45(2): 177-184.

de Boer, A. H., D. Gjaltema, et al.. (2002). "Characterization of inhalation aerosols: a critical evaluation of cascade impactor analysis and laser diffraction technique." International Journal of Pharmaceutics 249(1-2): 219-231.

de Boer, A. H., J. Wissink, et al.. (2008). "In vitro performance testing of the novel medspray (R) wet aerosol inhaler based on the principle of Rayleigh break-up." Pharmaceutical Research 25(5): 1186-1192.

De Ruysscher, D. and J. Vansteenkiste (2000). "Chest radiotherapy in limited-stage small cell lung cancer: facts, questions, prospects." Radiotherapy and Oncology 55(1): 1-9.

Denyer, J. and T. Dyche (2010). "The Adaptive Aerosol Delivery (AAD) Technology: Past, Present, and Future." Journal of Aerosol Medicine and Pulmonary Drug Delivery 23: S1-S10.

Derkach, S. R. (2009). "Rheology of emulsions." Advances in Colloid and Interface Science 151(1-2): 1-23.

Dershwitz, M., J. L. Walsh, et al.. (2000). "Pharmacokinetics and pharmacodynamics of inhaled versus intravenous morphine in healthy volunteers." Anesthesiology 93(3): 619-628.

Desai, T. R., R. E. W. Hancock, et al.. (2002). "A facile method of delivery of liposomes by nebulization." Journal of Controlled Release 84(1-2): 69-78.

Deshpande, D., J. Blanchard, et al.. (2002). "Aerosolization of lipoplexes using AERx (R) Pulmonary Delivery System." Aaps Pharmsci 4(3).

Deshpande, D. S., J. D. Blanchard, et al.. (2005). "Gamma scintigraphic evaluation of a miniaturized AERx (R) pulmonary delivery system for aerosol delivery to anesthetized animals using a positive pressure ventilation system." Journal of Aerosol Medicine-Deposition Clearance and Effects in the Lung 18(1): 34-44.

Dhanasekaran, M. and J. Ren (2005). "The emerging role of coenzyme Q-10 in aging, neurodegeneration, cardiovascular disease, cancer and diabetes mellitus." Current Neurovascular Research 2(5): 447-459.

Dhanikula, A. B. and R. Panchagnula (1999). "Localized paclitaxel delivery." International Journal of Pharmaceutics 183(2): 85-100.

Ding, L., T. Lee, et al.. (2005). "Fabrication of monodispersed Taxol-loaded particles using electrohydrodynamic atomization." Journal of Controlled Release 102(2): 395-413.

Dintaman, J. M. and J. A. Silverman (1999). "Inhibition of P-glycoprotein by D-alpha-tocopheryl polyethylene glycol 1000 succinate (TPGS)." Pharmaceutical Research 16(10): 1550-1556.

Diot, P., L. B. Palmer, et al.. (1997). "RhDNase I aerosol deposition and related factors in cystic fibrosis." American Journal of Respiratory and Critical Care Medicine 156(5): 1662-1668.

Dolovich, M. and R. Labiris (2004). "Imaging drug delivery and drug responses in the lung." Proc Am Thorac Soc 1(4): 329-37.

Dolovich, M. A. (2000). "Influence of inspiratory flow rate, particle size, and airway caliber on aerosolized drug delivery to the lung." Respir Care 45(6): 597-608.

Dolovich, M. B. (1992). Drugs and the Pharmaceutical Sciences. Pharmaceutical Inhalation Aerosol Technology. A. J. Hickey. New York, New York, USA., Marcel Dekker, Inc. 54: 171-213.

Dolovich, M. B. (2009). "18F-fluorodeoxyglucose positron emission tomographic imaging of pulmonary functions, pathology, and drug delivery." Proc Am Thorac Soc 6(5): 477-85.

Dolovich, M. B. and R. Dhand (2011). "Aerosol drug delivery: developments in device design and clinical use." Lancet 377(9770): 1032-1045.

Eberl, S., H. K. Chan, et al.. (2006). "SPECT imaging for radioaerosol deposition and clearance studies." Journal of Aerosol Medicine-Deposition Clearance and Effects in the Lung 19(1): 8-20.

Eberl, S., H. K. Chan, et al.. (2001). "Aerosol deposition and clearance measurement: a novel technique using dynamic SPET." European Journal of Nuclear Medicine 28(9): 1365-1372.

Edwards, D. A., J. Hanes, et al.. (1997). "Large porous particles for pulmonary drug delivery." Science 276(5320): 1868-1871.

Elhissi, A., H. Gill, et al.. (2011). "Vibrating-mesh nebulization of liposomes generated using an ethanol-based proliposome technology." Journal of Liposome Research 21(2): 173-180.

Elhissi, A. M. A., M. Faizi, et al.. (2007). "Physical stability and aerosol properties of liposomes delivered using an air-jet nebulizer and a novel micropump device with large mesh apertures." International Journal of Pharmaceutics 334(1-2): 62-70.

Elhissi, A. M. A., K. K. Karnam, et al.. (2006). "Formulations generated from ethanol-based proliposomes for delivery via medical nebulizers." Journal of Pharmacy and Pharmacology 58(7): 887-894.

Elhissi, A. M. A. and K. M. G. Taylor (2005). "Delivery of liposomes generated from proliposomes using air-jet, ultrasonic, and vibrating-mesh nebulisers." Journal of Drug Delivery Science and Technology 15(4): 261-265.

Emmen, H. H., E. M. G. Hoogendijk, et al.. (2000). "Human safety and pharmacokinetics of the CFC alternative propellants HFC 134a (1,1,1,2-tetrafluoroethane) and HFC 227 (1,1,1,2,3,3,3-heptafluoropropane) following whole-body exposure." Regulatory Toxicology and Pharmacology 32(1): 22-35.

Englander, T., D. Wiegel, et al.. (1996). "Dehydration of glass surfaces studied by contact angle measurements." Journal of Colloid and Interface Science 179(2): 635-636.

Erridge, S. C. and N. Murray (2003). "Thoracic radiotherapy for limited-stage small cell lung cancer: Issues of timing, volumes, dose, and fractionation." Seminars in Oncology 30(1): 26-37.

Esposito-Festen, J. E., P. Zanen, et al.. (2007). "Pharmacokinetics of inhaled monodisperse beclomethasone as a function of particle size." British Journal of Clinical Pharmacology 64(3): 328-334.

Esteban, E., M. Casillas, et al.. (2009). "Pemetrexed in first-line treatment of non-small cell lung cancer." Cancer Treatment Reviews 35(4): 364-373.

Faivre-Finn, C., L. W. Lee, et al.. (2005). "Thoracic Radiotherapy for Limited-stage Small-cell Lung Cancer: Controversies and Future developments." Clinical Oncology 17(8): 591-598.

Farr, S. J. (1996). "The physico-chemical basis of radiolabelling metered dose inhalers with Tc-99m." Journal of Aerosol Medicine-Deposition Clearance and Effects in the Lung 9: S27-S36.

Farr, S. J. and B. A. Otulana (2006). "Pulmonary delivery of opioids as pain therapeutics." Advanced Drug Delivery Reviews 58(9-10): 1076-1088.

Farr, S. J., S. J. Warren, et al.. (2000). "Comparison of in vitro and in vivo efficiencies of a novel unit-dose liquid aerosol generator and a pressurized metered dose inhaler." International Journal of Pharmaceutics 198(1): 63-70.

Fathi-Azarbayjani, A., A. Jouyban, et al.. (2009). "Impact of Surface Tension in Pharmaceutical Sciences." Journal of Pharmacy and Pharmaceutical Sciences 12(2): 218-228.

Fiel, S. B., H. J. Fuchs, et al.. (1995). "Comparison of Three Jet Nebulizer Aerosol Delivery Systems used to Administer Recombinant Human DNase-I to Patients with Cystic Fibrosis." Chest 108(1): 153-156.

Finer, N. N., T. A. Merritt, et al.. (2010). "An Open Label, Pilot Study of Aerosurf (R) Combined with nCPAP to Prevent RDS in Preterm Neonates." Journal of Aerosol Medicine and Pulmonary Drug Delivery 23(5): 303-309.

Finlay, W. H. (2001). Particle Deposition in the Respiratory Tract. The mechanics of inhaled pharmaceutical aerosols: an introduction. W. H. Finlay. San Diego, CA, Academic Press: 119-174.

Fischer, S., G. Darling, et al.. (2008). "Induction chemoradiation therapy followed by surgical resection for non-small cell lung cancer (NSCLC) invading the thoracic inlet." European Journal of Cardio-Thoracic Surgery 33(6): 1129-1133.

Flament, M. P., P. Leterme, et al.. (1999). "Influence of formulation on jet nebulisation quality of alpha(1) protease inhibitor." International Journal of Pharmaceutics 178(1): 101-109.

Flament, M. P., P. Leterme, et al.. (1999). "Influence of the technological parameters of ultrasonic nebulisation on the nebulisation quality of alpha 1 protease inhibitor (alpha 1I)." International Journal of Pharmaceutics 189(2): 197-204.

Fleming, J. S., A. H. Hashish, et al.. (1997). "A technique for simulating radionuclide images from the aerosol deposition pattern in the airway tree." Journal of Aerosol Medicine-Deposition Clearance and Effects in the Lung 10(3): 199-212.

Folkers, K., R. Brown, et al.. (1993). "Survival of Cancer Patients on Therapy with Coenzyme Q10." Biochemical and Biophysical Research Communications 192(1): 241-245.

Folkers, K., M. Morita, et al.. (1993). "The Activities of Coenzyme-Q(10) and Vitamin-B(6) for Immune-Responses." Biochemical and Biophysical Research Communications 193(1): 88-92.

Forde, G. M., J. Friend, et al.. (2006). "Straightforward biodegradable nanoparticle generation through megahertz-order ultrasonic atomization." Applied Physics Letters 89(6).

Freiberg, S. and X. Zhu (2004). "Polymer microspheres for controlled drug release." International Journal of Pharmaceutics 282(1-2): 1-18.

Freud, B. B. and H. Z. Freud (1930). "A Theory of the Ring Method for the Determination of Surface Tension." Journal of the American Chemical Society 52(5): 1772-1782.

Friend, J. and L. Y. Yeo (2011). "Microscale acoustofluidics: Microfluidics driven via acoustics and ultrasonics." Reviews of Modern Physics 83(2): 647-704.

Friend, J. R., L. Y. Yeo, et al.. (2008). "Evaporative self-assembly assisted synthesis of polymeric nanoparticles by surface acoustic wave atomization." Nanotechnology 19(14).

Fu, Y. J., S. S. Shyu, et al.. (2002). "Development of biodegradable co-poly(D,L-lactic/glycolic acid) microspheres for the controlled release of 5-FU by the spray drying method." Colloids and Surfaces B-Biointerfaces 25(4): 269-279.

Fulzele, S. V., A. Chatterjee, et al.. (2006). "Inhalation delivery and anti-tumor activity of celecoxib in human orthotopic non-small cell lung cancer xenograft model." Pharmaceutical Research 23(9): 2094-2106.

Fulzele, S. V., M. S. Shaik, et al.. (2006). "Anti-cancer effect of celecoxib and aerosolized docetaxel against human non-small cell lung cancer cell line, A549." Journal of Pharmacy and Pharmacology 58: 327-336.

Furlong, D. N. and S. Hartland (1980). "Wall Effects in Measurement of Surface Tension using a Vertical Cylinder.1. Theory." Journal of the Chemical Society-Faraday Transactions I 76: 457-466.

Furlong, D. N. and S. Hartland (1980). "Wall Effects in Measurement of Surface Tension using a Vertical Cylinder. 2. Experimental." Journal of the Chemical Society-Faraday Transactions I 76: 467-472.

Gagnadoux, F., J. Hureaux, et al.. (2008). "Aerosolized chemotherapy." J Aerosol Med Pulm Drug Deliv 21(1): 61-70.

Gagnadoux, F., A. Le Pape, et al.. (2005). "Safety of pulmonary administration of gemcitabine in rats." Journal of Aerosol Medicine-Deposition Clearance and Effects in the Lung 18(2): 198-206.

Gagnadoux, F., V. Leblond, et al.. (2006). "Gemcitabine aerosol: in vitro antitumor activity and deposition imaging for preclinical safety assessment in baboons." Cancer Chemotherapy and Pharmacology 58(2): 237-244.

Gagnadoux, F., A. L. Pape, et al.. (2005). "Aerosol delivery of chemotherapy in an orthotopic model of lung cancer." Eur Respir J 26(4): 657-661.

Ganguly, S., V. Moolchandani, et al.. (2008). "Phospholipid-Induced In Vivo Particle Migration to Enhance Pulmonary Deposition." Journal of Aerosol Medicine and Pulmonary Drug Delivery 21(4): 343-350.

Gaonkar, A. G. and R. D. Neuman (1987). "The Uncertainty in Absolute Values of Surface Tension of Water." Colloids and Surfaces 27(1-3): 1-14.

Gaspar, M. M., U. Bakowsky, et al.. (2008). "Inhaled Liposomes-Current Strategies and Future Challenges." Journal of Biomedical Nanotechnology 4(3): 245-257.

Geller, D., J. Thipphawong, et al.. (2003). "Bolus inhalation of rhDNase with the AERx system in subjects with cystic fibrosis." Journal of Aerosol Medicine-Deposition Clearance and Effects in the Lung 16(2): 175-182.

Geller, D. E. (2008). "The science of aerosol delivery in cystic fibrosis." Pediatric Pulmonology 43(9): S5-S17.

Geller, D. E., H. Eigen, et al.. (1998). "Effect of smaller droplet size of dornase alfa on lung function in mild cystic fibrosis." Pediatric Pulmonology 25(2): 83-87.

Ghazanfari, T., A. M. A. Elhissi, et al.. (2007). "The influence of fluid physicochemical properties on vibrating-mesh nebulization." International Journal of Pharmaceutics 339(1-2): 103-111.

Ghodrat, M. (2006). "Lung surfactants." American Journal of Health-System Pharmacy 63(16): 1504-1521.

Gilbert, B. E., A. Seryshev, et al.. (2002). "9-nitrocamptothecin liposome aerosol: Lack of subacute toxicity in dogs." Inhalation Toxicology 14(2): 185-197.

Glover, W., H.-K. Chan, et al.. (2008). "Effect of particle size of dry powder mannitol on the lung deposition in healthy volunteers." Int J Pharm 349(1-2): 314-22.

Glover, W., H. K. Chan, et al.. (2006). "Lung deposition of mannitol powder aerosol in healthy subjects." Journal of Aerosol Medicine-Deposition Clearance and Effects in the Lung 19(4): 522-532.

Goldberg, J., E. Freund, et al.. (2001). "Improved delivery of fenoterol plus ipratropium bromide using Respimat (R) compared with a conventional metered dose inhaler." European Respiratory Journal 17(2): 225-232.

Gonda, I. (2004). Targeting by Deposition. Pharmaceutical Inhalation Aerosol Technology. A. J. Hickey. New York, New York, USA., Marcel Dekker, Inc. 54: 65-88.

Gonda, I., J. A. Schuster, et al.. (1998). "Inhalation delivery systems with compliance and disease management capabilities." Journal of Controlled Release 53(1-3): 269-274.

Govindan, R., N. Page, et al.. (2006). "Changing Epidemiology of Small-Cell Lung Cancer in the United States Over the Last 30 Years: Analysis of the Surveillance, Epidemiologic, and End Results Database." J Clin Oncol 24(28): 4539-4544.

Guenther, K. J., S. Yoganathan, et al.. (2006). "Synthesis and in vitro evaluation of F-18- and F-19-labeled insulin: A new radiotracer for PET-based molecular imaging studies." Journal of Medicinal Chemistry 49(4): 1466-1474.

Gupta, R., M. Hindle, et al.. (2001). Solute and Concentration Effects in a Novel Pharmaceutical Condensation Aerosol Generator. AAPS PharmSci.

Gupta, R., M. Hindle, et al.. (2001). Vehicle Effects On The Performance Of A Novel Pharmaceutical Condensation Aerosol Generator. AAPS PharmSci.

Gurkan, A. S., Bozdag – Dundar, O. (2005). "Coenzyme Q10." J. Fac. Pharm, Ankara 34(2): 129-154.

Gurses, B. K. and G. C. Smaldone (2003). "Effect of tubing deposition, breathing pattern, and temperature on aerosol mass distribution measured by cascade impactor." Journal of Aerosol Medicine-Deposition Clearance and Effects in the Lung 16(4): 387-394.

Hande, K. R. (1998). "Etoposide: Four decades of development of a topoisomerase II inhibitor." European Journal of Cancer 34(10): 1514-1521.

Hansch, C., A. Leo, et al.. (1995). Exploring QSAR: Volume 2: Hydrophobic, Electronic, and Steric Constants. Washington, DC, An American Chemical Society Publication.

Hardaker, L. E. A. and R. H. M. Hatley (2010). "In Vitro Characterization of the I-neb Adaptive Aerosol Delivery (AAD) System." Journal of Aerosol Medicine and Pulmonary Drug Delivery 23: S11-S20.

Harkins, W. D. and H. F. Jordan (1930). "A Method for the Determination of Surface and Interfacial Tension from the Maximum Pull on a Ring." Journal of the American Chemical Society 52(5): 1751-1772.

Harris, K., L. Morra, et al.. (2007). In vitro effects of vibrating mesh nebulization and radiopharmaceuticals on interferon gamma. European Respiratory Society.

Hatefi, A. and B. Amsden (2002). "Camptothecin delivery methods." Pharmaceutical Research 19(10): 1389-1399.

Haughney, J., D. Price, et al.. (2010). "Choosing inhaler devices for people with asthma: current knowledge and outstanding research needs." Respiratory medicine 104(9): 1237-45.

Haynes, A., M. S. Shaik, et al.. (2003). "Evaluation of an aerosolized selective COX-2 inhibitor as a potentiator of doxorubicin in a non-small-cell lung cancer cell line." Pharmaceutical Research 20(9): 1485-1495.

Haynes, A., M. S. Shaik, et al.. (2005). "Formulation and evaluation of aerosolized celecoxib for the treatment of lung cancer." Pharmaceutical Research 22(3): 427-439.

Heinemann, L. (2011). "New ways of insulin delivery." International Journal of Clinical Practice 65: 31-46.

Hershey, A. E., I. D. Kurzman, et al.. (1999). "Inhalation Chemotherapy for Macroscopic Primary or Metastatic Lung Tumors: Proof of Principle Using Dogs with Spontaneously Occurring Tumors as a Model." Clin Cancer Res 5(9): 2653-2659.

Hertz, N. and R. E. Lister (2009). "Improved Survival in Patients with End-stage Cancer Treated with Coenzyme Q(10) and Other Antioxidants: a Pilot Study." Journal of International Medical Research 37(6): 1961-1971.

Hindle, M., Byron, P.R., Jashnani, R.N., Howell, T.M., Cox, K.A. (1998). High Efficiency Fine Particle Generation using Novel Condensation Technology. Respiratory Drug Delivery VI, Hilton Head, SC, USA, Interpharm Press, Buffalo Grove, IL, USA.

Hinds, W. C. (1999). Respiratory Deposition. Aerosol technology: properties, behavior, and measurement of airborne particles. W. C. Hinds. New York, Wiley: 233-259.

Hintze, J. (2001). NCSS and PASS. Kaysville, UT, USA, Number Cruncher Statistical Systems.

Hitzman, C. J., W. F. Elmquist, et al.. (2006). "Development of a respirable, sustained release microcarrier for 5-fluorouracil I: In vitro assessment of liposomes, microspheres, and lipid coated nanoparticles." Journal of Pharmaceutical Sciences 95(5): 1114-1126.

Hitzman, C. J., L. W. Wattenberg, et al.. (2006). "Pharmacokinetics of 5-fluorouracil in the hamster following inhalation delivery of lipid-coated nanoparticles." Journal of Pharmaceutical Sciences 95(6): 1196-1211.

Hochrainer, D., H. Holz, et al.. (2005). "Comparison of the aerosol velocity and spray duration of Respimat (R) Soft Mist (TM) Inhaler and pressurized metered dose inhalers." Journal of Aerosol Medicine-Deposition Clearance and Effects in the Lung 18(3): 273-282.

Hodder, R., D. Pavia, et al.. (2005). "Low incidence of paradoxical bronchoconstriction in asthma and COPD patients during chronic use of Respimat (R) soft mist (TM) inhaler." Respiratory Medicine 99(9): 1087-1095.

Hong, J. N., M. Hindle, et al.. (2002). "Control of particle size by coagulation of novel condensation aerosols in reservoir chambers." Journal of Aerosol Medicine-Deposition Clearance and Effects in the Lung 15(4): 359-368.

Hornby, J. M., E. C. Jensen, et al.. (2001). "Quorum sensing in the dimorphic fungus Candida albicans is mediated by farnesol." Applied and Environmental Microbiology 67(7): 2982-2992.

Hotta, K., K. Matsuo, et al.. (2006). "Advances in our understanding of postoperative adjuvant chemotherapy in resectable non-small-cell lung cancer." Current Opinion in Oncology 18(2): 144-150.

Howell, T. M. and W. R. Sweeney (1998). Aerosol and a Method and Apparatus for Generating Aerosol. USPTO. USA, Philip Morris Incorporated. New York, N.Y.: 14.

Iacono, P., P. Velicitat, et al.. (2000). "Improved delivery of ipratropium bromide using Respimat (R) (a new soft mist inhaler) compared with a conventional metered dose inhaler: cumulative dose response study in patients with COPD." Respiratory Medicine 94(5): 490-495.

Ijsebaert, J. C., K. B. Geerse, et al.. (2001). "Electro-hydrodynamic atomization of drug solutions for inhalation purposes." Journal of Applied Physiology 91(6): 2735-2741.

Iozzo, P., S. Osman, et al.. (2002). "In vivo imaging of insulin receptors by PET: preclinical evaluation of iodine-125 and iodine-124 labelled human insulin." Nuclear Medicine and Biology 29(1): 73-82.

Islam, N. and E. Gladki (2008). "Dry powder inhalers (DPIs) - A review of device reliability and innovation." International Journal of Pharmaceutics 360(1-2): 1-11.

Jaafar-Maalej, C., V. Andrieu, et al.. (2009). "Assessment methods of inhaled aerosols: technical aspects and applications." Expert Opinion on Drug Delivery 6(9): 941-959.

Jaworek, A. (2008). "Electrostatic micro- and nanoencapsulation and electroemulsification: A brief review." Journal of Microencapsulation 25(7): 443-468.

Jayasinghe, S. N. and M. J. Edirisinghe (2005). "Jet break-up in nano-suspensions during electrohydrodynamic atomization in the stable cone-jet mode." Journal of Nanoscience and Nanotechnology 5(6): 923-926.

Jin, Y. L., J. Y. Chen, et al.. (2006). "Refractive index measurement for biomaterial samples by total internal reflection." Physics in Medicine and Biology 51(20): N371-N379.

Joel, S. P., P. I. Clark, et al.. (1995). "PHARMACOLOGICAL ATTEMPTS TO IMPROVE THE BIOAVAILABILITY OF ORAL ETOPOSIDE." Cancer Chemotherapy and Pharmacology 37(1-2): 125-133.

Johnson, J. C., J. C. Waldrep, et al.. (2008). "Aerosol Delivery of Recombinant Human DNase I: In Vitro Comparison of a Vibrating-Mesh Nebulizer With a Jet Nebulizer." Respiratory Care 53(12): 1703-1708.

Joo, J. H., G. Liao, et al.. (2007). "Farnesol-induced apoptosis in human lung carcinoma cells is coupled to the endoplasmic reticulum stress response." Cancer Research 67(16): 7929-7936.

Julius, S. M., J. M. Sherman, et al.. (2002). "Accuracy of three electronic monitors for metered-dose inhalers." Chest 121(3): 871-876.

Jung, J. H. (2011). "Electrohydrodynamic nano-spraying of ethanolic natural plant extracts." Journal of Aerosol Science 42(10): 725-736.

Kallay, N., T. Preocanin, et al.. (2010). "Electrostatic Potentials at Solid/Liquid Interfaces." Croatica Chemica Acta 83(3): 357-370.

Kato, T., T. Yashiro, et al.. (2003). "Evidence that exogenous substances can be phagocytized by alveolar epithelial cells and transported into blood capillaries." Cell and Tissue Research 311(1): 47-51.

Kawaguchi, E., K. Shimokawa, et al.. (2008). "Physicochemical properties of structured phosphatidylcholine in drug carrier lipid emulsions for drug delivery systems." Colloids and Surfaces B-Biointerfaces 62(1): 130-135.

Kerstjens, H. A. M., B. Disse, et al.. (2011). "Tiotropium improves lung function in patients with severe uncontrolled asthma: A randomized controlled trial." Journal of Allergy and Clinical Immunology 128(2): 308-314.

Kesser, K. C. and D. E. Geller (2009). "New Aerosol Delivery Devices for Cystic Fibrosis." Respiratory Care 54(6): 754-767.

Khatri, L., K. M. G. Taylor, et al.. (2001). "An assessment of jet and ultrasonic nebulisers for the delivery of lactate dehydrogenase solutions." International Journal of Pharmaceutics 227(1-2): 121-131.

Kilfeather, S. A., H. H. Ponitz, et al.. (2004). "Improved delivery of ipratropium bromide/fenoterol from Respimat (R) Soft Mist (TM) Inhaler in patients with COPD." Respiratory Medicine 98(5): 387-397.

Kim, C. K. and S. J. Lim (2002). "Recent progress in drug delivery systems for anticancer agents." Archives of Pharmacal Research 25(3): 229-239.

Kim, C. S. and P. A. Jaques (2005). "Total lung deposition of ultrafine particles in elderly subjects during controlled breathing." Inhalation Toxicology 17(7-8): 387-399.

Kleeberger, L. and E. M. Rottinger (1993). "EFFECT OF PH AND MODERATE HYPERTHERMIA ON DOXORUBICIN, EPIRUBICIN AND ACLACINOMYCIN-A CYTOTOXICITY FOR CHINESE-HAMSTER OVARY CELLS." Cancer Chemotherapy and Pharmacology 33(2): 144-148.

Kleinstreuer, C., Z. Zhang, et al.. (2008). "Targeted drug-aerosol delivery in the human respiratory system." Annual Review of Biomedical Engineering 10: 195-220.

Knight, V., E. S. Kleinerman, et al.. (2000). "9-Nitrocamptothecin Liposome Aerosol Treatment of Human Cancer Subcutaneous Xenografts and Pulmonary Cancer Metastases in Mice." Annals of the New York Academy of Sciences 922(1): 151-163.

Knight, V., N. V. Koshkina, et al.. (2004). "Cyclosporin a aerosol improves the anticancer effect of Paclitaxel aerosol in mice." Trans Am Clin Climatol Assoc 115: 395-404.

Knight, V., N. V. Koshkina, et al.. (1999). "Anticancer exffect of 9-nitrocamptothecin liposome aerosol on human cancer xenografts in nude mice." Cancer Chemotherapy and Pharmacology 44(3): 177-186.

Koehler, D., D. Pavia, et al.. (2004). "Low incidence of paradoxical bronchoconstriction with bronchodilator drugs administered by Respimat (R) Soft Mist (TM) Inhaler: Results of phase II single-dose crossover studies." Respiration 71(5): 469-476.

Koehler, E., V. Sollich, et al.. (2003). "Lung Deposition in Cystic Fibrosis Patients Using an Ultrasonic or a Jet Nebulizer." Journal of Aerosol Medicine 16(1): 37-46.

Koshkina, N. V., B. E. Gilbert, et al.. (1999). "Distribution of camptothecin after delivery as a liposome aerosol or following intramuscular injection in mice." Cancer Chemotherapy and Pharmacology 44(3): 187-192.

Koshkina, N. V. and E. S. Kleinerman (2005). "Aerosol gemcitabine inhibits the growth of primary osteosarcoma and osteosarcoma lung metastases." International Journal of Cancer 116(3): 458-463.

Koshkina, N. V., V. Knight, et al.. (2001). "Improved respiratory delivery of the anticancer drugs, camptothecin and paclitaxel, with 5% CO2-enriched air: pharmacokinetic studies." Cancer Chemotherapy and Pharmacology 47(5): 451-456.

Koshkina, N. V., J. C. Waldrep, et al.. (2003). "Camptothecins and lung cancer: Improved delivery systems by aerosol." Current Cancer Drug Targets 3(4): 251-264.

Koshkina, N. V., J. C. Waldrep, et al.. (2001). "Paclitaxel Liposome Aerosol Treatment Induces Inhibition of Pulmonary Metastases in Murine Renal Carcinoma Model." Clin Cancer Res 7(10): 3258-3262.

Kumbar, S. G., S. Bhattacharyya, et al.. (2007). "A preliminary report on a novel electrospray technique for nanoparticle based biomedical implants coating: Precision electrospraying." Journal of Biomedical Materials Research Part B-Applied Biomaterials 81B(1): 91-103.

Kunkel, G., H. Magnussen, et al.. (2000). "Respimat (R) (a new soft mist inhaler) delivering fenoterol plus ipratropium bromide provides equivalent bronchodilation at half the cumulative dose compared with a conventional metered dose inhaler in asthmatic patients." Respiration 67(3): 306-314.

Labiris, N. R. and M. B. Dolovich (2003). "Pulmonary drug delivery. Part I: Physiological factors affecting therapeutic effectiveness of aerosolized medications." British Journal of Clinical Pharmacology 56(6): 588-599.

Labiris, N. R. and M. B. Dolovich (2003). "Pulmonary drug delivery. Part II: The role of inhalant delivery devices and drug formulations in therapeutic effectiveness of aerosolized medications." British Journal of Clinical Pharmacology 56(6): 600-612.

Lalloo, U. G., A. J. Fox, et al.. (1995). "CAPSAZEPINE INHIBITS COUGH INDUCED BY CAPSAICIN AND CITRIC-ACID BUT NOT BY HYPERTONIC SALINE IN GUINEA-PIGS." Journal of Applied Physiology 79(4): 1082-1087.

Lasch, J., V. Weissig, et al.. (2003). Preparation of Liposomes. Liposomes: a practical approach. V. P. Torchilin and V. Weissig. Oxford, UK, Oxford University Press: 3-29.

Lass, J. S., A. Sant, et al.. (2006). "New advances in aerosolised drug delivery: vibrating membrane nebuliser technology." Expert Opinion on Drug Delivery 3(5): 693-702.

Leach, C. L., P. J. Davidson, et al.. (1998). "Improved airway targeting with the CFC-free HFA-beclomethasone metered-dose inhaler compared with CFC-beclomethasone." European Respiratory Journal 12(6): 1346-1353.

Leach, C. L., P. J. Davidson, et al.. (2005). "Influence of particle size and patient dosing technique on lung deposition of HFA-beclomethasone from a metered dose inhaler." Journal of Aerosol Medicine-Deposition Clearance and Effects in the Lung 18(4): 379-385.

Leclerc, V., M. Lafferre, et al.. (2007). "Acute local tolerability of acidic aqueous vehicles delivered via Respimat (R) soft Mist(TM) inhaler in hyperreactive asthma patients." Respiration 74(6): 691-696.

Lentz, Y. K., T. J. Anchordoquy, et al.. (2006). "Rationale for the selection of an aerosol delivery system for gene delivery." Journal of Aerosol Medicine-Deposition Clearance and Effects in the Lung 19(3): 372-384.

Leung, K., D. Louca, et al.. (2004). "Comparison of breath-enhanced to breath-actuated nebulizers for rate, consistency, and efficiency." Chest 126(5): 1619-1627.

Li, C. B., P. L. Shi, et al.. (2010). "Tracing processes of rigor mortis and subsequent resolution of chicken breast muscle using a texture analyzer." Journal of Food Engineering 100(3): 388-391.

Li, H., J. R. Friend, et al.. (2007). "Surface acoustic wave concentration of particle and bioparticle suspensions." Biomedical Microdevices 9(5): 647-656.

Li, X. H., F. E. Blondino, et al.. (2005). "Stability and characterization of perphenazine aerosols generated using the capillary aerosol generator." International Journal of Pharmaceutics 303(1-2): 113-124.

Li, Z. L., Y. L. Zhang, et al.. (2008). "Characterization of nebulized liposomal amikacin (Arikace (TM)) as a function of droplet size." Journal of Aerosol Medicine and Pulmonary Drug Delivery 21(3): 245-253.

Longer, M. (2006). Rheology. Martin's physical pharmacy and pharmaceutical sciences. P. J. Sinko. Baltimore, MD, Lippincott Williams & Wilkins: 561-583.

Longest, P. W. and M. Hindle (2009). "Evaluation of the Respimat Soft Mist Inhaler using a Concurrent CFD and In Vitro Approach." Journal of Aerosol Medicine and Pulmonary Drug Delivery 22(2): 99-112.

Lou, Y. P. and J. M. Lundberg (1992). "INHIBITION OF LOW PH EVOKED ACTIVATION OF AIRWAY SENSORY NERVES BY CAPSAZEPINE, A NOVEL CAPSAICIN-RECEPTOR ANTAGONIST." Biochemical and Biophysical Research Communications 189(1): 537-544.

Lu, S., J. J. Chen, et al.. (2011). "Water mobility, rheological and textural properties of rice starch gel." Journal of Cereal Science 53(1): 31-36.

Lyklema, J. (2010). "Molecular interpretation of electrokinetic potentials." Current Opinion in Colloid & Interface Science 15(3): 125-130.

Mabrey, S. and J. M. Sturtevant (1976). "INVESTIGATION OF PHASE-TRANSITIONS OF LIPIDS AND LIPID MIXTURES BY HIGH SENSITIVITY DIFFERENTIAL SCANNING CALORIMETRY." Proceedings of the National Academy of Sciences of the United States of America 73(11): 3862-3866.

MacNeish, C. F., D. Meisner, et al.. (1997). "A comparison of pulmonary availability between ventolin (albuterol) nebules and ventolin (albuterol) respirator solution." Chest 111(1): 204-208.

Majzoobi, M., R. Ostovan, et al.. (2011). "Effects of Hydroxypropyl Cellulose on the Quality of Wheat Flour Spaghetti." Journal of Texture Studies 42(1): 20-30.

Malcolmson, R. J. and J. K. Embleton (1998). "Dry powder formulations for pulmonary delivery." Pharmaceutical Science & Technology Today 1(9): 394-398.

Mallol, J., S. Rattray, et al.. (1996). "Aerosol deposition in infants with cystic fibrosis." Pediatric Pulmonology 21(5): 276-281.

Marple, V. A., B. A. Olson, et al.. (2004). "Next generation pharmaceutical impactor: A new impactor for pharmaceutical inhaler testing. Part III. Extension of archival calibration to 15 L/min." Journal of Aerosol Medicine-Deposition Clearance and Effects in the Lung 17(4): 335-343.

Marple, V. A., D. L. Roberts, et al.. (2003). "Next generation pharmaceutical impactor (A new impactor for pharmaceutical inhaler testing). Part I: Design." Journal of Aerosol Medicine-Deposition Clearance and Effects in the Lung 16(3): 283-299.

Martin, A. R., R. B. Thompson, et al.. (2008). "MRI Measurement of Regional Lung Deposition in Mice Exposed Nose-Only to Nebulized Superparamagnetic Iron Oxide Nanoparticles." Journal of Aerosol Medicine and Pulmonary Drug Delivery 21(4): 335-341.

Martin, R. J. (2002). "Therapeutic significance of distal airway inflammation in asthma." Journal of Allergy and Clinical Immunology 109(2): S447-S460.

Martonen, T., J. Fleming, et al.. (2003). "In silico modeling of asthma." Advanced Drug Delivery Reviews 55(7): 829-849.

Martonen, T., K. Isaacs, et al.. (2005). "Three-dimensional simulations of airways within human lungs." Cell Biochemistry and Biophysics 42(3): 223-249.

Martonen, T. B., J. D. Schroeter, et al.. (2007). "3D in silico modeling of the human respiratory system for inhaled drug delivery and imaging analysis." Journal of Pharmaceutical Sciences 96(3): 603-617.

Marupudi, N. I., J. E. Han, et al.. (2007). "Paclitaxel: a review of adverse toxicities and novel delivery strategies." Expert Opinion on Drug Safety 6(5): 609-621.

Mastrandrea, L. D. and T. Quattrin (2006). "Clinical evaluation of inhaled insulin." Advanced Drug Delivery Reviews 58(9-10): 1061-1075.

Mather, L. E., Kam, P.C., Morishige, R.J., Otulana, B.A., Dayton, F., Rubsamen, R.M. (2000). "Pharmacokinetics of Orally Inhaled Fentanyl in Healthy Subjects." The Journal of Clinical Pharmacology 40(9): 1060.

McCallion, O. N. M. and M. J. Patel (1996). "Viscosity effects on nebulisation of aqueous solutions." International Journal of Pharmaceutics 130(2): 245-249.

McCallion, O. N. M., K. M. G. Taylor, et al.. (1996). "Jet nebulisers for pulmonary drug delivery." International Journal of Pharmaceutics 130(1): 1-11.

McCallion, O. N. M., K. M. G. Taylor, et al.. (1995). "Nebulization of Fluids of Different Physicochemical Properties with Air-Jet and Ultrasonic Nebulizers." Pharmaceutical Research 12(11): 1682-1688.

McCallion, O. N. M., K. M. G. Taylor, et al.. (1996). "The influence of surface tension on aerosols produced by medical nebulisers." International Journal of Pharmaceutics 129(1-2): 123-136.

McConville, J. T., K. A. Overhoff, et al.. (2006). "Targeted high lung concentrations of itraconazole using nebulized dispersions in a murine model." Pharmaceutical Research 23(5): 901-911.

Mei, X. H., F. M. Etzler, et al.. (2006). "Use of texture analysis to study hydrophilic solvent effects on the mechanical properties of hard gelatin capsules." International Journal of Pharmaceutics 324(2): 128-135.

Mercer, T. T. (1981). "Production of Therapeutic Aerosols - Principles and Techniques." Chest 80(6): 813-818.

Meyer, T., P. Brand, et al.. (2004). "Deposition of Foradil P in human lungs: Comparison of in vitro and in vivo data." Journal of Aerosol Medicine-Deposition Clearance and Effects in the Lung 17(1): 43-49.

Meyer, T., B. Muellinger, et al.. (2003). "Pulmonary deposition of monodisperse aerosols in patients with chronic obstructive pulmonary disease." Experimental Lung Research 29(7): 475-484.

Miller, F. J., R. R. Mercer, et al.. (1993). "LOWER RESPIRATORY-TRACT STRUCTURE OF LABORATORY-ANIMALS AND HUMANS - DOSIMETRY IMPLICATIONS." Aerosol Science and Technology 18(3): 257-271.

Minko, T. (2006). Interfacial Phenomena. Martin's physical pharmacy and pharmaceutical sciences. P. J. Sinko. Baltimore, MD, Lippincott Williams & Wilkins: 437-467.

Mitchell, J., R. Bauer, et al.. (2011). "Non-impactor-Based Methods for Sizing of Aerosols Emitted from Orally Inhaled and Nasal Drug Products (OINDPs)." AAPS PharmSciTech 12(3): 965-988.

Mitchell, J., S. Newman, et al.. (2007). "In Vitro and In Vivo Aspects of Cascade Impactor Tests and Inhaler Performance: A Review." Aaps Pharmscitech 8(4).

Mitchell, J. P., M.W. Nagel (2004). "Particle size analysis of aerosols from medicinal inhalers." KONA Powder and Particle 22: 32-65.

Mitchell, J. P. and M. W. Nagel (2003). "Cascade impactors for the size characterization of aerosols from medical inhalers: Their uses and limitations." Journal of Aerosol Medicine-Deposition Clearance and Effects in the Lung 16(4): 341-+.

Mitchell, J. P., M. W. Nagel, et al.. (2006). "Laser diffractometry as a technique for the rapid assessment of aerosol particle size from inhalers." Journal of Aerosol Medicine-Deposition Clearance and Effects in the Lung 19(4): 409-433.

Mogalian, E. and P. B. Myrdal (2007). Solvent systems and their selection in pharmaceutics and biopharmaceutics. P. Augustijns and M. Brewster, Springer; AAPS PRESS. VI: 427-441.

Moller, W., K. Felten, et al.. (2009). "Corrections in Dose Assessment of Tc-99m Radiolabeled Aerosol Particles Targeted to Central Human Airways Using Planar Gamma Camera Imaging." Journal of Aerosol Medicine and Pulmonary Drug Delivery 22(1): 45-54.

Moller, W., G. Meyer, et al.. (2009). "Left-to-Right Asymmetry of Aerosol Deposition after Shallow Bolus Inhalation Depends on Lung Ventilation." Journal of Aerosol Medicine and Pulmonary Drug Delivery 22(4): 333-339.

Montharu, J., S. Le Guellec, et al.. (2010). "Evaluation of Lung Tolerance of Ethanol, Propylene Glycol, and Sorbitan Monooleate as Solvents in Medical Aerosols." Journal of Aerosol Medicine and Pulmonary Drug Delivery 23(1): 41-46.

Moses, R. G., P. Bartley, et al.. (2009). "Safety and efficacy of inhaled insulin (AERx((R)) iDMS(1)) compared with subcutaneous insulin therapy in patients with Type 1 diabetes: 1-year data from a randomized, parallel group trial." Diabetic Medicine 26(3): 260-267.

Mountain, C. F. (1997). "Revisions in the International System for Staging Lung Cancer." Chest 111(6): 1710-1717.

Mudaliar, S. (2007). "Inhaled insulin using AERx (R) insulin diabetes management system (AERx (R) iDMS)." Expert Opinion on Investigational Drugs 16(10): 1673-1681.

Munnik, P., A. H. de Boer, et al.. (2009). "In Vivo Performance Testing of the Novel Medspray (R) Wet Aerosol Inhaler." Journal of Aerosol Medicine and Pulmonary Drug Delivery 22(4): 317-321.

Murariu, M., E. S. Dragan, et al.. (2010). "Model Peptide-Based System Used for the Investigation of Metal Ions Binding to Histidine-Containing Polypeptides." Biopolymers 93(6): 497-508.

Myrdal, P. B., K. L. Karlage, et al.. (2004). "Optimized dose delivery of the peptide cyclosporine using hydrofluoroalkane-based metered dose inhalers." Journal of Pharmaceutical Sciences 93(4): 1054-1061.

Nagvekar, A. A., W. J. Trickler, et al.. (2009). "Current Analytical Methods Used in the In Vitro Evaluation of Nano-Drug Delivery Systems." Current Pharmaceutical Analysis 5(4): 358-366.

Narain, N. R., J. Li, et al.. (2004). "Coenzyme Q10 inhibits the proliferation of oncogenic cells while stabilizing growth in primary cells in vitro." Journal of Investigative Dermatology 122(3): 167.

Narain, N. R., J. Li, et al.. (2004). "Coenzyme Q10 induces apoptosis in human melanoma cells." Journal of Investigative Dermatology 122(3): 958.

Newman, S., S. Malik, et al.. (2002). "Lung deposition of salbutamol in healthy human subjects from the MAGhaler dry powder inhaler." Respiratory Medicine 96(12): 1026-1032.

Newman, S. P. (1993). "Scintigraphic assessment of therapeutic aerosols." Critical reviews in therapeutic drug carrier systems 10(1): 65-109.

Newman, S. P. and H. K. Chan (2008). "In vitro/in vivo comparisons in pulmonary drug delivery." Journal of Aerosol Medicine and Pulmonary Drug Delivery 21(1): 77-84.

Newman, S. P., G. R. Pitcairn, et al.. (2003). "Radionuclide imaging technologies and their use in evaluating asthma drug deposition in the lungs." Advanced Drug Delivery Reviews 55(7): 851-867.

Newman, S. P., K. P. Steed, et al.. (2007). "An in vitro study to assess facial and ocular deposition from Respimat (R) Soft Mist (TM) inhaler." Journal of Aerosol Medicine-Deposition Clearance and Effects in the Lung 20(1): 7-12.

Newman, S. P. and I. R. Wilding (1999). "Imaging techniques for assessing drug delivery in man." Pharmaceutical Science & Technology Today 2(5): 181-189.

Nietz, A. H. and R. H. Lambert (1929). "Effect of Some Factors on the Ring Method for determining Surface Tension." The Journal of Physical Chemistry 33(10): 1460-1467.

Nikander, K., M. Turpeinen, et al.. (1999). "The conventional ultrasonic nebulizer proved inefficient in nebulizing a suspension." Journal of Aerosol Medicine-Deposition Clearance and Effects in the Lung 12(2): 47-53.

NIOSH (2005). Strategic Plan for NIOSH Nanotechnology Research and Guidance - Filling the Knowledge Gap, Nanotechnology Research Program, Centers for Disease Control and Prevention, National Institute for Occupational Safety and Health. Draft: 103.

Niven, R. W., S. J. Prestrelski, et al.. (1996). "Protein nebulization .2. Stabilization of G-CSF to air-jet nebulization and the role of protectants." International Journal of Pharmaceutics 127(2): 191-201.

Ocallaghan, C., A. R. Clarke, et al.. (1989). "Inaccurate Calculation of Drug Output from Nebulizers." European Journal of Pediatrics 148(5): 473-474.

Okumu, F. W., R. Y. Lee, et al.. (2002). "Evaluation of the AERx pulmonary delivery system for systemic delivery of a poorly soluble selective D-1 agonist, ABT-431." Pharmaceutical Research 19(7): 1009-1012.

Ondarroa, M., S. K. Sharma, et al.. (1986). "Solvation properties of ubiquinone-10 in solvents of different polarity." Biosci Rep 6(9): 783-96.

Osman, R., P. L. Kan, et al.. (2011). "Enhanced properties of discrete pulmonary deoxyribonuclease I (DNaseI) loaded PLGA nanoparticles during encapsulation and activity determination." International Journal of Pharmaceutics 408(1-2): 257-265.

Otterson, G. A., M. A. Villalona-Calero, et al.. (2007). "Phase I study of inhaled doxorubicin for patients with metastatic tumors to the lungs." Clinical Cancer Research 13(4): 1246-1252.

Otulana, B., J. Okikawa, et al.. (2004). "Safety and pharmacokinetics of inhaled morphine delivered using the AERx System in patients with moderate-to-severe asthma." International Journal of Clinical Pharmacology and Therapeutics 42(8): 456-462.

Owens, D. R., B. Zinman, et al.. (2003). "Alternative routes of insulin delivery." Diabetic Medicine 20(11): 886-898.

Packhaeuser, C. B., K. Lahnstein, et al.. (2009). "Stabilization of Aerosolizable Nano-carriers by Freeze-Drying." Pharmaceutical Research 26(1): 129-138.

Padday, J. F., A. R. Pitt, et al.. (1975). "Menisci at a Free Liquid Surface - Surface Tension from Maximum Pull on a Rod." Journal of the Chemical Society-Faraday Transactions I 71: 1919-1931.

Pallas, N. R. and B. A. Pethica (1983). "The Surface Tension of Water." Colloids and Surfaces 6(3): 221-227.

Pardeike, J., S. Weber, et al.. (2011). "Development of an Itraconazole-loaded nanostructured lipid carrier (NLC) formulation for pulmonary application." International Journal of Pharmaceutics.

Pareta, R., A. Brindley, et al.. (2005). "Electrohydrodynamic atomization of protein (bovine serum albumin)." Journal of Materials Science-Materials in Medicine 16(10): 919-925.

Partridge, A. H., J. Avorn, et al.. (2002). "Adherence to therapy with oral antineoplastic agents." Journal of the National Cancer Institute 94(9): 652-661.

Patel, K. R., D. Pavia, et al.. (2006). "Inhaled ethanolic and aqueous solutions via respimat soft mist inhaler are well-tolerated in asthma patients." Respiration 73(4): 434-440.

Patton, J. S., C. S. Fishburn, et al.. (2004). "The lungs as a portal of entry for systemic drug delivery." Proc Am Thorac Soc 1(4): 338-44.

Phalen, R. F. (2008). Inhalation Studies: Foundations and Techniques. R. F. Phalen. New York, NY, USA, Informa Health Care: 187-214.

Phalen, R. F. (2008). The Respiractory Tract. Inhalation Studies: Foundations and Techniques. R. F. Phalen. New York, NY, USA, Informa Health Care: 33-68.

Pickering, H., G. R. Pitcairn, et al.. (2000). "Regional lung deposition of a technetium 99m-labeled formulation of mometasone furoate administered by hydrofluoroalkane 227 metered-dose inhaler." Clinical Therapeutics 22(12): 1483-1493.

Pignon, J. P., R. Arriagada, et al.. (1992). "A METAANALYSIS OF THORACIC RADIOTHERAPY FOR SMALL-CELL LUNG-CANCER." New England Journal of Medicine 327(23): 1618-1624.

Pilcer, G. and K. Amighi (2010). "Formulation strategy and use of excipients in pulmonary drug delivery." International Journal of Pharmaceutics 392(1-2): 1-19.

Pilcer, G., F. Vanderbist, et al.. (2008). "Correlations between cascade impactor analysis and laser diffraction techniques for the determination of the particle size of aerosolised powder formulations." International Journal of Pharmaceutics 358(1-2): 75-81.

Pili, B., C. Bourgaux, et al.. (2009). "Interaction of an anticancer drug, gemcitabine, with phospholipid bilayers." Journal of Thermal Analysis and Calorimetry 98(1): 19-28.

Pinto, L., A. Sloan, et al.. (2009). "Normalization of BCL-2 Family Members in Breast Cancer by Coenzyme Q10." Ethnicity & Disease 19(2): S17-S18.

Pitance, L., Vecellio, L., Leal, T., Reychler, G., Reychler, H., Liistro, G. (2010). "Delivery Efficacy of a Vibrating Mesh Nebulizer and a Jet Nebulizer under Different Configurations." Journal of Aerosol Medicine and Pulmonary Drug Delivery 23(6): 389-396.

Pitcairn, G., S. Reader, et al.. (2005). "Deposition of corticosteroid aerosol in the human lung by Respimat (R) Soft Mist (TM) Inhaler compared to deposition by metered dose inhaler or by Turbuhaler (R) dry powder inhaler." Journal of Aerosol Medicine-Deposition Clearance and Effects in the Lung 18(3): 264-272.

Posther, K. E. and D. H. Harpole (2006). "The surgical management of lung cancer." Cancer Investigation 24(1): 56-67.

Prokop, R. M., W. H. Finlay, et al.. (1995). "AN IN-VITRO TECHNIQUE FOR CALCULATING THE REGIONAL DOSAGES OF DRUGS DELIVERED BY AN ULTRASONIC NEBULIZER." Journal of Aerosol Science 26(5): 847-860.

Qi, A., L. Yeo, et al.. (2009). "The extraction of liquid, protein molecules and yeast cells from paper through surface acoustic wave atomization." Lab on a Chip 10(4): 470-476.

Qi, A., L. Y. Yeo, et al.. (2008). "Interfacial destabilization and atomization driven by surface acoustic waves." Physics of Fluids 20(7).

Qi, A. S., J. R. Friend, et al.. (2009). "Miniature inhalation therapy platform using surface acoustic wave microfluidic atomization." Lab on a Chip 9(15): 2184-2193.

Randall, C. (1995). Particle Size Distribution. Physical characterization of pharmaceutical solids. H. G. Brittain. New York, NY, M. Dekker. 70: 157-186.

Rautio, J. and P. J. Chikhale (2004). "Drug delivery systems for brain tumor therapy." Current Pharmaceutical Design 10(12): 1341-1353.

Rayleigh, L. (1878). "On the Instability of Jets." Proceedings of the London Mathematical society 10: 4-13.

Richards, T. W. and E. K. Carver (1921). "A Critical Study of the Capillary Rise Method of Determining Surface Tension, with Data for Water, Benzene, Toluene, Chloroform, Carbon Tetrachloride, Ether and Dimethyl Aniline[Second Paper]." Journal of the American Chemical Society 43(4): 827-847.

Riedel, R. F. and J. Crawford (2003). "Small-cell lung cancer: a review of clinical trials." Seminars in Thoracic and Cardiovascular Surgery 15(4): 448-456.

Rodriguez, C. O., T. A. Crabbs, et al.. (2009). "Aerosol Gemcitabine: Preclinical Safety and In Vivo Antitumor Activity in Osteosarcoma-Bearing Dogs." Journal of Aerosol Medicine and Pulmonary Drug Delivery.

Rosell J., S. J., Liu K., Gonda, I., Srinivassan, S., Deshpande, D. (2001). "Suppression of electrostatic changing of AERx aerosols." Journal of Aerosol Medicine 14(3): 405-405.

Rostami, A. A. (2009). "Computational Modeling of Aerosol Deposition in Respiratory Tract: A Review." Inhalation Toxicology 21(4): 262-290.

Rottier, B. L., C. J. P. van Erp, et al.. (2009). "Changes in Performance of the Pari eFlow (R) Rapid and Pari LC Plus (TM) during 6 Months Use by CF Patients." Journal of Aerosol Medicine and Pulmonary Drug Delivery 22(3): 263-269.

Ruenraroengsak, P., J. M. Cook, et al.. (2009). "Nanosystem drug targeting: Facing up to complex realities." Journal of Controlled Release 141(3): 265-276.

Rusciani, L., I. Proietti, et al.. (2006). "Low plasma coenzyme Q10 levels as an independent prognostic factor for melanoma progression." Journal of the American Academy of Dermatology 54(2): 234-241.

Ruzer, L. S. and M. G. Apte (2010). "Unattached radon progeny as an experimental tool for dosimetry of nanoaerosols: Proposed method and research strategy." Inhalation Toxicology 22(9): 760-766.

Rytting, E., J. Nguyen, et al.. (2008). "Biodegradable polymeric nanocarriers for pulmonary drug delivery." Expert Opinion on Drug Delivery 5(6): 629-639.

Sangwan, S., J. M. Agosti, et al.. (2001). "Aerosolized protein delivery in asthma: Gamma camera analysis of regional deposition and perfusion." Journal of Aerosol Medicine-Deposition Clearance and Effects in the Lung 14(2): 185-195.

Sangwan, S., R. Condos, et al.. (2003). "Lung deposition and respirable mass during wet nebulization." Journal of Aerosol Medicine-Deposition Clearance and Effects in the Lung 16(4): 379-386.

Schanker, L. S. and M. J. Less (1977). "LUNG PH AND PULMONARY ABSORPTION OF NONVOLATILE DRUGS IN RAT." Drug Metabolism and Disposition 5(2): 174-178.

Schlesinger, R. B. (1985). "COMPARATIVE DEPOSITION OF INHALED AEROSOLS IN EXPERIMENTAL-ANIMALS AND HUMANS - A REVIEW." Journal of Toxicology and Environmental Health 15(2): 197-214.

Schmekel, B., H. Hedenstrom, et al.. (2002). "Deposition of terbutaline in the large or small airways: A single-center pilot study of ventilation-perfusion distributions and airway tone." Current Therapeutic Research-Clinical and Experimental 63(9): 536-548.

Schnaare, R. L., L. H. Block, et al.. (2005). Rheology. Remington: The Science and Practice of Pharmacy. R. Hendrickson. Baltimore, MD, Lippincott Williams & Wilkins: 338-357.

Schuepp, K. G., S. Devadason, et al.. (2004). "A complementary combination of delivery device and drug formulation for inhalation therapy in preschool children." Swiss Medical Weekly 134(13-14): 198-200.

Schuepp, K. G., D. Straub, et al.. (2004). "Deposition of aerosols in infants and children." Journal of Aerosol Medicine-Deposition Clearance and Effects in the Lung 17(2): 153-156.

Schulz, M., B. Fussnegger, et al.. (2010). "Drug release and adhesive properties of crospovidone-containing matrix patches based on polyisobutene and acrylic adhesives." European Journal of Pharmaceutical Sciences 41(5): 675-684.

Schuster, J., R. Rubsamen, et al.. (1997). "The AER(X)(TM) aerosol delivery system." Pharmaceutical Research 14(3): 354-357.

Seedher, N. and S. Bhatia (2003). "Solubility enhancement of Cox-2 inhibitors using various solvent systems." AAPS PharmSciTech 4(3): E33.

Shaik, M. S., A. Chatterjee, et al.. (2006). "Enhancement of antitumor activity of docetaxel by celecoxib in lung tumors." International Journal of Cancer 118(2): 396-404.

Shaik, M. S., A. Haynes, et al.. (2002). "Inhalation delivery of HFA-based metered dose anticancer agents via inhaler using methotrexate as a model drug." Journal of Aerosol Medicine-Deposition Clearance and Effects in the Lung 15(3): 261-270.

Sharma, S., D. White, et al.. (2001). "Development of inhalational agents for oncologic use." Journal of Clinical Oncology 19(6): 1839-1847.

Shekunov, B. Y., P. Chattopadhyay, et al.. (2007). "Particle size analysis in pharmaceutics: Principles, methods and applications." Pharmaceutical Research 24(2): 203-227.

Shen, X., A. Hindle, et al.. (2004). "Effect of energy on propylene glycol aerosols using the capillary aerosol generator." International Journal of Pharmaceutics 275(1-2): 249-258.

Shoyele, S. A. and S. Cawthome (2006). "Particle engineering techniques for inhaled biopharmaceuticals." Advanced Drug Delivery Reviews 58(9-10): 1009-1029.

Siekmann, B. and K. Westesen (1995). "Preparation and Physicochemical Characterization of Aqueous Dispersions of Coenzyme Q10 Nanoparticles." Pharmaceutical Research 12(2): 201-208.

Simon, G. R. and H. Wagner (2003). "Small cell lung cancer." Chest 123(1): 259S-271S.

Simonsson, B. G., F. M. Jacobs, et al.. (1967). "ROLE OF AUTONOMIC NERVOUS SYSTEM AND COUGH REFLEX IN INCREASED RESPONSIVENESS OF

AIRWAYS IN PATIENTS WITH OBSTRUCTIVE AIRWAY DISEASE." Journal of Clinical Investigation 46(11): 1812-&.

Singh, S., Y. K. Loke, et al.. (2011). "Mortality associated with tiotropium mist inhaler in patients with chronic obstructive pulmonary disease: systematic review and meta-analysis of randomised controlled trials." British Medical Journal 342.

Skaria, S. and G. C. Smaldone (2010). "Omron NE U22: Comparison Between Vibrating Mesh and Jet Nebulizer." Journal of Aerosol Medicine and Pulmonary Drug Delivery 23(3): 173-180.

Smart, J., Berg, E., Nerbrink, O., Zuban, R., Blakey, D., New, M. (2002). TouchSprayTM Technology: Comparison of the Droplet Size Measured with Cascade Impaction and Laser Diffraction. Respiratory Drug Delivery VIII, Tucson, AZ, USA, Virginia Commonwealth University, Richmond, VA, USA.

Smith, E. C., J. Denyer, et al.. (1995). "Comparison of 23 Nebulizer Compressor Combinations for Domiciliary Use." European Respiratory Journal 8(7): 1214-1221.

Smith, J. R. H., M. R. Bailey, et al.. (2008). "Effect of particle size on slow particle clearance from the bronchial tree." Exp Lung Res 34(6): 287-312.

Smyth, W. F. and V. Rodriguez (2007). "Recent studies of the electrospray ionisation behaviour of selected drugs and their application in capillary electrophoresis-mass spectrometry and liquid chromatography-mass spectrometry." Journal of Chromatography A 1159(1-2): 159-174.

Son, Y. J. and J. T. McConville (2008). "Advancements in dry powder delivery to the lung." Drug Development and Industrial Pharmacy 34(9): 948-959.

Sonnichsen, D. S., Q. Liu, et al.. (1995). "VARIABILITY IN HUMAN CYTOCHROME-P450 PACLITAXEL METABOLISM." Journal of Pharmacology and Experimental Therapeutics 275(2): 566-575.

Sood, B. G., J. Peterson, et al.. (2007). "Jet nebulization of prostaglandin E-1 during neonatal mechanical ventilation: Stability, emitted dose and aerosol particle size." Pharmacological Research 56(6): 531-541.

Spallek, M. W., Hochrainer, D., Wachtel, H. (2002). Optimizing Nozzles for Soft Mist Inhalers. Respiratory Drug Delivery VIII, Tucson, AZ, USA, Virginia Commonwealth University, Richmond, VA, USA.

Stahlhofen, W., G. Rudolf, et al.. (1989). "Intercomparison of Experimental Regional Aerosol Deposition Data." Journal of Aerosol Medicine 2(3): 285-308.

Steckel, H. and F. Eskandar (2003). "Factors affecting aerosol performance during nebulization with jet and ultrasonic nebulizers." European Journal of Pharmaceutical Sciences 19(5): 443-455.

Steckel, H., F. Eskandar, et al.. (2003). "Effect of cryoprotectants on the stability and aerosol performance of nebulized aviscumine, a 57-kDa protein." European Journal of Pharmaceutics and Biopharmaceutics 56(1): 11-21.

Stella, B., S. Arpicco, et al.. (2007). "Encapsulation of gemcitabine lipophilic derivatives into polycyanoacrylate nanospheres and nanocapsules." International Journal of Pharmaceutics 344(1-2): 71-77.

Tadros, M. I. (2008). "The influence of sodium hyaluronate, L-leucine and sodium taurocholate on the nebulization of aqueous betamethasone-17-valerate suspensions." Aaps Pharmscitech 9(1): 243-249.

Taeusch, H. W., K. Lu, et al.. (2002). "Improving pulmonary surfactants." Acta Pharmacologica Sinica 23: 11-15.

Tam, J. M., J. T. McConville, et al.. (2008). "Amorphous Cyclosporin Nanodispersions for Enhanced Pulmonary Deposition and Dissolution." Journal of Pharmaceutical Sciences 97(11): 4915-4933.

Tan, M. K., J. R. Friend, et al.. (2007). "Microparticle collection and concentration via a miniature surface acoustic wave device." Lab on a Chip 7(5): 618-625.

Tang, K. and A. Gomez (1994). "Generation by Electrospray of Monodisperse Water Droplets for Targeted Drug-Delivery by Inhalation." Journal of Aerosol Science 25(6): 1237-1249.

Terzano, C., A. Ricci, et al.. (2003). "Comparison of the efficacy of beclometasone dipropionate and fluticasone propionate suspensions for nebulization in adult patients with persistent asthma." Respiratory Medicine 97: S35-S40.

Thi, T. H. H., N. Azaroual, et al.. (2009). "Characterization and in vitro evaluation of the formoterol/cyclodextrin complex for pulmonary administration by nebulization." European Journal of Pharmaceutics and Biopharmaceutics 72(1): 214-218.

Thipphawong, J. B., N. Babul, et al.. (2003). "Analgesic efficacy of inhaled morphine in patients after bunionectomy surgery." Anesthesiology 99(3): 693-700.

Thorsson, L., C. Kenyon, et al.. (1998). "Lung deposition of budesonide in asthmatics: a comparison of different formulations." International Journal of Pharmaceutics 168(1): 119-127.

Tillery, M. and R. Buchan (2002). "Determination of large aerosol particle size by elutriation." Appl Occup Environ Hyg 17(10): 717-22.

Tukaram, B. N., I. V. Rajagopalan, et al.. (2010). "The Effects of Lactose, Microcrystalline Cellulose and Dicalcium Phosphate on Swelling and Erosion of Compressed HPMC Matrix Tablets: Texture Analyzer." Iranian Journal of Pharmaceutical Research 9(4): 349-358.

Ugarcic, Z., D. K. Vohra, et al.. (1981). "Measurement of Surface Tension using a Vertical Cone." Journal of the Chemical Society-Faraday Transactions I 77: 49-61.

UNEP (1987). The Montreal Protocol on substances that deplete the ozone layer, United Nations Environment Programme, Nairobi. Last ammended: 1999: 54.

Usmani, O. S. (2009). Delivery of drugs to the airways. Lung Biology in Health and Disease. O. S. Usmani. 234: 143-161.

Usmani, O. S., M. F. Biddiscombe, et al.. (2005). "Regional lung deposition and bronchodilator response as a function of beta(2)-agonist particle size." American Journal of Respiratory and Critical Care Medicine 172(12): 1497-1504.

USP (2011). "<1601> Products for Nebulization - Characterization Tests."

Vaghi, A., E. Berg, et al.. (2005). "In vitro comparison of nebulised budesonide (Pulmicort Respuless (R)) and beclomethasone dipropionate (Clenil (R) per Aerosol)." Pulmonary Pharmacology & Therapeutics 18(2): 151-153.

van Waarde, A., B. Maas, et al.. (2005). "Positron emission tomography studies of human airways using an inhaled beta-adrenoceptor antagonist, S-C-11-CGP 12388." Chest 128(4): 3020-3027.

Vanden Burgt, J. A., W. W. Busse, et al.. (2000). "Efficacy and safety overview of a new inhaled corticosteroid, QVAR (hydrofluoroalkane-beclomethasone extrafine inhalation aerosol), in asthma." J Allergy Clin Immunol 106(6): 1209-26.

Vaughn, J. M., J. T. McConville, et al.. (2006). "Single dose and multiple dose studies of itraconazole nanoparticles." European Journal of Pharmaceutics and Biopharmaceutics 63(2): 95-102.

Vaughn, J. M., N. P. Wiederhold, et al.. (2007). "Murine airway histology and intracellular uptake of inhaled amorphous itraconazole." International Journal of Pharmaceutics 338(1-2): 219-224.

Verschraegen, C. F., B. E. Gilbert, et al.. (2004). "Clinical Evaluation of the Delivery and Safety of Aerosolized Liposomal 9-Nitro-20(S)-Camptothecin in Patients with Advanced Pulmonary Malignancies." Clin Cancer Res 10(7): 2319-2326.

Videira, M. A., M. F. Botelho, et al.. (2002). "Lymphatic uptake of pulmonary delivered radiolabelled solid lipid nanoparticles." Journal of Drug Targeting 10(8): 607-613.

Vincken, W., T. Bantje, et al.. (2004). "Long-term efficacy and safety of ipratropium bromide plus fenoterol via Respimat (R) Soft Mist (TM) inhaler (SMI) versus a pressurised metered-dose inhaler in asthma." Clinical Drug Investigation 24(1): 17-28.

Visser, T. J., A. van Waarde, et al.. (1998). "Characterisation of beta(2)-adrenoceptors, using the agonist [C-11]formoterol and positron emission tomography." European Journal of Pharmacology 361(1): 35-41.

von Berg, A., P. M. Jeena, et al.. (2004). "Efficacy and safety of Ipratropium bromide plus fenoterol inhaled via Respimat (R) Soft Mist (TM) inhaler vs. a conventional metered dose inhaler plus Spacer in children with asthma." Pediatric Pulmonology 37(3): 264-272.

Waldrep, J. C., J. Arppe, et al.. (1997). "High dose cyclosporin A and budesonide-liposome aerosols." International Journal of Pharmaceutics 152(1): 27-36.

Waldrep, J. C., A. Berlinski, et al.. (2007). "Comparative analysis of methods to measure aerosols generated by a vibrating mesh nebulizer." Journal of Aerosol Medicine-Deposition Clearance and Effects in the Lung 20(3): 310-319.

Wang, Z., H. T. Chen, et al.. (2003). "Farnesol for aerosol inhalation: Nebulization and activity against human lung cancer cells." Journal of Pharmacy and Pharmaceutical Sciences 6(1): 95-100.

Ward, M. E., A. Woodhouse, et al.. (1997). "Morphine pharmacokinetics after pulmonary administration from a novel aerosol delivery system." Clinical Pharmacology & Therapeutics 62(6): 596-609.

Warde, P. and D. Payne (1992). "DOES THORACIC IRRADIATION IMPROVE SURVIVAL AND LOCAL-CONTROL IN LIMITED-STAGE SMALL-CELL CARCINOMA OF THE LUNG - A METAANALYSIS." Journal of Clinical Oncology 10(6): 890-895.

Washington, C. (1996). "Stability of lipid emulsions for drug delivery." Advanced Drug Delivery Reviews 20(2-3): 131-145.

Watts, A. B., J. T. McConville, et al.. (2008). "Current therapies and technological advances in aqueous aerosol drug delivery." Drug Development and Industrial Pharmacy 34(9): 913-922.

Weber, C. (1931). "Zum Zerfall eines Flussigkeitsstrahles." Journal of Applied Mathematics and Mechanics / Zeitschrift fur Angewandte Mathematik und Mechanik 11(2): 136-154.

Wilbanks, T. M. and J. A. Schuster (2005). Aerosol drug delivery to the lung periphery using nano-scale technologies. 2005 International Conference on MEMS, NANO and Smart Systems, Proceedings: 127-128.

Windt, H., H. Kock, et al.. (2010). "Particle deposition in the lung of the Gottingen minipig." Inhal Toxicol 22(10): 828-34.

Wittgen, B. P. H., P. W. A. Kunst, et al.. (2007). "Phase I study of aerosolized SLIT cisplatin in the treatment of patients with carcinoma of the lung." Clinical Cancer Research 13(8): 2414-2421.

Wu, Y. Z. and T. Wang (2003). "Phospholipid class and FA compositions of modified soybeans processed with two extraction methods." Journal of the American Oil Chemists Society 80(2): 127-132.

Wu, Y. Z. and T. Wang (2003). "Soybean lecithin fractionation and functionality." Journal of the American Oil Chemists Society 80(4): 319-326.

Xie, J., L. K. Lim, et al.. (2006). "Electrohydrodynamic atomization for biodegradable polymeric particle production." Journal of Colloid and Interface Science 302(1): 103-112.

Xie, Y. Y., P. Y. Zeng, et al.. (2010). "Magnetic Deposition of Aerosols Composed of Aggregated Superparamagnetic Nanoparticles." Pharmaceutical Research 27(5): 855-865.

Yeo, L. Y. and J. R. Friend (2009). "Ultrafast microfluidics using surface acoustic waves." Biomicrofluidics 3(1).

Yeo, L. Y., J. R. Friend, et al.. (2010). "Ultrasonic nebulization platforms for pulmonary drug delivery." Expert Opinion on Drug Delivery 7(6): 663-679.

Yi, D., A. Price, et al.. (2010). "Measurement of the distribution of aerosols among mouse lobes by fluorescent imaging." Analytical Biochemistry 403(1-2): 88-93.

Yi, D. and T. S. Wiedmann (2010). "Inhalation Adjuvant Therapy for Lung Cancer." Journal of Aerosol Medicine and Pulmonary Drug Delivery: ahead of print.

Yim D., C. D., Boyd B. (2001). "Feasibility of Pulmonary Delivery of Nano-suspension Formulations using the AERx® System." Journal of Aerosol Medicine 18(1): 101-102.

Yurteri, C. U., R. P. A. Hartman, et al.. (2010). "Producing Pharmaceutical Particles via Electrospraying with an Emphasis on Nano and Nano Structured Particles - A Review." Kona Powder and Particle Journal(28): 91-115.

Zakharian, T. Y., A. Seryshev, et al.. (2005). "A fullerene-paclitaxel chemotherapeutic: Synthesis, characterization, and study of biological activity in tissue culture." Journal of the American Chemical Society 127(36): 12508-12509.

Zanen, P., L. T. Go, et al.. (1995). "THE OPTIMAL PARTICLE-SIZE FOR PARASYMPATHICOLYTIC AEROSOLS IN MILD ASTHMATICS." International Journal of Pharmaceutics 114(1): 111-115.

Zanen, P., L. T. Go, et al.. (1996). "Optimal particle size for beta(2) agonist and anticholinergic aerosols in patients with severe airflow obstruction." Thorax 51(10): 977-980.

Zanen, P., L. T. Go, et al.. (1998). "The efficacy of a low-dose, monodisperse parasympathicolytic aerosol compared with a standard aerosol from a metered-dose inhaler." European Journal of Clinical Pharmacology 54(1): 27-30.

Zaru, M., S. Mourtas, et al.. (2007). "Liposomes for drug delivery to the lungs by nebulization." European Journal of Pharmaceutics and Biopharmaceutics 67: 655-666.

Zeng, X. M., G. P. Martin, et al.. (2001). Medicinal Aerosols. Particulate interactions in dry powder formulations for inhalation. X. M. Zeng, G. P. Martin and C. Marriott. New York, NY, Taylor & Francis: 65-102.

Zhang, G., A. David, et al.. (2007). "Performance of the vibrating membrane aerosol generation device: Aeroneb micropump nebulizer (TM)." Journal of Aerosol Medicine-Deposition Clearance and Effects in the Lung 20(4): 408-416.

Zhang, L.-J., B. Xing, et al.. (2008). "Biodistribution in mice and severity of damage in rat lungs following pulmonary delivery of 9-nitrocamptothecin liposomes." Pulm Pharmacol Ther 21(1): 239-46.

Zierenberg, B. (1999). "Optimizing the in vitro performance of Respimat." Journal of Aerosol Medicine-Deposition Clearance and Effects in the Lung 12: S19-S24.

Zimlich, W. C., Ding, J.Y., Busick, D.R., Moutvic, R.R., Placke, M.E., Hirst, P.H., Pitcairn, G.R., Malik, S., Newman, S.P., Macintyre, F., Miller, P.R., Shepherd,

M., Lukas, T.M. (2000). The Development of a Novel Electrohydrodynamic Pulmonary Drug Delivery Device. Respiratory Dru Delivery VII, Tarpon Springs, FL, USA, Serentec Press, Raleigh, NC, USA.

Zou, Y., H. Fu, et al.. (2004). "Antitumor Activity of Hydrophilic Paclitaxel Copolymer Prodrug Using Locoregional Delivery in Human Orthotopic Non-Small Cell Lung Cancer Xenograft Models." Clin Cancer Res 10(21): 7382-7391.

ZuWallack, R., M. C. De Salvo, et al.. (2010). "Efficacy and safety of ipratropium bromide/albuterol delivered via Respimat (R) inhaler versus MDI." Respiratory Medicine 104(8): 1179-1188.

Vita

Thiago Cardoso Carvalho has attended public educational institutions in Brazil from elementary school to college. He graduated from Escola Estadual de Furnas in São José da Barra, in 1997. After that, he attended the College of Pharmacy at Universidade Federal de Minas Gerais (UFMG) in Belo Horizonte. In 2004, he joined the pharmaceutics research laboratory of Dr. Robert O. Williams III for an internship period of 5 months, working under the direct supervision of the then *Post Doc* scientist Dr. Jason T. McConville. During the following years, he was employed by Novo Nordisk Produção Farmacêutica do Brasil, in Montes Claros, Brazil, as Insulin Production Analyst and, later on, as Supervisor. In fall 2007, he started his doctorate program in Pharmaceutics at The University of Texas at Austin, under the supervision of Dr. Jason T. McConville.

Permanent address: thiago.carvalho@utexas.edu

This dissertation was typed by the author.